Determining Internal Leakages of High Pressure and Temperature Steam Valves

by

Sulaiman Ahmed Sadeck Bapeekee

(BPKSUL001)

Thesis submitted to the University of Cape Town in fulfilment of the requirements for the degree of

Master of Science in Engineering (MSc Eng)

Mechanical Engineering

Department of Mechanical Engineering

University of Cape Town

Private Bag X3, Rondebosch 7701, South Africa

Supervisor:

Mr Dirk Findeis

July 2015

Declaration

I, the undersigned, hereby declare that I know the meaning of plagiarism and that all the work in the document, save for that which is properly acknowledged, is my own original work and that I have not previously in its entirety or in part submitted it at any university for a degree.

Signature: ..... Signed by candidate ..... Signature Removed

Sulaiman AS Bapeekee (8612135045080)

Date: 23/07/2015

Summary

Internal leakages of high pressure and temperature steam valves have been identified as a potential contributor to a loss in power generating plant efficiency. These losses are often neglected due to it being difficult to detect problematic valves and quantify the internal leakages through them. A non-intrusive NDT technique that detects and quantifies internal leakages through valves will be a very favourable tool to any power generating plant as it will allow for the early detection of internal leakages and could possibly provide considerable financial savings.

This research evaluates different monitoring techniques suitable for detecting and quantifying internal leakages through valves and selects a technique that is most suitable for application in a power generating plant environment.

The proposed technique utilises infra-red thermography to calculate pipe surface temperatures on a length of un-insulated pipe located downstream of a valve that is leaking internally. As the leakage steam flows through the length of un-insulated pipe, it will lose a portion of its heat energy through the pipe wall to the surrounding environment. This will result in a drop in temperature of the steam from the upstream to downstream points of the un-insulated length of pipe. By calculating the heat loss and the drop in temperature of the leakage steam, a mass flow rate of the leakage steam can be determined.

A mathematical model was derived which with inputs of upstream and downstream pipe surface temperatures of the un-insulated pipe, pipe properties and ambient air conditions, calculates the heat loss, the temperature drop and the resulting mass flow rate of the leakage flow through the valve.

A detailed experimental study was conducted to validate the proposed technique in determining internal leakages thought steam valves. Steam generated from a mini steam generating plant was allowed to flow through an experimental test rig, which contained a length of un-insulated pipe, at different flow rates. Pipe surface temperature measurements of the un-insulated pipe were made using an infrared thermal camera and a mass flow rate of the steam was calculated using the derived mathematical model. In all experiments, the mass flow rate calculated using the mathematical model was compared to a mass flow rate acquired from a flow measuring device installed in-line with the experimental test rig.

The results indicate that an increase in mass flow rate causes an increase in pipe surface temperatures of the un-insulated pipe which translates to an increase in heat loss of the

leakage steam through the length of un-insulated pipe. The mass flow rate calculated using the proposed technique closely approximates the mass flow rate acquired from the flow measuring device. This indicates that the proposed technique, using infrared thermography, is capable of detecting and quantifying possible internal valve leakages encountered in online operation.

Onsite tests were performed using the proposed technique on two different boiler drain valves at Majuba Power Station. It was found that one of the valves was internally leaking steam to the atmosphere at a rate of 0.039 kg/s whilst the other valve was sealing correctly. A comprehensive financial impact study was conducted, and it was found that this leakage steam will result in a total loss of R 730 108 per annum if the leak is left unattended. This is the loss for a single valve that has a relatively small leak. The financial loss for a combination of all valves that are internally leaking in a power plant could be substantial and can clearly justify plant personnel in utilising the proposed technique to identify problematic valves.

With its portability, non-intrusiveness and ease of use the proposed technique provides a cost effective means to determine internal leakages through power plant valves.

Acknowledgements

I would like to express my sincere gratitude to the following people who have contributed to making this work possible:

- Mr D. Findeis of the University of Cape Town and Mr P. Magner of Eskom as my mentors and supervisors.
- Mr A. Cassim of Eskom Majuba Power Station for his assistance on the experimental test rig.
- Eskom Power Plant Engineering Institute for granting me the opportunity to conduct this research.
- Eskom Majuba Power Station for their financial support.
- Eskom Academy of Learning for allowing me to utilise equipment used in the experimentation.

I would also like to thank my family and friends for their steady love and support. Most of all, I thank the Almighty Lord for His continual grace and guidance, without which this study with not have been possible.

Contents

List of Figures

List of Tables

Nomenclature

Variables:

A	Area [m^2]
C	Specific heat capacity [kJ/kg K] or coefficient
D	Diameter [m]
g	Gravitational acceleration [9.81 m/s^2]
H	Head [m]
h	Convective heat transfer coefficient [W/m^2 k] or enthalpy [kJ/kg]
k	Resistance coefficient
L	Length [m]
$\dot{m}$	Mass flow rate [kg/s]
N	Shaft speed [rpm]
Nu	Nusselt Number
P	Pressure [pa] or Power [W]
Pr	Prandtl Number
Q	Heat Loss [W] or Volumetric flow rate [m^3/s]
Ra	Rayleigh Number
S	Specific gravity [m^3/kg]
T	Temperature [K] or [^oC]
t	wall thickness [m]
V	Volumetric flow rate [l/s]
v	Velocity [m/s]

Greek Symbols:

β	Ratio of orifice diameter to pipe diameter or thermal expansion coefficient
Δ	Differential
ε	Thermal emissivity or expansibility factor
ρ	Density [kg/m^3] or reflectivity
σ	Stefan-Boltzmann constant [$5.67 \times 10^{-8} W/m^2K^4$]
α	Thermal diffusity or sound velocity
τ	Transmittivity
μ	Dynamic viscosity [kg/sm]
ν	kinematic viscosity [m^3/sm]
κ	Thermal conductivity [W/mk]
η	Efficiency
λ	Wavelength

Subscripts:

a	Air
amb	Ambient air
avg	Average
b	Boiler
c	Convection
f	fluid
i	internal

r	Radiation
s	Surface
t	turbine

Abbreviations

AE	Acoustic Emission
ASL	Average Signal level
BFP	Boiler Feed Pump
CEP	Condensate Extraction Pump
CFD	Computational Fluid Dynamics
HP	High pressure
IP	Intermediate pressure
IRT	Infrared Thermography
kW	Kilowatt
LP	Low pressure
MW	Megawatt
NDT	Non-Destructive Testing
SMEs	Small or Medium Enterprises

1. Introduction

1.1 Power generation in South Africa

Eskom is a South African public utility and the largest electricity generating utility in Africa. It currently generates approximately 95% of the electricity used in South Africa and approximately 45% of the electricity used in Africa. Eskom has 23 power generating plants and is currently capable of generating a net maximum capacity of 44 084 MW of electricity. The generation of electricity is mainly from coal-fired power plants due to the rich coal deposits concentrated in the north east of the country.

Towards the end of 2007, South Africa experienced widespread rolling blackouts as supply fell behind demand, threatening to destabilise the national grid. This had a severe impact on the economy of the country as mines were first shut down and subsequently restricted in their electricity use and retailers reported large losses due to spoiled frozen and chilled foods. The country's economic growth slowed down substantially and estimates on the direct cost of the blackouts were calculated to be in the region of R 50 billion during the period November 2007 to January 2008. The economy slowed down to 4.0 % in the first quarter of 2008 from 5.8 % for the same period in 2007 mainly as a result of the mining industry which contracted by 22.1 % in the first quarter of 2008. This also had a severe impact on the investor confidence in the country since the Johannesburg Stock Exchange, dominated by large mining companies, and the South African currency depreciated significantly in 2008 due to the energy crisis.

The energy crisis had a severe impact on small and medium enterprises (SMEs) in South Africa. Unlike larger businesses, SMEs generally lack the resources necessary to invest in alternate sources of energy and are completely reliant on Eskom for their energy requirements making them extremely vulnerable to an unstable energy environment. There were various reports covering the extent of damage to SMEs, examples of this include damaged equipment, perishables damaged in refrigerators, loss of clients due to failure to meet deadlines and loss of trade or productivity due to carrying the cost of overheads while not trading.

The impact of the energy crisis extends well beyond South Africa's borders. Eskom supplies electricity to the Southern Africa Power Pool (SAPP), which was established to create a regional market in 11 Southern African countries. As the power crisis unfolded in South Africa, countries that were supplied by Eskom were also confronted with blackouts since the pool could not absorb the capacity shortfall of South Africa.

A number of problems combined to cause the South African power crisis. The most significant being the insufficient generation capacity available. A clear indication of this can be seen from analysing the country's reserve margin, the gap between maximum generating capacity and the peak electricity demand, which fell from 15% in 2001 to a mere 7% in 2008. Internationally, a reserve margin of 20% is seen as adequate to cater comfortably for planned maintenance and breakdowns. This decrease in reserve margin was as a result of higher than expected economic development in the country which created a growing demand for electricity.

To increase the reserve margin back to acceptable levels, more generation capacity needed to be added to the national grid, which meant that more power plants needed to be constructed. The construction of power plants is a lengthy process which takes many years to complete. Thus, to mitigate the power crisis, Eskom and other role players embarked upon many short to medium type initiatives to stabilise the national grid.

One of the key initiatives embarked upon by Eskom was a fleet wide energy efficiency drive. This entailed a comprehensive analysis of all power plants to determine system inefficiencies which result in power plants operating inefficiently and power plants not being able to generate maximum capacity when required. Identifying and rectifying inefficiencies of existing power plants was identified as a cost effective and fast way to increase production capacity and save money which could be reinvested into Eskom's new capital expansion projects.

1.2 Coal-fired power plants

The generation of electricity from coal-fired power stations accounts for 88 % of the total generating capacity of the country. The balance is generated from nuclear, hydroelectric, pumped storage and open cycle gas turbine power plants.

Fundamentally a coal-fired power plant converts the chemical energy contained in coal to heat energy, converts the heat energy into mechanical energy and uses the mechanical energy to rotate a generator to produce electrical energy. The fundamental operating cycle of a coal-fired power plant is the Rankine cycle and is shown in figure 1 below.

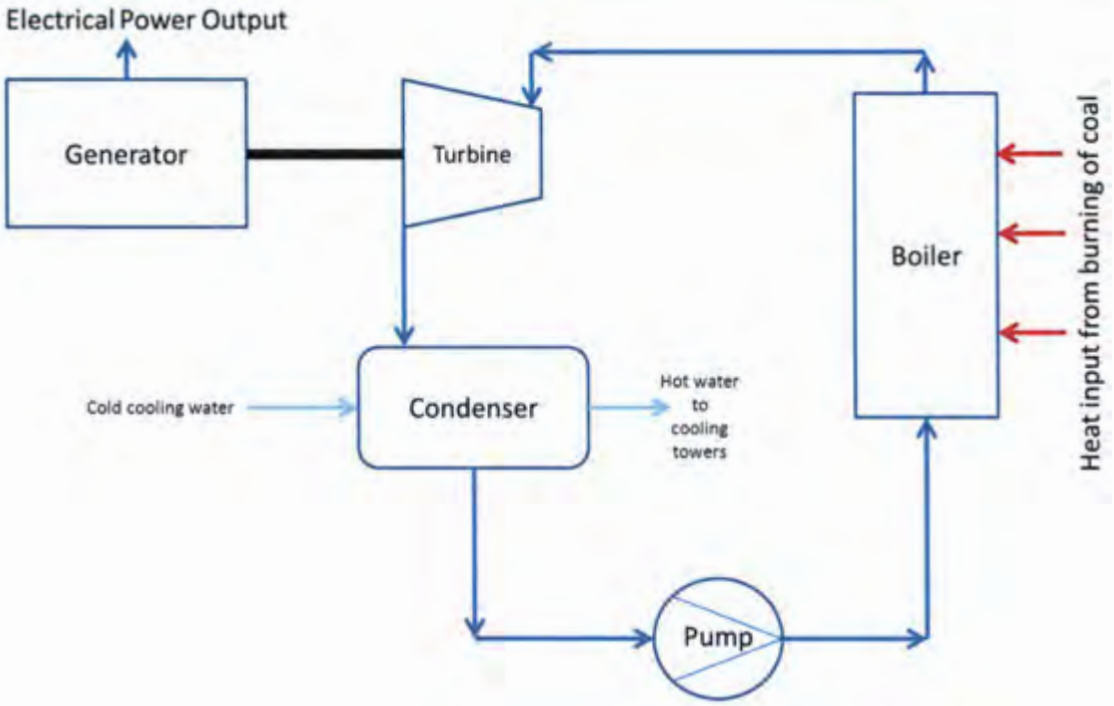

Figure 1: The Rankine cycle for a coal-fired power plant

Coal is transported to the boiler were it is ignited and burned. The heat energy from the burning coal is supplied externally to a closed loop, which uses water as the working fluid. High pressure water is pumped into the boiler were it is heated by the heat energy from the burning coal into steam. The steam is then transported to the turbine were it expands, resulting in rotation of a shaft or mechanical energy. The generator, located on a common shaft with the turbine, converts this mechanical energy into electrical energy which is transmitted to electricity consumers. To transport the expanded steam from the outlet of the turbine to the boiler, it is necessary to condense it to a liquid by removing the remaining heat contained in the steam. This is done in the condenser were the steam loses its heat to the cold cooling water which transports the heat to cooling towers expelling it to the environment. The condensed liquid is then transferred back to the boiler via pumps thus completing the circuit. The above is a simplified description on the generation of electricity from a coal-fired power plant. In reality, coupled to the above cycle, coal-fired power plants typically contain heaters to heat the water before entering the boiler, a high pressure (HP), intermediate pressure (IP) and low pressure (LP) turbine all rotating on a common shaft, superheaters to superheat the steam before entering the HP turbine and reheaters to reheat the steam before entering the IP turbine. Figure 2 below illustrates a typical water-steam cycle flow path for a coal-fired power plant. There are many different types of configurations installed in steam generators worldwide. The below figure illustrates the process of the Benson type steam generator installed at Majuba Power Station.

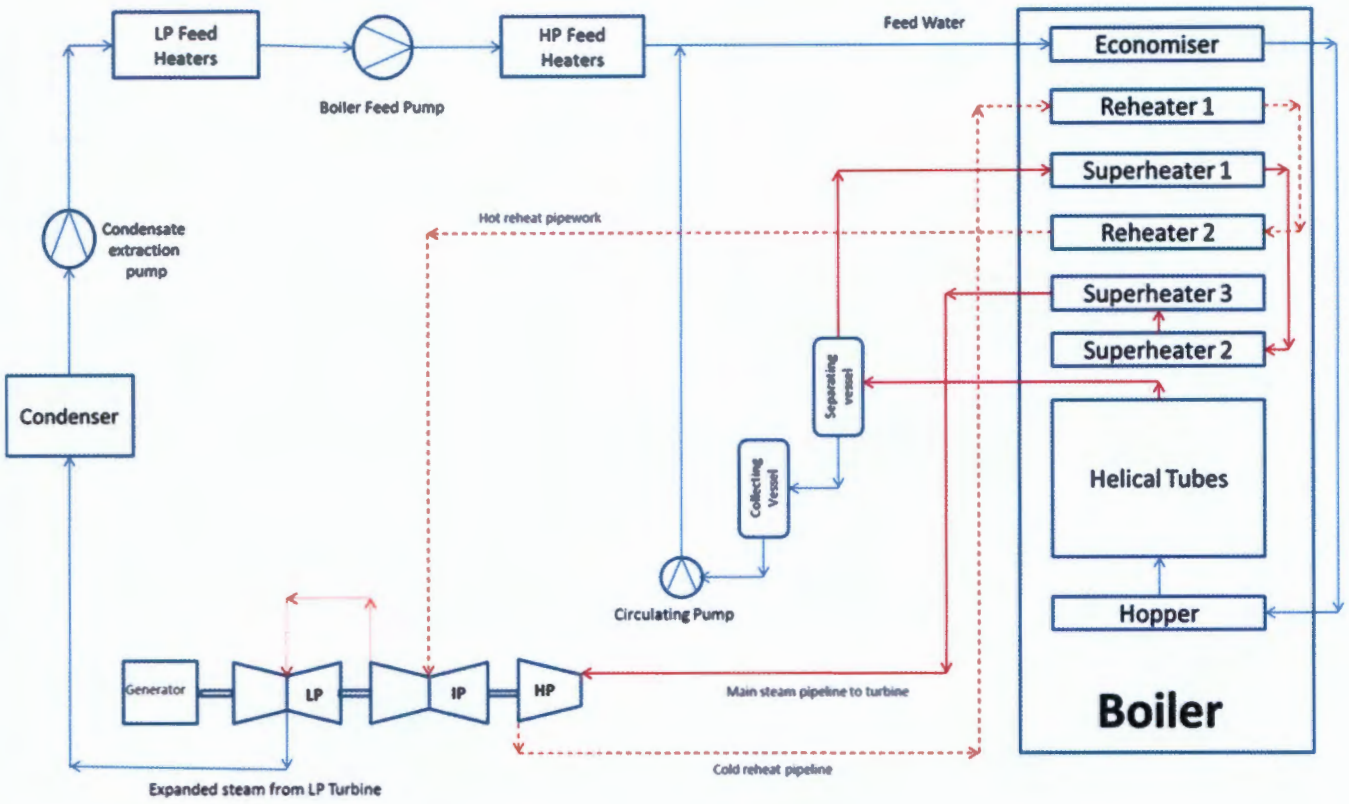

Figure 2: Water-steam cycle flow path for typical coal fired power plant

The boiler contains many water-steam flow paths to facilitate efficient heating of the fluid pumped into the boiler. These components are made up of bundles of tubes. Pulverised coal and air is fed into the boiler by tangential-type burners located along the walls of the boiler. The ignition of the coal creates a fireball in the boiler releasing heat energy to the boiler components. The heat energy is then conducted through the tube walls and transferred to the water/steam flowing in them.

Initially the water is pumped into the economiser section of the boiler, located horizontally at the tail end of the boiler gas path, were it is heated to a certain temperature and passed to the evaporator (hopper tubes and helical tubes) located along the boiler walls were the water is heated to the saturation temperature and converted into steam by the heat energy released from the burning coal.

The steam then travels into the separating vessel were any water present is drained to the collecting vessel and pumped back into pipes that feed the economiser. This is to ensure that only steam is allowed to flow to the turbine. Steam from the separating vessel cascades into the superheaters, were it is superheated and transferred to the HP turbine. The heat energy contained in the steam is used to drive the HP turbine. The expanded steam is then returned to the boiler were it is reheated in the reheaters and transferred to the IP turbine. The dashed red lines in figure 2 show this process. After expanding in the IP turbine the steam cascades to the

LP turbine. The steam from the LP turbine is then expanded into the condenser, were it is condensed and returned to the boiler via LP heaters and HP heaters. The heaters preheat the feedwater, before entering the boiler, with steam tapped off from the turbines.

Many valves, serving different purposes, are installed on the water-steam cycle. Feed regulating valves are installed after the boiler feed pumps and control the amount of feed water that is pumped into the boiler. Pressure relief valves are installed on various components to protect them against over pressurisation. Vent valves are installed on components to remove air ingress into the system and drain valves are installed to facilitate the draining of components in shut down and emergency conditions.

Drain valves are installed on drain lines which are tapped off from the lowest location on a component. This facilitates quick draining of components if needed. Primarily, components are drained to a sink, maintained at much lower pressures, to remove any condensation formed in components during start-up conditions and to preserve component pipework in shutdown conditions. Standing water in components during shutdown conditions can cause severe corrosion which compromises the integrity of components. Under normal operating conditions drain valves are maintained in the fully closed position and are meant to completely isolate (shut-off) flow preventing high pressure and temperature steam from escaping to the lower pressure sink.

1.3 Problem due to internally leaking valves

Drain valves have been identified as a potential contributor to an energy loss on a power plant due to valves leaking fluid internally when they are meant to completely isolate (shut-off) the fluid under normal operating conditions as explained above. Due to high pressure steam being isolated by the drain valves, a small leak path generated between the valve mating surfaces, when it is in the fully closed position, will cause high energy steam to leak internally through the valve to the lower pressure sink. This leakage steam is dumped into the atmosphere resulting in a loss to the power generating cycle due to the energy contained in the steam being lost. To supplement this loss more water needs to be added to the cycle and more coal needs to be burned to maintain the energy levels of the steam produced and delivered to the turbine to meet the generating requirements of the plant. This additional fuel directly impacts the efficiency of the power plant.

Figure 3 below illustrates the severity of the leakages of steam to the environment from internally leaking valves at an Eskom power station.

Figure 3: Steam loss due to internally leaking drain valves

Currently not much knowledge is known in any of Eskom's power plants as to which valves are leaking internally, by how much they are leaking and to what extent it affects the performance of the power plant.

1.4 Objectives of current study

The main objectives of this dissertation can be listed as follows:

1. To develop an understanding of high energy valves and identify valves which are main contributors to energy losses in a power plant.
2. To evaluate, by practical application, the suitability of different techniques to detect and quantify internal leakages through valves.
3. To evaluate all losses associated with valves that are leaking internally.

2. Background

2.1 Reasons for internal valve leakages on Eskom power plants

Drain valves are considered isolating valves since they isolate (shut-off) a fluid from flowing through it, to the downstream piping, when they are in the fully closed position under normal operating conditions. In shut down and emergency conditions, these valves are usually in the fully open position allowing quick draining predominantly to the atmosphere. Thus, these valves are designed to either operate in the fully open state or fully closed state.

A valve that is thought to be in the fully closed position but allows fluid to pass is considered an internally leaking valve. The leak occurs as a result of a leak path created between the valve mating surfaces. This leak path is thought to be generated by one or a combination of the following factors:

- **Lack of maintenance opportunities**

Due to the severe shortage of electricity as explained in chapter 1, planned maintenance on power generating plants are regularly postponed to meet high energy demand. These postponements result in valves not being refurbished as per maintenance strategy.

Valves are mechanical devices and the internals are susceptible to wear. Typically, over a period of time, valve seats and discs begin to wear and need to be refurbished or replaced. Continual operation with a worn seat and disc, compromises the integrity of the mating surfaces and result in high pressure steam passing between the mating surfaces into the downstream piping network.

- **Foreign or abrasive debris in the pipeline**

Foreign debris such as used welding rods, grinder discs etc. left in the pipeline after repairs can settle in the valve cavity. This debris can get lodged between the valve seat and disc and can potentially cause the mating surface not to tightly seal the fluid when the valve is in the closed condition resulting in fluid leaking internally through the valve to the downstream pipework.

- **Incorrect "stroking" of valves**

Many valves in a power plant are installed with motor operated actuators to automatically drive the valve stem to a desired position. With regard to the boiler drain valves, motor operated actuators are installed to drive the valve stem and disc assembly to either a fully open position or a fully closed position. The valve stem and disc assembly being in the fully open position will allow fluid to flow through to the downstream piping network, whilst the valve stem and disc assembly in the fully closed position will allow for the valve disk to make contact with the valve seat, thereby creating a sealing surface which will prevent a fluid from flowing through to the downstream piping network.

To ensure that the actuator correctly drives the valve stem and disc assembly to a desired position, the valve needs to be "stroked". "Stroking" a valve is a process whereby an operator drives the valve manually to a fully closed position and sets a closed limit switch, thereafter the operator drives the valve to a fully open position and sets an open limit switch. The valve then operates between these two limit switches. When the valve is required to be in the fully closed position, the actuator automatically drives the valve stem and disc assembly until the closed limit switch makes contact. This will indicate that the valve is in a fully closed position and the disk is in contact with the seat, creating a leak tight seal.

It has been observed by the author on many occasions that the closed limit is set in an incorrect position resulting in the valve disk not coming into full contact with the valve seat. This will result in fluid being allowed to flow through the valve to the downstream pipework whilst the valve is thought to be in the fully closed position.

If a leak-path is generated from any of the above mentioned reasons, the "leak-hole" will deteriorate rapidly due to the leaking high pressure steam eroding away the valve internal material resulting in an increased leakage rate with time. Thus, identifying a leak early can prove very advantages.

2.2 Valves that are main contributors to energy losses on a power plant

The scales of losses due to internally leaking valves will vary depending on where in the water-steam cycle the leak occurs. If a leak occurs immediately after the condensate extraction pumps (CEP), where most of the energy contained in the steam has been used to generate electricity, a loss of steam at this point will not have a significant impact on the efficiency of the cycle compared to a leak occurring before the inlet to the HP turbine, where the steam contains the most energy in the entire cycle. Thus, to identify an internally leaking valve that is part of the high energy steam network will be more preferable than identifying an internally leaking valve on the low energy steam side of the network.

The most energy added to the fluid in the water-steam cycle is in the boiler. Figure 4 below illustrates the energy content of the fluid at different locations in a typical coal-fired power plant. Typically, feed water is pumped into the boiler at pressures and temperatures of 21 MPa and 240 °C respectively. Once heated in the boiler, the steam leaves the boiler at pressures and temperatures of 17 MPa and 540 °C respectively. This amounts to approximately 2400 kJ/kg of energy being added to the fluid in the boiler. If any drain valve around the boiler leaks it will potentially have the largest impact on the plant efficiency due to the high concentration of energy contained in the leaking steam.

Taking this into consideration, it was decided to concentrate this study on the boiler drain valves.

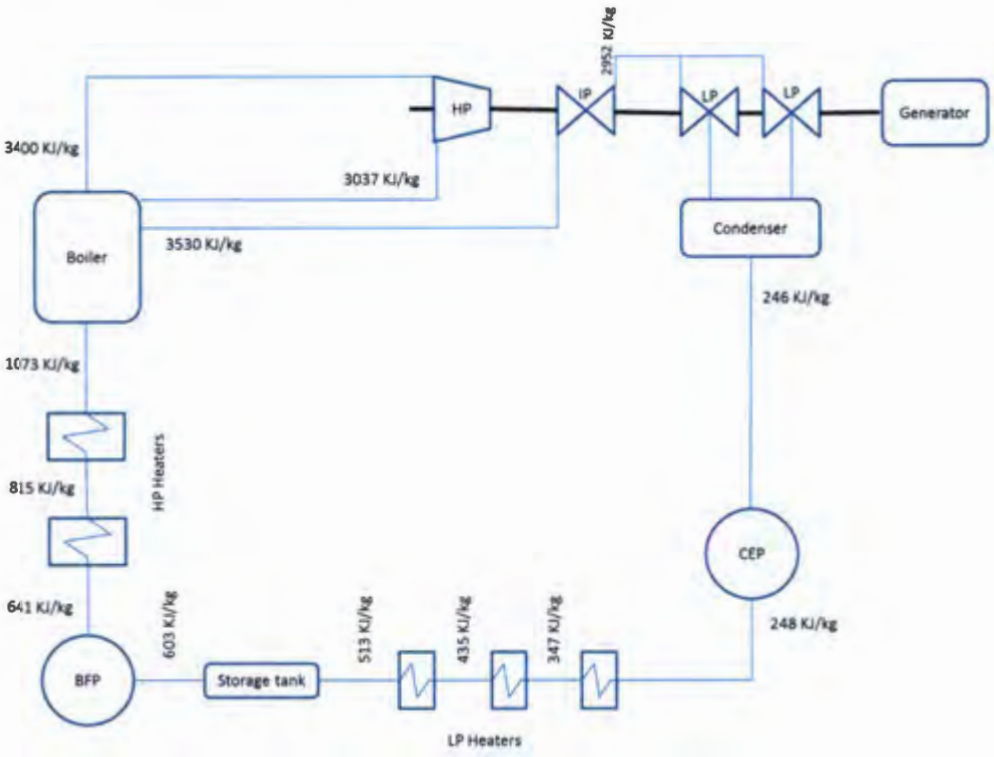

Figure 4: Energy level of fluid in typical coal-fired power plant along the water/steam cycle

2.3 Boiler drain valve configuration

Drain lines are installed on most components of the boiler to allow for draining of the boiler components in start-up, shut down and emergency conditions. Drain lines are usually installed on the lowest point of the component to ensure effective draining. Generally, there are two valves installed on a drain line, a motor operated valve and a hand operated valve. These valves are installed in series with each other with the motor operated valve installed before the hand operated valve in the direction of flow. The hand operated valve is usually installed close to the common manifold where all boiler drain lines discharge into, before going into the boiler blow down vessel. Figure 5 below shows a schematic of a typical boiler drain valve configuration.

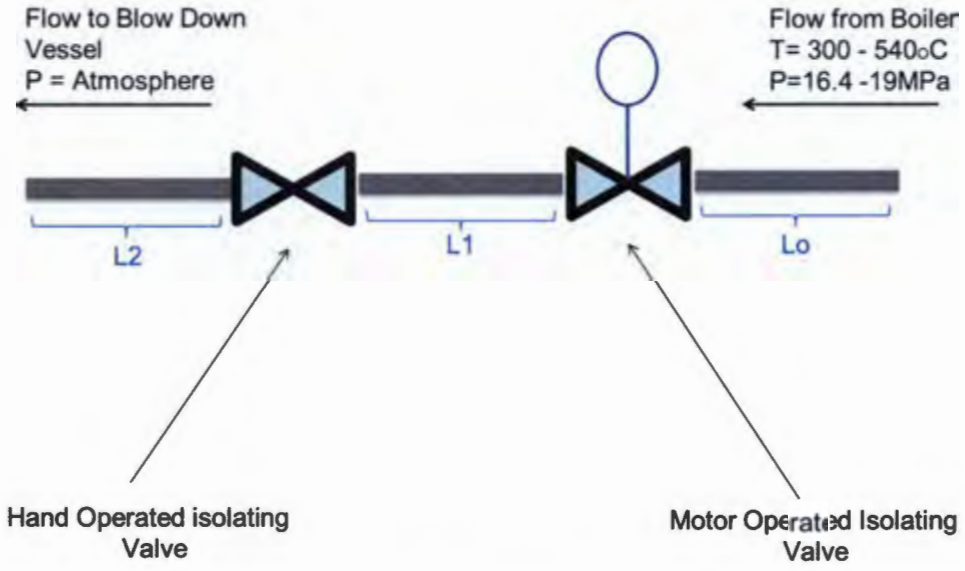

Figure 5: Typical boiler drain line and drain valve configuration

In the above figure, lengths L0, L1 and L2, pipe diameters and the upstream pressure and temperature vary between different boiler drain lines. Table 1 below shows typical values of pressures and temperatures experienced by different boiler drain lines.

Table 1: Typical upstream steam temperatures and pressures and pipe diameters for different boiler drain lines

Drain lines	Upstream temperature (°C)	Upstream Pressure (MPa)	Pipe Diameter (mm)
Evaporator drains	306	23.4	50
Superheater drains	470	21.4	50
Reheater drains	462	5.8	50
Main steam piping drains	545	19.4	50/65
Hot reheat piping drains	545	5	50/65
Cold reheat drains	430	5.35	50/65

All pipes are insulated on their outer surface with mineral fibre mats and galvanised metal sheets as a safety precaution. No measuring instrumentations are available on any pipework upstream or downstream of the boiler drain valves. This means that one is unable to determine any fluid properties such as temperature or pressure upstream and downstream of the drain valves. There is also no means whatsoever to determine the leak diameter/ path of an internally leaking valve.

All boiler drain and vent valves discharge into a common manifold which discharge into the boiler blow down vessel. The boiler blow down vessel vents to atmosphere. Figure 6 below illustrates the discharge of the drain valves into the boiler blow down vessel.

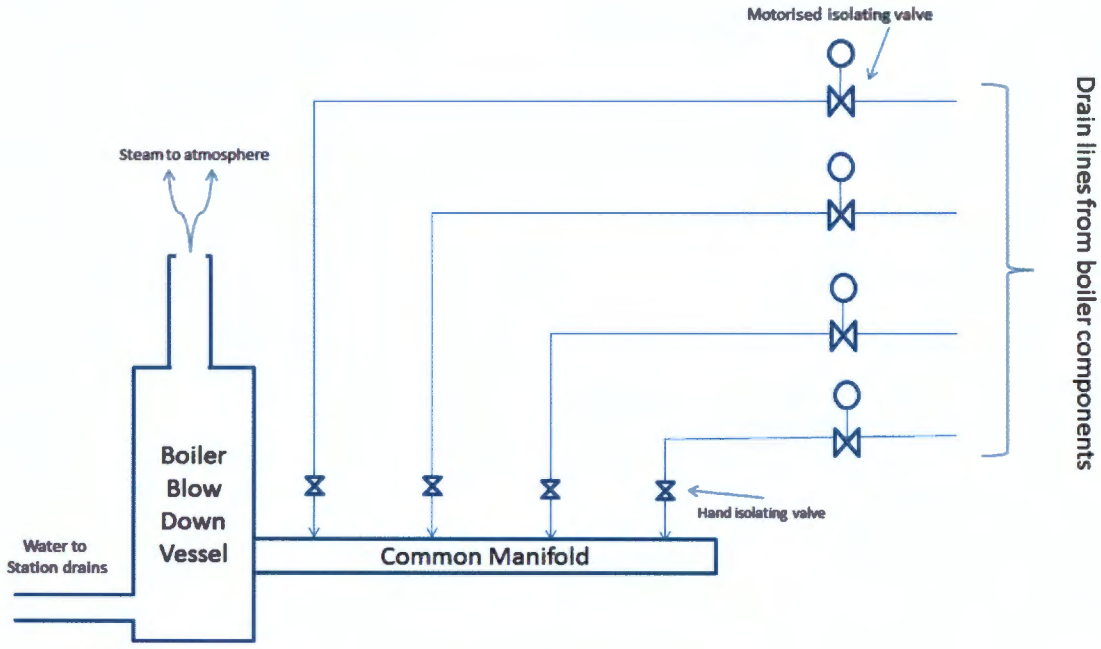

Figure 6: Discharge of boiler drain valves into boiler blow down vessel

Under start-up, shutdown and emergency conditions the motorised isolation valve is in the fully open position whilst it is in the fully closed position under normal operating conditions. The hand isolation valve is always in the fully open position.

2.4 Factors in considering a suitable detection and quantification technique

To choose a suitable technique to detect and quantify internal leakages of valves one needs to consider the following factors:

- The proposed technique needs to be quick and easy to enable responsible personnel in identifying problematic valves swiftly.
- It needs to be an in-situ inspection method. Authorities are reluctant to shut down power plants due to the high demand of electricity currently experienced in the country as explained in chapter 1.
- The technique needs to be non-intrusive as it will not be feasible to install instrumentation on all drain lines in the boilers across all power stations.
- The proposed technique needs to take into consideration the high pressures and temperatures of the steam flow upstream of the drain valves and the fact that steam is a compressible fluid.
- All piping upstream and downstream of the drain valves are insulated with mineral fibre mats. The mineral fibre mats are covered with galvanised metal sheeting.
- Noise levels are high in the vicinity of the drain valves.

3. Literature review

3.1 Valves

A valve is a mechanical device that can be used to control, regulate or direct the flow of a fluid by opening, closing or partially obstructing a pipeline or duct. Valves have many uses and are found in virtually every industrial process. In power plants, valves are installed to control the amount of flow required by a system, to drain a component when required, to protect a component from over pressurisation and to vent air that ingresses into systems.

Valves come in a variety of types, shapes and sizes. The most common types of valves in use today are gate, plug, ball, butterfly, check, pressure-relief, and globe valves [1]. Generally, valves can be classified into three main function areas: on-off (isolation), non-return and throttling. On-off or isolation valves provide the function of blocking or isolating a fluid from flowing through it when in the fully closed position whilst allowing fluid to flow through it in the fully open position. Non-return valves allow a fluid to flow through in one direction only and throttling valves allow for the control and regulation of flow at any point between fully open to fully closed.

3.1.1 Valve components

Although valves come in a variety of types, shapes and sizes, they all have the same basic parts [2]. A schematic of a valve is shown in figure 7 below. The main parts include a body, bonnet, disc, seat, packing, stem and actuator. The valve body is the outer casing of the valve and houses all valve internals. The bonnet acts as a cover for the valve body and is usually bolted or screwed into the valve body. The disc is a movable obstruction located in the valve body and provides the capability of permitting and prohibiting fluid flow. The seat is located in the interior surface of the valve and provides the seating surface for the disc. It remains stationary relative to the valve body and provides a leak-tight seal when in contact with the disc.

The stem connects the actuator and the disc and transmits motion from the actuator to the disc, thereby positioning the disc as required. The actuator operates the stem and disc assembly. Actuators can be manually operated by hand wheels and levers or automatically

operated by electric, pneumatic or hydraulic systems. Packing is installed in valves to prevent leakage of the working medium to the environment from the space between the stem and the bonnet.

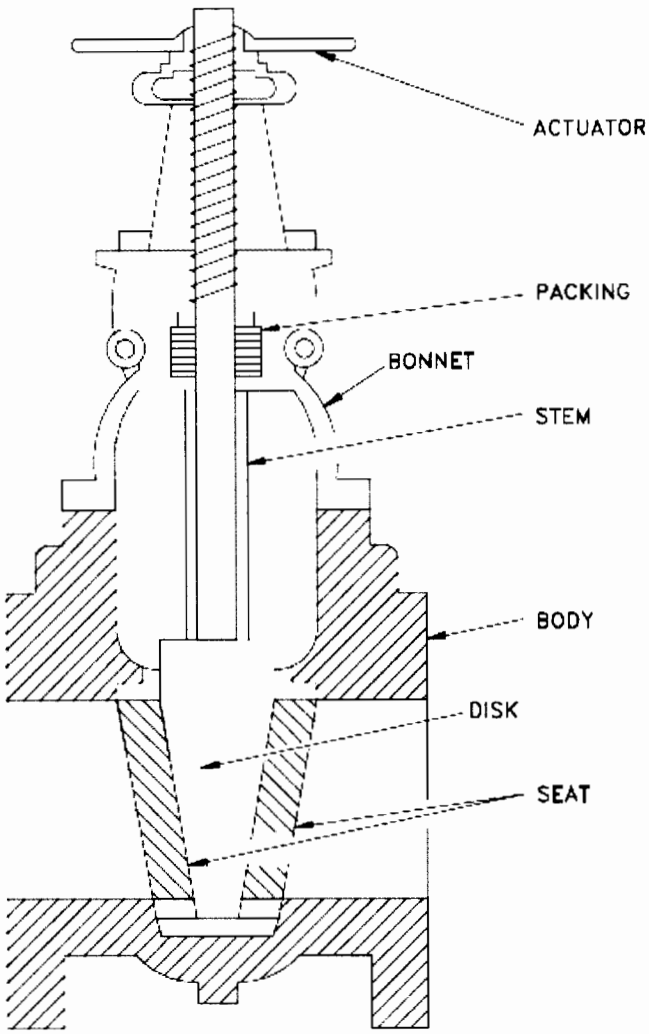

Figure 7: Basic parts of a valve [2]

3.1.2 Common drain valve types in power generating plants

A large number of valve designs, types and shapes have been developed to accommodate different fluids, system conditions and different operating environments. Below is a brief description of a gate valve and a globe valve, which are common valves, installed on power plant drain lines in Eskom power stations.

A gate valve is a valve that is primarily used to start and stop a fluid. In the fully open position the disc is completely removed from the flow path, allowing no resistance to the fluid flow thereby permitting the fluid to flow through the valve. In the fully closed position the disc

comes into contact with the seat, thus restricting the flow through the valve. With proper mating between the disk and the seat no leakage occurs through the valve. Figure 8 shows a schematic of a typical gate valve.

Gate valves are not used for regulating or controlling fluid flow since the flow rate is non-linear with respect to the percentage of disc opening [2]. They are generally installed on systems that require on-off operations where either full flow through the valve is required or complete restriction of flow is required as is the case for drain valves.

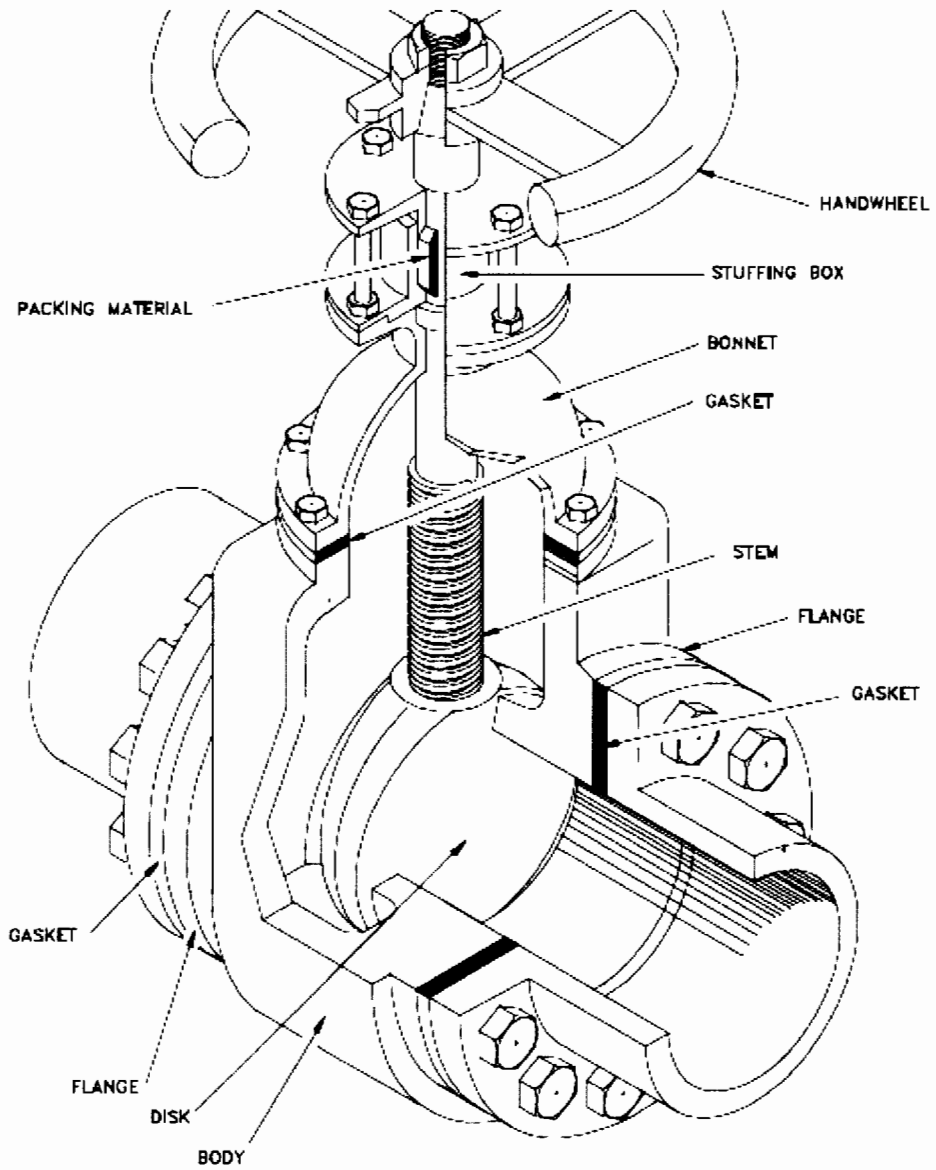

Figure 8: Schematic of a gate valve [2]

A globe valve is a valve that is used to regulate flow. Globe valves differ from gate valves in that the disc moves perpendicular to the seat. This is shown in figure 9 below. The perpendicular movement allows for the annular space between the disc and the seat to gradually close as the valve is closed. This gives the globe valve good throttling ability which allows for the regulation of flow [2].

Globe valves are generally used on high pressure drain line applications in Eskom power plants due to the disk-to-seat position. The disk makes contact with the seat at a right angle which permits the force of closing to tightly seat the disc. This provides less seat leakage when compared to gate valves. Eskom utilises both gate and globe valves on the drain system depending on the pressure of the fluid. High pressure drain systems usually contain globe valves, whilst lower pressure systems contain gate valves.

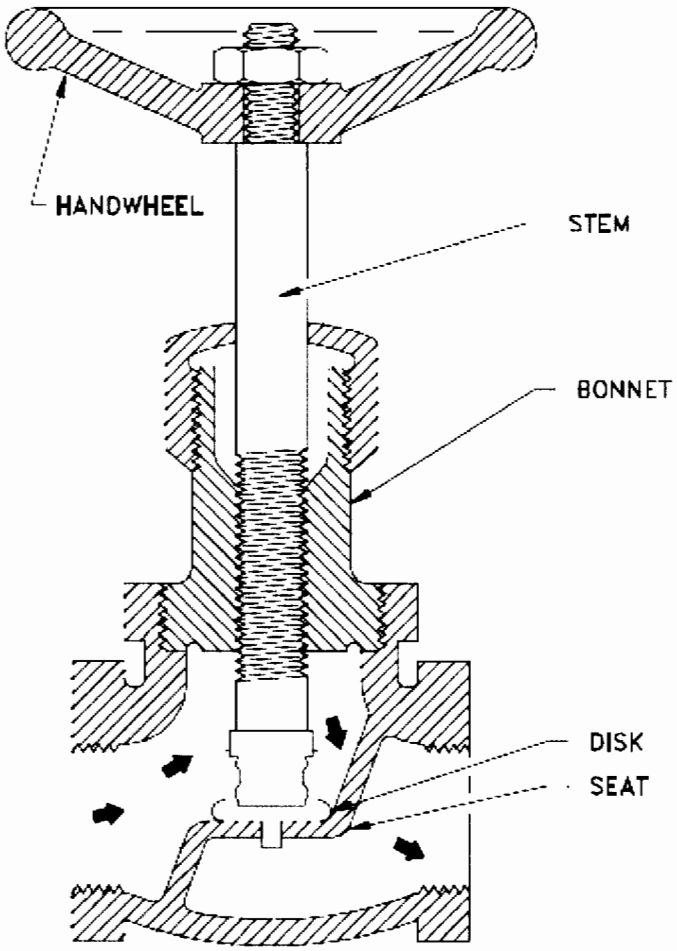

Figure 9: Schematic of a globe valve [2]

3.2 Monitoring techniques

A survey of the literature indicates that techniques previously developed to detect the onset of internal valve leakages used predominantly acoustic emission and infrared thermography principles and techniques.

3.2.1 Acoustic Emission

Acoustic emission (AE) is a form of energy emitted as transient elastic waves or sound waves emanating from within a material. For internally leaking valves, the AE signal is generated from turbulent flow resulting from the high pressure and high velocity flow through the 'leak' hole as shown in figure 10 below.

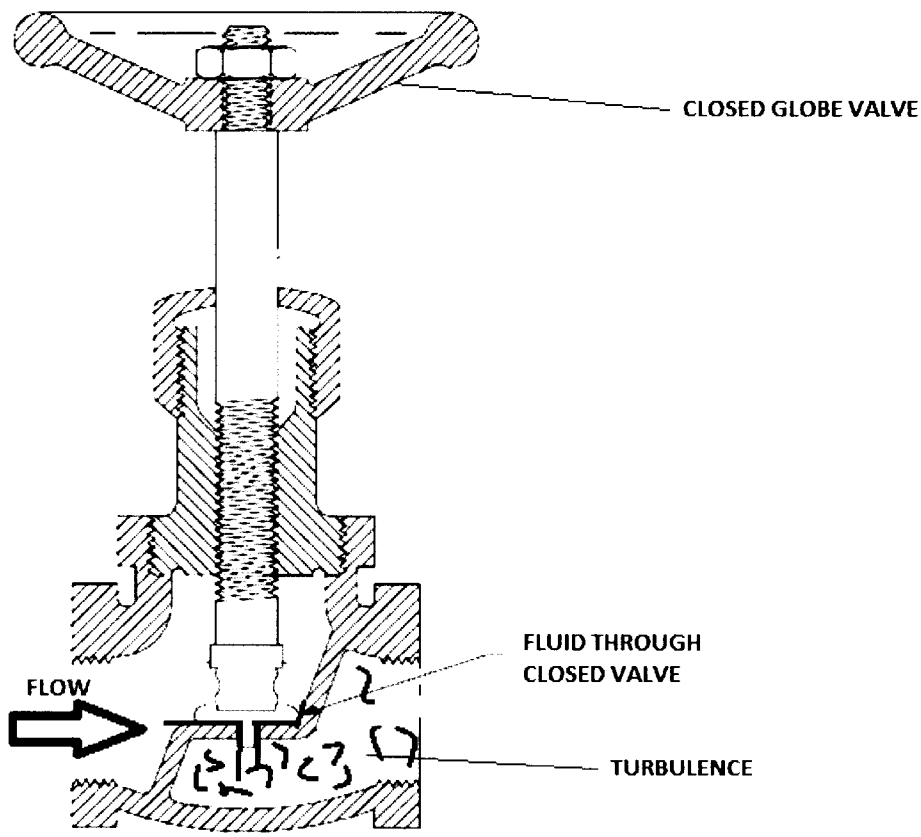

Figure 10: Illustration of an internally leaking valve

AE instrumentation are generally installed downstream of a valve. A typical system can contain an AE sensor, preamplifier, filters, and amplifiers, along with measurement, display and storage equipment. The AE sensors are piezoelectric devices that respond to dynamic motion caused by an AE event. The sensors convert elastic waves to electric signals which travel through amplification and filtration devices to the AE mainframe for analysis and storage. This is shown in figure 11 below.

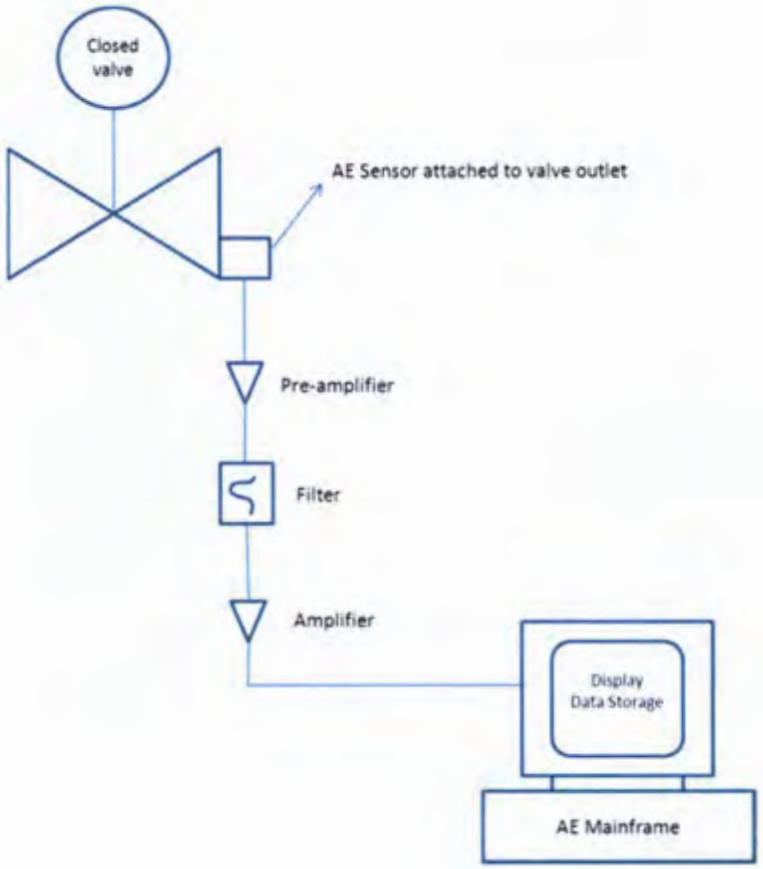

Figure 11: Schematic diagram of valve leakage monitoring using an AE system

AE signals are either continuous (random noise with amplitudes varying according to the AE events) or burst type. In the case of an internally leaking valve the AE signal is a continuous signal since the beginning and the end of the signal (in time domain) cannot be identified [3]. For continuous signals, the most frequently used AE parameters are the average energy (AErms) and the average signal level (ASL). AErms is the root mean square value of the AE signal. Since acoustic emission activity is attributed to the rapid release of energy in a material, the energy content of the acoustic emission is related to this energy release and it is suitable to use as a means of detecting internal leakages through valves [4].

Acoustic emission technology has many applications and is extensively used in industry. Some of its uses are; assessing structural integrity of components, detecting flaws in materials, monitoring weld quality, detecting leaks in pressure vessels and detecting internal leaks

through valves. Drouillard [5] gives a comprehensive review of acoustic emission, the history of its development and a brief description of applications of AE in leak detection. Delarue [6] and Rajtar et al [7] successfully used AE to detect leakages in process pipelines. They also concluded that the initial symptoms of abnormalities such as microstructure cracks in the structure of pipelines can be detected using AE. Williams [8] provided detailed descriptions of the applications of AE in chemical plants, nuclear reactors, and in iron and steel making plants.

Sharif and Grosvenor [9] researched the development of non-destructive methods that could be used in an industrial environment to detect the onset of internal valve leakages reliably for both liquids and gases. They conducted tests to determine the lowest detectable compressed air leakage rate through a 1 inch valve that can be reliably detected using the AE technique. The research concluded that very low leakage rates can be reliably detected using AE at differential pressures of 1 bar. It was further concluded that a unique leak-related trend exists in the frequency spectrum which could be distinguished from that produced due to background noise. This makes AE testing a suitable technique for use in an industrial environment.

Detecting internal leakages of valves using AE is a proven technology and is utilised extensively in industry, but quantifying these losses is still a challenge. Recently many researches have tried to determine a method to quantify the losses of internal valve leakages using the AE signals [3]-[11], [10].

Meland et al. [11] mentions that generally there are two ways to estimate internal leakages through valves. The first uses analytical methods based on known physical relationships from which empirical expressions are deduced. The use of empirical expressions here is due to the problem being too complex to model by pure analytical expressions [11]. The second way is by direct comparison with other valves that are known to have leaks. The data from these reference 'leaking' valves are collected in a test rig and a match between signals on site and a reference signal will indicate the leakage rate. This is often referred to as a fingerprinting approach.

Kaewwaewnoi et al [3] & [4] used the first method described above to estimate leakage rates from internally leaking valves. Kaewwaewnoi et al [3] researched the relationship between the AE signals generated from three different sizes of internally leaking ball valves (1, 2, 3 inch) at different inlet pressure (1-5 bars) conditions using air as the medium. The research concluded that the average energy (AErms) and the average signal level (ASL) of the AE signal increased with an increase in leakage rate and in upstream pressure. They attributed this increase in AErms and ASL to an increase in turbulence with an increase in leakage rate. Although it was noted, that at higher leakage rates the signal decreased due to the degree of turbulence decreasing as the leakage "hole" increased. Kaewwaewnoi et al [3] concludes that the parameters that affect AE signals are valve inlet pressure, valve size and leakage rate.

Following the findings of Kaewwaewnoi et al [3], Kaewwaewnoi et al [4] used a theoretical model to predict internal leakage rates through valves. This is shown in equation 1 below which

when rearranged can be used to calculate the volumetric flow rate through an internally leaking valve. The model was reported to be successful based on experiments from liquid flow in ball and globe valves. Meland et al. [12] mentioned that the model derived by Kaewwaewnoi et al [4] would be only valid for liquids.

$$AErms = C_1 \frac{1}{\alpha^5 \rho^3 D^{14}} \left(\frac{Q}{C_v}\right)^8 \left(\frac{P_1 S}{\Delta P}\right)^4 \quad \textbf{Equation 1}$$

Where:

C1 is a constant covering fluid variables

α is the sound velocity in the fluid

ρ is the fluid density

D is the valve size

Q is the volume flow rate

ΔP is the pressure drop across the valve

P_1 is the inlet pressure

C_v is the valve flow coefficient

S is the specific gravity of the liquid

Prateepasen et al. [10] extended Kaewwaewnoi et al [4] findings for gas in their work and created a new model for gas shown in equation 2 below. They conducted experiments with two different sizes of ball valves (1 inch and 2 inch) as well as at different pressures (1-5 bars). Their research concluded that AErms greatly depended on the valve design, valve shape and valve size.

$$Q = 0.31\, e^{2x10^{-5}} \left(\left[\frac{AErms^2 \alpha^5 D^{14} RT}{P_1} \right]^{\frac{1}{8}} \right) \quad \textbf{Equation 2}$$

Meland et al. [12] analysed all previous work carried out on AE for detecting and quantifying internal leakages of valves. The research concentrated on determining factors that affect the power level in the frequency spectra of AE signals. They established that the fluid density, sound velocity in the fluid, pressure, temperature, leak rate, viscosity, size and geometry of the

leak and properties of the valve and piping all affect the power level of the AE signal. The research concluded that AE is deemed to be effective for the detection of leaks but the quantification of leaks is a rather complex matter and warrants further investigation.

From the above analysis of the literature it can be seen that there are generally two methods of quantifying internal leakages through valves. In the first method researchers have created empirical models that use the generated AE signals to quantify internal leakages through valves. These models are sensitive to valve design, valve type, valve size and upstream pressure. The second method to quantify internal leakages from valves is by comparing the AE signal generated with a similar valves AE signal trend signature, i.e. a fingerprinting exercise. Both methods require an experimental facility to be set-up so that empirical relationships or AE signal signatures can be generated for different valves. It will be extremely difficult to set-up such an experiment due to the high pressures and temperatures needed for such an experiment to acquire accurate AE signals to generate the empirical relationships or the AE signal signatures for each valve. Coupled with the above, there is a variation in valve sizes, valve types, valve designs and upstream pressures experienced by different drain valves. Setting up an experiment that caters for all the variables will be a difficult task to accomplish.

3.2.2 Infrared Thermography

Infrared thermography (IRT) is a non-contact, non-intrusive, non-destructive testing (NDT) technique, which enables one to view energy radiated by an object. Objects at a temperature above absolute zero emit electromagnetic radiation in the form of waves which fall into the infrared (IR) portion of the electromagnetic spectrum. The energy emitted by the object is mainly a function of its temperature and so IRT may be considered as a technique to measure an object's temperature [14].

Infrared thermography comprises of a camera that is equipped with a series of changeable optics, and a computer. An object's surface temperature can be obtained by focussing the IRT camera on the object. The core of the camera is the infrared detector. This absorbs the IR energy emitted by the object and converts it into an electrical voltage or current which is analysed by the computer and processed to produce thermal images and perform temperature calculations.

The radiation emitted from a blackbody, the maximum value radiated by a body for a given temperature, was derived by Planck and is given in equation 3 below.

$$E_{yb} = \frac{C_1}{\lambda^5\left(e^{\frac{C_2}{\lambda T}}-1\right)}$$ **Equation 3**

Where:

E_{yb} is the blackbody radiation intensity

C_1 and C_2 are first and second radiation constants respectively

λ is the wavelength of the radiation being considered

T is the absolute temperature of the blackbody

Wien's displacement law is obtained by integrating Planck's law with respect to the wavelength and is shown in equation 4 below.

$$\lambda_{max} = \frac{2898}{T} \qquad \textbf{Equation 4}$$

This law states that there is an inverse relationship between the wavelength of maximum emission of any body and its temperature when expressed as a function of wavelength. Wien's law mathematically expresses the common observation that colours vary from red to orange to yellow, as the temperature of the thermal radiator increases [14].

The total hemispherical radiation intensity can be obtained by integrating Planck's law over the entire spectrum. This is shown in equation 5 below.

$$E_b = \sigma T^4 \qquad \textbf{Equation 5}$$

Where:

σ is the Stephan-Boltzmann constant.

With the above equation, if the total radiation emitted by a blackbody in all directions is known, one can calculate the temperature of the blackbody. Generally, a real body does not comply with Planck's law and only emits a portion of the radiation emitted by a blackbody at the same temperature and at the same wavelength. Since IRT is based on Planck's law in calculating temperatures of objects, considerations need to be made to account for the variation experienced with real bodies.

The total radiation energy leaving from an objects surface is called radiosity, which is equal to the sum of reflected, emitted and transmitted energy. This is quantified by Kirchhoff's radiation law and is shown in equation 6 below.

$$\varepsilon + \rho + \tau = 1 \qquad \textbf{Equation 6}$$

Where:

ε is the emissivity

ρ is the reflectivity

τ is the transmittivity

The emissivity of a material is the relative ability of its surface to emit energy by radiation and is the ratio of the total thermal radiation emitted from an object to the total thermal radiation emitted from a blackbody at the same temperature. This is shown in equation 7 below. The emissivity is a dimensionless quantity and ranges between 0 and 1. A blackbody has an emissivity of 1.

$$\varepsilon = \frac{E_y}{E_{yb}} \qquad \textbf{Equation 7}$$

Where:

E_y is the thermal radiation emitted by an object

The reflectivity is the fraction of incident energy that is reflected at an object. Reflectivity is a property of the material. For opaque objects, the transmittivity is zero and equation 4 reduces to:

$$\varepsilon + \rho = 1 \qquad \textbf{Equation 8}$$

The above equation indicates that a high emissivity equates to a low reflectivity and a low emissivity equates to a high reflectivity. Modern day IRT cameras allow for users to insert values for the emissivity and the background (reflected) temperature. They measure the total radiosity from the object, subtract the reflective component, and scale the results by the objects emissivity to determine an accurate temperature measurement of the object [15].

IRT has a variety of applications and is extensively used in industries including agriculture, architecture, power industry, manufacturing industry, and the medical industry. Some of the applications were IRT can be used is in electrical systems to detect localised high temperatures which indicate faulty connectors or overloaded circuits, mechanical equipment to detect abnormally high motor temperatures or bearing failures, in building applications to detect missing insulation or air infiltration and in fluid systems to detect line blockages and recently it is increasingly used for fluid leak detection [16], [17].

The underlying principle in fluid leak detection is that the hot fluid that is leaking internally through the valve will increase the temperature of the downstream piping network. As the fluid flows through the downstream pipework, heat energy contained in the fluid will be transferred from the high temperature fluid through the pipe walls to the pipe surroundings. This will result in an increase in the outer surface temperature of the pipe. The thermal radiation from the pipe surface can then be measured by an IRT camera which will indicate the temperature of the pipe. A relatively high pipe surface temperature will indicate a leak, whilst a temperature close to room temperature will indicate no internal leakages through the valve. This is illustrated in figure 12 below.

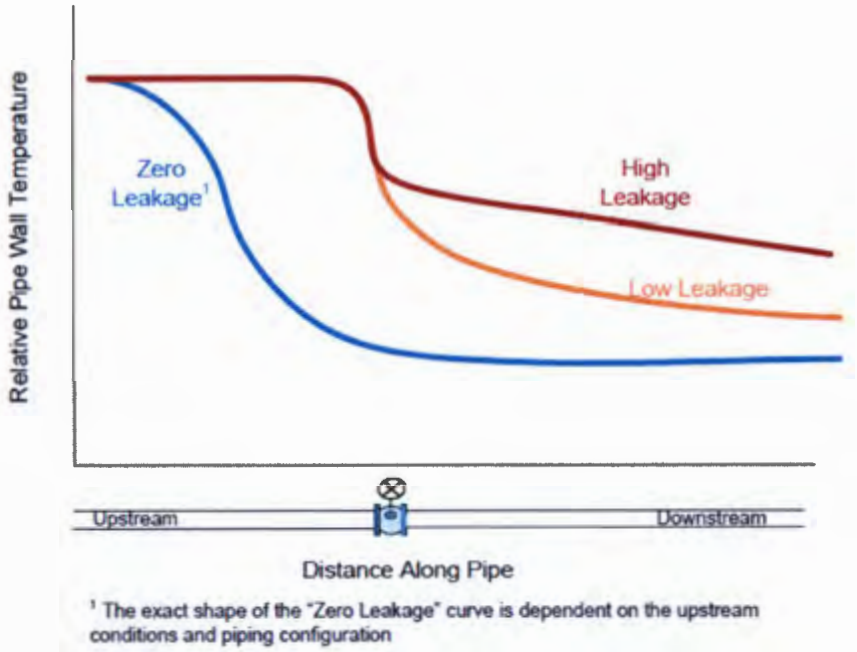

Figure 12: Pipe wall temperature along distance of pipe [16]

The number of scientific papers that deal with IRT detection and quantification of internally leaking high pressure and temperature steam valves is minimal. Korellis [16] conducted a study to evaluate IRT as a possible means to quantify internally leaking valves. The authors derived mathematical models that use pipe surface temperatures to calculate the flow rate of the leakage flow. Figure 13 illustrates a schematic of their proposed technique.

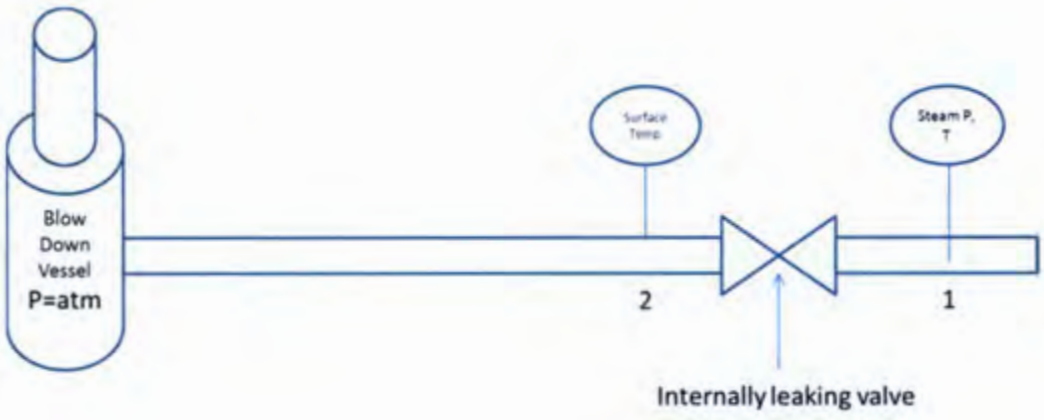

Figure 13: Korellis [16] technique to calculate internal leakages from steam valves

Infrared thermography is applied to point 2, located downstream of a valve to measure the pipe surface temperature at this point. The pipe surface temperature is then assumed to be the fluid leakage temperature. With a known upstream fluid temperature and pressure, a

downstream pressure at point 2 is calculated by assuming an isentropic efficiency of 70 % for the expansion of the leakage flow through the valve. This assumption, made by Korellis [16], is based on comparing the expansion of steam across a valve to the expansion of steam across a diaphragm in a steam turbine. Korellis [16] states, "If a typical turbine, designed for an aerodynamic pressure drop/velocity increase, has an efficiency of 95%, estimating an efficiency of 70% for an unintentional process that would be less reversible represents an acceptable approximation."

Once the pressure at point 2 is calculated Korellis [16] then proposed equations to calculate the velocity of the leakage flow between point 2 and the blow down vessel, which is maintained at atmospheric pressure. An example of a proposed equation is shown in equation 9 below.

$$\Delta H = K\left(\frac{v^2}{2g}\right) \qquad \textbf{Equation 9}$$

Where:

ΔH is the head loss in the pipe (i.e. pressure change)

K is the resistance coefficient

v is the downstream velocity of the medium

Equation 9 is the Darcy head loss equation and is generally used to calculate the head loss between two points in a pipeline. To account for steam being a compressible gas, an expansion factor is added to the above equation. Once the velocity is calculated, Korellis [9] uses equation 10 below to calculate the flow rate of the leakage.

$$\dot{m} = \rho A v \qquad \textbf{Equation 10}$$

Where:

ṁ is the mass flow rate

A is the pipe cross sectional area

In the method derived by Korellis [16], the upstream temperature and pressure before the valve is used to calculate the immediate downstream pressure of the valve. In the power plant, there are no instruments installed immediately upstream of the valve to acquire the pressure and temperature of the fluid. One can assume these properties to be the live steam properties, but as mentioned in chapter 2.3, the valves installed on the drain lines are installed at various different lengths away from the main steam pipe work and there will be a slight drop in temperature and pressure immediately upstream of the drain valve due to heat loss through the piping and head loss along the piping. It should also be noted that Korellis [16] does not provide any experimental validation for the technique proposed.

Sherikar [17] proposed a technique that uses IRT to quantify internal leakages from steam valves by measuring surface temperatures from a length of un-insulated pipe downstream of the relevant internally leaking valve. The underlying principle upon which the leakage flow may be determined is that the heat loss across a length of bare pipe causes a drop in temperature of the leakage flow, which corresponds to a loss of enthalpy of the steam flow across the length of pipe. Figure 14 below illustrates this technique. As a fluid flows through the section of un-insulated pipe, heat energy is transferred from the fluid via the pipe wall to the surrounding atmosphere. By measuring the surface temperatures at point $T_{1,pipe\ surface}$ and point $T_{2,pipe\ surface}$, the heat loss from the length of un-insulated pipe can be calculated. Since energy is conserved the heat loss from the fluid flow through the length of un-insulated pipe is equal to the heat loss from the pipe surface for the same length of pipe.

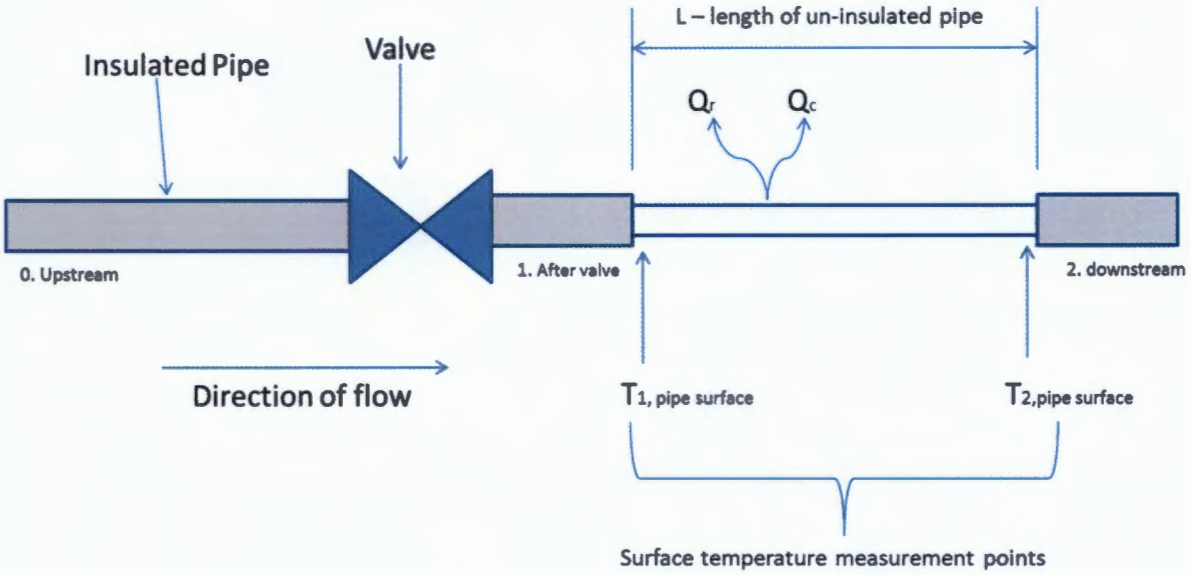

Figure 14: Sherikar [17] technique to quantify internal leakages from steam valves

By assuming the expansion of steam through the valve an isenthalpic process, Sherikar [17] concludes that the loss of enthalpy of the fluid downstream of the valve is equivalent to the heat loss of the downstream un-insulated length of pipe. This relationship is often expressed as in equation 11 below:

$$Q_{flow} = \dot{m}(h_1 - h_{2-L}) \qquad \textbf{Equation 11}$$

Where:

Q_{flow} is the heat loss from the fluid,

$h_1 - h_{2\text{-}L}$ is the loss of enthalpy of the fluid across the un-insulated pipe.

To calculate the enthalpy of the steam at upstream and downstream points of the un-insulated length of pipe is extremely difficult as no instrumentation to measure steam intrinsic properties are available on a power plant environment. Sherikar assumes that since the steam expands to atmosphere immediately after an internally leaking valve one can make an ideal gas approximation for the loss of enthalpy,$(h_1 - h_{2-L})$, due to most gases behaving similar to an ideal gas at high temperatures and low pressures. This ideal gas approximation is shown in equation 12 below.

$$\Delta \boldsymbol{h} = \boldsymbol{C_p}\,(\Delta \boldsymbol{T}) \qquad \textbf{Equation 12}$$

Where:

Cp is an average specific heat of a fluid at constant pressure

ΔT is the change in temperature of the fluid measured at two locations in the system.

By substituting equation 12 into equation 11, the heat loss equation can be written as:

$$\boldsymbol{Q_{flow}} = \boldsymbol{\dot{m} C_p (T_{1,steam} - T_{2,steam})} \qquad \textbf{Equation 13}$$

Q_{flow} is the heat loss from the steam flow through the pipe. Since energy is conserved the heat loss from the steam is equal to the heat loss from the outer pipe surface, a combination of convection and radiation heat transfer, and can be expressed as equation 14 below:

$$\boldsymbol{Q_{flow}} = \boldsymbol{Q_c + Q_r} \qquad \textbf{Equation 14}$$

Therefore by combining equations 13 and 14, the leakage flow rate can be determined from the following expression:

$$\boldsymbol{\dot{m} C_p (T_{1,steam} - T_{2,steam}) = Q_c + Q_r} \qquad \textbf{Equation 15}$$

$T_{1,steam} - T_{2,steam}$, is the change in temperature of the steam flow through the un-insulated length of pipe. Since there is no instruments installed on the system to measure this steam temperature, Sherikar [17] assumes that the change in pipe surface temperature $T_{1,pipe\ surface} - T_{2,pipe\ surface}$ is equal to the change in steam temperature $T_{1,steam} - T_{2,steam}$. Rearranging the above equation and substituting the change in steam temperature with the change in pipe surface temperature, Sherikar [17] calculates the mass flow rate from an internally leaking valve from equation 16 below.

$$\dot{m} = \frac{Q_c + Q_r}{C_P \left(T_{1,pipe\ surface} - T_{2,pipe\ surface} \right)}$$ **Equation 16**

Where:

Q_c is the convection heat loss from the surface of the un-insulated pipe

Q_r is the radiation heat loss from the surface of the un-insulated pipe

It should be noted that Sherikar [17] is a patent document and no experimental validation was provided for the proposed technique. An extensive literature review on Sherikar [17] revealed no other information on the proposed technique

Sherikar's [17] proposed technique fulfils most of the requirements listed in section 2.4. It is a non-intrusive technique which can be conducted whilst the generating unit is in operation. The drawback of this proposed technique is that a length of insulation material downstream of the valve needs to be removed to conduct the tests. Although it should be noted that the removal of the insulation material will not affect the efficiency of the plant as the drain lines dump its contents into the boiler blow down vessel and any fluid recovered will be recovered at atmospheric conditions. Removal of the insulation might however be a safety risk if people work or walk in the vicinity of the area where the insulation material is removed. This however can be mitigated by demarcating the area and restricting people from walking close to the exposed pipework.

The assumption made by the author equating the change in steam temperature to the change in pipe surface temperature of the un-insulated pipe needs to be verified as the author merely states the assumption and does not provide any verification.

The assumption made that the expansion of steam through an internally leaking valve is an isenthalpic process needs to be validated as this assumption is only valid for normal flow through valves. Due to the high pressures differential across internally leaking valves one can expect high velocities downstream of the valve which will result in an increase in kinetic energy and the process will not be isenthalpic as assumed by the author.

This technique will also be needed to be experimentally validated before implementation on the power plant.

3.2.3 Other Techniques

3.2.3.1 Pressure Change Monitoring

Pressure change monitoring is a technique whereby the system pressures on either side of a component is monitored or the difference in pressure between 2 points in a system is measured. This is more commonly termed differential pressure monitoring. Differential pressure monitoring is accomplished by the use of differential pressure gauges, which are visual indicators designed to measure and display the difference in pressure between two pressure points in a system. The differential gauges typically have two inlet ports, each connected to the pressure points that are being monitored. The gauges perform the mathematical operation of subtraction through mechanical means. This eliminates the need for an operator or control system to watch two separate pressure gauges and calculate the difference in readings [18].

Differential pressure monitoring is extensively used in industry. Applications include, filter blockage monitoring, liquid level monitoring, flow rate monitoring and backflow prevention, through components. For filter blockage monitoring, a differential pressure gauge is installed on either side of a filter by means of impulse lines, as is shown in figure 15 below. By monitoring the differential pressure, one can determine the condition of the filter. A high differential pressure will indicate the presence of a blockage whilst a lower differential pressure will indicate a clean filter.

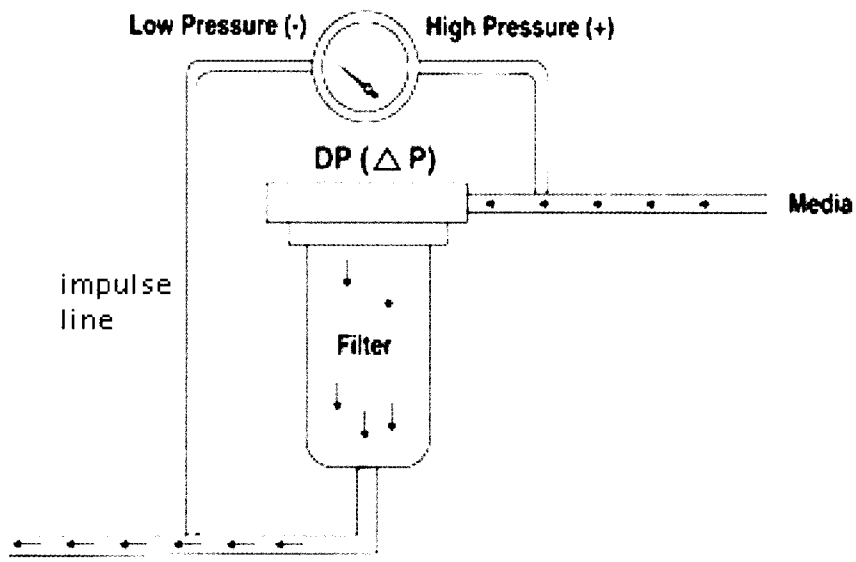

Figure 15: Filter blockage monitoring by differential pressure technique [18]

Measuring flow rates by means of differential pressure monitoring is a common practice. Here, differential pressure gauges/transmitters are installed on either side of a restriction device, such as an orifice plate. By measuring the differential pressure across the orifice and knowing the orifice diameter and the upstream fluid conditions, a flow rate can be calculated.

The number of scientific papers that deal with pressure change monitoring for the detection and quantification of internally leaking valves is extremely minimal. Thompson et al. [19] mentions that a valve that is leaking internally can be detected by monitoring the system pressures on either side of the valve. This will entail inserting impulse lines to upstream and downstream pipework before and after a valve and installing a differential pressure gauge to the impulse lines as is shown in figure 16 below.

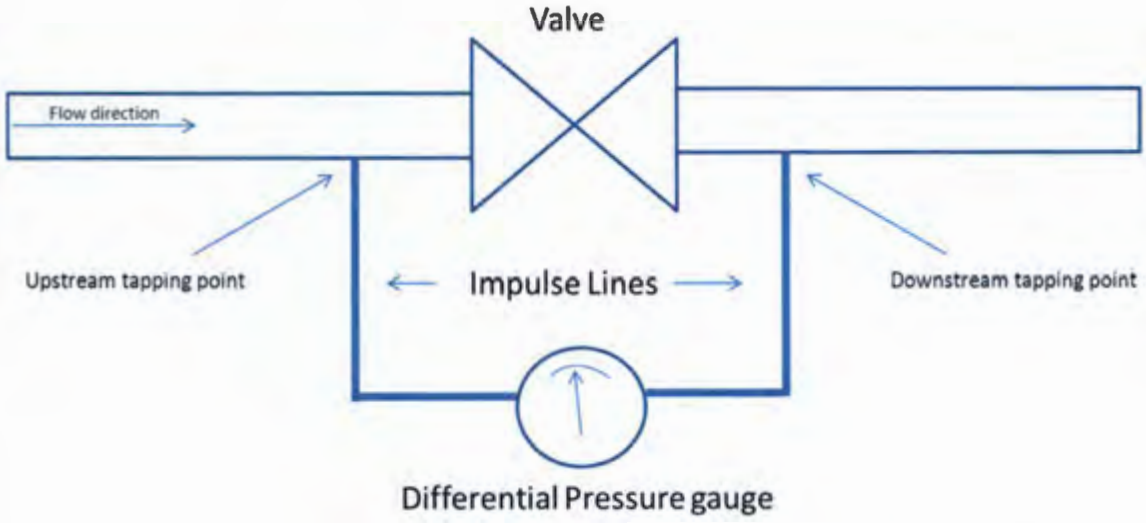

Figure 16: Schematic of differential pressure monitoring for internal leakages through valves

A properly closed valve will not allow fluid to flow through resulting in a high upstream pressure and a low downstream pressure. As fluids flows through a supposedly closed valve, the upstream pressure before the valve will decrease whilst the downstream pressure after the valve will increase resulting in a change of differential pressure across the valve, and an indication of valve leakage [19].

Thompson et al. [19] did not conduct any experimentation using this technique. An extensive survey of the literature found no other information on this technique to detect and quantify internal leakages of steam valves.

This method is an intrusive monitoring technique that requires impulse lines to be permanently installed to the upstream and downstream piping network of the drain valve. This will not be a feasible approach as there are many drain lines installed on a power plant. Coupled to this, due

to the high pressure differentials across the valve, the differential pressure transmitter/gauge might not have sufficient resolution to measure small pressure differences on the low pressure side of the valve.

3.2.3.2 Vibration Analysis

Vibration can be considered to be an oscillation or repetitive motion of an object around an equilibrium position [20]. Vibration analysis is a technique whereby vibrations are measured from a component using vibration sensors. The information from these sensors is generally used for condition monitoring purposes. A common application which uses vibration analysis is condition monitoring of roller bearings.

For internally leaking valves, vibration is generated in the valve body from the turbulent flow resulting from the leakage. Vibration analysis to detect internal leakages of valves is similar to the acoustic emission technology in that a vibration sensor is installed on the downstream face of the valve body. This is illustrated in figure 17 below. The sensors convert the mechanical vibration into an electric signal and transmit it to a data collector. Within the data collector the electric signal is transformed into digital signals which are then manipulated in a variety of ways depending on what aspects of the data is required. The vibration information is then transformed to a frequency spectrum and converted into an RMS reading [21].

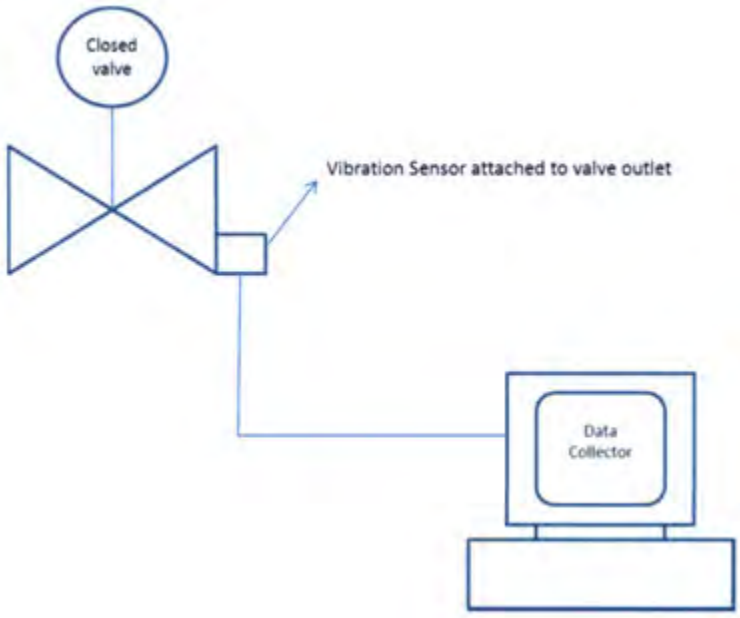

Figure 17: Vibration analysis system configuration to detect internal leakages through valves

Thompson and Wijesundra [22] conducted experiments to determine whether significant leak-dependant frequency peaks existed in the frequency spectrum below 25 kHz for valves that are internally leaking fluid. They experimented with air and water and different sizes and types of

valves. Their results show that the air leakage through the valves excites the valve to vibrate at certain frequencies whilst water leakages show a general increase in signal level in wide frequency bands for all valves.

Thompson and Zolkieswki [19] did extensive research on the frequencies exited by gases that leak internally through valves. They concluded that the vibration analysis technique could be used satisfactorily to detect internal leakage of gasses through valves under laboratory conditions, where the background noise is controllable. It was mentioned that under industrial environments, were the levels of background noise is high, this technique cannot be used.

The sound power level from power plant equipment can range from about 120 dB to well over 155 dB depending on the size and type of the machines. This makes the vibration analysis technique not a suitable technique to detect and quantify internal leakages from boiler drain valves.

4. Internally Leaking Valves in a Power Station

4.1 Impact of internally leaking valves

Listed below are the main losses associated with internally leaking valves:

- Loss in power plant efficiency. The steam lost due to internally leaking valves has already had its energy level increased by the fuel combustion process and since this energy is not available for generating purposes more fuel needs to be burned in order to meet the generating requirements of the plant.
- Loss in revenue. If the power plant is required to operate at maximum capacity, the losses from internal valve leakages can impede the plant from attaining maximum capacity due to limitations in performance of components such as pumps, turbines etc. resulting in a loss of revenue.
- Loss of demineralised water. The water being used in the power plant is clarified, filtered and demineralised to remove impurities and to prevent corrosion and calcification of pipework. There is a cost associated with the production of demineralised water. Hence the loss of demineralised water which needs to be replaced has a direct financial impact. Coupled to this is the scarce availability of water resources in South Africa.
- High auxiliary power consumption. More water needs to be fed into the boiler as a result of water losses from internally leaking valves. This results in the Boiler Feed Pump's Variable Speed Drives drawing more auxiliary power to pump the excess feed water into the boiler.
- Valve damage. As a result of the high operating pressures and temperatures of the steam, the steam begins to erode the seat of the valve causing damage to the valve components. This result in higher maintenance costs associated with refurbishing or replacing valves that are left to leak internally.

- Cost of Repairs. If the leakage is not identified, the cost of repairs to the valve will increase as the deterioration of the valve increases.

- Damage to downstream piping. The high velocities of steam resulting from leaking valves causes erosion of the downstream pipework. Erosion of pipework can result in pipe rupture which will result in the plant being forced shut down. This will result in loss of revenue.

Shutting down a generating unit for an unplanned outage will result in a significant revenue loss for the company. In this study the revenue loss for shutting down the generating unit is not considered due to the following reasons:

- The objective of this study is to evaluate all losses associated with valves that are leaking internally. Shutting down of the generating unit is ultimately a management decision and management can use the information on internally leaking valves to make an executive decision bearing in mind the actual revenue loss.
- Eskom follows an outage philosophy for the generating units. The duration between different outages per unit is 18 months. As mentioned earlier, due to the shortage of generating capacity these planned outages are deferred, resulting in the unit staying on load for longer durations than planned. The quantification of losses by internally leaking valves will provide guidance to management as to the losses experienced and might provide reasons to management to shut down the unit to maintain identified valves and complete all maintenance activities, on all plant areas, schedule for that specific outage. The loss of revenue here will not apply as it would have already been factored into the planning of the outage.
- The loss of revenue varies. Shutting down the generating unit during off-peak times like weekends, long weekends, public holidays and school holidays will not affect loss of revenue severely as the demand during these times are low and generators are usually on low load conditions or on cold reserve.

4.2 Flow properties upstream and downstream of an internally leaking boiler drain valve

An understanding of the nature of steam flow upstream and downstream of an internally leaking drain valve is paramount in considering a suitable detection and quantification method. The upstream temperatures and pressures vary with different drain valves depending on the location of the drain valve in the cycle. There will also be a variation from similar drain valves in different power plants due to different plant designs.

Typically the boiler feed pump delivers the working fluid into the boiler via the HP heaters at pressures and temperatures in the region of 21 MPa and 240 ^{o}C respectively. As the fluid progresses through the boiler the temperature is raised whilst there is a decrease in pressure due to head losses. At the outlet of the boiler (inlet to the turbine) the fluid has a pressure and temperature of 16.4 MPa and 540 ^{o}C respectively (Majuba Power Station). At this point the fluid contains the most energy in the cycle and a leak at this point, through internally leaking valves, will result in the greatest loss in power plant efficiency as previously discussed.

For the configuration mentioned in section 2.3, the upstream steam condition, before the drain valve, is maintained at pressures above 16.4 MPa and the downstream pressure (boiler blow down vessel) is maintained at atmosphere. Hence the internal leakage of steam through the valve will expand to atmosphere. The steam upstream of the valve is in the superheated state, since the saturation temperature of steam at 16.4 MPa is 349 °C, which is far less than the steam temperature of 540°C.

Internal leakages of valves result from the valve not appropriately isolating the upstream flow. These valves are meant to be in the fully closed position but due to reasons mentioned in section 2.1, sometimes a leak path is generated between the mating surfaces which cause steam to 'pass' through the valve.

As steam flows through the leak path to the downstream pipework which is at a significantly lower pressure than the upstream pipework, the steam will expand. Equation 17 below shows the steady flow energy equation, in specific quantities, for a fluid flow in an open system.

$$\boldsymbol{h_1 + \frac{v_1^2}{2} + gz_1 + \Delta q = h_2 + \frac{v_2^2}{2} + gz_2 + \Delta w} \qquad \textbf{Equation 17}$$

Where:

Point 1 is upstream of the valve

Point 2 is downstream of the valve

$\frac{v^2}{2}$ is the kinetic energy component

gz_1 is the potential energy component

Δq is the change in heat input/output

Δw is the change in work

Since there is no work being done by an internally leaking valve, the change in work component from the above equation can be neglected. It can be assumed that the valve is adiabatic i.e. no heat energy is added or lost through the valve. This will enable us to neglect the change in heat component from equation 17. Since it is a gas the potential energy component can also be neglected. Thus equation 17 will reduce to equation 18 below, which means that the total energy of the system will be conserved

$$h_1 + \frac{v_1^2}{2} = h_2 + \frac{v_2^2}{2}$$ **Equation 18**

As the fluid flows through an internally leaking valve the cross sectional area of the flow path reduces significantly. To ensure continuity, the velocity of the fluid has to increase as the area reduces. Many researches have mentioned that although the outlet velocity through a valve is often relatively higher than the inlet velocity, the change in kinetic energy of the gas between upstream and downstream locations is small and can be neglected [27][28]. By neglecting the kinetic energy terms in equation 18 above, one can deduce that the upstream enthalpy is approximately equal to the downstream enthalpy. This relationship will only hold true if the velocity difference between upstream and downstream conditions are not significant.

However, in the case of an internally leaking valve, leaking fluid from a very high pressure to a very low pressure, one can expect that the velocity downstream of the leaking valve will be significant and that the kinetic energy terms of equation 18 is relevant and cannot be neglected. Computational fluid dynamic simulations provided in the following section will prove that the downstream velocity is indeed significantly higher for certain conditions.

Since the density of steam varies significantly, compressibility effects have to be taken into consideration. As the fluid flows through the restriction the velocity increases as mentioned above. Due to the high pressure difference across the valve there is a possibility of the fluid reaching sonic velocity. This occurs when the fluid velocity equals the speed of sound in that specific medium. At this point the mass flow rate will be choked and no further increase in flow rate is possible under those specific conditions. The flow rate will only change if the leak path is changed or if the upstream steam conditions are changed.

4.2.1 Temperature and pressure change downstream of an internally leaking valve

To gain a better understanding of the fluid properties downstream of an internally leaking valve a Flownex SE model was built and is shown in figure 18 below. Flownex is an integrated systems CFD code used for the design, simulation and optimization of complete thermal-fluid systems such as gas, steam or combined cycle power plants.

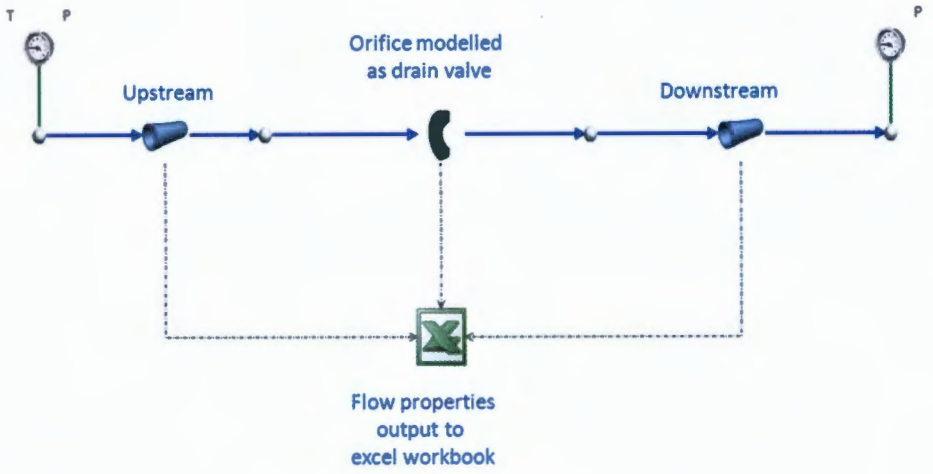

Figure 18: Flownex model of typical drain valve

An internally leaking valve potentially has a leak "hole" that is miniscule and thus it was decided to model the valve as an orifice plate, since the orifice diameter can be varied in small percentages of the total pipe internal diameter. It should be noted that majority of the flow elements in Flownex, including the orifice element, takes compressible flow effects into consideration when solving the relevant flow and energy equations.

The upstream conditions in the model were kept at a constant pressure and temperature of 16.4 MPa and 540 °C respectively, the downstream pressure at the discharge node was kept constant at atmospheric pressure, and the orifice diameter was varied between 1 to 30% of pipe internal diameter. Upstream and downstream pipe lengths were kept constant at 10 meters.

Flow properties along upstream and downstream pipework were output to an excel workbook. The data from the simulations are shown in appendix A. The figures below show how fluid properties such as pressure, temperature, enthalpy, velocity and the Mach number varies along the length of upstream and downstream pipework for orifice diameters between 1 and 20 % of pipe internal diameters. Figure 19 and 20 show the pressure profile along upstream and downstream piping whilst figure 21 and 22 show the temperature profile along upstream and

downstream piping. Figure 23 shows the enthalpy profile whilst figure 24 and figure 25 show the velocity profile and Mach number profile respectively.

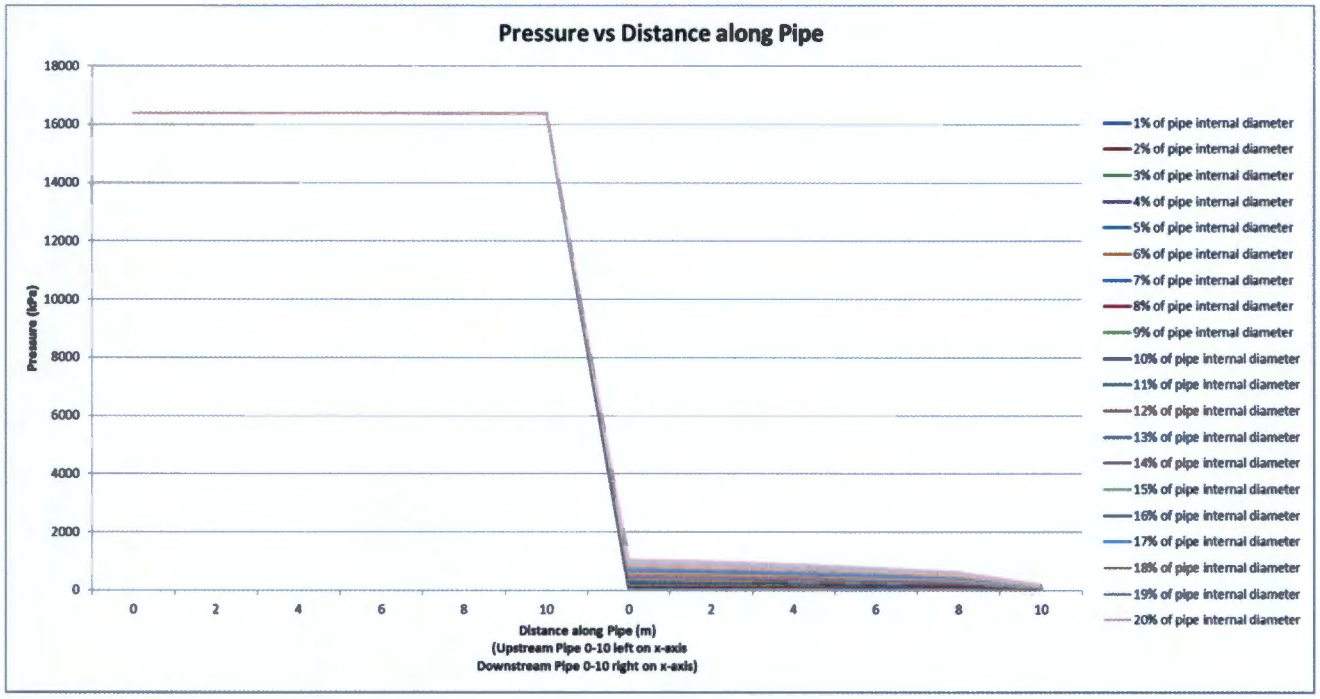

Figure 19: Pressure profile of the steam flow from upstream to downstream of an internally leaking drain valve

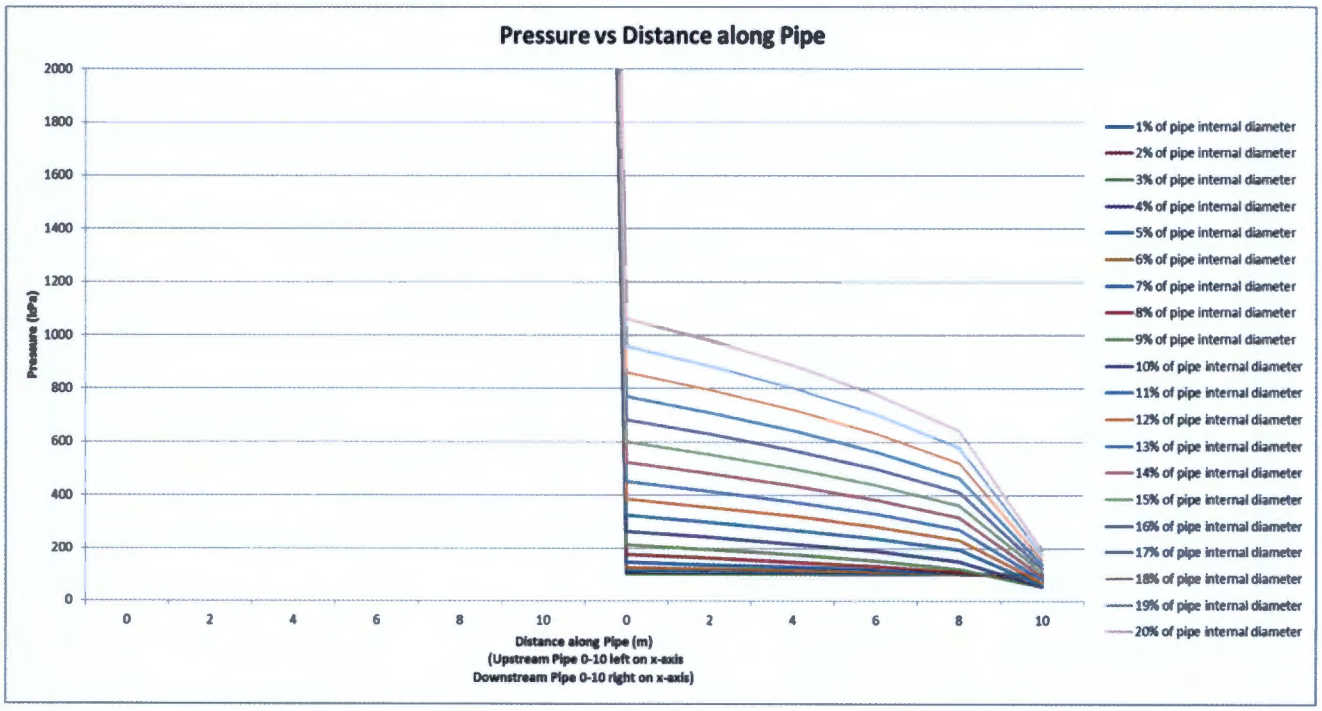

Figure 20: Downstream pressure profile from an internally leaking valve (Expanded in the downstream region to show pressures)

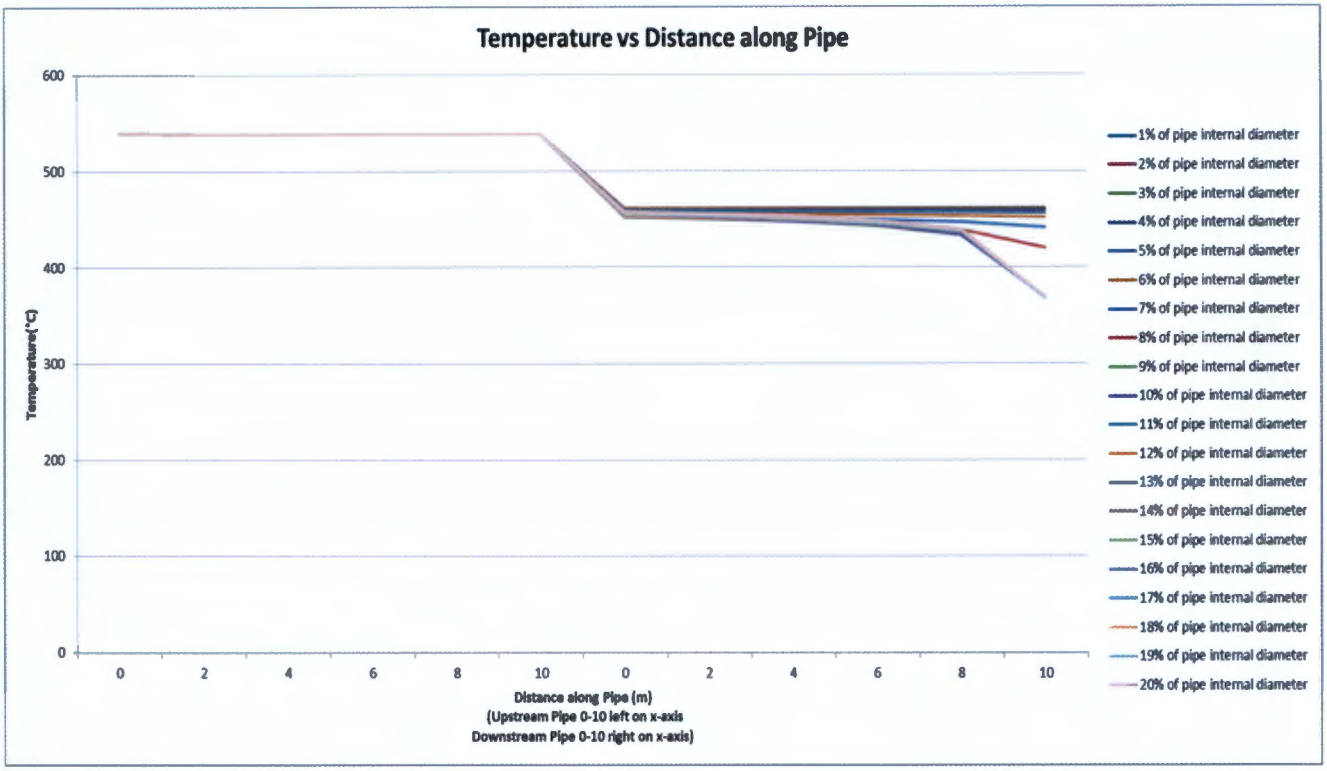

Figure 21: Temperature profile of the steam flow from upstream to downstream of an internally leaking drain valve

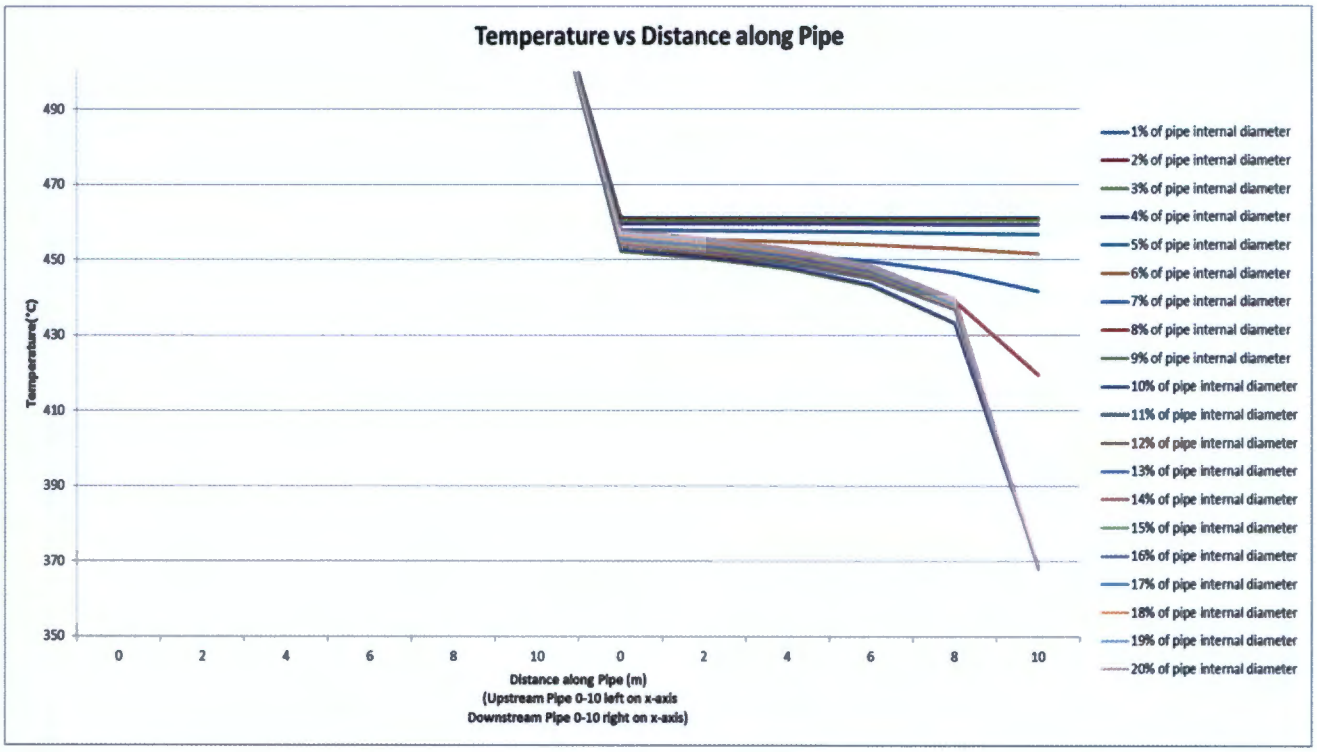

Figure 22: Downstream temperature profile of an internally leaking valve (Expanded in the downstream portion to show temperatures)

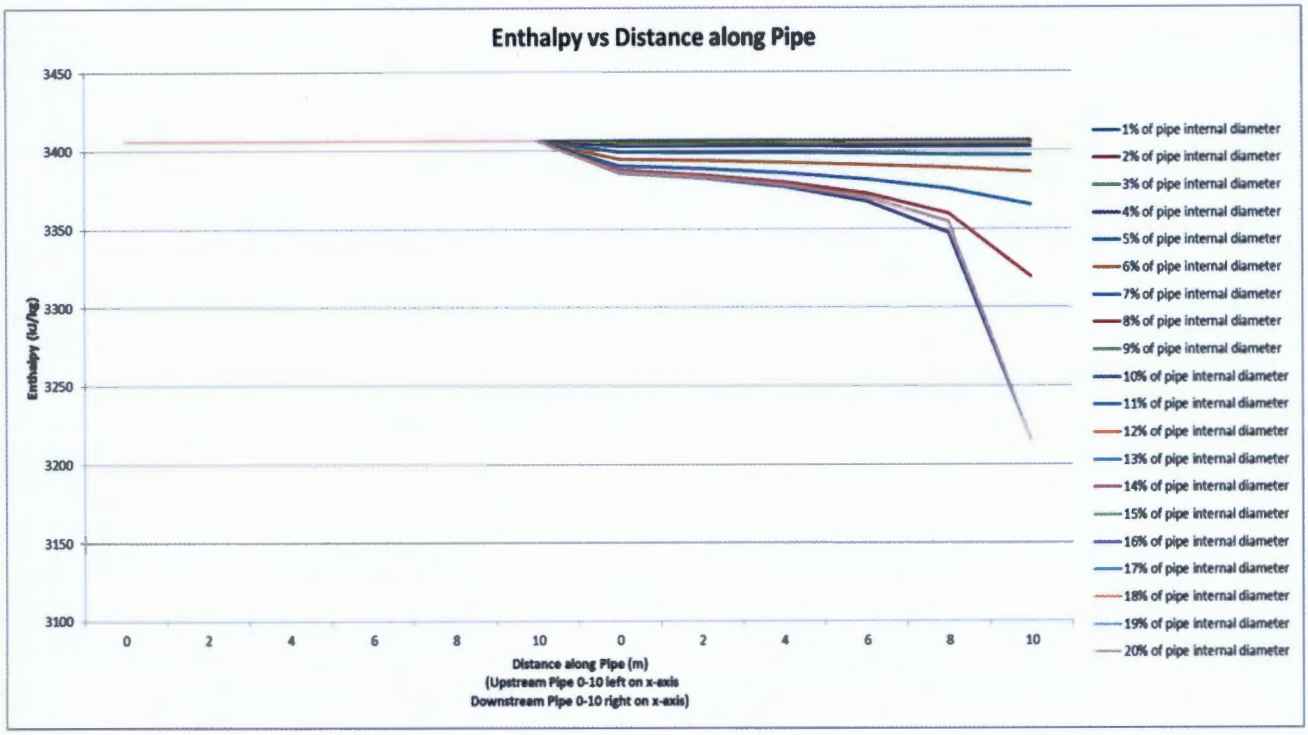

Figure 23: Enthalpy profile of the steam flow from upstream to downstream of an internally leaking drain valve

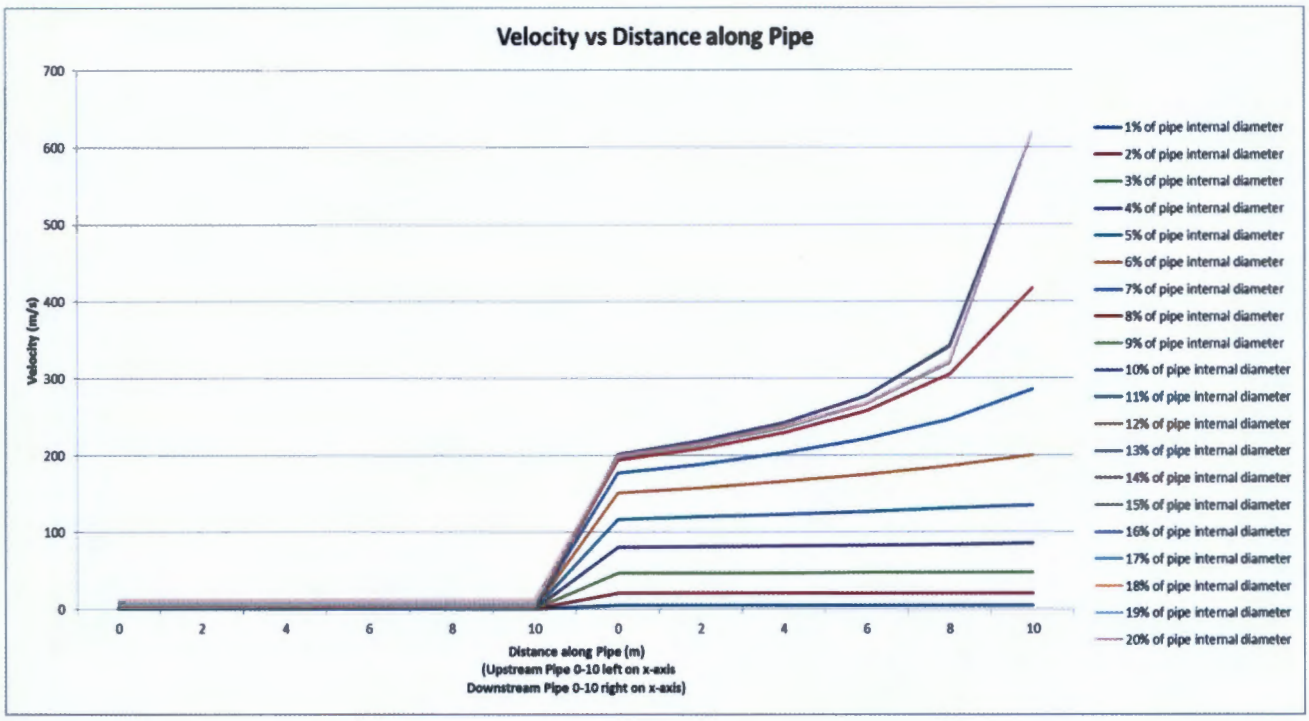

Figure 24: Velocity profile of the steam flow from upstream to downstream of an internally leaking drain valve

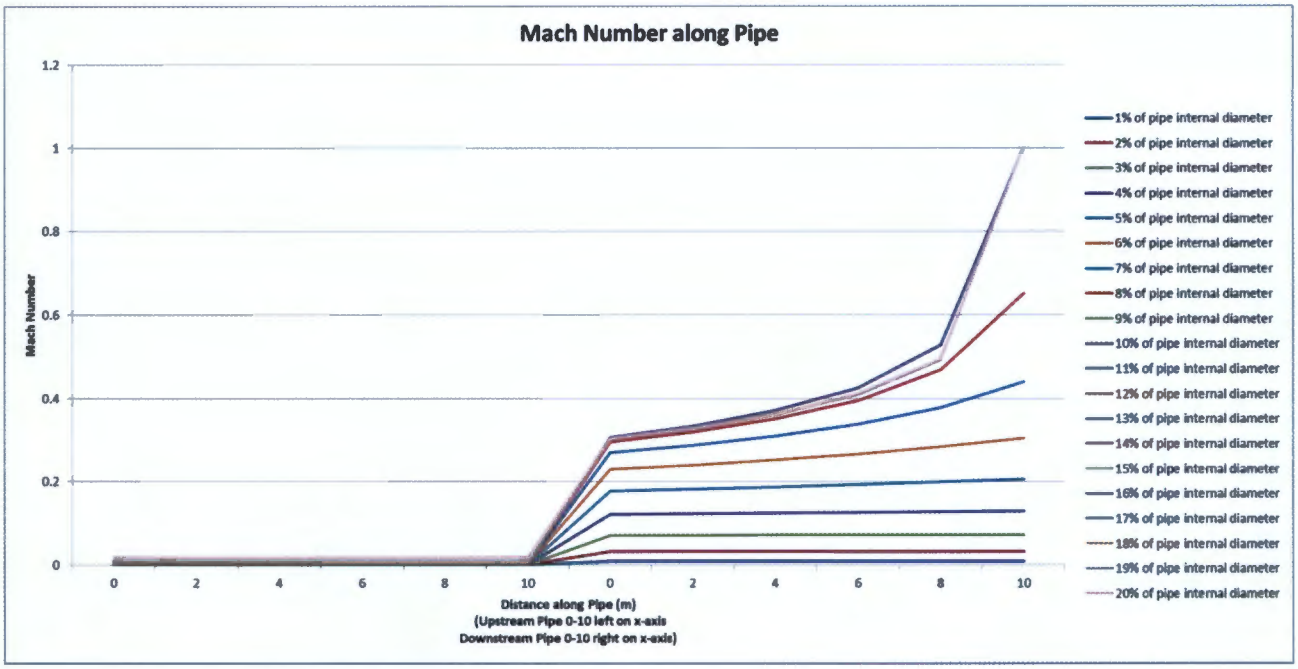

Figure 25: Mach Number profile along upstream and downstream pipe

On analysing the pressure profiles along upstream and downstream pipe lengths for different orifice openings in figure 19 and 20 it can be seen that there is a drastic pressure drop across the restriction for all orifice openings. For orifice openings from 1% to 10% of pipe diameter the downstream pressure immediately after the restriction is between 100-300 kPa and for orifice openings from 11% to 20% the downstream pressure immediately after the restriction is between 300-1100kPa.

Figure 21 and 22 shows the temperature profile along upstream and downstream pipe lengths for orifice openings from 1% to 20% of pipe internal diameter. The graphs indicate that there will be a drop in temperature across the restriction for all openings. After the restriction, the temperature for all openings ranges between 369 to 461 °C. This indicates that the steam is still in the superheated condition since the temperature is above the saturation temperature. With this knowledge one can assume that the steam expanding to atmosphere through an internally leaking valve is in the single superheated phase, and not in a two-phase state.

The enthalpy profile shown in figure 23 indicates that the enthalpy changes across the restriction for all orifice openings. On analysing the velocity profile, it can be seen that the velocity upstream of the restriction remains fairly constant whilst the velocity downstream increases significantly as the flow expands through the downstream pipework. Since the velocity increases, the effect of the kinetic energy component in equation 18 becomes more pronounced thus decreasing the enthalpy value downstream of the restriction.

The table below shows the enthalpy values downstream of the restriction together with the difference between upstream enthalpy and that specific enthalpy and the percentage deviation

of that enthalpy with the upstream enthalpy. It is illustrated here to indicate the change in enthalpy from upstream to downstream conditions for orifice openings from 1% to 30% of pipe internal diameter.

Table 2: Downstream Enthalpy Analysis

	0 meter downstream			2 meter downstream			4 meter downstream			6 meter downstream			8 meter downstream			10 meter downstream		
Orifice Opening	Enthalpy	Difference between upstream enthalpy and node enthalpy	Percentage Deviation from upstream enthalpy	Enthalpy	Difference between upstream enthalpy and node enthalpy	Percentage Deviation from upstream enthalpy	Enthalpy	Difference between upstream enthalpy and node enthalpy	Percentage Deviation from upstream enthalpy	Enthalpy	Difference between upstream enthalpy and node enthalpy	Percentage Deviation from upstream enthalpy	Enthalpy	Difference between upstream enthalpy and node enthalpy	Percentage Deviation from upstream enthalpy	Enthalpy	Difference between upstream enthalpy and node enthalpy	Percentage Deviation from upstream enthalpy
[%]	[kJ/kg]	[kJ/kg]	[%]	[kJ/kg]	[kJ/kg]	[%]	[kJ/kg]	[kJ/kg]	[%]	[kJ/kg]	[kJ/kg]	[%]	[kJ/kg]	[kJ/kg]	[%]	[kJ/kg]	[kJ/kg]	[%]
1	3406.14	0.01	0.00	3406.14	0.01	0.00	3406.14	0.01	0.00	3406.14	0.01	0.00	3406.14	0.01	0.00	3406.14	0.01	0.00
2	3405.93	0.22	0.01	3405.93	0.22	0.01	3405.93	0.22	0.01	3405.93	0.22	0.01	3405.93	0.22	0.01	3405.93	0.23	0.01
3	3405.06	1.09	0.03	3405.05	1.10	0.03	3405.04	1.11	0.03	3405.03	1.12	0.03	3405.02	1.14	0.03	3405.01	1.15	0.03
4	3402.94	3.21	0.09	3402.86	3.30	0.10	3402.77	3.38	0.10	3402.68	3.47	0.10	3402.59	3.56	0.10	3402.49	3.66	0.11
5	3399.33	6.83	0.20	3398.96	7.19	0.21	3398.55	7.60	0.22	3398.09	8.06	0.24	3397.57	8.58	0.25	3396.98	9.17	0.27
6	3394.78	11.37	0.33	3393.73	12.42	0.36	3392.45	13.70	0.40	3390.86	15.29	0.45	3388.83	17.32	0.51	3386.15	20.01	0.59
7	3390.51	15.65	0.46	3388.41	17.74	0.52	3385.63	20.53	0.60	3381.72	24.44	0.72	3375.75	30.40	0.89	3365.28	40.87	1.20
8	3387.47	18.68	0.55	3384.38	21.78	0.64	3379.94	26.21	0.77	3372.94	33.21	0.97	3359.77	46.38	1.36	3319.17	86.98	2.55
9	3386.98	20.17	0.59	3382.31	23.84	0.70	3376.85	29.30	0.86	3367.62	38.53	1.13	3347.37	58.78	1.73	3215.56	190.59	5.60
10	3386.94	20.21	0.59	3382.29	23.86	0.70	3376.84	29.31	0.86	3367.68	38.47	1.13	3347.79	58.36	1.71	3215.42	190.73	5.60
11	3386.63	19.51	0.57	3383.28	22.87	0.67	3378.40	27.75	0.81	3370.51	35.64	1.05	3354.89	51.26	1.50	3215.22	190.92	5.61
12	3386.58	19.56	0.57	3383.22	22.92	0.67	3378.33	27.81	0.82	3370.42	35.72	1.05	3354.80	51.35	1.51	3215.23	190.91	5.60
13	3386.53	19.61	0.58	3383.17	22.97	0.67	3378.28	27.86	0.82	3370.35	35.79	1.05	3354.69	51.44	1.51	3215.24	190.90	5.60
14	3386.50	19.63	0.58	3383.12	23.01	0.68	3378.22	27.91	0.82	3370.30	35.84	1.05	3354.62	51.52	1.51	3215.26	190.87	5.60
15	3386.49	19.64	0.58	3383.11	23.02	0.68	3378.17	27.95	0.82	3370.24	35.88	1.05	3354.58	51.55	1.51	3215.28	190.85	5.60
16	3386.47	19.65	0.58	3383.10	23.02	0.68	3378.18	27.94	0.82	3370.20	35.92	1.05	3354.54	51.58	1.51	3215.30	190.82	5.60
17	3386.45	19.66	0.58	3383.08	23.03	0.68	3378.17	27.95	0.82	3370.21	35.91	1.05	3354.48	51.63	1.52	3215.35	190.77	5.60
18	3386.42	19.68	0.58	3383.05	23.05	0.68	3378.14	27.96	0.82	3370.20	35.90	1.05	3354.45	51.65	1.52	3215.39	190.71	5.60
19	3386.39	19.70	0.58	3383.02	23.07	0.68	3378.12	27.97	0.82	3370.18	35.91	1.05	3354.48	51.61	1.52	3215.43	190.66	5.60
20	3386.40	19.67	0.58	3382.99	23.08	0.68	3378.09	27.98	0.82	3370.16	35.92	1.05	3354.49	51.58	1.51	3215.46	190.61	5.60
21	3386.41	19.64	0.58	3383.01	23.05	0.68	3378.05	28.01	0.82	3370.11	35.94	1.06	3354.45	51.60	1.51	3215.49	190.57	5.59
22	3386.42	19.62	0.58	3383.03	23.01	0.68	3378.07	27.96	0.82	3370.07	35.97	1.06	3354.41	51.62	1.52	3215.51	190.52	5.59
23	3386.41	19.60	0.58	3383.03	22.98	0.67	3378.10	27.91	0.82	3370.06	35.95	1.06	3354.37	51.64	1.52	3215.54	190.47	5.59
24	3386.40	19.59	0.58	3383.03	22.96	0.67	3378.11	27.88	0.82	3370.11	35.87	1.05	3354.33	51.66	1.52	3215.56	190.42	5.59
25	3386.38	19.57	0.57	3383.01	22.94	0.67	3378.11	27.85	0.82	3370.14	35.82	1.05	3354.29	51.67	1.52	3215.59	190.37	5.59
26	3386.36	19.56	0.57	3382.99	22.93	0.67	3378.09	27.83	0.82	3370.14	35.78	1.05	3354.38	51.54	1.51	3215.61	190.31	5.59
27	3386.36	19.56	0.57	3382.99	22.93	0.67	3378.09	27.83	0.82	3370.14	35.78	1.05	3354.38	51.54	1.51	3215.61	190.31	5.59
28	3386.32	19.52	0.57	3382.92	22.92	0.67	3378.02	27.82	0.82	3370.09	35.75	1.05	3354.40	51.44	1.51	3215.69	190.15	5.58
29	3386.34	19.45	0.57	3382.91	22.88	0.67	3377.98	27.81	0.82	3370.06	35.74	1.05	3354.40	51.39	1.51	3215.73	190.06	5.58
30	3386.35	19.39	0.57	3382.94	22.80	0.67	3377.95	27.80	0.82	3370.02	35.72	1.05	3354.39	51.35	1.51	3215.78	189.96	5.58
Average		**16.31**	**0.48**		**19.03**	**0.56**		**22.97**	**0.67**		**29.32**	**0.86**		**41.85**	**1.23**		**145.15**	**4.26**

It can be seen from the above table that the average enthalpy difference immediately after the restriction is 16.31kJ/kg. This equates to a 0.48% average percentage deviation from upstream enthalpy for all orifice openings. At 2 meters downstream of the restriction, the average difference in enthalpy is 19.03kJ/kg which equates to a 0.56% average percentage deviation from upstream enthalpy. At 4 meters downstream of the restriction, the average difference is 22.97kJ/kg which equates to a 0.67% average percentage deviation from upstream enthalpy. At 6 meters and 8 meters the average percentage deviation is 0.86% and 1.23 % respectively. At 10 meters, which is the discharge into the sink, the average enthalpy difference is 145.15kJ/kg and the average percentage deviation is 4.46% for all orifice openings from 1-30% of pipe internal diameter. This indicates that, although there is a change in enthalpy across the restriction, the change is in essence very small for most of the length of the downstream pipework. The largest difference in enthalpy occurs at the discharge from the downstream pipework into the boiler blow down vessel.

It can also be seen from the above table that the difference between upstream enthalpy and downstream enthalpy becomes approximately constant for all downstream points from 9% to 30 % of orifice openings, the difference remains fixed despite the orifice opening increasing.

On analysing the downstream velocity profile, it can be seen that the velocity immediately after the restriction ranges between 5 m/s to 200 m/s. As the steam expands through the downstream pipework, the velocity steadily increases. The simulations indicate that for larger orifice openings, orifice openings greater than 8% of pipe internal diameter, the velocity increases rapidly in the last segments of the discharge pipe. The graph in figure 25 shows that

the Mach number in the last segment of the discharge pipe for orifice openings greater than 9% of pipe internal diameter is 1 which indicates that the velocity of flow is equal to the sonic velocity, and the mass flow rate is choked.

5. Proposed technique to detect and quantify internal leakages of drain valves

5.1 Chosen detection and quantification technique

In section 2.4, mention is made of the factors that need to be considered in choosing a suitable technique to detect and quantify internal leakages from drain valves. Coupled with these conditions since the velocities in the discharge pipe sometimes reach sonic velocity, choked flow condition needs to be considered.

The literature survey makes mentions of all the different types of technique available to detect the onset of internal valve leakages an also critically evaluates each technique with respect to suitability to detect and quantify leakages in a power plant environment. Below is a summary of this evaluation, repeated here so that all techniques are evaluated and a suitable technique can be chosen and pursued.

Techniques using acoustic emission technology to detect the onset of internal leakages from valves are a well proven science. Researchers have recently created empirical models that use the generated AE signal to quantify internal leakages although these models are sensitive to valve design, valve type, valve size and upstream pressure. Other researchers mention that one can quantify internal leakages from valves by comparing the AE signal generated with a similar valves AE signal trend signature, i.e. a fingerprinting exercise. Both methods require an experimental facility to be set-up so that empirical relationships or AE signal signatures can be generated for different valves. It will be extremely difficult to set-up such an experiment due to the high pressures and temperatures needed for such an experiment to acquire accurate AE signals to generate the empirical relationships or the AE signal signatures for each valve. Coupled with the above, there is a variation in valve sizes, valve types, valve designs and upstream pressures experienced by different drain valves. Setting up an experiment that caters for all the variables will be a difficult task to accomplish.

Pressure change monitoring is an intrusive monitoring technique that requires impulse lines to be permanently installed to the upstream and downstream piping network of the drain valve. This will not be a feasible approach as there are many drain lines installed on a power plant. Coupled to this, due to the high pressure differentials across the valve, the differential pressure transmitter/gauge might not have sufficient resolution to measure small pressure differences on the low pressure side of the valve.

Vibration analyses technique to detect internal leakages from valves is susceptible to background noise. Researchers have mentioned that this technique cannot be used in environments were background noises are high. The sound power level from power plant equipment can range from about 120 dB to well over 155 dB depending on the size and type of the machines. This makes vibration analyses not a suitable technique for power plant environments.

Detecting internal leakages of steam valves using infrared thermography is a simple exercise. As the leakage steam flow passes through the valve to the downstream pipework, the steam loses a portion of its energy to the pipework, thereby increasing the temperature of the piping network. By measuring the temperature of the downstream pipework using an IRT camera, one can determine if the valve is internally leaking or not. Quantification of the leakage flow is still a challenge. Korellis [16] and Sherikar [17] proposed techniques to quantify the leakage flow from power plant drain valves although none provided experimental validation of their techniques.

In the method derived by Korellis [16], the upstream temperature and pressure before the valve is used to calculate the downstream pressure of the valve. In the power plant, there are no instruments installed immediately upstream of the valve to acquire the pressure and temperature of the fluid and installing these instrumentation on all drain lines will be unfeasible. One can assume these properties to be the live steam properties, but as mentioned in chapter 2.3, the valves installed on the drain lines are installed at various different lengths away from the main steam pipe work and there will be a slight drop in temperature and pressure immediately upstream of the drain valve due to heat loss through the piping and head loss along the piping.

Sherikar's [17] proposed technique fulfils most of the requirements listed in section 2.4. It is a non-intrusive technique which can be conducted whilst the generating unit is in operation. The assumption made by the author equating the change in steam temperature to the change in pipe surface temperature of the un-insulated pipe needs to be verified as the author merely states the assumption and does not provide any verification.

In the simulations conducted in the previous section, it can be seen that the flow will be choked at the last segment of the downstream pipework in certain conditions. In Sherikar's [17] technique, if the length of insulation material is removed from a section well above the downstream discharge into the boiler blow down vessel, the effects of choked flow, i.e. shock

waves will not be seen by the length of un-insulated pipe as it will be upstream of the point of choking. Even for orifice openings as high as 30% of pipe internal diameter, shown in appendix A, it can be seen that the velocity only in the last segment of the downstream pipe is sonic velocity. Further to this, Sherikar's technique uses the heat lost from an un-insulated pipe to calculate a mass flow rate. If a choked flow condition exists the mass flow rate will not increase beyond a certain value with the upstream conditions and restriction opening remaining constant. Hence, the flow rate will remain constant which infers that heat loss from the un-insulated pipe will remain constant and the problem can be analysed as a steady state problem.

Sherikar [17] assumes in his technique that the expansion of fluid through an internally leaking valve follows an isenthalpic process, i.e. the enthalpy is conserved between upstream and downstream of the valve. From this assumption Sherikar [17] further goes on to mention that since the enthalpy is conserved, if a length of insulation is removed from a section of pipework downstream of an internally leaking valve, the heat loss from that section of un-insulated pipework will result in an enthalpy loss of the fluid and thus this forms the basis of the mass flow rate calculation. In section 4.2, it was shown that for internally leaking valves the effects of kinetic energy cannot be ignored and the process is not isenthalpic. However, on analysing the enthalpy profile downstream of an internally leaking valve, figure 23 and table 2, it can be concluded that the effects of kinetic energy is minimal along most of the initial parts of the downstream piping network and can be neglected. The effects of kinetic energy are more pronounced as the flow discharges into the boiler blow down vessel and thus in the last segment of the downstream pipe work one cannot neglect the effects of kinetic energy. This means that in utilising Sherikar's [17] technique, the length of un-insulated pipe must be removed from well above the discharge of the downstream piping to the boiler blow down vessel to avoid the effects of kinetic energy on the calculations.

Although this technique seems promising it first needs to be experimentally validated before implementation. Thus it was decided to pursue Sherikar's [17] proposed technique to detect and quantify internal leakages of valves.

5.2 Theory

The technique proposed by Sherikar [17] to detect and quantify internal leakages from drain valves uses infrared thermography technology to measure surface temperatures of an un-insulated pipe located downstream of a valve. As explained previously, the underlying principle upon which the leakage flow rate may be determined is that the heat loss along a length of un-insulated pipe will cause a drop in temperature of the leakage flow through the pipe. The change in temperature across the length of un-insulated pipe corresponds to a loss of enthalpy across the length which is representative of the heat loss from the un-insulated pipe length. The calculated heat loss is then correlated to a leakage flow rate. Figure 26 below illustrates a schematic of the proposed technique set-up.

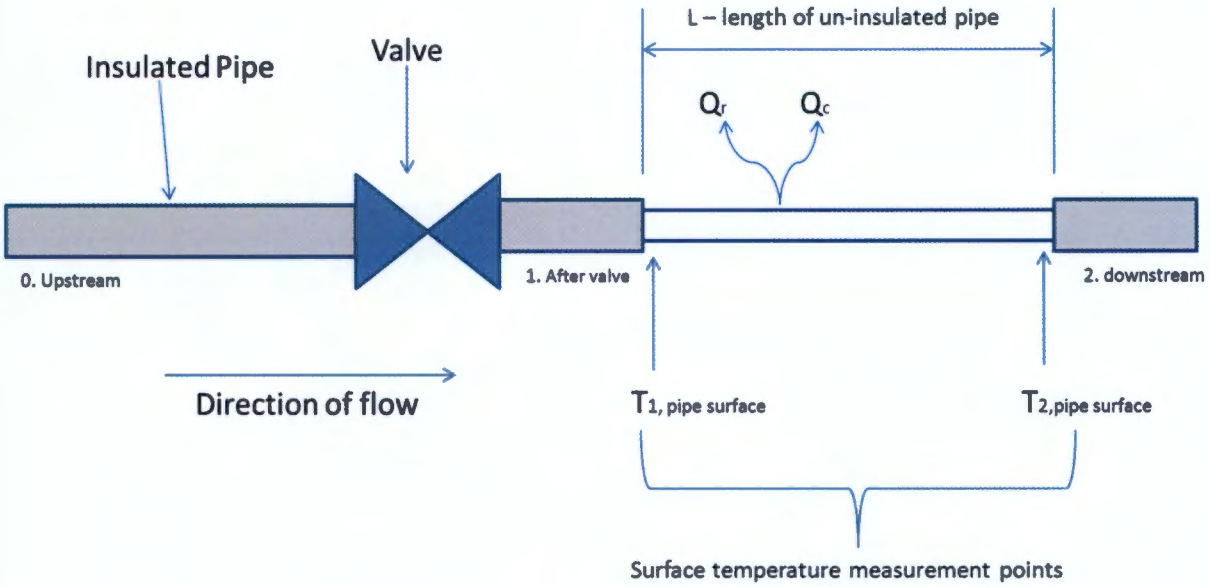

Figure 26: Schematic of proposed technique set-up

A length of pipe is provided in the bare (un-insulated) condition as is depicted in figure 26 above. As steam passes through the un-insulated length of pipe in a steady state condition, a portion of the heat energy contained in the steam is transferred via convection from the steam to the inner pipe surface. The heat energy is then conducted through the pipe wall to the outer surface of the pipe and thereafter lost to the surroundings by convection and radiation heat transfer. Since energy is conserved the heat loss from the steam flow is equal to the heat loss from the outer pipe surface.

As discussed and derived in section 3.2.2, Sherikar [17] calculates the mass flow rate of the fluid by the below mentioned equation.

$$\dot{m} = \frac{Q_C + Q_r}{C_P\,(T_{1,pipe\ surface} - T_{2,pipe\ surface})}$$ **Equation 19**

Where:

Q_C is the convection heat loss from the surface of the un-insulated pipe

Q_r is the radiation heat loss from the surface of the un-insulated pipe

C_p is the average specific heat of the fluid at constant pressure

$T_{1,pipe\ surface}$ and $T_{2,pipe\ surface}$ are pipe surface temperatures as indicated in figure 26

The convection heat transfer from the surface of the un-insulated pipe can be calculated from equation 20 below [23].

$$Q_C = h_c A_{out}(T_{surface\ avg} - T_{amb})$$ **Equation 20**

Where:

h is the heat transfer coefficient

A_{out} is the surface area of the outer surface along length L of the un-insulated pipe

$T_{surface,avg}$ is an average temperature of $T_{1,pipe\ surface}$ and $T_{2,pipe\ surface}$

T_{amb} is the ambient temperature

The radiation heat transfer from the surface of the un-insulated pipe can be calculated from equation 21 below [23]. By using the average pipe surface temperature across the length of the un-insulated pipe in equation 20 and 21, it is assumed that the heat transfer rate is uniform across the length of un-insulated pipe.

$$Q_r = \varepsilon\sigma AF(T^4_{surface,avg} - T^4_{amb})$$ **Equation 21**

Where:

ε is the thermal emissivity of the pipe surface

σ is the Stefan-Boltzmann constant

F is the shape factor

The heat transfer coefficient h_c, in equation 20 above, may be determined from the Nusselt number approximation as shown in equation 22 below:

$$Nu_D = \frac{h_C D_{out}}{k} \qquad \textbf{Equation 22}$$

Where:

Nu_D is a dimensionless Nusselt number

k is the thermal conductivity of air

D_{out} is the outer diameter of the un-insulated pipe length.

The Nusselt number is a ratio of the total heat transfer of a system to the conduction heat transfer of the same system. Churchill and Chu [23] derived an empirical relationship for the calculation of the Nusselt number as a function of the Rayleigh number (Ra_D) and Prandtl number (Pr) for free convection heat loss from an isothermal horizontal cylinder and is shown in equation 23 below.

$$Nu_D = \left\{ 0.60 + \frac{0.387\, Ra_D^{1/6}}{\left[1+\left(\frac{0.559}{Pr}\right)^{\frac{9}{16}}\right]^{\frac{8}{27}}} \right\}^2 \qquad \textbf{Equation 23}$$

The Rayleigh number and Prandtl number can be calculated from equations 24 and 25 respectively [23]:

$$Ra_D = \frac{g\beta_a(T_{surface\,avg} - T_{amb})D_{out}^3}{v_a \alpha_a} \qquad \textbf{Equation 24}$$

$$P_r = \frac{v_a}{\alpha_a} \qquad \textbf{Equation 25}$$

Where:

g is the gravitation acceleration

β_a is the thermal expansion coefficient of air

v_a is the kinematic viscosity of air

α_a is the thermal diffusity of air

Equations to calculate the thermos physical properties of air are shown in Appendix B.

Solving for the Nusselt number in equation 23 and substituting in equation 22 one can solve for the heat transfer coefficient. The mass flow rate of the leakage flow through the length of un-insulated pipe can then be calculated by equation 26 below:

$$\dot{m} = \frac{h_{cA_{out}}(T_{surface\ avg} - T_{amb}) + \varepsilon\sigma A_{out}(T^4_{surface\ avg} - T^4_{amb})}{C_p\,(T_{1,pipe\ surface} - T_{2,pipe\ surface})} \qquad \textbf{Equation 26}$$

The following assumptions are made in the above equation:

- The heat transfer rate across the length of un-insulated pipe is uniform throughout the length.
- The heat transfer from the steam through the pipe wall is one dimensional, i.e. heat is only transferred in the radial direction through the pipe wall across the pipe length.
- The change in pipe surface temperature is equal to the change in steam temperature across the length of the un-insulated pipe. As mentioned earlier, this assumption is made due to the fact that no instrumentation is available on site to measure steam temperature or any other steam properties. It will be shown, in section 6.5, that this assumption is not entirely accurate

The above equation will be referred to as the mathematical model to calculate mass flow rate of a leakage flow through an internally leaking valve. The process to follow in utilising this mathematical model will be referred to as the proposed technique. The proposed technique comprises the following procedure:

- Remove a length of insulation from the downstream pipe work of an internally leaking valve
- Take surface temperature measurements of the upstream and downstream points of the un-insulated pipe using an infrared thermal camera
- Calculating the mass flow rate of the leakage flow by using the mathematical model

Once problematic valves have been identified and the quantity of leakage flow is established, one can calculate the costs associated with an internally leaking valve.

5.3 Evaluation of losses associated with internally leaking valves

In section 4.1, the impact of internally leaking valves were listed and discussed. In this section the equations to calculate the financial impact of the main losses are given.

5.3.1 Loss in revenue

The amount of steam lost from a combination of internally leaking valves could prevent a power plant from attaining maximum generating capabilities. This could be due to the boiler feed pump not being able to feed the excess water lost by the leakage flow. This will result in a loss of revenue from the power generating plant if it cannot reach maximum generating capacity.

To calculate this loss of revenue, the energy lost from the leakage flow needs to be calculated first. This is determined by multiplying the difference in enthalpy of the leakage flow and the enthalpy of the demineralised water make-up to the mass flow rate of the leakage flow. This is shown in equation 27 below.

$$\boldsymbol{P_{leak} = (h_0 - h_{ref})\, x\, \dot{m}} \qquad \textbf{Equation 27}$$

Where:

P_{leak} is the energy lost from the leakage flow

h_0 is the enthalpy of the leakage steam

h_{ref} is the enthalpy of the demineralised water make-up to the system

$\dot{m}$ is the mass flow rate

The demineralised water make-up to the station is usually fed to the station at temperatures very close to ambient temperatures making the enthalpy of the make-up water small in comparison with the enthalpy of the leakage steam. The leakage steam enthalpy is in the region of 3000 - 3400 kJ/kg whilst the enthalpy of the make-up water is in the region of 50 -100 kJ/kg depending on the ambient conditions. Thus, since the make-up water enthalpy is much smaller than the leakage steam enthalpy, it can be ignored in the above equation.

The loss of revenue can be calculated from equation 28 below taking into consideration the turbine efficiency (η_t) since not all the energy available in the steam is converted into electricity. Typically, the efficiency of a turbine set, including HP,IP and LP turbines, in a 660 MW power plant is between 90-93%.

$$\boldsymbol{Loss\ of\ revenue} = \boldsymbol{P_{leak}\ x\ \eta_T\ x\ Cost\ of\ electricity}\left(\frac{R}{kwh}\right)\boldsymbol{\ x\ time\ on\ full\ load}\ (\%)$$

Equation 28

5.3.2 Cost of excess coal required

The steam lost due to internally leaking valves has already had its energy level increased by the fuel combustion process and since this energy is not available for generating purposes more fuel needs to be burned in order to meet the generating requirements of the plant.

Not all of the chemical energy contained in the coal is transferred to the fluid in the boiler. A portion of the energy is lost in the combustion process. To determine the amount of excess coal required to supplement the energy lost from the leakage flow, the energy required from the excess coal ($P_{excess\ coal}$) needs to be determined. This can be calculated by dividing the energy lost from the leakage flow (P_{leak}), as determined in equation 27 above, by the boiler efficiency (η_B). This is shown in equation 29 below. Typically, the efficiency of a boiler in a 660 MW power plant is between 85-89 %.

$$\boldsymbol{P_{excess\ coal}} = \frac{\boldsymbol{P_{leak}}}{\boldsymbol{\eta_B}}$$ **Equation 29**

Once the energy required from the excess coal is calculated, the quantity of excess coal can be determined by dividing the energy required from the excess coal by the average calorific value of coal ($C_{v,coal}$), which is the amount of potential energy in the coal that can be converted into heating ability. This is shown in equation 30 below.

$$\boldsymbol{Excess\ Coal\ (per\ hour\ per\ kg)} = \frac{\boldsymbol{P_{excess\ coal}}}{\boldsymbol{C_{v,coal}}}\ \boldsymbol{x\ 3600}$$ **Equation 30**

The cost of the excess coal can then be calculated by multiplying the excess coal per ton to the cost of coal per ton.

5.3.3 Loss of demineralised water

The working fluid used in a power plant is demineralised to prevent corrosion of pipework. There is a cost associated with the production of demineralised water and any loss of it will result in a financial impact. By knowing the quantity of leakage flow from internally leaking drain valves one can calculate the financial losses that results from the leakage flow from equation 31 below.

$$\boldsymbol{Cost\ of\ excess\ demin\ water\ per\ year = lost\ water\ per\ year\ (l) x\ cost\ per\ l\ to\ manufacture\ demin\ water}$$

Equation 31

5.3.4 Cost of excess auxiliary power consumption

Water is pumped into the boiler by means of boiler feed pumps (BFP). Three BFP's are installed on each power generating unit. Each is capable of supplying 50% of the required flow rate. Thus, two are in service at any given time whilst the third is on standby. The BFP's are driven by variable speed drives, which allow the pump to vary the flow rate required by the system.

Internally leaking valves results in the BFP's consuming more power to feed the additional feed water into the boiler. The determination of the excess power required by the BFP's for an increase in flow rate can be determined by pump affinity laws for centrifugal pumps. The affinity laws are derived from a dimensionless analysis of three important parameters that describe pump performance: flow, total head and power [24]. These laws describe the impact of changes in speed on pump flow, head and power for centrifugal pumps. As formulae, the affinity laws are shown in equation 32, 33 and 34 below.

$$\frac{V_1}{V_2} = \frac{N_1}{N_2}$$

Equation 32

$$\frac{H_1}{H_2} = \left(\frac{N_1}{N_2}\right)^2$$

Equation 33

$$\frac{P_1}{P_2} = \left(\frac{N_1}{N_2}\right)^3$$ **Equation 34**

Where:

V is the volumetric flow rate

N is the shaft speed

H is the pump head

P is the pump power

From the above equations one can see that an increase in flow rate will result in an increase in shaft speed which will result in an increase in power required by the pumps. Once the excess power consumed by the BFP's are calculated, the cost of the excess power can be calculated by multiplying the excess power to the cost of electricity.

It should be noted that if there is a loss of water in the boiler through internally leaking valves, the system will automatically send signals requesting more feedwater from the boiler feed pumps. Since the BFP's are fitted with variable speed drives, the pump is able to speed up and transfer more feed water into the boiler as requested. However, there is a limit to the amount of excess feedwater that the BFP's can supply. The drives are fitted with an overload function, which will inform the unit operator when the BFP's are delivering close to their maximum amount. Once this point is reached, the operator will then have to de-load the unit and take a load loss. The system also monitors the boiler pressure and informs the operator if the boiler pressure is exceeding its maximum allowable value. If the pressure is exceeded, the operator will then have to de-load the unit and take a load loss to protect components from over pressurisation.

All the above losses are the major losses that will be encountered from internally leaking valves. Other losses like blowing more air through the boiler to facilitate the excess coal being burned is not considered in this analysis as the additional power required by the fans to blow the excess air will be insignificant as the power consumption ratio to air volume is small in fans.

6. Experimental Investigation

In chapter 5.2 equation 26, a mathematical model was formulated to calculate the mass flow rate from an internally leaking valve. For it to be established as an accurate indication of internal valve leakages on a power plant environment, the mathematical model needs to be validated experimentally. The validation process should consist of a mass flow rate reading calculated from the mathematical model, to be compared with a mass flow rate reading generated from a reliable flow measurement device at varying flow properties.

Ideally the experiments should be conducted using steam similar to that experienced by the drain valves in a power plant. Unfortunately generating steam at such high temperatures and pressures is extremely difficult in a controlled environment and for this reason it was decided to conduct the experiments using steam at lower pressures and temperatures, whilst still maintaining the superheated nature of the steam.

6.1 Cussons mini steam power plant

The Cussons mini steam power plant was utilised in generating superheated steam required for the experiments. This steam plant is owned by Eskom and is located in the Eskom Academy of Learning in Midrand, Johannesburg. The Cussons Mini Steam Power Plant has been specifically designed to allow institutes of education to study the principles and operations of an industrial steam power plant. The plant can operate as a steam boiler, turbo-generator or complete power plant. Steam generated from the boiler can be transferred to a set of experimental test benches to conduct tests. Available tests include: thermal and total efficiency consumption, boiler capacity, efficiency, heat balance, turbine power and specific steam consumption. Figure 27 below shows a picture of the power plant.

Figure 27: Picture of Cussons mini power plant located in Eskom Academy of Learning Midrand

6.1.2 Overview on the operation of the Cussons mini power plant

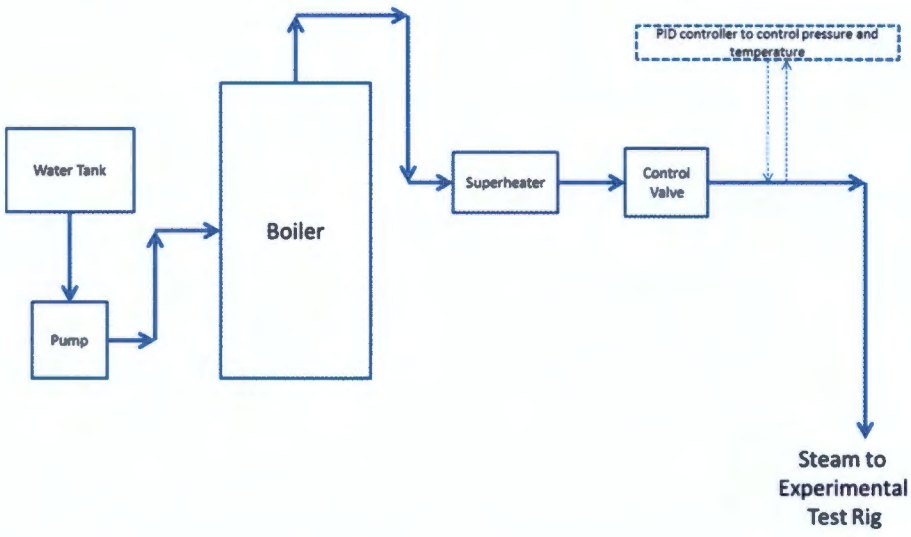

Figure 28: Water/Steam flow diagram of Cussons mini steam plant

Figure 28 above illustrates the water/steam flow path through the Cussons mini steam plant. Water is suctioned from the water tank by a pump and discharged into the boiler at a pressure

of 8 bars. The diesel fired boiler then heats the fluid to a temperature of 173 °C. The steam is then transferred to a superheater to further increase the temperature of the steam to a user defined value. A control valve is installed immediately after the superheater to control the pressure to a user defined value. Thus, the outlet steam temperature and pressure can be controlled by the operator although not exceeding a maximum of 250°C and 6 bar respectively.

The machine maintains a user defined outlet temperature and pressure and thus the mass flow rate cannot be user controlled but is a function of the back pressure in the system. The back pressure is the pressure in the exhaust region, at the discharge of a nozzle, pipe, orifice or valve. When the back pressure is equal to the supply pressure, there is no flow, since a fluid will flow from a region of high pressure to a region of lower pressure. As the back pressure is decreased to below the supply pressure the flow rate increases. Or if the supply pressure is increased above the back pressure, the flow rate increases. Thus to vary the mass flow rate of steam through the system the outlet pressure of the machine needs to be varied or the back pressure in the downstream piping needs to be adjusted.

As indicated earlier, steam generated from the Cussons boiler can be transferred to a set of experimental benches which utilise the steam for experimental purposes. Some of the experimental benches and their purposes are listed below.

- Pressure and Temperature Bench – to investigate the relationship between temperature and pressure of saturated steam.
- Separating and Throttling Calorimeter Steam Bench – to determine the dryness fraction of steam i.e. the quantity of dry vapour present in any wet vapour mixture.
- Condenser Bench - to illustrate to students the operation of a condenser.

For purposes of this investigation an experimental test rig was designed and connected to the Cussons power plant to facilitate experiments that needed to be conducted to validate the mathematical model derived.

6.2 Experimental test rig

6.2.1 Description of test rig

An experimental test rig to validate the proposed technique was designed and connected to the Cussons mini power plant. Figure 29 below shows a picture of the experimental test rig set-up.

Figure 29: Picture of experimental test rig installed to Cussons power plant

For purposes of this investigation, the experimental benches, installed on the Cussons mini steam plant, were disconnected and the above experimental test rig was connected to the main steam supply line from the Cussons plant. The below picture indicates the location were the experimental benches where disconnected and were the experimental test rig was connected.

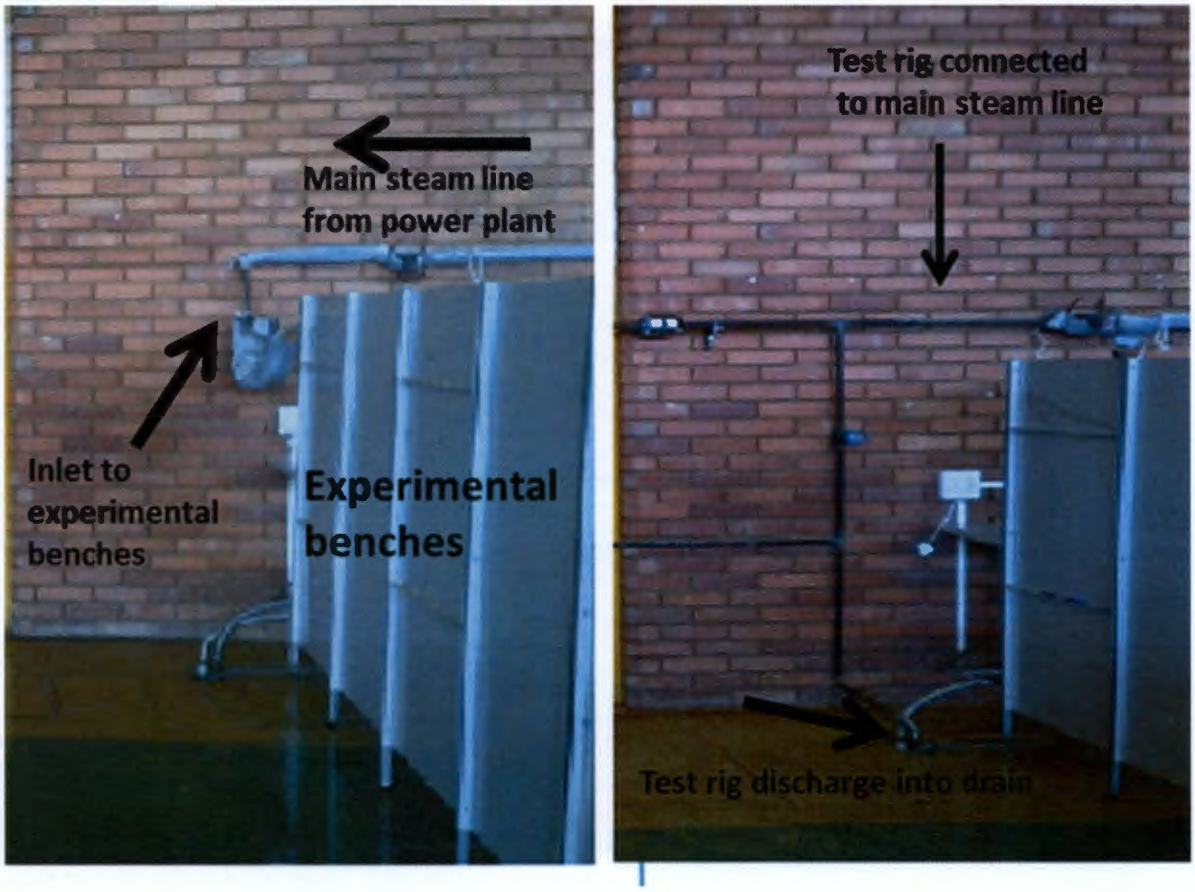

Figure 30: Test rig connection to Cussons plant

The experimental test rig consisted of the following components. Figure 31 shows the location of the different components in the test rig.

a) Steel piping

Steel piping made up the bulk of the test rig and was installed to transport steam from the Cussons plant to the test length and to discharge the steam into the drain system. All steam piping was made up of ASTM A106 GRB carbon steel piping. The maximum working temperature and pressure ratings for the steel piping is 343 °C and 7.6 MPa respectively. The dimensions of the piping were as follows:

Internal diameter (d_i) = 15 mm

Outer diameter (d_o) = 20.54 mm

Wall thickness (t) = 2.77 mm

Total length of piping = 11.8 m

b) Pipe fittings (90° elbows, tee-pieces, sockets)

Pipe fittings were installed to the steel piping to change the direction of the fluid flow (90° elbows) or to split the flow into two branches (tee-pieces). All pipe fittings were of the butt-weld type and designed for use with ASTM A106 steel piping. All fittings were selected from standard catalogues. Altogether the rig consisted of six 90° elbows, two tee-pieces and two sockets. All components were welded together by the TIG (tungsten inert gas) welding process.

c) Orifice plate

An orifice plate was installed in line with the experimental test rig. An orifice is a flow restriction device that provides a means to calculate a mass flow rate. The orifice plate was installed to calculate the actual mass flow rate in the test rig, which was used to compare with the mass flow rate obtained from the mathematical model. The orifice plate was designed to ISO 5167-2003, the international standard relating to the design and use of orifice plates. It should be noted that since the mass flow rate is conserved in the system, the orifice plate was installed upstream of the test valve so that any choked flow effects, occurring downstream of the test valve, will not affect the mass flow rate readings in any way.

d) Impulse lines

Instrumentation Impulse lines were installed to connect the upstream and downstream tapping points of the orifice plate to a differential pressure gauge. The Impulse lines were made from aluminium tubes. Impulse lines contain the process fluid and are generally used to transmit the pressure signal from the process to the transmitter.

e) Differential pressure transmitter

A Siemens differential pressure transmitter was installed across the orifice plate, by means of impulse lines, to read the differential pressure of the fluid flow caused by the orifice.

f) Pressure gauge

A digital pressure gauge was installed upstream of the orifice plate. This allowed for the pressure to be recorded upstream of the orifice which was used to calculate the density of the fluid. The density is needed in the calculation of mass flow rate by means of an orifice plate.

g) Valves

Two hand operated wedge gate type valves were installed on the experimental test rig, a test valve and a bypass valve. By varying the opening of the test valve, one could vary the back

pressure of the system and thus the mass flow rate could be controlled as explained earlier. The bypass valve was purely installed to bypass flow from the experimental test rig.

h) Length of un-insulated pipe

The design of the experimental test rig saw the length of un-insulated pipe (test length) being installed a distance of one meter away from the surface of the building wall. This was done to avoid the wall from influencing heat transfer from the un-insulated pipe. The length of the un-insulated pipe was maintained at 1.9 meters for all experiments performed.

Before commencing experimentation the test section was sanded down and painted with a matt black paint to maintain a constant emissivity along the length. The emissivity of the pipe surface is a vital parameter since the infrared camera, used for pipe surface temperature measurements, depends on an accurate emissivity input for an accurate surface temperature output. The emissivity influences the radiation heat transfer rate from the pipe surface as well.

In all experiments, surface temperature measurements were conducted on the upstream surface of the un-insulated wall as well as the downstream surface of the un-insulated pipe. Surface temperature measurements were also conducted on 9 equi spaced points along the length of un-insulated pipe.

i) Pipe insulation material

All steel piping, except the test length was insulated with mineral fibre insulation material to avoid heat loss. The conductivity of mineral fibre is very low, making it a suitable material for insulation purposes.

j) Pipe supports

Pipe supports and pipe hangers were installed to fasten the test rig to the building wall.

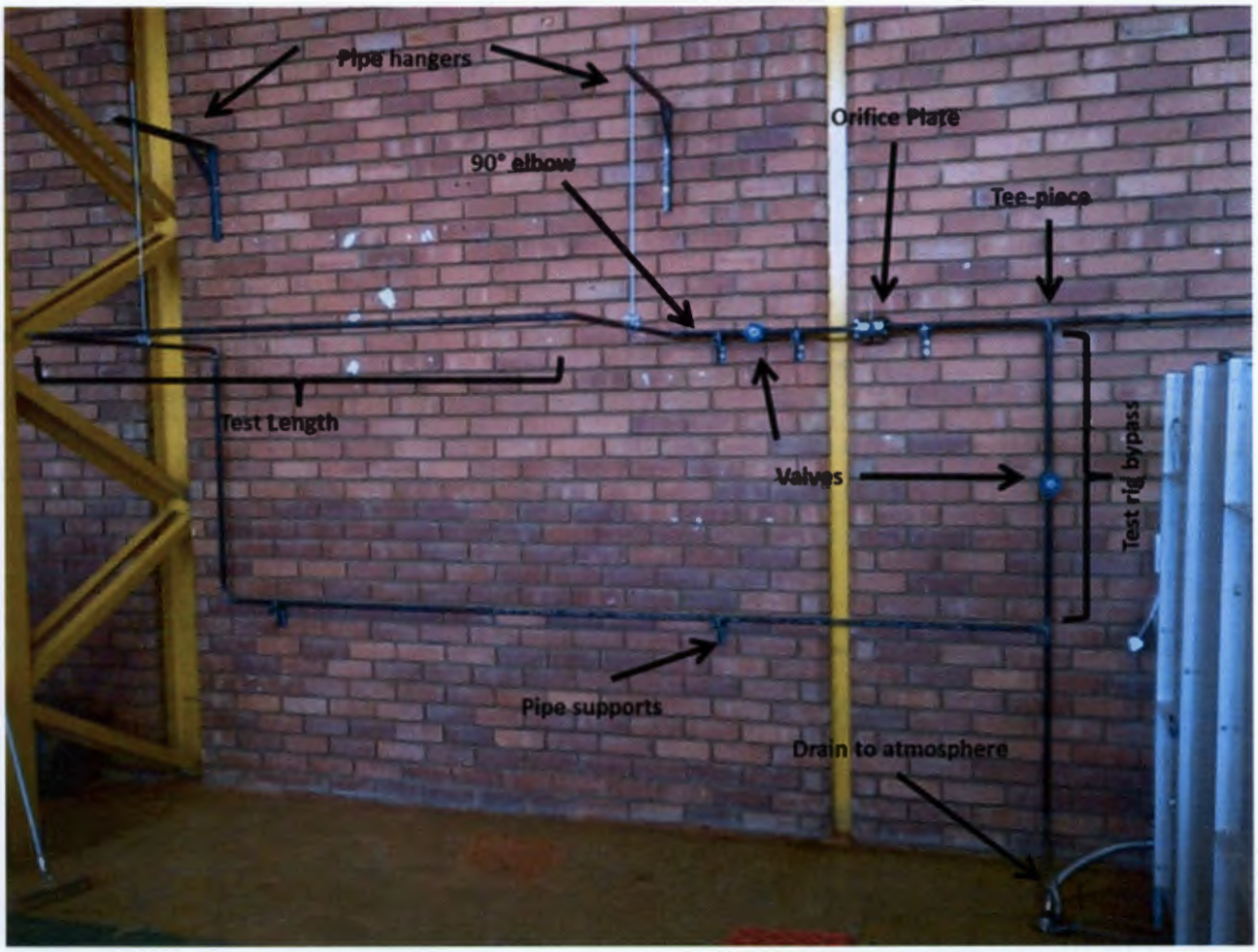

Figure 31: Test rig components

6.2.2 Steam flow through experimental test rig

Steam at pressure and temperature P_0 and T_0, generated by the Cussons power plant was allowed to flow through the experimental test rig. Figure 32 below shows the steam flow path through the experimental test rig. The steam flow first passes an installed flow measuring device and then on to an installed test valve. The steam expands to atmospheric pressure after passing the test valve. A length of pipe is provided in the un-insulated (bare) state downstream of the valve to conduct the experiments. A bypass valve was installed to bypass steam from the bare pipe and was kept in the fully closed position throughout all experiments conducted.

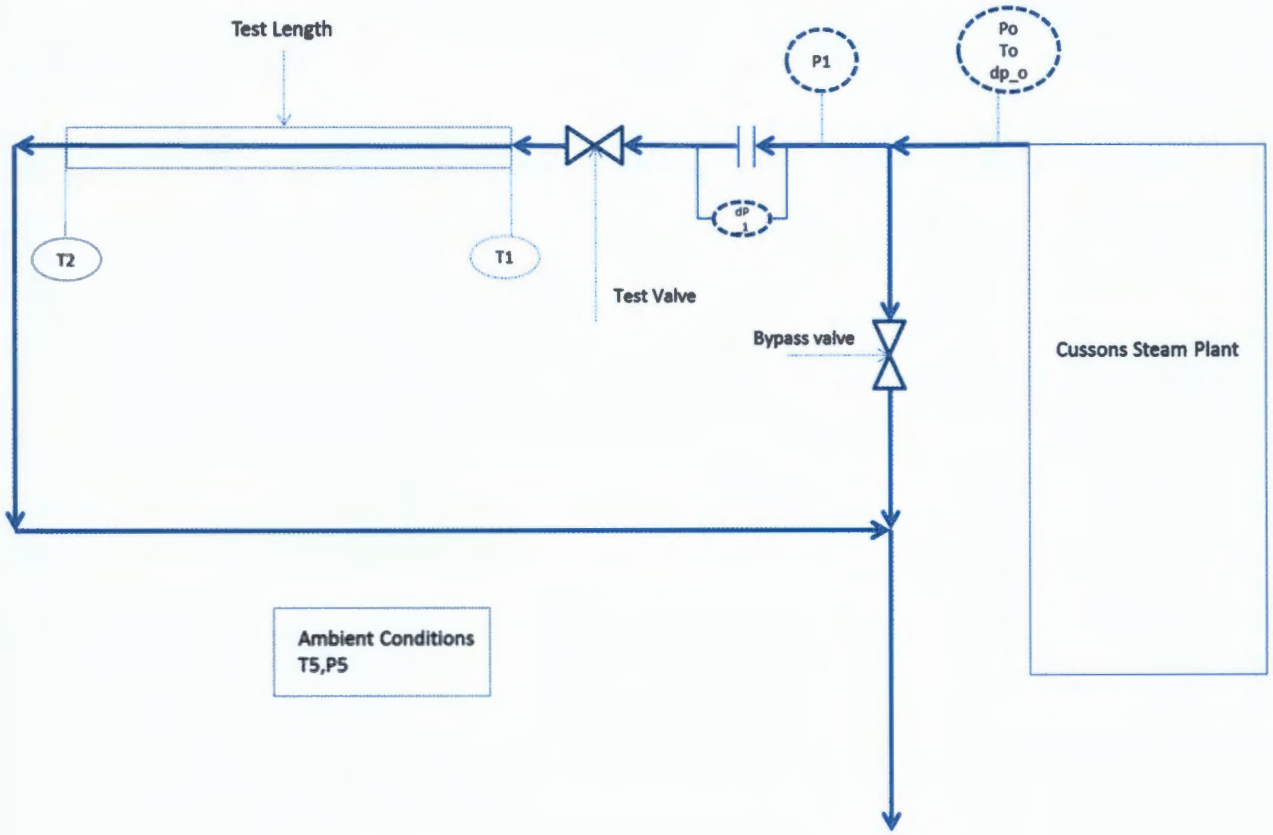

Figure 32: Steam flow through experimental test rig

6.2.3 Orifice plate and associated components

In all experiments, flow measurement was accomplished by the use of an orifice plate installed in line with the experimental test rig, upstream of the test valve. A Siemens differential pressure transmitter was installed across the orifice, by means of impulse lines, to read the differential pressure caused by the restriction device. A pressure gauge was also installed on the upstream face of the orifice in order to calculate fluid density which is necessary for mass flow rate calculation. The standard equation used to calculate mass flow rate for an orifice plate is given below.

$$\dot{m} = \frac{C}{\sqrt{1-\beta^4}} \varepsilon \frac{\pi}{4} d^2 \sqrt{2\Delta p \rho_1} \qquad \textbf{Equation 35}$$

Where:

ṁ is the mass flow rate

C is the discharge coefficient

β is the ratio of orifice diameter to pipe internal diameter

ε is the expansibility factor

d is the orifice diameter

Δp is the differential pressure across the orifice

ρ_1 is the upstream density of the fluid.

ISO 5167-2003, the international standard relating to the design and use of orifice plates, contains the relevant equations on the calculation of the discharge coefficient and the expansibility factor. Appendix C elucidates these equations and other relevant information pertaining to the orifice plate. As mentioned earlier the orifice plate was installed upstream of the test valve so that any effects due to the high pressure differentials across the test valve will not affect the calculation of the mass flow rate used for verification purposes.

6.2.4 Surface temperature measurement

Surface temperature measurements were obtained using the FLIR i7 infrared thermal imaging camera. The operation of an IRT camera is explained in section 3.2.2.

The FLIR i7 IRT camera can measure objects from -20 °C to +250 °C, has a field of view of 29°X29°, minimum focus distance of 0.6, accuracy of ±2°C or ±2% (whichever is greater) and a thermal resolution of 140X140 pixels. Below is a picture of the FLIR i7 camera as well as a thermal image generated from the camera.

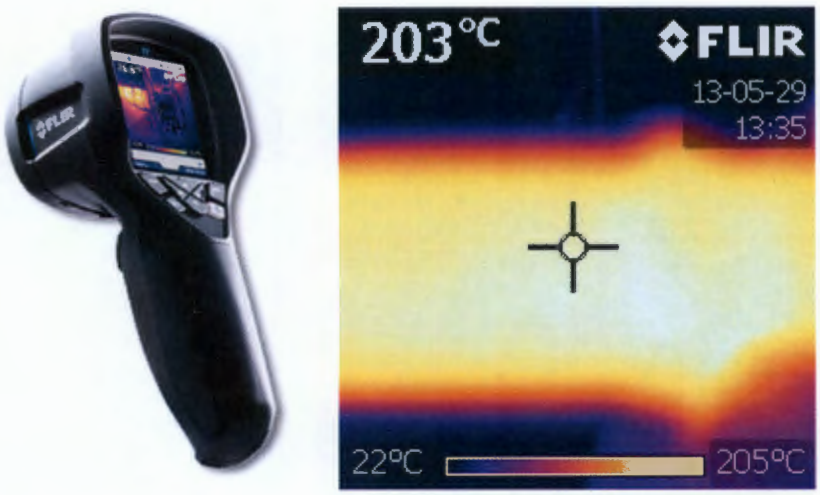

Figure 33: Picture of FLIR i7 infrared camera and infrared thermal image generated from camera

6.3 Experimental Procedure

Steam generated at pressure (P_0) and temperature (T_0) from the Cussons mini steam plant was allowed to flow through the test rig set-up as is shown in figure 32.

As discussed previously, either the back pressure of the system or the outlet pressure of the machine needed to be varied to vary the mass flow rate through the experimental test rig. Varying the opening of the installed test valve caused the back pressure of the system to vary and thus the mass flow rate through the system to vary. Both methods were used in the experiments to vary the mass flow rate through the experimental test rig i.e. the valve opening and the machine outlet pressure was varied.

To acquire a mass flow rate reading from the installed orifice an upstream pressure (P_1) and differential pressure (dP_1) was recorded for all tests performed. On the length of un-insulated pipe, surface temperature measurements were taken on the upstream location T_1 and downstream location T_2. Measurements were only taken once pipe surface temperatures stabilised, the duration being 30 minutes from commencement of any particular test. The ambient temperature was recorded from the ambient temperature gauge installed on the Cussons plant for each individual test.

There were 5 different sets of experiments conducted as explained below:

1. Outlet Pressure and temperature from Cussons Steam Generating Plant fixed at 3.5 bar and 230°C respectively whilst the test valve's opening varied from 0.5 turns to 2 turns in 0.25 turn increments.

2. Outlet Pressure and temperature from Cussons Steam Generating Plant fixed at 4 bar and 230°C respectively whilst the test valve's opening varied from 1 turn to fully opened in 0.25 turn increments.

3. Outlet Pressure and temperature from Cussons Steam Generating Plant fixed at 4.5 bar and 250°C respectively whilst the test valve's opening varied from 1 turn to fully opened in 0.25 turn increments.

4. Outlet Pressure and temperature from Cussons Steam Generating Plant fixed at 5 bar and 230°C respectively whilst the test valve's opening varied from 1 turn to fully opened in 0.25 turn increments.

5. The test valve fixed at 1 turn whist the outlet pressure from Cussons Steam Generating Plant was varied from 2.5 bar to 6.5 bar in 0.5 bar increments and the outlet temperature maintained at 230 °C.

Data collected from the experiments were recorded and used to calculate the mass flow rate by the mathematical model which was modelled in Microsoft Excel. With an input of pipe dimensions, ambient temperature and the un-insulated pipe surface temperatures the model calculates the mass flow rate of the fluid flowing through the un-insulated pipe. Table 4 in the following section shows the excel model. In this table each column is numbered 1-33. Table 3 below shows an explanation of each column and how the values in the model are calculated.

In the mathematical model the convection coefficient was calculated using the Nusselt number correlation given in equations 22 and 23 in section 5.2. The Nusselt number is a function of the Prandtl number and the Raleigh number. These are calculated from equation 24 and 25 respectively shown in section 5.2. The Prandtl number and the Raleigh numbers are functions of the thermo physical properties of air and the surface temperature of the pipe for free convection from a horizontal pipe. Thus the convection coefficient varies as these properties vary and was calculated for each individual test performed. The convection coefficient varied between 8.5 and 9.9.

To acquire a constant emissivity of the test length pipe surface; the entire test length was painted with a matt black paint giving the surface an emissivity of 0.95. This emissivity was used in all calculations.

The surface area of the test length was calculated using equation 36 below and remained constant for all experiments performed. For the test length the surface area was 0.1278 m^2.

$$A_{out} = \pi d_o L \qquad \textbf{Equation 36}$$

Where:

A_{out} is the surface area of the test length

d_0 is the pipe outer diameter

L is the length of the un-insulated pipe (test length)

Table 3: Explanation as to how columns are calculated in the Excel model

Column Number in Model	Description of Column	Abb	Units	Explanation
1	Length of un-insulated pipe	L	*[m]*	User input value
2	Outer Diameter of Pipe	Do	*[m]*	User input value
3	Inner Diameter of Pipe	Di	*[m]*	User input value
4	Pipe Wall Thichness	t	*[m]*	User input value
5	Pipe emissivity	ε		User input value
6	Test Valve Opening		*[turns]*	User input value
7	Ambient Temperature	Tamb	*[° C]*	User input value
8	Upstream un-insulated Pipe Surface Temperature	T1,s	*[° C]*	User input value
9	Downstream un-insulated Pipe Surface temperature	T2,s	*[° C]*	User input value
10	Average Pipe Surface Temperature	Ts,avg	*[° C]*	Ts,avg = (T1,s+T2,s)/2
11	Pipe Surface Area	A_ps	*[m^2]*	Calculated using equation 36
12	Radiation Heat Transfer from un-insulated pipe surface	Qrad_ps	*[W]*	Calculated using equation 21
13	Convection Heat Transfer from un-insulated pipe surface	Qconv,ps	*[W]*	Calculated using equation 20 using convection coefficient that is calculated in column 25
14	Film Temperature	Tfilm	*[k]*	Calculated using Equation B.8
15	Density of air	ρ_a	*[kg/m^3]*	Calculated using Equation B.1
16	Specific heat of air	Cp_a	*[J/kgK]*	Calculated using Equation B.2
17	Dynamic viscosity	μ_a	*[kg/sm]*	Calculated using Equation B.3
18	Thermal conductivity of air	k_a	*[W/mk]*	Calculated using Equation B.4
19	Kinematic viscosity	v_a	*[m^2/s]*	Calculated using Equation B.5
20	Thermal diffusity	α_a	*[m^2/s]*	Calculated using Equation B.6
21	Thermal expansion coefficient	β_a	*[1/K]*	Calculated using Equation B.7
22	Prandtl Number	Pr		Calculated using Equation 25
23	Raleigh Number	Ra		Calculated using Equation 24
24	Nusselt Number	Nu		Calculated using Equation 23
25	Convection coefficient	h	*[W/m^2 k]*	Calculated using Equation 22
26	Total Heat Loss	Q_tot	*[W]*	Q_tot = Qrad_ps + Qconv,ps
27	Speciic heat of steam	Cp_s	*[J/kg o C]*	From steam tables using upstream pipe surface temp as steam temp and atmospheric pressure
28	change in pipe surface temperature	ΔTps	*[° C]*	ΔTps = T1,s - T2,s
29	Estimated mass flow rate	ṁ_est	*[kg/s]*	Calculated using Equation 26
30	Upstream pressure before orifice	Po	*[kPa]*	User input value
31	Upstream Temperature before orifice	To	*[° C]*	User input value
32	Differential Pressure	dP_1	*[kPa]*	User input value
33	Mass Flow rate calculation using orifice	ṁ_orifice	*[kg/s]*	Calculated using Equation C.1

6.4 Experimental Results

6.4.1 Results for experiment 1

In experiment 1, the steam set point pressure and temperature from the Cussons plant was set to 3.5 bar and 230 °C respectively. Steam at this pressure and temperature was then allowed to flow through the test rig. To vary the mass flow rate through the rig, the test valve's opening was varied between 0.5 turns and 2 turns in 0.25 turn increments. An increase in the valves opening caused an increase in flow rate through the test length.

Table 4 below illustrates the experimental data, calculated variables and resultant mass flow rates calculated from the mathematical model as well as the verification mass flow rate calculated from the orifice plate. Figure 34 below shows a graphical comparison between the two mass flow rates.

Table 4: Data for experiment 1

	Experimental Input Data								
	Pipe Properties						Temperatures		
	1	2	3	4	5	6	7	8	9
	Length of un-insulated pipe	Outer Diameter of Pipe	Inner Diameter of Pipe	Pipe Wall Thichness	Pipe emissivity	Test Valve Opening	Ambient Temperature	Upstream un-insulated Pipe Surface Temperature	Downstream un-insulated Pipe Surface temperature
	L	Do	Di	t	ε		Tamb	T1,s	T2,s
	[m]	[m]	[m]	[m]		[turns]	[°C]	[°C]	[°C]
1	1.9	0.0213	0.01576	2.77	0.95	0.5	22.8	116.00	97.50
2	1.9	0.0213	0.01576	2.77	0.95	1	22.2	136.00	118.00
3	1.9	0.0213	0.01576	2.77	0.95	1.25	23	154.00	137.00
4	1.9	0.0213	0.01576	2.77	0.95	1.5	22.8	168.00	152.00
5	1.9	0.0213	0.01576	2.77	0.95	1.75	23.1	172.00	157.00
6	1.9	0.0213	0.01576	2.77	0.95	2	22.5	173.00	158.00

	Calculation Sheet 1											
	Heat Loss from the entire length of un-insulated pipe				Thermophysical Properties of Air							
	10	11	12	13	14	15	16	17	18	19	20	21
	Average Pipe Surface Temperature	Pipe Surface Area	Radiation Heat Transfer from un-insulated pipe surface	Convection Heat Transfer from un-insulated pipe surface	Film Temperature	Density of air	Specific heat of air	Dynamic viscosity	Thermal conductivity of air	Kinematic viscosity	Thermal diffusity	Thermal expansion coefficient
	Ts,avg	A_ps	Qrad_ps	Qconv,ps	Tfilm	ρ_a	Cp_a	μ_a	k_a	v_a	α_a	β_a
	[°C]	[m^2]	[W]	[W]	[k]	[kg/m^3]	[J/kgK]	[kg/sm]	[W/mk]	[m^2/s]	[m^2/s]	[1/K]
	106.75	0.12714	89.99	91.73	337.78	1.04	1008.95	2.0173E-05	0.0291	1.9305E-05	2.7598E-05	0.0030
	127.00	0.12714	123.31	120.09	347.60	1.02	1009.68	2.0605E-05	0.0298	2.0293E-05	2.9095E-05	0.0029
	145.50	0.12714	157.50	144.81	357.25	0.99	1010.48	2.1025E-05	0.0305	2.1282E-05	3.0593E-05	0.0028
	160.00	0.12714	188.31	165.90	364.40	0.97	1011.11	2.1334E-05	0.0311	2.2026E-05	3.172E-05	0.0027
	164.50	0.12714	198.26	171.94	366.80	0.96	1011.34	2.1437E-05	0.0312	2.2279E-05	3.2102E-05	0.0027
	165.50	0.12714	200.98	174.36	367.00	0.96	1011.36	2.1446E-05	0.0313	2.23E-05	3.2134E-05	0.0027

Calculation Sheet 2								Orifice Flow Properties			
Free convection coefficients for horizontal cylinder				Mass flow rate calculation							
22	23	24	25	26	27	28	29	30	31	32	33
Prandtl Number	Raleigh Number	Nusselt Number	Convection coefficient	Total Heat Loss	Speciic heat of steam	change in pipe surface temperature	Estimated mass flow rate	Upstream pressure before orifice	Upstream Temperature before orifice	Differential Pressure	Mass Flow rate calculation using orifice
Pr	Ra	Nu	h	Q_tot	Cp_s	ΔTps	ṁ_est	Po	To	dP_1	ṁ_orifice
			[W/m^2 k]	*[W]*	*[J/kg o C]*	*[° C]*	*[kg/s]*	*[kPa]*	*[° C]*	*[kPa]*	*[kg/s]*
0.70	44222.01	6.29	8.59	181.73	2026.22	18.50	0.0048	331	159	0.44	0.0031
0.70	48410.13	6.44	9.01	243.40	1997.10	18.00	0.0068	317	190	1.06	0.0045
0.70	49928.76	6.48	9.30	302.31	1983.33	17.00	0.0090	283	201	2.67	0.0067
0.69	51086.38	6.52	9.51	354.21	1977.73	16.00	0.0112	230	210	5.87	0.0091
0.69	51098.46	6.52	9.56	370.20	1976.75	15.00	0.0125	190	210	7.4	0.0095
0.69	51548.48	6.54	9.59	375.34	1976.55	15.00	0.0127	180	211	9.25	0.0104

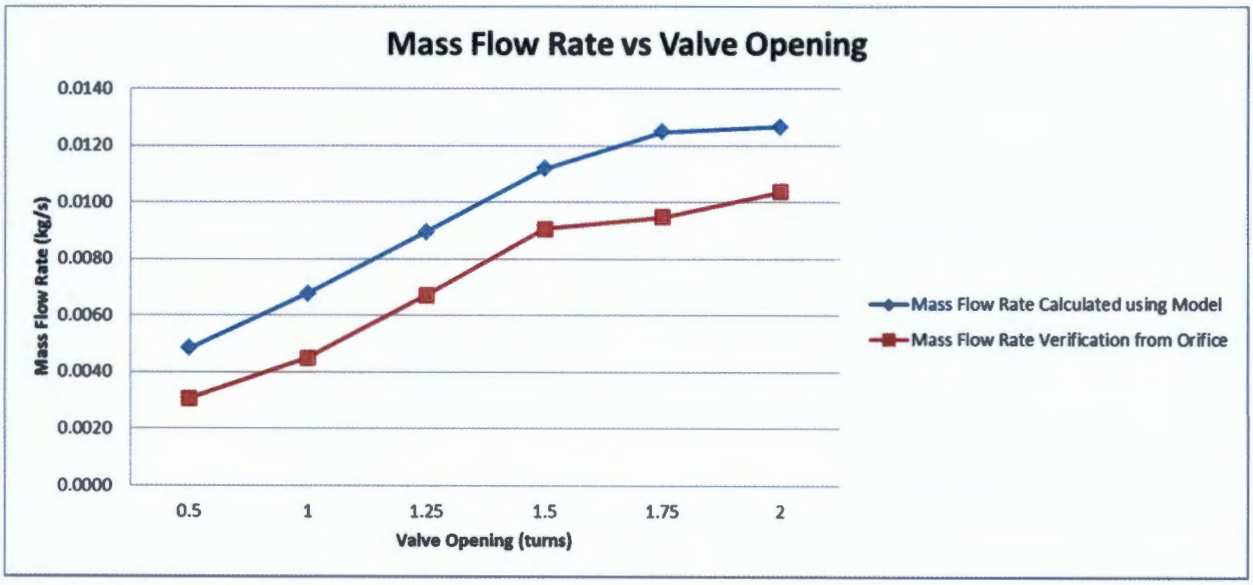

Figure 34: Comparison of mass flow rates for experiment 1

6.4.2 Results for experiment 2

In experiment 2, the steam set point pressure and temperature from the Cussons plant was set to 4 bar and 230 °C respectively. Steam at this pressure and temperature was then allowed to flow through the test rig. To vary the mass flow rate through the rig, the test valve's opening was varied between 1 turn to fully open in 0.25 turn increments.

Table 5 below illustrates the experimental data, calculated variables and resultant mass flow rates calculated from the mathematical model as well as the verification mass flow rate calculated from the orifice plate. Figure 35 below shows a graphical comparison between the two mass flow rates.

Table 5: Data for experiment 2

	Experimental Input Data								
	Pipe Properties						Temperatures		
	1	2	3	4	5	6	7	8	9
	Length of un-insulated pipe	Outer Diameter of Pipe	Inner Diameter of Pipe	Pipe Wall Thichness	Pipe emissivity	Test Valve Opening	Ambient Temperature	Upstream un-insulated Pipe Surface Temperature	Downstream un-insulated Pipe Surface temperature
	L	Do	Di	t	ε		Tamb	T1,s	T2,s
	[m]	[m]	[m]	[m]		[turns]	[°C]	[°C]	[°C]
1	1.9	0.0213	0.01576	2.77	0.95	1	20.8	137.00	119.00
2	1.9	0.0213	0.01576	2.77	0.95	1.25	21	160.00	145.00
3	1.9	0.0213	0.01576	2.77	0.95	1.5	21.8	172.00	157.00
4	1.9	0.0213	0.01576	2.77	0.95	1.75	22	178.00	164.00
5	1.9	0.0213	0.01576	2.77	0.95	2	22	180.00	166.00
6	1.9	0.0213	0.01576	2.77	0.95	2.25	22.5	182.00	168.00
7	1.9	0.0213	0.01576	2.77	0.95	2.5	23	182.00	169.00
8	1.9	0.0213	0.01576	2.77	0.95	2.75	23.2	182.00	170.00
9	1.9	0.0213	0.01576	2.77	0.95	3	23.2	182.00	169.00
10	1.9	0.0213	0.01576	2.77	0.95	fully open	23.8	183.00	171.00

	Calculation Sheet 1											
	Heat Loss from the entire length of un-insulated pipe				Thermophysical Properties of Air							
	10	11	12	13	14	15	16	17	18	19	20	21
	Average Pipe Surface Temperature	Pipe Surface Area	Radiation Heat Transfer from un-insulated pipe surface	Convection Heat Transfer from un-insulated pipe surface	Film Temperature	Density of air	Specific heat of air	Dynamic viscosity	Thermal conductivity of air	Kinematic viscosity	Thermal diffusity	Thermal expansion coefficient
	Ts,avg	A_ps	Qrad_ps	Qconv,ps	Tfilm	ρ_a	Cp_a	μ_a	k_a	v_a	α_a	β_a
	[°C]	[m^2]	[W]	[W]	[k]	[kg/m^3]	[J/kgK]	[kg/sm]	[W/mk]	[m^2/s]	[m^2/s]	[1/K]
	128.00	0.12714	126.05	123.57	347.40	1.02	1009.67	2.0596E-05	0.0298	2.0272E-05	2.9064E-05	0.0029
	152.50	0.12714	173.32	157.94	359.75	0.98	1010.69	2.1134E-05	0.0307	2.1541E-05	3.0985E-05	0.0028
	164.50	0.12714	199.18	174.03	366.15	0.96	1011.28	2.1409E-05	0.0312	2.221E-05	3.1999E-05	0.0027
	171.00	0.12714	214.28	183.19	369.50	0.96	1011.60	2.1553E-05	0.0314	2.2564E-05	3.2534E-05	0.0027
	173.00	0.12714	219.11	186.13	370.50	0.95	1011.69	2.1596E-05	0.0315	2.267E-05	3.2694E-05	0.0027
	175.00	0.12714	223.65	188.25	371.75	0.95	1011.82	2.1649E-05	0.0316	2.2802E-05	3.2895E-05	0.0027
	175.50	0.12714	224.53	188.17	372.25	0.95	1011.86	2.1671E-05	0.0316	2.2855E-05	3.2975E-05	0.0027
	176.00	0.12714	225.63	188.58	372.60	0.95	1011.90	2.1685E-05	0.0317	2.2893E-05	3.3032E-05	0.0027
	175.50	0.12714	224.39	187.84	372.35	0.95	1011.87	2.1675E-05	0.0316	2.2866E-05	3.2991E-05	0.0027
	177.00	0.12714	227.68	189.07	373.40	0.95	1011.98	2.172E-05	0.0317	2.2978E-05	3.3161E-05	0.0027

	Calculation Sheet 2								Orifice Flow Properties			
	Free convection coefficients for horizontal cylinder				Mass flow rate calculation							
	22	23	24	25	26	27	28	29	30	31	32	33
	Prandtl Number	Raleigh Number	Nusselt Number	Convection coefficient	Total Heat Loss	Specific heat of steam	change in pipe surface temperature	Estimated mass flow rate	Upstream pressure before orifice	Upstream Temperature before orifice	Differential Pressure	Mass Flow rate calculation using orifice
	Pr	Ra	Nu	h	Q_tot	Cp_s	ΔTps	ṁ_est	Po	To	dP_1	ṁ_orifice
				[W/m^2 k]	[W]	[J/kg o C]	[°C]	[kg/s]	[kPa]	[°C]	[kPa]	[kg/s]
	0.70	49649.35	6.48	9.07	249.62	1996.09	18.00	0.0069	375	179	0.45	0.0032
	0.70	51917.76	6.55	9.45	331.26	1980.47	15.00	0.0112	336	201	2.13	0.0064
	0.69	51986.68	6.55	9.59	373.20	1976.75	15.00	0.0126	295	210	5.2	0.0094
	0.69	52076.00	6.55	9.67	397.48	1975.74	14.00	0.0144	253	212	8.17	0.0110
	0.69	52129.62	6.55	9.69	405.24	1975.51	14.00	0.0147	228	212	10.26	0.0118
	0.69	51846.53	6.54	9.71	411.90	1975.33	14.00	0.0149	210	213	11.89	0.0123
	0.69	51530.38	6.53	9.70	412.70	1975.33	13.00	0.0161	195	213	12.85	0.0125
	0.69	51411.44	6.53	9.71	414.20	1975.33	12.00	0.0175	185	213	13.35	0.0125
	0.69	51399.94	6.53	9.70	412.23	1975.33	13.00	0.0161	165	213	12.62	0.0117
	0.69	51045.50	6.52	9.71	416.75	1975.26	12.00	0.0176	178	213	14.98	0.0130

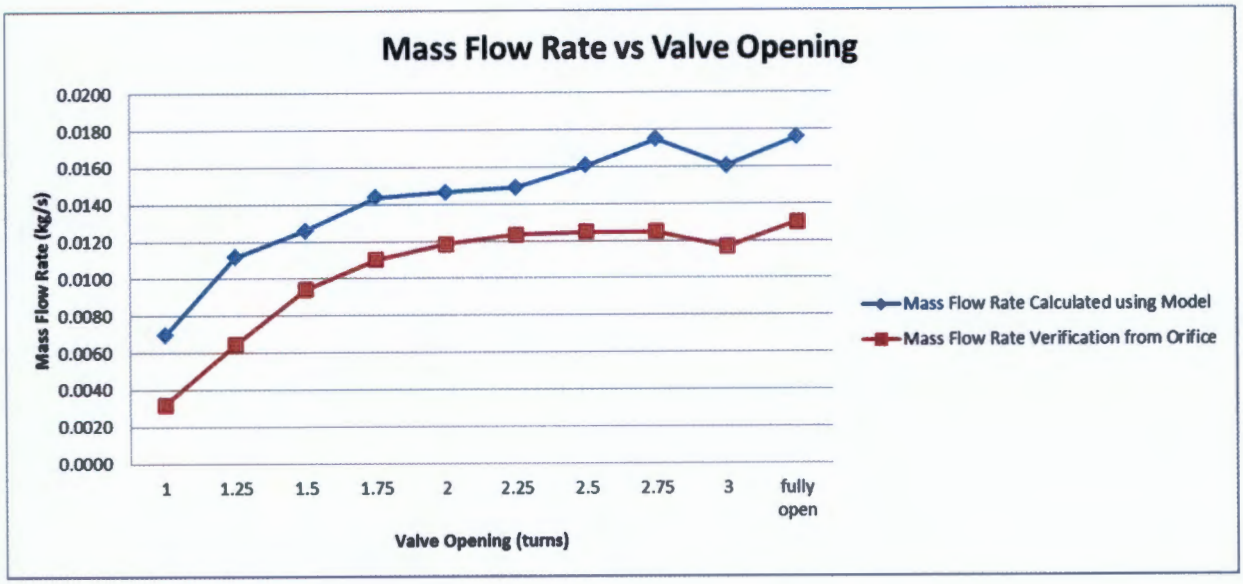

Figure 35: Comparison of mass flow rates for experiment 2

6.4.3 Results for experiment 3

In experiment 3, the steam set point pressure and temperature from the Cussons plant was set to 4.5 bar and 250 °C respectively. Steam at this pressure and temperature was then allowed to flow through the test rig. To vary the mass flow rate through the rig, the test valve's opening was varied between 1 turn and fully open in 0.25 turn increments.

Table 6 below illustrates the experimental data, calculated variables and resultant mass flow rates calculated from the mathematical model as well as the verification mass flow rate calculated from the orifice plate. Figure 36 below shows a graphical comparison between the two mass flow rates.

Table 6: Data for experiment 3

	Experimental Input Data								
	Pipe Properties						Temperatures		
	1	2	3	4	5	6	7	8	9
	Length of un-insulated pipe	Outer Diameter of Pipe	Inner Diameter of Pipe	Pipe Wall Thichness	Pipe emissivity	Test Valve Opening	Ambient Temperature	Upstream un-insulated Pipe Surface Temperature	Downstream un-insulated Pipe Surface temperature
	L	Do	Di	t	ε		Tamb	T1,s	T2,s
	[m]	*[m]*	*[m]*	*[m]*		*[turns]*	*[°C]*	*[°C]*	*[°C]*
1	1.9	0.0213	0.01576	2.77	0.95	1	21.5	153.00	134.00
2	1.9	0.0213	0.01576	2.77	0.95	1.25	22	183.00	166.00
3	1.9	0.0213	0.01576	2.77	0.95	1.5	22.2	194.00	179.00
4	1.9	0.0213	0.01576	2.77	0.95	1.75	22.8	198.00	184.00
5	1.9	0.0213	0.01576	2.77	0.95	2	23	201.00	187.00
6	1.9	0.0213	0.01576	2.77	0.95	2.25	23	203.00	189.00
7	1.9	0.0213	0.01576	2.77	0.95	2.5	23.5	203.00	189.00
8	1.9	0.0213	0.01576	2.77	0.95	2.75	23.5	203.00	189.00
9	1.9	0.0213	0.01576	2.77	0.95	3	24	203.00	190.00
10	1.9	0.0213	0.01576	2.77	0.95	3.25	24	203.00	189.00

Calculation Sheet 1											
Heat Loss from the entire length of un-insulated pipe				Thermophysical Properties of Air							
10	11	12	13	14	15	16	17	18	19	20	21
Average Pipe Surface Temperature	Pipe Surface Area	Radiation Heat Transfer from un-insulated pipe surface	Convection Heat Transfer from un-insulated pipe surface	Film Temperature	Density of air	Specific heat of air	Dynamic viscosity	Thermal conductivity of air	Kinematic viscosity	Thermal diffusity	Thermal expansion coefficient
Ts,avg	A_ps	Qrad_ps	Qconv,ps	Tfilm	ρ_a	Cp_a	μ_a	k_a	ν_a	α_a	β_a
[°C]	[m^2]	[W]	[W]	[k]	[kg/m^3]	[J/kgK]	[kg/sm]	[W/mk]	[m^2/s]	[m^2/s]	[1/K]
143.50	0.12714	154.57	144.29	355.50	0.99	1010.33	2.095E-05	0.0304	2.1101E-05	3.0319E-05	0.0028
174.50	0.12714	222.77	188.33	371.25	0.95	1011.77	2.1628E-05	0.0316	2.2749E-05	3.2814E-05	0.0027
186.50	0.12714	253.30	205.73	377.35	0.94	1012.38	2.1888E-05	0.0320	2.3401E-05	3.38E-05	0.0027
191.00	0.12714	265.01	211.42	379.90	0.93	1012.64	2.1996E-05	0.0322	2.3675E-05	3.4215E-05	0.0026
194.00	0.12714	273.16	215.56	381.50	0.93	1012.81	2.2063E-05	0.0323	2.3848E-05	3.4476E-05	0.0026
196.00	0.12714	278.77	218.55	382.50	0.92	1012.92	2.2106E-05	0.0324	2.3956E-05	3.464E-05	0.0026
196.00	0.12714	278.42	217.71	382.75	0.92	1012.95	2.2116E-05	0.0324	2.3983E-05	3.4681E-05	0.0026
196.00	0.12714	278.42	217.71	382.75	0.92	1012.95	2.2116E-05	0.0324	2.3983E-05	3.4681E-05	0.0026
196.50	0.12714	279.47	217.62	383.25	0.92	1013.00	2.2137E-05	0.0324	2.4038E-05	3.4763E-05	0.0026
196.00	0.12714	278.06	216.87	383.00	0.92	1012.97	2.2127E-05	0.0324	2.401E-05	3.4722E-05	0.0026

Calculation Sheet 2							
Free convection coefficients for horizontal cylinder				Mass flow rate calculation			
22	23	24	25	26	27	28	29
Prandtl Number	Raleigh Number	Nusselt Number	Convection coefficient	Total Heat Loss	Speciic heat of steam	change in pipe surface temperature	Estimated mass flow rate
Pr	Ra	Nu	h	Q_tot	Cp_s	ΔTps	ṁ_est
			[W/m^2 k]	[W]	[J/kg o C]	[°C]	[kg/s]
0.70	50852.70	6.52	9.30	298.86	1983.87	19.00	0.0079
0.69	52165.08	6.55	9.71	411.10	1975.26	17.00	0.0122
0.69	52186.27	6.55	9.85	459.03	1975.21	15.00	0.0155
0.69	51814.95	6.54	9.89	476.43	1975.49	14.00	0.0172
0.69	51681.62	6.54	9.91	488.72	1975.80	14.00	0.0177
0.69	51668.36	6.54	9.94	497.32	1976.05	14.00	0.0180
0.69	51366.45	6.53	9.93	496.13	1976.05	14.00	0.0179
0.69	51366.45	6.53	9.93	496.13	1976.05	14.00	0.0179
0.69	51062.99	6.52	9.92	497.10	1976.05	13.00	0.0194
0.69	51065.99	6.52	9.92	494.93	1976.05	14.00	0.0179

Orifice Flow Properties			
30	31	32	33
Upstream pressure before orifice	Upstream Temperature before orifice	Differential Pressure	Mass Flow rate calculation using orifice
Po	To	dP_1	ṁ_orifice
[kPa]	[°C]	[kPa]	[kg/s]
416	223	2.43	0.0073
375	228	4.5	0.0094
331	230	6.5	0.0107
291	232	9.44	0.0122
258	233	11.97	0.0131
240	234	13.3	0.0134
223	234	14.59	0.0137
215	234	15.55	0.0139
209	234	16.17	0.0140
204	234	16.69	0.0141

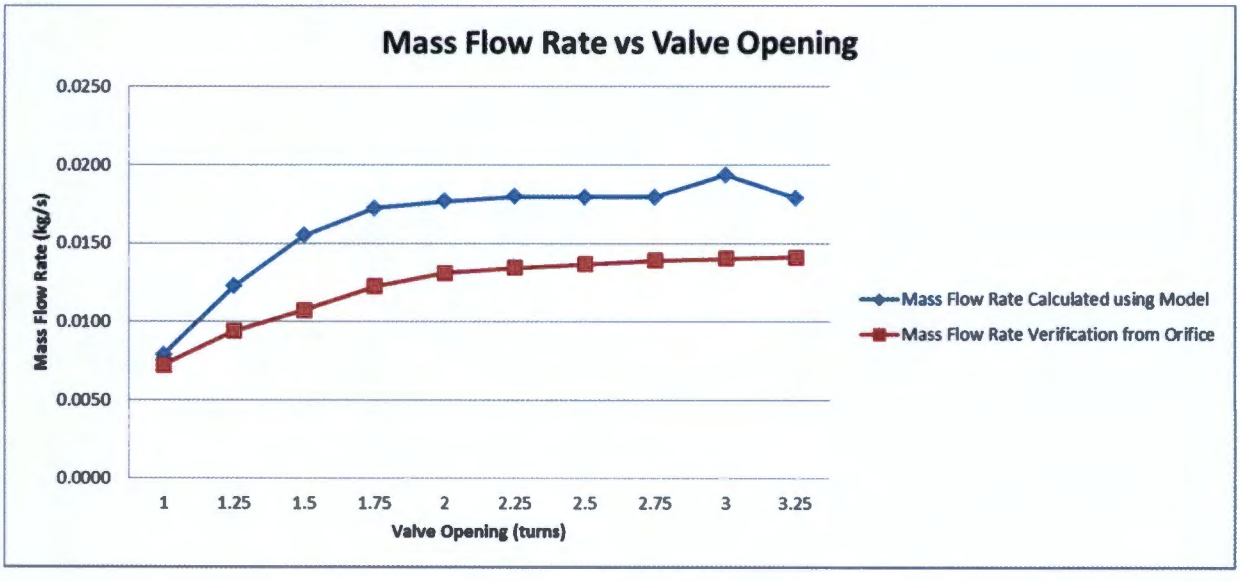

Figure 36: Comparison of mass flow rates for experiment 3

6.4.4 Results for experiment 4

In experiment 4, the steam set point pressure and temperature from the Cussons plant was set to 5 bar and 230 °C respectively. Steam at this pressure and temperature was then allowed to flow through the test rig. To vary the mass flow rate through the rig, the test valve's opening was varied between 1 turn and fully open in 0.25 turn increments.

Table 7 below illustrates the experimental data, calculated variables and resultant mass flow rates calculated from the mathematical model as well as the verification mass flow rate calculated from the orifice plate. Figure 37 below shows a graphical comparison between the two mass flow rates.

Table 7: Data for experiment 4

	Experimental Input Data								
	Pipe Properties						Temperatures		
	1	2	3	4	5	6	7	8	9
	Length of un-insulated pipe	Outer Diameter of Pipe	Inner Diameter of Pipe	Pipe Wall Thichness	Pipe emissivity	Test Valve Opening	Ambient Temperature	Upstream un-insulated Pipe Surface Temperature	Downstream un-insulated Pipe Surface temperature
	L	Do	Di	t	ε		Tamb	T1,s	T2,s
	[m]	[m]	[m]	[m]		[turns]	[°C]	[°C]	[°C]
1	1.9	0.0213	0.01576	2.77	0.95	0.75	23	119.00	104.00
2	1.9	0.0213	0.01576	2.77	0.95	1	23.5	146.00	130.00
3	1.9	0.0213	0.01576	2.77	0.95	1.25	23.5	165.00	151.00
4	1.9	0.0213	0.01576	2.77	0.95	1.5	23.2	177.00	165.00
5	1.9	0.0213	0.01576	2.77	0.95	1.75	23.2	182.00	170.00
6	1.9	0.0213	0.01576	2.77	0.95	2	23.2	184.00	172.00
7	1.9	0.0213	0.01576	2.77	0.95	2.25	23	184.00	171.00
8	1.9	0.0213	0.01576	2.77	0.95	2.5	23	184.00	171.00
9	1.9	0.0213	0.01576	2.77	0.95	2.75	23	184.00	171.00
10	1.9	0.0213	0.01576	2.77	0.95	fully open	23	184.00	171.00

Calculation Sheet 1											
Heat Loss from the entire length of un-insulated pipe				Thermophysical Properties of Air							
10	11	12	13	14	15	16	17	18	19	20	21
Average Pipe Surface Temperature	Pipe Surface Area	Radiation Heat Transfer from un-insulated pipe surface	Convection Heat Transfer from un-insulated pipe surface	Film Temperature	Density of air	Specific heat of air	Dynamic viscosity	Thermal conductivity of air	Kinematic viscosity	Thermal diffusity	Thermal expansion coefficient
Ts,avg	A_ps	Qrad_ps	Qconv,ps	Tfilm	ρ_a	Cp_a	μ_a	k_a	v_a	α_a	β_a
[°C]	[m^2]	[W]	[W]	[k]	[kg/m^3]	[J/kgK]	[kg/sm]	[W/mk]	[m^2/s]	[m^2/s]	[1/K]
111.50	0.12714	97.11	97.79	340.25	1.04	1009.13	2.0282E-05	0.0293	1.9552E-05	2.7972E-05	0.0029
138.00	0.12714	142.49	133.46	353.75	1.00	1010.18	2.0873E-05	0.0303	2.0921E-05	3.0046E-05	0.0028
158.00	0.12714	183.39	161.91	363.75	0.97	1011.05	2.1306E-05	0.0310	2.1958E-05	3.1617E-05	0.0027
171.00	0.12714	213.43	181.25	370.10	0.95	1011.65	2.1579E-05	0.0315	2.2627E-05	3.263E-05	0.0027
176.00	0.12714	225.63	188.58	372.60	0.95	1011.90	2.1685E-05	0.0317	2.2893E-05	3.3032E-05	0.0027
178.00	0.12714	230.62	191.52	373.60	0.94	1012.00	2.1728E-05	0.0317	2.2999E-05	3.3193E-05	0.0027
177.50	0.12714	229.51	191.11	373.25	0.95	1011.96	2.1713E-05	0.0317	2.2962E-05	3.3136E-05	0.0027
177.50	0.12714	229.51	191.11	373.25	0.95	1011.96	2.1713E-05	0.0317	2.2962E-05	3.3136E-05	0.0027
177.50	0.12714	229.51	191.11	373.25	0.95	1011.96	2.1713E-05	0.0317	2.2962E-05	3.3136E-05	0.0027
177.50	0.12714	229.51	191.11	373.25	0.95	1011.96	2.1713E-05	0.0317	2.2962E-05	3.3136E-05	0.0027

Calculation Sheet 2								Orifice Flow Properties			
Free convection coefficients for horizontal cylinder				Mass flow rate calculation							
22	23	24	25	26	27	28	29	30	31	32	33
Prandtl Number	Raleigh Number	Nusselt Number	Convection coefficient	Total Heat Loss	Specific heat of steam	change in pipe surface temperature	Estimated mass flow rate	Upstream pressure before orifice	Upstream Temperature before orifice	Differential Pressure	Mass Flow rate calculation using orifice
Pr	Ra	Nu	h	Q_tot	Cp_s	ΔTps	ṁ_est	Po	To	dP_1	ṁ_orifice
			[W/m^2 k]	[W]	[J/kg o C]	[° C]	[kg/s]	[kPa]	[° C]	[kPa]	[kg/s]
0.70	45084.26	6.32	8.69	194.90	2020.49	15.00	0.0064	486	179.1	0.4	0.0034
0.70	48814.76	6.45	9.17	275.94	1988.38	16.00	0.0087	465	197.1	1.18	0.0055
0.69	50490.32	6.50	9.47	345.30	1978.62	14.00	0.0125	430	207.9	2.77	0.0080
0.69	51276.42	6.53	9.65	394.68	1975.87	12.00	0.0166	380	212	6.75	0.0118
0.69	51411.44	6.53	9.71	414.20	1975.33	12.00	0.0175	320	214	9.8	0.0132
0.69	51453.13	6.53	9.73	422.13	1975.20	12.00	0.0178	280	214	11.96	0.0138
0.69	51572.84	6.54	9.73	420.61	1975.20	13.00	0.0164	240	214	12.9	0.0135
0.69	51572.84	6.54	9.73	420.61	1975.20	13.00	0.0164	215	214	14.3	0.0136
0.69	51572.84	6.54	9.73	420.61	1975.20	13.00	0.0164	214	214	15.57	0.0141
0.69	51572.84	6.54	9.73	420.61	1975.20	13.00	0.0164	196	214	16.17	0.0139

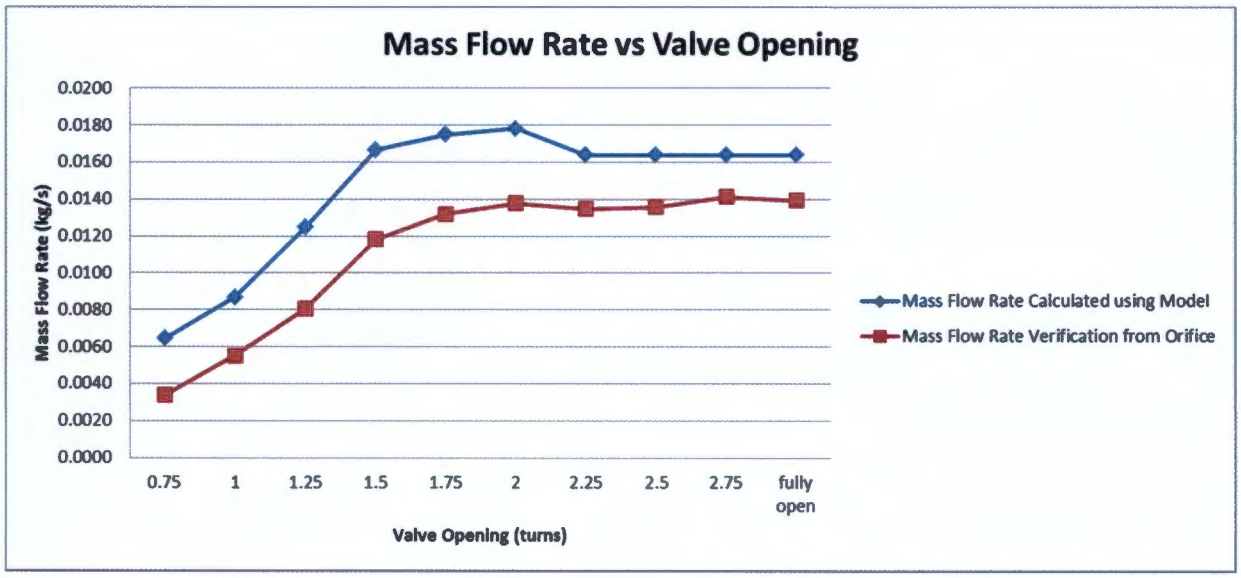

Figure 37: Comparison of mass flow rates for experiment 4

6.4.5 Results for experiment 5

In experiment 5, the steam set point pressure and temperature from the Cussons plant was varied between 2.5 bar and 6.5 bar in 0.5 bar increments whilst the test valve's position was maintained at 1 turn and the outlet temperature from the machine was maintained at 230 °C.

Table 8 below illustrates the experimental data, calculated variables and resultant mass flow rates calculated from the mathematical model as well as the verification mass flow rate calculated from the orifice plate. Figure 38 below shows a graphical comparison between the two mass flow rates.

Table 8: Data for experiment 5

Experimental Input Data									
	Pipe Properties						Temperatures		
	1	2	3	4	5	6	7	8	9
	Length of un-insulated pipe	Outer Diameter of Pipe	Inner Diameter of Pipe	Pipe Wall Thichness	Pipe emissivity	Test Valve Opening	Ambient Temperature	Upstream un-insulated Pipe Surface Temperature	Downstream un-insulated Pipe Surface temperature
	L	Do	Di	t	ε		Tamb	T1,s	T2,s
	[m]	*[m]*	*[m]*	*[m]*		*[turns]*	*[° C]*	*[° C]*	*[° C]*
1	1.9	0.0213	0.01576	2.77	0.95	1	20.9	120.00	102.00
2	1.9	0.0213	0.01576	2.77	0.95	1	22.8	128.00	110.00
3	1.9	0.0213	0.01576	2.77	0.95	1	22.1	135.00	117.00
4	1.9	0.0213	0.01576	2.77	0.95	1	22.1	140.00	122.00
5	1.9	0.0213	0.01576	2.77	0.95	1	22.9	145.00	128.00
6	1.9	0.0213	0.01576	2.77	0.95	1	23.2	149.00	133.00
7	1.9	0.0213	0.01576	2.77	0.95	1	23	154.00	138.00
8	1.9	0.0213	0.01576	2.77	0.95	1	23.5	156.00	141.00
9	1.9	0.0213	0.01576	2.77	0.95	1	23	159.00	144.00

Calculation Sheet 1											
Heat Loss from the entire length of un-insulated pipe				Thermophysical Properties of Air							
10	11	12	13	14	15	16	17	18	19	20	21
Average Pipe Surface Temperature	Pipe Surface Area	Radiation Heat Transfer from un-insulated pipe surface	Convection Heat Transfer from un-insulated pipe surface	Film Temperature	Density of air	Specific heat of air	Dynamic viscosity	Thermal conductivity of air	Kinematic viscosity	Thermal diffusity	Thermal expansion coefficient
Ts,avg	A_ps	Qrad_ps	Qconv,ps	Tfilm	ρ_a	Cp_a	μ_a	k_a	v_a	α_a	β_a
[° C]	*[m^2]*	*[W]*	*[W]*	*[k]*	*[kg/m^3]*	*[J/kgK]*	*[kg/sm]*	*[W/mk]*	*[m^2/s]*	*[m^2/s]*	*[1/K]*
111.00	0.12714	97.81	100.13	338.95	1.04	1009.04	2.0225E-05	0.0292	1.9422E-05	2.7776E-05	0.0030
119.00	0.12714	109.28	108.22	343.90	1.03	1009.40	2.0443E-05	0.0296	1.9919E-05	2.8528E-05	0.0029
126.00	0.12714	121.64	118.85	347.05	1.02	1009.64	2.0581E-05	0.0298	2.0237E-05	2.901E-05	0.0029
131.00	0.12714	130.50	125.79	349.55	1.01	1009.84	2.069E-05	0.0300	2.0491E-05	2.9395E-05	0.0029
136.50	0.12714	140.08	132.26	352.70	1.00	1010.09	2.0828E-05	0.0302	2.0813E-05	2.9883E-05	0.0028
141.00	0.12714	148.47	138.13	355.10	0.99	1010.29	2.0932E-05	0.0304	2.106E-05	3.0256E-05	0.0028
146.00	0.12714	158.51	145.52	357.50	0.99	1010.50	2.1036E-05	0.0306	2.1307E-05	3.0632E-05	0.0028
148.50	0.12714	163.23	148.30	359.00	0.98	1010.63	2.1101E-05	0.0307	2.1463E-05	3.0867E-05	0.0028
151.50	0.12714	169.81	153.36	360.25	0.98	1010.74	2.1155E-05	0.0308	2.1593E-05	3.1064E-05	0.0028

Calculation Sheet 2								Orifice Flow Properties			
Free convection coefficients for horizontal cylinder				Mass flow rate calculation							
22	23	24	25	26	27	28	29	30	31	32	33
Prandtl Number	Raleigh Number	Nusselt Number	Convection coefficient	Total Heat Loss	Speciic heat of steam	change in pipe surface temperature	Estimated mass flow rate	Upstream pressure before orifice	Upstream Temperature before orifice	Differential Pressure	Mass Flow rate calculation using orifice
Pr	Ra	Nu	h	Q_tot	Cp_s	ΔTps	ṁ_est	Po	To	dP_1	ṁ_orifice
			[W/m^2 k]	*[W]*	*[J/kg o C]*	*[° C]*	*[kg/s]*	*[kPa]*	*[° C]*	*[kPa]*	*[kg/s]*
0.70	46711.88	6.38	8.74	197.94	2018.72	18.00	0.0054	225.4	179	0.73	0.0033
0.70	46668.71	6.38	8.85	217.50	2006.50	18.00	0.0060	278	179	0.78	0.0037
0.70	48343.45	6.43	9.00	240.49	1998.15	18.00	0.0067	325	190.1	0.91	0.0042
0.70	49032.94	6.46	9.09	256.29	1993.25	18.00	0.0071	365	190.1	1.01	0.0047
0.70	49093.50	6.46	9.16	272.34	1989.12	17.00	0.0081	420	197	1.17	0.0053
0.70	49355.20	6.47	9.22	286.60	1986.30	16.00	0.0090	470	197	1.3	0.0058
0.70	49972.68	6.49	9.31	304.03	1983.33	16.00	0.0096	510	201	1.4	0.0062
0.70	49823.77	6.48	9.33	311.53	1982.29	15.00	0.0105	570	201	1.52	0.0068
0.70	50412.81	6.50	9.39	323.17	1980.90	15.00	0.0109	617	205	1.7	0.0074

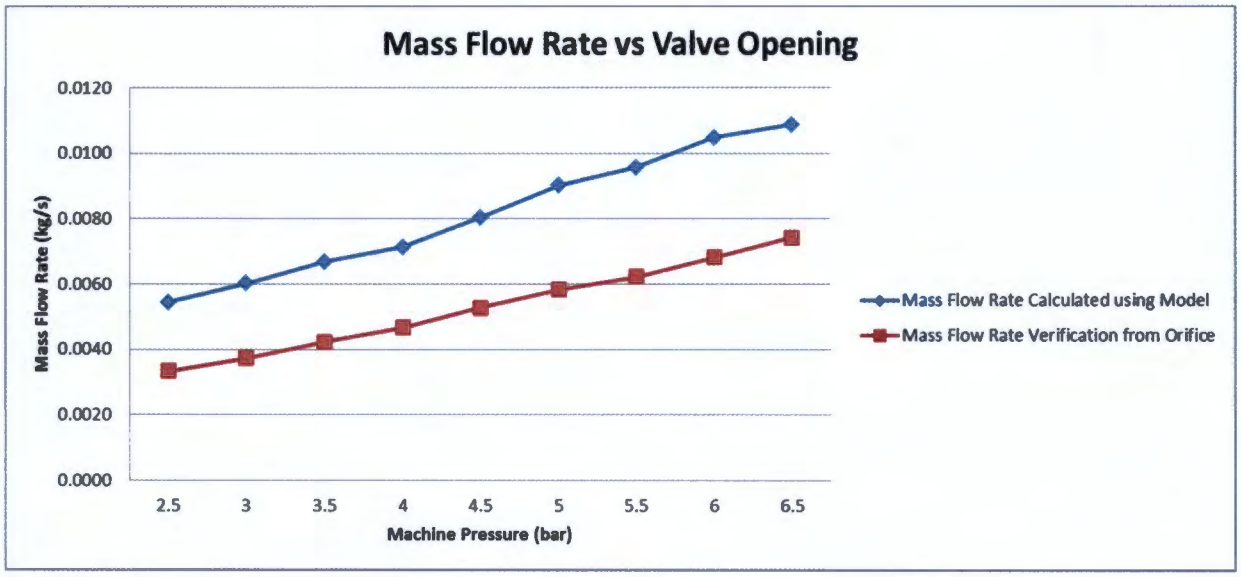

Figure 38: Comparison of mass flow rates for experiment 5

6.5 Discussion on experimental results

In experiment 1 to 4, it can be seen that as the test valve's opening was increased it resulted in an increase in flow rate through the test rig. The increase in flow rate results in more energy being transferred through the un-insulated pipe which results in more energy being transferred through the pipe wall to the surroundings. This is evident from the experimentation: as the mass flow rate increased through the test length, the surface temperatures of the un-insulated pipe increased resulting in an increase in the total heat loss from the un-insulated pipe length. In experiment 5, the increase in mass flow rate through the rig was accomplished by varying the outlet pressure of the mini steam plant. It can be seen in figure 36, that an increase in pressure resulted in an increase in flow rate through the test rig.

In all experiments 1 to 5 it can be seen that the mass flow rate calculated using the mathematical model and the mass flow rate calculated using the orifice plate trend each other, although the mass flow rate calculated using the mathematical model is always greater than the mass flow rate calculated using the orifice. Figure 39 below shows the difference between the mass flow rate calculated using the mathematical model and the mass flow rate calculated using the verification orifice.

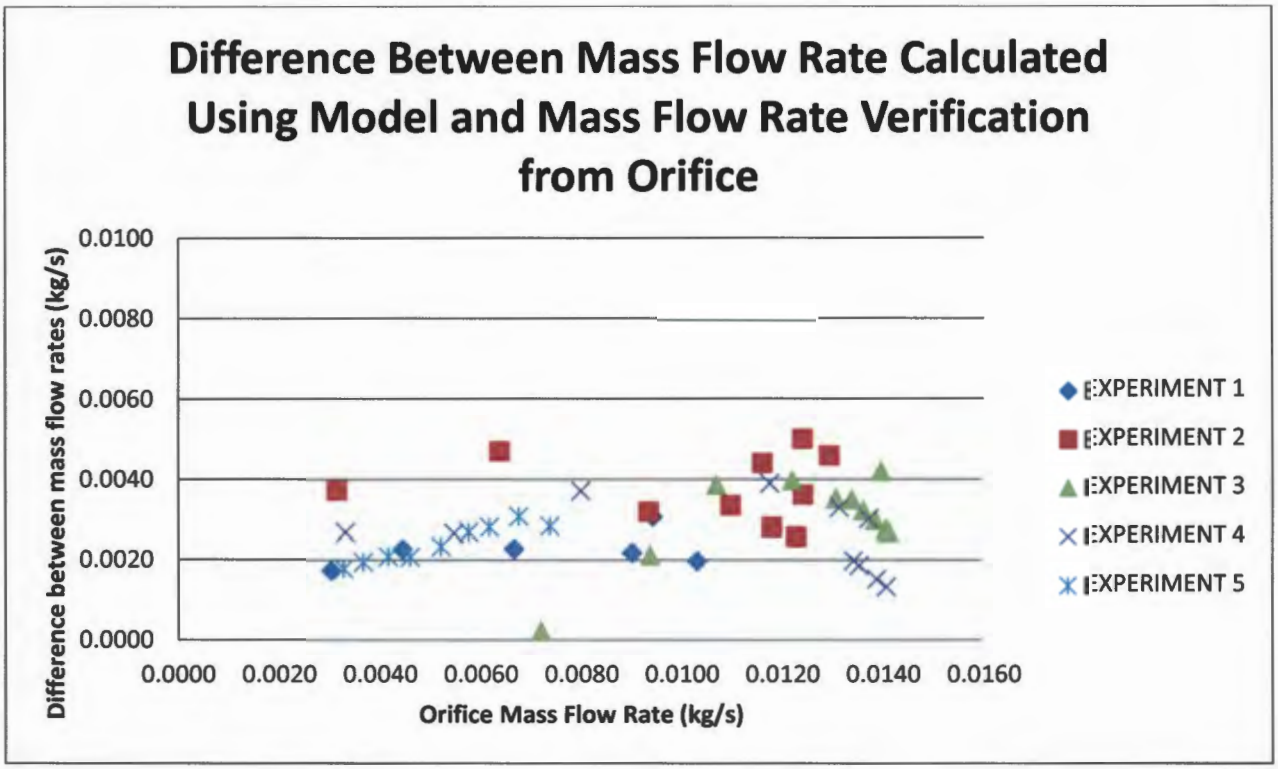

Figure 39: Difference between mass flow rates calculated using model and mass flow rate calculated using orifice plate

From the above figure one can see that the difference between the mass flow rate calculated using the mathematical model and the mass flow rate calculated using the orifice plate varies between 0.002 kg/s and 0.004 kg/s for all mass flow rates experienced in the experiments. It can roughly be concluded that the difference remains constant for all flow rates experienced during the experimentation. This means that for lower mass flow rates, the percentage difference between model and actual will be greater whilst for higher mass flow rates the percentage difference will be smaller.

It was pointed out that due to no instrumentation being available to measure steam temperature on the drain lines in the power plant, an assumption needed to be made to calculate the mass flow rate using the proposed technique. It was assumed that the change in steam temperature ($T_{1,steam} - T_{2,steam}$) across the length of un-insulated pipe is equal to the change in pipe surface temperature ($T_{1,pipe\ surface} - T_{2,pipe\ surface}$) across the same length . To prove the validity of this assumption, one needs to measure the change in steam temperature on upstream and downstream points of the un-insulated pipe and compare with the change in pipe surface temperatures along the same length. It was decided to simulate a computational model identical to the experimental test rig set-up in Flownex SE and compare these two temperatures. Figure 40 below illustrates the computational model created in Flownex.

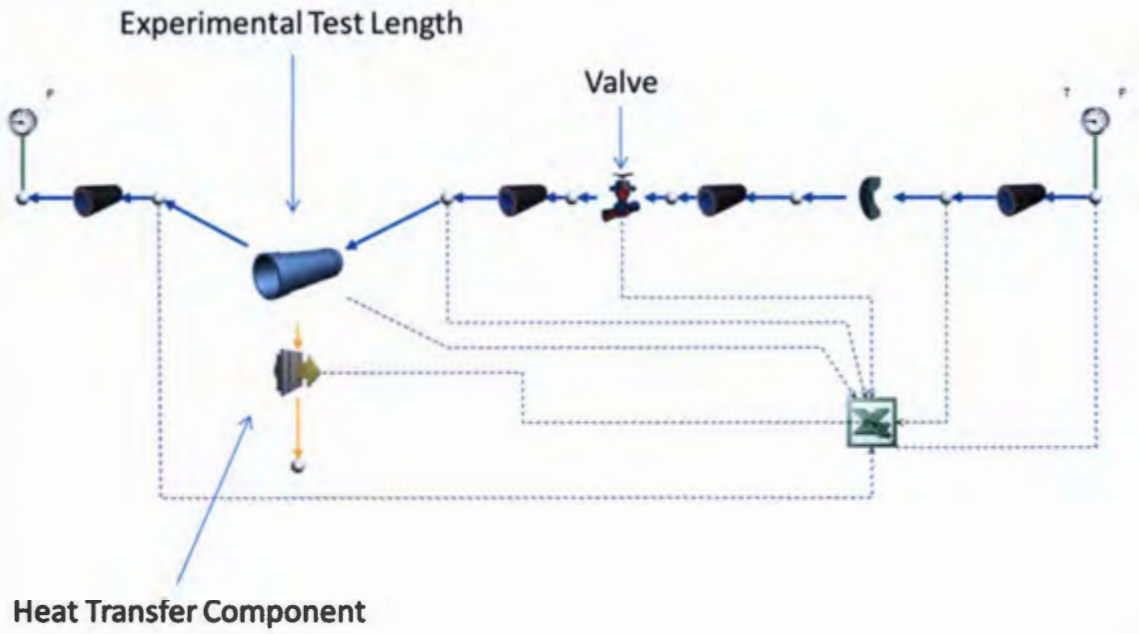

Figure 40: Flownex model based on experimental test rig

The above computational model identically resembled the experimental test rig set-up. The computational model was simulated with steam flowing at 0.001 kg/s to 0.04 kg/s at a fixed temperature of 230 °C. Relevant properties were output to an excel spread sheet and analysed.

The results from the simulation are given in Appendix D. Figure 41 shows a graphical representation of the change in temperatures on the pipe surface and the steam flow.

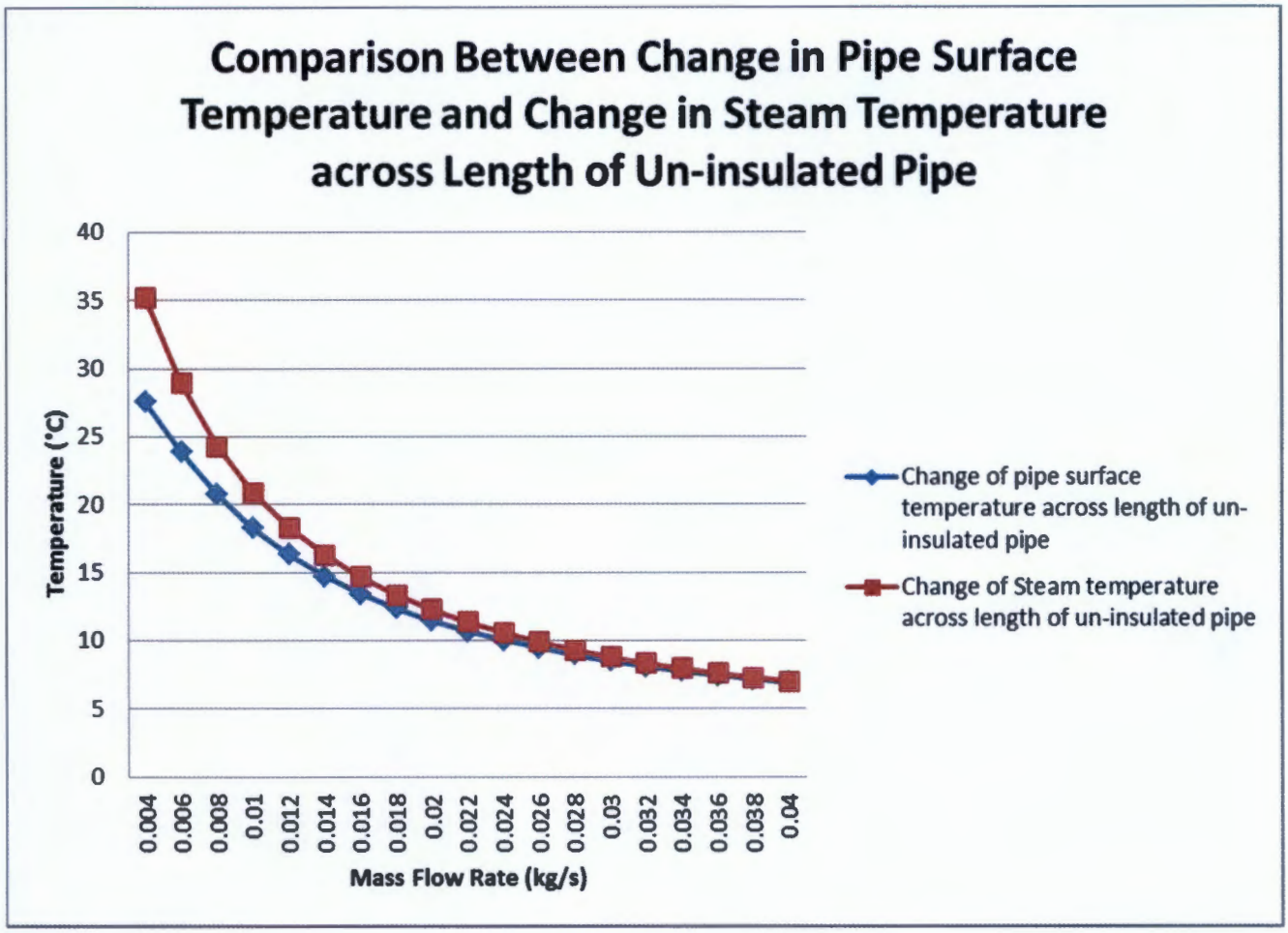

Figure 41: Comparison between change in pipe surface temperature to change in steam temperature over length of un-insulated pipe

It is clearly evident from the above graph that the change in pipe surface temperature deviates from the change in steam temperature at low mass flow rates. At higher mass flow rates the change in pipe surface temperature equals the change in steam temperature across the length of the un-insulated pipe. This indicates that the assumption made in the mathematical model that equated the change in steam temperature across the length of un-insulated pipe to the change in pipe surface temperature across the same length is not valid for all mass flow rates. To mitigate this, one needs to find a method to calculate the change in steam temperature.

6.6 Calculating the change in steam temperature

To calculate the change in steam temperature, it was decided to try and calculate the steam temperatures at upstream and downstream points of the un-insulated pipe. The difference of these two temperatures is the change in steam temperature across the length of un-insulated pipe. To accomplish this, the upstream and downstream of the un-insulated pipe were broken up into two increments as shown in figure 42 below. Upstream and downstream points were labelled 1 and 2 respectively. The upstream and downstream control volumes were analysed as is shown in figure 43.

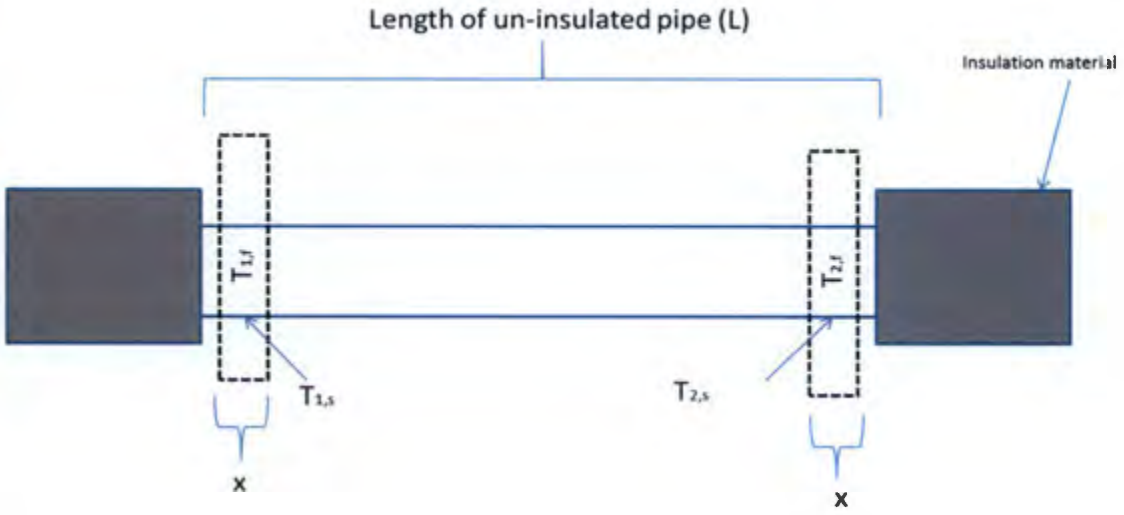

Figure 42: Schematic of un-insulated pipe showing upstream and downstream increments

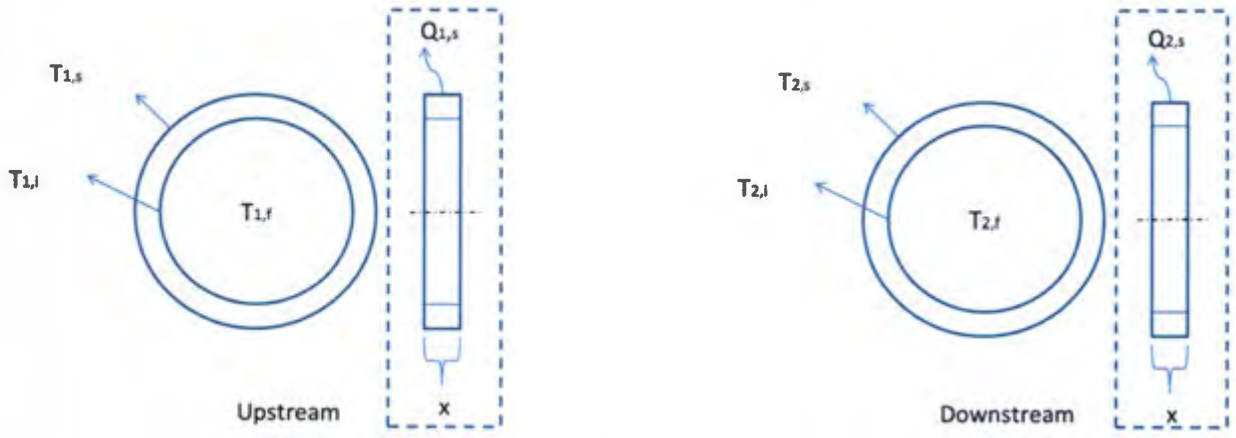

Figure 43: Upstream and downstream control volumes

6.6.1 Calculating upstream steam temperature

As the fluid flows through the upstream control volume, x, heat energy is lost from the fluid to the pipe internal wall by convection heat transfer in the radial direction. The heat energy is then transferred in the radial direction to the pipe surface by conduction heat transfer and thereafter the heat energy is lost to the surrounding atmosphere by convection and radiation heat transfer. Since energy is conserved, the total heat lost from the fluid in the upstream control volume is equal to the heat lost through the pipe wall which is equal to the heat lost from the pipe surface, assuming one dimensional heat transfer. This is shown in equation 37 below.

$$Q_{1,f} = Q_{1,i} = Q_{1,s} \qquad \textbf{Equation 37}$$

Where:

$Q_{1,f}$ is the heat lost from the fluid by convection heat transfer for control volume 1

$Q_{1,i}$ is the heat transferred through the pipe wall by conduction for control volume 1

$Q_{1,S}$ is the heat lost to the surrounding atmosphere for control volume 1

The heat lost to the surrounding atmosphere is a combination of convection and radiation heat transfer and can be calculated by equation 38 below.

$$Q_{1,s} = h_{1,S}A_{1,sx}(T_{1,s} - T_{amb}) + \varepsilon\sigma A_{1,sx}(T_{1,s}^4 - T_{amb}^4) \qquad \textbf{Equation 38}$$

Where:

$A_{1,sx}$ is the surface area of the pipe for control volume 1

$T_{1,s}$ is the upstream pipe surface temperature

$h_{1,s}$ is the free convection coefficient

T_{amb} is the air temperature in the vicinity of the un-insulated pipe

In the above equation, the convection coefficient ($h_{1,s}$) can be solved from the Nusselt number correlation given in section 5.2, the surface area can be calculated using equation 36 in section 5.2 and the pipe surface temperature can be acquired by means of an infrared thermal camera. Equation 38 can then be used to solve for the total heat loss from the pipe surface of the control volume. From equation 37, the total heat lost from the pipe surface is equal to the total heat lost through the pipe wall.

The heat lost through the pipe wall by conduction heat transfer for the control volume can be expressed by equation 39 below.

$$Q_{1,i} = \frac{2\pi x k_i}{\ln\left(\frac{r_0}{r_i}\right)} \left(T_{1,i} - T_{1,s}\right) \qquad \textbf{Equation 39}$$

Where:

X is the length of the control volume

K_i is the thermal conductivity of the material

r_o and r_i are the pipe outer radius and inner radius respectively

$T_{1,i}$ is the pipe internal wall temperature for the upstream control volume

By rearranging equation 39 above, one can calculate the pipe internal wall temperature at point 1.

The heat lost from the fluid by convection heat transfer can be expressed by equation 40 below.

$$Q_{1,f} = 2\pi r_i x h_{1,f} \left(T_{1,f} - T_{1,i}\right) \qquad \textbf{Equation 40}$$

Where:

$T_{1,f}$ is the fluid temperature at the upstream control volume

$h_{1,f}$ is the fluid convection coefficient

Before removing the insulation of the downstream pipe, the flow is both hydrodynamically and thermally fully developed. Once the insulation is removed, the heat transfer regime changes abruptly and the flow, although being hydrodynamically fully developed, will not be thermally fully developed anymore. Thus, the thermal entrance length will need to be considered.

If a fluid enters the tube, with a uniform temperature, greater or less than the tube surface temperature, heat transfer will occur and a thermal boundary layer begins to develop. In the thermal entrance region, the temperature of the central portion of the flow outside the thermal boundary layer remains unchanged, but in the boundary layer the temperature either decreases or increases sharply depending if the fluid is at a higher or lower temperature than

the pipe wall. At the thermal entrance length, $X_{fd,t}$, the thermal boundary layer has filled the tube and the thermally fully developed flow condition has been reached. The convection coefficient varies in the thermal entrance region compared to the fully developed region, were it is a constant, and thus it is important to take the thermal entrance region into consideration.

Laminar and turbulent flow conditions defer significantly with regards to the calculation of thermal entrance lengths. Due to the high pressure drop across the internally leaking valve, it can safely be assumed that the flow will be turbulent. Reynolds number will be calculated in the analysis that will follow and it will be proven that the flow is indeed turbulent.

For turbulent flow, results for $X_{fd,t}$ are based on experimental data. In general lengths are much shorter than their corresponding laminar flow values [29]. The following equation provides a guide for estimating the thermal entrance length for turbulent flow.

$$\left(\frac{X_{fd,t}}{D}\right)_{turb} = 10 \qquad \textbf{Equation 41}$$

In many applications, the tube length will exceed the thermal entry length. Hence, it is often reasonable to assume that the average Nusselt number for the entire tube is equal to the value associated with the fully developed region. Only for short tubes, $\left(\frac{X_{fd,t}}{D}\right)_{turb} \leq 10$, the Nusselt number for the thermally fully developed flow will exceed the Nusselt number for the thermal entrance length, requiring that the entrance region effects must be considered [29][30].

For laminar flow there are many empirical correlations available in literature to calculate the Nusselt number in the entry length. However, for turbulent flow majority of the literature discard the thermal entry length as the entry length is usually significantly smaller than the pipe length and an average Nusselt number is assumed for the entire tube. In the book 'A Heat Transfer Textbook' [29], the author mentions that for $0.01 \leq \mathrm{Pr} \leq 3.0$, the Nusselt number in the thermal entry length will be no more than 5 % above its fully developed value in turbulent flow.

Bhatti and Shah [29] provide the following correlation for the Nusselt number in the thermal entrance region, with L/D > 3 for air and other fluids with Pr ≈ 0.7. In this technique the ratio of length of un-insulated to pipe diameter is significantly larger than 3 and the Prandtl number for steam at atmospheric pressure and temperature greater than 200 °C is approximately 0.9-0,95.

$$\frac{\overline{Nu_D}}{Nu_\infty} = 1 + \frac{C}{\left(\frac{L}{D}\right)^n} \qquad \textbf{Equation 42}$$

Where:

$\overline{Nu_D}$ is the Nusselt number in the thermal entrance region

Nu_∞ is the Nusselt number in the fully developed region

C and n are constant depending on inlet configuration. For straight pipe C = 0.9756 and

n = 0,760

By substituting values for the length and diameter of the un-insulated pipe and values for C and n, the ratio $\frac{\overline{Nu_D}}{Nu_\infty}$, equates to 1.024, which means that the Nusselt number in the thermal entry region is 1.024 times, or 2% greater than the Nusselt number in the fully developed region.

The Nusselt number for forced convection in fully developed pipe flow can be calculated by the empirical correlation given by Dittus-Boelter [23] shown in equation 44 below. The Nusselt number for the thermal entry length, for the upstream increment, can then be calculated by multiplying the Nusselt number for fully developed flow by the ratio $\frac{\overline{Nu_D}}{Nu_\infty}$. The convection coefficient can then be calculated using equation 43 below.

$$h_{1,f} = \frac{Nu.k}{d_i} \qquad \textbf{Equation 43}$$

$$Nu = 0.023\, Re_{1,f}^{0.8} Pr_{1,f}^{0.3} \qquad \textbf{Equation 44}$$

Where:

$K_{1,f}$ is the thermal conductivity of the fluid at point 1

d_i is the pipe internal diameter

$Re_{1,f}$ is the Reynolds number for the fluid flow at point 1

$Pr_{1,f}$ is the Prandtl number for the fluid flow at point 1

The Reynolds number can be calculated from equation 45 below.

$$Re_{1,f} = \frac{4\dot{m}}{\pi d_i \mu_{1,f}} \qquad \textbf{Equation 45}$$

Where:

$\mu_{1,f}$ is the dynamic viscosity of the fluid at point 1

It can be seen that the Reynolds number is a function of the mass flow rate. The Prandtl number, thermal conductivity of the fluid and the dynamic viscosity is a function of the fluid pressure and temperature. The mass flow rate and the fluid temperatures are unknown and needs to be estimated first and then solved iteratively.

The following is a procedure that can be followed to calculate an estimate of the mass flow rate and the fluid temperature. The mass flow rate can be calculated using equation 26 derived in section 5.2. This equation formed the bases of the mathematical model to calculate the mass flow rate and it was shown in the experimental result that the mass flow rate calculated using the mathematical model trended the mass flow rate acquired from the orifice plate. The fluid temperature can be estimated to be the pipe internal wall temperature, $T_{1,i}$, which can be calculated using equation 39 above.

Once an estimate of the mass flow rate and the fluid temperature is acquired, the Reynolds number, the Nusselt number and the convection coefficient of the steam flow can be calculated from equations 45, 44 and 43 respectively. Once the heat transfer coefficient is calculated, equation 40 can be rearranged to calculate a first estimate of the upstream fluid temperature ($T_{1,f}$).

6.6.2 Calculating downstream steam temperature

The calculation of the downstream steam temperature will follow the exact same procedure as calculating the upstream steam temperature explained above. All subscript 1 in equations 37 to 45 should be changed to subscript 2.

As is the case above, the mass flow rate and the fluid temperature for the downstream control volume is unknown and has to be estimated. The mass flow rate estimate will be the same as above and the fluid temperature can be estimated to be the pipe internal wall temperature ($T_{2,i}$). The Reynolds number, Nusselt number, Prandtl number and heat transfer coefficient at downstream conditions can then be calculated and equation 40, with subscript 2 instead of 1, can be rearranged to calculate an estimated downstream steam temperature. It should be noted that at the downstream location the flow will be thermally fully developed and equation 44 can be used to calculate the Nusselt number approximation and equation 42 can be ignored.

An estimated change in steam temperature can be calculated by subtracting the estimated upstream steam temperature to the estimated downstream steam temperature. The mathematical model can now be used to calculate a mass flow rate by using the change in

steam temperature and neglecting the change in pipe surface temperature. This is shown in equation 46 below.

$$\dot{m} = \frac{h_{cA_{out}}\left(T_{surface\ avg} - T_{amb}\right) + \varepsilon\sigma A_{out}\left(T^4_{surface\ avg} - T^4_{amb}\right)}{C_p\left(T_{1,f} - T_{2,f}\right)} \qquad \textbf{Equation 46}$$

Initially, the mass flow rate calculated using the above equation will be an estimate since the change in steam temperature along the length of un-insulated pipe was calculated from estimated values. To acquire a more accurate mass flow rate value, an iteration process needs to be pursued. This will require the estimated mass flow rate value calculated from equation 46 to be used to recalculate the Reynolds number, Nusselt number and convection coefficient for the upstream and downstream steam flow using equations 45, 44 and 43 respectively. Once these properties are calculated, equation 40, with subscript 1 can be used to recalculate the upstream steam temperature and with subscript 2 can be used to calculate the downstream steam temperature. The change in steam temperature can then be calculated and a mass flow rate can be recalculated using equation 46 above. The above process can then be repeated until the estimated mass flow rate converges to the resulting mass flow rate.

To simplify the calculation process, all the relevant equations were modelled in Microsoft Excel. An example of the spreadsheet is shown in table 10 below. Excel has a built in iterative solver that allows for repeatedly recalculating a worksheet until a specific numerical condition is met. The spreadsheet requires inputs of the pipe surface temperatures of the un-insulated pipe, the ambient temperatures and the pipe properties such as, length of un-insulated pipe, pipe diameters, pipe thickness, pipe emissivity and the thermal conductivity of the pipe material. The spreadsheet thereafter calculates an estimated mass flow rate by using equation 26, an estimated Reynolds number, Nusselt number, convection coefficient for the upstream and downstream steam flow, an estimated upstream and downstream steam temperature and a resulting mass flow rate is calculated using equation 46. A circular reference is then created by equating the resulting mass flow rate with the initial estimate of the mass flow rate, resulting in a closed loop calculation. This allows excel to solve the mathematical model iteratively until the estimated mass flow rate converges to the resulting mass flow rate.

6.6.3 Validation of method to calculate steam temperatures

The method to calculate steam temperatures derived above needs to be validated to determine its accuracy in calculating the upstream and downstream steam temperatures and resulting mass flow rate. This was done by applying the methods derived above to the Flownex

simulations conducted in chapter 6.5. The results from the simulation, upstream and downstream temperatures of the steam, upstream and downstream temperatures of the pipe surface, and the change of these temperatures are shown in Appendix D.

The pipe surface temperatures generated in Flownex was inserted into the model created in Microsoft Excel to calculate the steam temperatures and a mass flow rate for an internally leaking valve. Table 10 below shows the excel model created to calculate mass flow rate. It should be noted that the excel model has a built in program called X-steam version 2.6, that uses IAPWS IF97 steam tables to calculate relevant steam properties. Due to the size of the spreadsheet, the spreadsheet was broken up into segments and is all shown under table 10. Each column is numbered column 1 to column 113. The below table list each column number and shows how that relevant column was calculated.

Table 9 : Explanation as to how columns are calculated in Excel model

Column Number	Description	Abb	units	Explanation
1	Length of un-insulated pipe	L	*[m]*	User input value
2	Outer Diameter of Pipe	Do	*[m]*	User input value
3	Inner Diameter of Pipe	Di	*[m]*	User input value
4	Pipe Wall Thichness	t	*[m]*	User input value
5	Pipe emissivity	ε		User input value
6	Thermal conductivity of pipe	k-pipe	*[W/mK]*	User input value
7	Ambient Temperature	Tamb	*[°C]*	User input value
8	Upstream un-insulated Pipe Surface Temperature	T1,s	*[°C]*	User input value
9	Downstream un-insulated Pipe Surface temperature	T2,s	*[°C]*	User input value
10	Average Pipe Surface Temperature	Ts,avg	*[°C]*	Average temperature of T1,s and T2,s
11	Surface Area of un-insulated pipe	A_ps	*[m^2]*	A_ps = ∏ x Do x L
12	Radiation Heat Transfer from un-insulated pipe surface	Qrad_ps	*[W]*	Equation 21
13	Convection Heat Transfer from un-insulated pipe surface	Qconv,ps	*[W]*	Equation 20
14	Film Temperature	Tfilm	*[k]*	Equation B.8
15	Density of air	ρ_a	*[kg/m^3]*	Equation B.1
16	Specific heat of air	Cp_a	*[J/kgK]*	Equation B.2
17	Dynamic viscosity	μ_a	*[kg/sm]*	Equation B.3
18	Thermal conductivity of air	k_a	*[W/mk]*	Equation B.4
19	Kinematic viscosity	v_a	*[m^2/s]*	Equation B.5
20	Thermal diffusity	α_a	*[m^2/s]*	Equation B.6

Column Number	Description	Abb	units	Explanation
21	Thermal expansion coefficient	β_a	*[1/K]*	Equation B.7
22	Prandtl Number	Pr		Equation 25
23	Raleigh Number	Ra		Equation 24
24	Nusselt Number	Nu		Equation 23
25	Convection coefficient	h	*[W/m^2 k]*	Equation 22
26	Total Heat Loss	Q_tot	*[W]*	Qrad_ps + Qconv,ps
27	Specific heat of steam	Cp_s	*[J/kg o C]*	From steam tables
28	change in pipe surface temperature	ΔTps	*[°C]*	T1,s - T2,s
29	Estimated mass flow rate	ṁ_est	*[kg/s]*	Equation 26
30	Length of increment on upstream pipe surface	x_1	*[m]*	User input value
31	Surface Area of increment	A_1x	*[m^2]*	A_ps = ∏ x Do x X_1
32	Pipe Surface temperature at increment	T_1s	*[°C]*	T1,s
33	Radiation heat transfer from increment	Q_rad, 1s	*[W]*	Equation 21
34	Convection heat transfer from increment	Q_conv,1s	*[W]*	Equation 20
35	Film Temperature	Tf	*[k]*	Equation B.8
36	Density of air	ρ_a	*[kg/m^3]*	Equation B.1
37	Specific heat of air	Cp_a	*[J/kgK]*	Equation B.2
38	Dynamic viscosity	μ_a	*[kg/sm]*	Equation B.3
39	Thermal conductivity of air	k_a	*[W/mk]*	Equation B.4
40	Kinematic viscosity	v_a	*[m^2/s]*	Equation B.5

Column Number	Description	Abb	units	Explanation
41	Thermal diffusity	**α_a**	*[m^2/s]*	Equation B.6
42	Thermal expansion coefficient	**β_a**	*[1/K]*	Equation B.7
43	Prandtl Number	**Pr**		Equation 25
44	Raleigh Number	**Ra**		Equation 24
45	Nusselt Number	**Nu**		Equation 23
46	Convection coefficient	**h**	*[W/m^2 k]*	Equation 22
47	Total heat transfer from increment	**Q_1,s**	*[W]*	Qrad_1s + Qconv,1s
48	Upstream Pipe wall internal temperature	**T_1,i**	*[°C]*	Equation 39
49	Dynamic viscosity of steam flow	**μ_steam**	*[Pa.s]*	From steam tables assuming T_1i as steam temperature and pressure as atmospheric pressure
50	Reynolds Number	**Re_steam**		Equation 45
51	Prandtl Number	**Pr_steam**		From steam tables assuming T_1i as steam temperature and pressure as atmospheric pressure
52	Nusselt Number	**Nu_steam**		Equation 44 x Equation 42
53	Thermal conductivity of steam	**k_steam**	*[W/mK]*	From steam tables assuming T_1i as steam temperature and pressure as atmospheric pressure
54	Convection coefficient	**h_steam**	*[W/m^2 k]*	Equation 43
55	Upstream steam temperature Estimate	**T_1,f**	*[°C]*	Equation 40
56	Length of increment on Downstream pipe surface	**x_2**	*[m]*	User input value
57	Surface Area of increment	**A_2s**	*[m^2]*	A_ps = ∏ x Do x X_2
58	Downstream pipe surface temperature increment	**T_2,s**	*[°C]*	T_2,s
59	Radiation heat transfer from increment	**Q_rad, 2,s**	*[W]*	Equation 21
60	Convection heat transfer from increment	**Q_conv, 2,s**	*[w]*	Equation 20

Column Number	Description	Abb	units	Explanation
61	Film Temperature	**Tf**	*[k]*	Equation B.8
62	Density of air	**ρ_a**	*[kg/m^3]*	Equation B.1
63	Specific heat of air	**Cp_a**	*[J/kgK]*	Equation B.2
64	Dynamic viscosity	**μ_a**	*[kg/sm]*	Equation B.3
65	Thermal conductivity of air	**k_a**	*[W/mk]*	Equation B.4
66	Kinematic viscosity	**v_a**	*[m^2/s]*	Equation B.5
67	Thermal diffusity	**α_a**	*[m^2/s]*	Equation B.6
68	Thermal expansion coefficient	**β_a**	*[1/K]*	Equation B.7
69	Prandtl Number	**Pr**		Equation 25
70	Raleigh Number	**Ra**		Equation 24
71	Nusselt Number	**Nu**		Equation 23
72	Convection coefficient	**h**	*[W/m^2 k]*	Equation 22
73	Total heat transfer from increment	**Q_2,s**	*[W]*	Q_rad, 2s + Q_conv,2s
74	Downstream Pipe wall internal temperature	**T_2,i**	*[°C]*	Equation 39
75	Dynamic viscosity of steam flow	**μ_steam**	*[Pa.s]*	From steam tables assuming T_2i as steam temperature and pressure as atmospheric pressure
76	Reynolds Number	**Re_steam**		Equation 45
77	Prandtl Number	**Pr_steam**		From steam tables assuming T_2i as steam temperature and pressure as atmospheric pressure
78	Nusselt Number	**Nu_steam**		Equation 44
79	Thermal conductivity of steam	**k_steam**	*[W/mK]*	From steam tables assuming T_2i as steam temperature and pressure as atmospheric pressure
80	Convection coefficient	**h_steam**	*[W/m^2 k]*	Equation 43

Column Number	Description	Abb	units	Explanation
81	Downstream steam temperature estimate	**T_2,f**	*[°C]*	Equation 40
82	Average steam temp		*[°C]*	Average temperature of T1,f and T2,f
83	Specific Heat of Steam	**Cp_steam**	*[J/kg o C]*	From steam tables using average steam temp and pressure as atmospheric pressure
84	Change in steam temperature	**ΔT**	*[°C]*	T_1,f - T_2,f
85	Mass flow rate estimate 2	**ṁ_2est**	*[kg/s]*	Eqaution 46
86	Estimate mass flow rate for iterative solver	**ṁ_est**	*[kg/s]*	Is equal to column 85 as first estimate therafter is iteratively solved with column 113
87	Internal Diameter	**Di**	*[m]*	User input value
88	Estimated upstream steam temp	**T_1f_est**	*[°C]*	column 55
89	Estimated downstream steam temp	**T_2f_est**	*[°C]*	column 81
90	upstream steam temp	**T_1f_est**	*[°C]*	Is equal to column 88 as first estimate therafter is iteratively solved with column 102
91	downstream steam temp	**T_2f_est**	*[°C]*	Is equal to column 89 as first estimate therafter is iteratively solved with column 109
92	Heat loss from increment 1	**Q_1s**	*[W]*	column 47
93	Heat loss from increment 2	**Q_2s**	*[W]*	column 73
94	Pipe upstream internal temp	**T_1i**	*[°C]*	column 48
95	Pipe downstream internal temp	**T_2i**	*[°C]*	column 74
96	Dynamic viscosity of steam flow	**μ_steam**	*[Pa.s]*	From steam tables using T_1f_est and atmospheric pressure
97	Reynolds Number	**Re_steam**		Equation 45
98	Prandtl Number	**Pr_steam**		From steam tables using T_1f_est and atmospheric pressure
99	Nusselt Number	**Nu_steam**		Equation 44 x Equation 42
100	Thermal conductivity of steam	**k_steam**	*[W/mK]*	From steam tables using T_1f_est and atmospheric pressure

Column Number	Description	Abb	units	Explanation
101	Convection coefficient	**h_steam**	*[W/m^2 k]*	Equation 43
102	Upstream steam temperature	**T_1,f**	*[°C]*	Equation 40
103	Dynamic viscosity of steam flow	**μ_steam**	*[Pa.s]*	From steam tables using T_2f_est and atmospheric pressure
104	Reynolds Number	**Re_steam**		Equation 45
105	Prandtl Number	**Pr_steam**		From steam tables using T_2f_est and atmospheric pressure
106	Nusselt Number	**Nu_steam**		Equation 44
107	Thermal conductivity of steam	**k_steam**	*[W/mK]*	From steam tables using T_2f_est and atmospheric pressure
108	Convection coefficient	**h_steam**	*[W/m^2 k]*	Equation 43
109	Downstream steam temperature	**T_2,f**	*[°C]*	Equation 40
110	Average steam temperature		*[°C]*	(T_1,f + T_2,f) /2
111	Specific Heat of Steam	**Cp_steam**	*[J/kg o C]*	From steam tables using average steam temp and atmospheric pressure
112	Change in steam temperature	**ΔT**	*[°C]*	T_1,f - T_2,f
113	Mass flow rate	**ṁ**	*[kg/s]*	Equation 46

Table 10: Model to calculate mass flow rate

Experimental Data- Input Data								
Pipe Properties						Temperatures		
1	2	3	4	5	6	7	8	9
Length of un-insulated pipe	Outer Diameter of Pipe	Inner Diameter of Pipe	Pipe Wall Thichness	Pipe emissivity	Thermal conductivity of pipe	Ambient Temperature	Upstream un-insulated Pipe Surface Temperature	Downstream un-insulated Pipe Surface temperature
L	Do	Di	t	ε	k-pipe	Tamb	T1,s	T2,s
[m]	*[m]*	*[m]*	*[m]*		*[W/mK]*	*[°C]*	*[°C]*	*[°C]*
2	0.0213	0.01576	2.77	0.95	50	20	150.28	122.71
2	0.0213	0.01576	2.77	0.95	50	20	169.04	145.17
2	0.0213	0.01576	2.77	0.95	50	20	179.89	159.14
2	0.0213	0.01576	2.77	0.95	50	20	186.97	168.71
2	0.0213	0.01576	2.77	0.95	50	20	191.93	175.62
2	0.0213	0.01576	2.77	0.95	50	20	195.59	180.85
2	0.0213	0.01576	2.77	0.95	50	20	198.36	184.92
2	0.0213	0.01576	2.77	0.95	50	20	200.54	188.18
2	0.0213	0.01576	2.77	0.95	50	20	202.28	190.83
2	0.0213	0.01576	2.77	0.95	50	20	203.70	193.01
2	0.0213	0.01576	2.77	0.95	50	20	204.86	194.83
2	0.0213	0.01576	2.77	0.95	50	20	205.78	196.33
2	0.0213	0.01576	2.77	0.95	50	20	206.54	197.59
2	0.0213	0.01576	2.77	0.95	50	20	207.17	198.66
2	0.0213	0.01576	2.77	0.95	50	20	207.70	199.58
2	0.0213	0.01576	2.77	0.95	50	20	208.14	200.37
2	0.0213	0.01576	2.77	0.95	50	20	208.51	201.04
2	0.0213	0.01576	2.77	0.95	50	20	208.81	201.63
2	0.0213	0.01576	2.77	0.95	50	20	209.07	202.13

First Estimate of Mass Flow Rate (1)											
Heat Loss from the entire length of un-insulated pipe				Thermophysical Properties of Air							
10	11	12	13	14	15	16	17	18	19	20	21
Average Pipe Surface Temperature	Surface Area of un-insulated pipe	Radiation Heat Transfer from un-insulated pipe surface	Convection Heat Transfer from un-insulated pipe surface	Film Temperature	Density of air	Specific heat of air	Dynamic viscosity	Thermal conductivity of air	Kinematic viscosity	Thermal diffusity	Thermal expansion coefficient
Ts,avg	A_ps	Qrad_ps	Qconv,ps	Tfilm	ρ_a	Cp_a	μ_a	k_a	v_a	α_a	β_a
[°C]	*[m^2]*	*[W]*	*[W]*	*[k]*	*[kg/m^3]*	*[J/kgK]*	*[kg/sm]*	*[W/mk]*	*[m^2/s]*	*[m^2/s]*	*[1/K]*
136.50	0.133832	149.57	143.88	351.25	1.00	1009.97	2.0764E-05	0.0301	2.0664E-05	2.9658E-05	0.0028
157.10	0.133832	193.56	174.91	361.55	0.98	1010.86	2.1211E-05	0.0309	2.1728E-05	3.1269E-05	0.0028
169.51	0.133832	223.29	193.96	367.76	0.96	1011.43	2.1478E-05	0.0313	2.2379E-05	3.2255E-05	0.0027
177.84	0.133832	244.70	206.88	371.92	0.95	1011.83	2.1656E-05	0.0316	2.282E-05	3.2922E-05	0.0027
183.78	0.133832	260.69	216.14	374.89	0.94	1012.13	2.1783E-05	0.0318	2.3137E-05	3.3401E-05	0.0027
188.22	0.133832	273.07	223.10	377.11	0.94	1012.35	2.1877E-05	0.0320	2.3375E-05	3.3761E-05	0.0027
191.64	0.133832	282.87	228.49	378.82	0.93	1012.53	2.195E-05	0.0321	2.3559E-05	3.4039E-05	0.0026
194.36	0.133832	290.80	232.78	380.18	0.93	1012.67	2.2007E-05	0.0322	2.3705E-05	3.4261E-05	0.0026
196.55	0.133832	297.31	236.24	381.28	0.93	1012.79	2.2054E-05	0.0323	2.3824E-05	3.444E-05	0.0026
198.35	0.133832	302.71	239.09	382.18	0.92	1012.88	2.2092E-05	0.0324	2.3921E-05	3.4587E-05	0.0026
199.85	0.133832	307.24	241.45	382.92	0.92	1012.96	2.2123E-05	0.0324	2.4002E-05	3.471E-05	0.0026
201.05	0.133832	310.93	243.37	383.53	0.92	1013.03	2.2149E-05	0.0325	2.4068E-05	3.4808E-05	0.0026
202.06	0.133832	314.04	244.97	384.03	0.92	1013.08	2.217E-05	0.0325	2.4122E-05	3.4891E-05	0.0026
202.92	0.133832	316.68	246.32	384.46	0.92	1013.13	2.2188E-05	0.0325	2.4169E-05	3.4961E-05	0.0026
203.64	0.133832	318.94	247.47	384.82	0.92	1013.17	2.2203E-05	0.0325	2.4208E-05	3.5021E-05	0.0026
204.25	0.133832	320.86	248.44	385.13	0.92	1013.20	2.2216E-05	0.0326	2.4242E-05	3.5071E-05	0.0026
204.78	0.133832	322.50	249.28	385.39	0.92	1013.23	2.2227E-05	0.0326	2.427E-05	3.5114E-05	0.0026
205.22	0.133832	323.91	249.99	385.61	0.92	1013.26	2.2237E-05	0.0326	2.4294E-05	3.5151E-05	0.0026
205.60	0.133832	325.11	250.59	385.80	0.91	1013.28	2.2245E-05	0.0326	2.4315E-05	3.5182E-05	0.0026

First Estimate of Mass Flow Rate (2)							
Free convection coefficients for horizontal cylinder				Mass flow rate calculation			
22	23	24	25	26	27	28	29
Prandtl Number	Raleigh Number	Nusselt Number	Convection coefficient	Total Heat Loss	Speciic heat of steam	change in pipe surface temperature	Estimated mass flow rate
Pr	Ra	Nu	h	Q_tot	Cp_s	ΔTps	ṁ_est
			[W/m^2 k]	[W]	[J/kg o C]	[° C]	[kg/s]
0.70	51303.38	6.53	9.23	293.45	1985.49	27.56	0.0054
0.69	52910.25	6.58	9.53	368.48	1977.45	23.86	0.0078
0.69	53393.10	6.59	9.69	417.26	1975.52	20.75	0.0102
0.69	53550.49	6.60	9.79	451.57	1975.09	18.26	0.0125
0.69	53591.14	6.60	9.86	476.83	1975.12	16.32	0.0148
0.69	53586.12	6.60	9.91	496.17	1975.30	14.74	0.0170
0.69	53562.91	6.60	9.95	511.36	1975.52	13.44	0.0193
0.69	53533.13	6.60	9.98	523.58	1975.75	12.35	0.0215
0.69	53502.08	6.60	10.00	533.54	1975.95	11.45	0.0236
0.69	53472.07	6.59	10.02	541.80	1976.14	10.69	0.0257
0.69	53444.15	6.59	10.03	548.70	1976.31	10.03	0.0277
0.69	53419.67	6.59	10.04	554.30	1976.44	9.46	0.0297
0.69	53397.87	6.59	10.05	559.01	1976.56	8.95	0.0316
0.69	53378.55	6.59	10.06	563.00	1976.67	8.51	0.0335
0.69	53361.52	6.59	10.07	566.40	1976.75	8.12	0.0353
0.69	53346.58	6.59	10.08	569.30	1976.83	7.77	0.0371
0.69	53333.51	6.59	10.08	571.78	1976.89	7.46	0.0388
0.69	53322.12	6.59	10.08	573.89	1976.95	7.18	0.0404
0.69	53312.24	6.59	10.09	575.70	1976.99	6.94	0.0420

Calculating Estimate of upstream steam temperature (1)												
					Thermophysical Properties of Air							
30	31	32	33	34	35	36	37	38	39	40	41	42
Length of increment on upstream pipe surface	Surface Area of increment	Pipe Surface temperature at increment	Radiation heat transfer from increment	Convection heat transfer from increment	Film Temperature	Density of air	Specific heat of air	Dynamic viscosity	Thermal conductivity of air	Kinematic viscosity	Thermal diffusity	Thermal expansion coefficient
x_1	A_1x	T_1s	Q_rad, 1s	Q_conv,1s	Tf	ρ_a	Cp_a	μ_a	k_a	v_a	α_a	β_a
[m]	[m^2]	[° C]	[W]	[W]	[k]	[kg/m^3]	[J/kgK]	[kg/sm]	[W/mk]	[m^2/s]	[m^2/s]	[1/K]
0.005	0.000335	150.28	0.4457	0.4114	358.14	0.99	1010.55	2.106E-05	0.031	2.1374E-05	3.0732E-05	0.0028
0.005	0.000335	169.04	0.5553	0.4831	367.52	0.96	1011.41	2.147E-05	0.031	2.2354E-05	3.2217E-05	0.0027
0.005	0.000335	179.89	0.6254	0.5252	372.94	0.95	1011.93	2.17E-05	0.032	2.2929E-05	3.3087E-05	0.0027
0.005	0.000335	186.97	0.6739	0.5529	376.49	0.94	1012.29	2.185E-05	0.032	2.3308E-05	3.366E-05	0.0027
0.005	0.000335	191.93	0.7093	0.5724	378.97	0.93	1012.55	2.196E-05	0.032	2.3575E-05	3.4063E-05	0.0026
0.005	0.000335	195.59	0.7361	0.5868	380.79	0.93	1012.74	2.203E-05	0.032	2.3772E-05	3.4361E-05	0.0026
0.005	0.000335	198.36	0.7568	0.5977	382.18	0.92	1012.89	2.209E-05	0.032	2.3922E-05	3.4588E-05	0.0026
0.005	0.000335	200.54	0.7734	0.6064	383.27	0.92	1013.00	2.214E-05	0.032	2.404E-05	3.4766E-05	0.0026
0.005	0.000335	202.28	0.7868	0.6133	384.14	0.92	1013.10	2.217E-05	0.032	2.4134E-05	3.4909E-05	0.0026
0.005	0.000335	203.70	0.7978	0.6189	384.85	0.92	1013.17	2.22E-05	0.033	2.4211E-05	3.5026E-05	0.0026
0.005	0.000335	204.86	0.8070	0.6235	385.43	0.92	1013.24	2.223E-05	0.033	2.4275E-05	3.5122E-05	0.0026
0.005	0.000335	205.78	0.8142	0.6272	385.89	0.91	1013.29	2.225E-05	0.033	2.4325E-05	3.5197E-05	0.0026
0.005	0.000335	206.54	0.8202	0.6302	386.27	0.91	1013.33	2.226E-05	0.033	2.4366E-05	3.526E-05	0.0026
0.005	0.000335	207.17	0.8252	0.6327	386.59	0.91	1013.36	2.228E-05	0.033	2.4401E-05	3.5312E-05	0.0026
0.005	0.000335	207.70	0.8294	0.6348	386.85	0.91	1013.39	2.229E-05	0.033	2.4429E-05	3.5355E-05	0.0026
0.005	0.000335	208.14	0.8330	0.6366	387.07	0.91	1013.42	2.23E-05	0.033	2.4453E-05	3.5391E-05	0.0026
0.005	0.000335	208.51	0.8359	0.6380	387.25	0.91	1013.44	2.231E-05	0.033	2.4474E-05	3.5422E-05	0.0026
0.005	0.000335	208.81	0.8384	0.6393	387.41	0.91	1013.45	2.231E-05	0.033	2.449E-05	3.5447E-05	0.0026
0.005	0.000335	209.07	0.8405	0.6403	387.54	0.91	1013.47	2.232E-05	0.033	2.4504E-05	3.5468E-05	0.0026

Calculating Estimate of upstream steam temperature (2)												
Free convection coefficients for increment				Calculating internal pipe wall temperature		Upstream steam properties						
43	44	45	46	47	48	49	50	51	52	53	54	55
Prandtl Number	Raleigh Number	Nusselt Number	Convection coefficient	Total heat transfer from increment	Upstream Pipe wall internal temperature	Dynamic viscosity of steam flow	Reynolds Number	Prandtl Number	Nusselt Number	Thermal conductivity of steam	Convection coefficient	Upstream steam temperature Estimate
Pr	Ra	Nu	h	Q_1,s	T_1,i	μ_steam	Re_steam	Pr_steam	Nu_steam	k_steam	h_steam	T_1,f
			[W/m^2 k]	[W]	[° C]	[Pa.s]				[W/mK]	[W/m^2 k]	[° C]
0.70	52499.72	6.57	9.44	0.857	150.38	1.41978E-05	30512.68	0.98	88.38	0.029	161.70	171.79
0.69	53380.23	6.59	9.69	1.038	169.16	1.49394E-05	42225.81	0.97	114.29	0.031	221.21	188.12
0.69	53570.90	6.60	9.82	1.151	180.02	1.53729E-05	53496.01	0.96	137.92	0.031	275.64	196.89
0.69	53590.44	6.60	9.90	1.227	187.12	1.56574E-05	64588.84	0.96	160.24	0.032	326.94	202.28
0.69	53560.17	6.60	9.95	1.282	192.09	1.58573E-05	75370.22	0.96	181.21	0.033	375.08	205.89
0.69	53516.54	6.60	9.99	1.323	195.74	1.60048E-05	86028.46	0.96	201.37	0.033	421.20	208.43
0.69	53471.96	6.59	10.02	1.355	198.52	1.61171E-05	96556.82	0.96	220.80	0.033	465.52	210.27
0.69	53430.38	6.59	10.04	1.380	200.70	1.62052E-05	106948.57	0.96	239.57	0.033	508.24	211.67
0.69	53393.01	6.59	10.06	1.400	202.45	1.62759E-05	117019.42	0.96	257.41	0.034	548.81	212.75
0.69	53360.06	6.59	10.07	1.417	203.87	1.63334E-05	126873.78	0.96	274.58	0.034	587.78	213.60
0.69	53331.24	6.59	10.08	1.431	205.03	1.63808E-05	136475.31	0.96	291.05	0.034	625.11	214.28
0.69	53307.52	6.59	10.09	1.441	205.95	1.64181E-05	145929.80	0.96	307.05	0.034	661.18	214.76
0.69	53287.25	6.59	10.10	1.450	206.71	1.64489E-05	155132.29	0.96	322.42	0.034	695.78	215.13
0.69	53269.90	6.59	10.10	1.458	207.34	1.64745E-05	164127.36	0.96	337.28	0.034	729.13	215.42
0.69	53255.09	6.59	10.11	1.464	207.87	1.64959E-05	172856.91	0.96	351.54	0.034	761.09	215.64
0.69	53242.48	6.59	10.11	1.470	208.31	1.65138E-05	181309.83	0.96	365.21	0.034	791.67	215.81
0.69	53231.76	6.59	10.12	1.474	208.68	1.65288E-05	189478.01	0.96	378.30	0.034	820.91	215.93
0.69	53222.69	6.59	10.12	1.478	208.99	1.65413E-05	197351.82	0.96	390.82	0.034	848.80	216.02
0.69	53215.08	6.59	10.12	1.481	209.25	1.65518E-05	204922.83	0.96	402.76	0.034	875.37	216.08

Calculating Estimate of Downstream steam temperature (1)												
					Thermophysical Properties of Air							
56	57	58	59	60	61	62	63	64	65	66	67	68
Length of increment on Downstream pipe surface	Surface Area of increment	Downstream pipe surface temperature increment	Radiation heat transfer from increment	Convection heat transfer from increment	Film Temperature	Density of air	Specific heat of air	Dynamic viscosity	Thermal conductivity of air	Kinematic viscosity	Thermal diffusity	Thermal expansion coefficient
x_2	A_2s	T_2,s	Q_rad, 2,s	Q_conv, 2,s	Tf	ρ_a	Cp_a	μ_a	k_a	v_a	α_a	β_a
[m]	[m^2]	[° C]	[W]	[w]	[k]	[kg/m^3]	[J/kgK]	[kg/sm]	[W/mk]	[m^2/s]	[m^2/s]	[1/K]
0.005	0.000335	122.71	0.309	0.309	344.36	1.02	1009.43	2.0463E-05	0.03	1.9965E-05	2.86E-05	0.00
0.005	0.000335	145.17	0.418	0.392	355.59	0.99	1010.33	2.0953E-05	0.03	2.111E-05	3.033E-05	0.00
0.005	0.000335	159.14	0.496	0.445	362.57	0.97	1010.95	2.1255E-05	0.03	2.1835E-05	3.143E-05	0.00
0.005	0.000335	168.71	0.553	0.482	367.35	0.96	1011.39	2.1461E-05	0.03	2.2337E-05	3.219E-05	0.00
0.005	0.000335	175.62	0.597	0.509	370.81	0.95	1011.72	2.1609E-05	0.03	2.2702E-05	3.274E-05	0.00
0.005	0.000335	180.85	0.632	0.529	373.42	0.95	1011.98	2.1721E-05	0.03	2.298E-05	3.316E-05	0.00
0.005	0.000335	184.92	0.660	0.545	375.46	0.94	1012.19	2.1807E-05	0.03	2.3198E-05	3.349E-05	0.00
0.005	0.000335	188.18	0.682	0.558	377.09	0.94	1012.35	2.1877E-05	0.03	2.3373E-05	3.376E-05	0.00
0.005	0.000335	190.83	0.701	0.568	378.41	0.93	1012.49	2.1933E-05	0.03	2.3515E-05	3.397E-05	0.00
0.005	0.000335	193.01	0.717	0.577	379.50	0.93	1012.60	2.1979E-05	0.03	2.3632E-05	3.415E-05	0.00
0.005	0.000335	194.83	0.730	0.584	380.42	0.93	1012.70	2.2017E-05	0.03	2.3731E-05	3.43E-05	0.00
0.005	0.000335	196.33	0.742	0.590	381.16	0.93	1012.78	2.2049E-05	0.03	2.3811E-05	3.442E-05	0.00
0.005	0.000335	197.59	0.751	0.595	381.79	0.92	1012.84	2.2076E-05	0.03	2.388E-05	3.452E-05	0.00
0.005	0.000335	198.66	0.759	0.599	382.33	0.92	1012.90	2.2098E-05	0.03	2.3938E-05	3.461E-05	0.00
0.005	0.000335	199.58	0.766	0.603	382.79	0.92	1012.95	2.2118E-05	0.03	2.3988E-05	3.469E-05	0.00
0.005	0.000335	200.37	0.772	0.606	383.18	0.92	1012.99	2.2134E-05	0.03	2.403E-05	3.475E-05	0.00
0.005	0.000335	201.04	0.777	0.608	383.52	0.92	1013.03	2.2149E-05	0.03	2.4067E-05	3.481E-05	0.00
0.005	0.000335	201.63	0.782	0.611	383.81	0.92	1013.06	2.2161E-05	0.03	2.4099E-05	3.486E-05	0.00
0.005	0.000335	202.13	0.786	0.613	384.07	0.92	1013.09	2.2172E-05	0.03	2.4126E-05	3.49E-05	0.00

Calculating Estimate of Downstream steam temperature (2)												
Free convection coefficients for increment				Calculating internal pipe wall temperature		Downstream steam properties						
69	70	71	72	73	74	75	76	77	78	79	80	81
Prandtl Number	Raleigh Number	Nusselt Number	Convection coefficient	Total heat transfer from increment	Downstream Pipe wall internal temperature	Dynamic viscosity of steam flow	Reynolds Number	Prandtl Number	Nusselt Number	Thermal conductivity of steam	Convection coefficient	Downstream steam temperature estimate
Pr	Ra	Nu	h	Q_2,s	T_2,i	μ_steam	Re_steam	Pr_steam	Nu_steam	k_steam	h_steam	T_2,f
			[W/m^2 k]	[W]	[°C]	[Pa.s]				[W/mK]	[W/m^2 k]	[°C]
0.70	49526.61	6.47	8.99	0.62	122.79	1.3129E-05	32995.79	1.00	94.63	0.03	159.20	138.47
0.70	52117.22	6.56	9.36	0.81	145.27	1.3998E-05	45066.12	0.98	120.62	0.03	217.28	160.33
0.69	53011.76	6.58	9.56	0.94	159.25	1.4547E-05	56533.67	0.97	144.15	0.03	270.87	173.28
0.69	53371.19	6.59	9.68	1.04	168.83	1.4926E-05	67752.21	0.97	166.31	0.03	321.58	181.83
0.69	53520.36	6.60	9.77	1.11	175.75	1.5202E-05	78620.12	0.97	187.12	0.03	369.29	187.84
0.69	53578.11	6.60	9.83	1.16	180.98	1.5411E-05	89341.57	0.96	207.10	0.03	415.05	192.28
0.69	53592.65	6.60	9.87	1.20	185.06	1.5575E-05	99917.79	0.96	226.35	0.03	459.08	195.66
0.69	53586.26	6.60	9.91	1.24	188.33	1.5706E-05	110347.03	0.96	244.96	0.03	501.54	198.32
0.69	53569.90	6.60	9.94	1.27	190.98	1.5813E-05	120447.79	0.96	262.64	0.03	541.88	200.44
0.69	53549.15	6.60	9.96	1.29	193.16	1.5901E-05	130326.49	0.96	279.66	0.03	580.64	202.16
0.69	53526.98	6.60	9.98	1.31	194.99	1.5974E-05	139948.08	0.96	295.99	0.03	617.77	203.58
0.69	53505.59	6.60	10.00	1.33	196.48	1.6035E-05	149418.67	0.96	311.85	0.03	653.68	204.71
0.69	53485.37	6.59	10.01	1.35	197.74	1.6086E-05	158634.57	0.96	327.10	0.03	688.11	205.64
0.69	53466.57	6.59	10.02	1.36	198.82	1.6129E-05	167640.93	0.96	341.83	0.03	721.31	206.43
0.69	53449.38	6.59	10.03	1.37	199.74	1.6166E-05	176380.02	0.96	355.97	0.03	753.13	207.08
0.69	53433.83	6.59	10.04	1.38	200.53	1.6198E-05	184841.02	0.96	369.53	0.03	783.58	207.63
0.69	53419.86	6.59	10.04	1.39	201.21	1.6226E-05	193016.09	0.96	382.52	0.03	812.69	208.10
0.69	53407.37	6.59	10.05	1.39	201.79	1.625E-05	200895.76	0.96	394.93	0.03	840.47	208.49
0.69	53396.28	6.59	10.05	1.40	202.30	1.627E-05	208471.75	0.96	406.78	0.03	866.92	208.82

Second Estimate of Mass Flow Rate			
82	83	84	85
Average steam temp	Specific Heat of Steam	Change in steam temperature	Mass flow rate estimate 2
	Cp_steam	ΔT	ṁ_2est
[°C]	[J/kg o C]	[°C]	[kg/s]
155.13	1982.73	33.32	0.0044
174.23	1976.32	27.79	0.0067
185.08	1975.14	23.61	0.0089
192.05	1975.12	20.44	0.0112
196.87	1975.40	18.05	0.0134
200.35	1975.73	16.15	0.0156
202.97	1976.04	14.61	0.0177
204.99	1976.33	13.35	0.0198
206.60	1976.57	12.31	0.0219
207.88	1976.78	11.44	0.0240
208.93	1976.97	10.70	0.0259
209.73	1977.11	10.05	0.0279
210.39	1977.23	9.49	0.0298
210.92	1977.33	8.99	0.0317
211.36	1977.42	8.56	0.0335
211.72	1977.49	8.18	0.0352
212.01	1977.55	7.84	0.0369
212.25	1977.60	7.53	0.0385
212.45	1977.63	7.26	0.0401

Iterative solver to calculate mass flow rate and steam temperatures (1)									
86	87	88	89	90	91	92	93	94	95
Estimate mass flow rate for iterative solver	Internal Diameter	Estimated upstream steam temp	Estimated downstream steam temp	upstream steam temp	downstream steam temp	Heat loss from increment 1	Heat loss from increment 2	Pipe upstream internal temp	Pipe downstream internal temp
ṁ_est	Di	T_1f_est	T_2f_est	T_1f_est	T_2f_est	Q_1s	Q_2s	T_1i	T_2i
[kg/s]	[m]	[°C]	[°C]	[°C]	[°C]	[W]	[W]	[°C]	[°C]
0.0044	0.01576	171.79	138.47	174.57	140.95	0.857	0.618	150.38	122.79
0.0066	0.01576	188.12	160.33	190.60	162.33	1.038	0.810	169.16	145.27
0.0088	0.01576	196.89	173.28	198.74	174.81	1.151	0.941	180.02	159.25
0.0111	0.01576	202.28	181.83	203.73	183.05	1.227	1.035	187.12	168.83
0.0132	0.01576	205.89	187.84	207.07	188.85	1.282	1.106	192.09	175.75
0.0154	0.01576	208.43	192.28	209.42	193.13	1.323	1.161	195.74	180.98
0.0176	0.01576	210.27	195.66	211.12	196.39	1.355	1.204	198.52	185.06
0.0197	0.01576	211.67	198.32	212.40	198.95	1.380	1.240	200.70	188.33
0.0218	0.01576	212.75	200.44	213.39	200.99	1.400	1.269	202.45	190.98
0.0238	0.01576	213.60	202.16	214.18	202.66	1.417	1.294	203.87	193.16
0.0258	0.01576	214.28	203.58	214.80	204.03	1.431	1.314	205.03	194.99
0.0277	0.01576	214.76	204.71	215.23	205.12	1.441	1.331	205.95	196.48
0.0296	0.01576	215.13	205.64	215.56	206.02	1.450	1.346	206.71	197.74
0.0314	0.01576	215.42	206.43	215.82	206.77	1.458	1.358	207.34	198.82
0.0332	0.01576	215.64	207.08	216.01	207.40	1.464	1.369	207.87	199.74
0.0350	0.01576	215.81	207.63	216.15	207.93	1.470	1.378	208.31	200.53
0.0367	0.01576	215.93	208.10	216.26	208.37	1.474	1.386	208.68	201.21
0.0383	0.01576	216.02	208.49	216.33	208.75	1.478	1.392	208.99	201.79
0.0398	0.01576	216.08	208.82	216.37	209.06	1.481	1.398	209.25	202.30

Iterative solver to calculate mass flow rate and steam temperatures (2)													
Upstream steam properties							Downstream steam properties						
96	97	98	99	100	101	102	103	104	105	106	107	108	109
Dynamic viscosity of steam flow	Reynolds Number	Prandtl Number	Nusselt Number	Thermal conductivity of steam	Convection coefficient	Upstream steam temperature	Dynamic viscosity of steam flow	Reynolds Number	Prandtl Number	Nusselt Number	Thermal conductivity of steam	Convection coefficient	Downstream steam temperature
μ_steam	Re_steam	Pr_steam	Nu_steam	k_steam	h_steam	T_1,f	μ_steam	Re_steam	Pr_steam	Nu_steam	k_steam	h_steam	T_2,f
[Pa.s]				[W/mK]	[W/m^2 k]	[°C]	[Pa.s]				[W/mK]	[W/m^2 k]	[°C]
1.5155E-05	23550.06	0.97	72.77	0.031	143.12	174.57	1.383E-05	25806.37	0.98	77.30	0.028	137.44	140.95
1.5797E-05	33748.14	0.96	94.92	0.032	195.62	190.60	1.4668E-05	36345.56	0.97	101.17	0.030	191.87	162.33
1.6126E-05	44228.09	0.96	117.72	0.033	248.36	198.74	1.5165E-05	47031.62	0.97	124.07	0.031	244.18	174.81
1.6328E-05	54690.92	0.96	139.44	0.034	298.38	203.73	1.5494E-05	57633.37	0.96	145.79	0.032	293.96	183.05
1.6463E-05	64953.69	0.96	159.95	0.034	345.51	207.07	1.5727E-05	67995.79	0.96	166.28	0.032	340.96	188.85
1.6559E-05	75166.51	0.96	179.72	0.034	390.80	209.42	1.5899E-05	78284.10	0.96	186.01	0.033	386.17	193.13
1.6628E-05	85304.90	0.95	198.83	0.034	434.42	211.12	1.6031E-05	88481.46	0.96	205.07	0.033	429.74	196.39
1.668E-05	95349.81	0.95	217.32	0.035	476.52	212.40	1.6134E-05	98573.76	0.96	223.51	0.033	471.82	198.95
1.672E-05	105113.10	0.95	234.92	0.035	516.56	213.39	1.6217E-05	108375.60	0.96	241.06	0.033	511.85	200.99
1.6752E-05	114689.70	0.95	251.88	0.035	555.05	214.18	1.6285E-05	117984.19	0.96	257.97	0.034	550.33	202.66
1.6778E-05	124039.26	0.95	268.16	0.035	591.95	214.80	1.634E-05	127360.60	0.96	274.20	0.034	587.24	204.03
1.6795E-05	133262.81	0.95	283.98	0.035	627.64	215.23	1.6384E-05	136606.44	0.96	289.98	0.034	622.94	205.12
1.6809E-05	142253.61	0.95	299.20	0.035	661.88	215.56	1.6421E-05	145616.20	0.96	305.15	0.034	657.21	206.02
1.6819E-05	151052.86	0.95	313.91	0.035	694.91	215.82	1.6451E-05	154431.74	0.96	319.81	0.034	690.25	206.77
1.6827E-05	159601.67	0.95	328.03	0.035	726.58	216.01	1.6477E-05	162994.60	0.96	333.90	0.034	721.94	207.40
1.6833E-05	167887.45	0.95	341.58	0.035	756.89	216.15	1.6498E-05	171292.54	0.96	347.41	0.034	752.27	207.93
1.6837E-05	175900.83	0.95	354.56	0.035	785.87	216.26	1.6516E-05	179316.50	0.96	360.35	0.034	781.28	208.37
1.684E-05	183631.16	0.95	366.97	0.035	813.54	216.33	1.6532E-05	187056.02	0.96	372.73	0.034	808.96	208.75
1.6842E-05	191069.14	0.95	378.81	0.035	839.89	216.37	1.6544E-05	194502.03	0.96	384.54	0.034	835.33	209.06

Iterative solver to calculate mass flow rate and steam temperatures (3)			
110	111	112	113
Average steam temperature	Specific Heat of Steam	Change in steam temperature	Mass flow rate
	Cp_steam	ΔT	ṁ
[°C]	[J/kg o C]	[°C]	[kg/s]
157.76	1976.26	33.61	0.0044
176.46	1975.09	28.27	0.0066
186.78	1975.56	23.92	0.0088
193.39	1976.14	20.67	0.0111
197.96	1976.65	18.22	0.0132
201.27	1977.05	16.29	0.0154
203.75	1977.37	14.73	0.0176
205.67	1977.62	13.45	0.0197
207.19	1977.83	12.40	0.0218
208.42	1977.99	11.52	0.0238
209.41	1978.13	10.77	0.0258
210.17	1978.22	10.11	0.0277
210.79	1978.30	9.55	0.0296
211.29	1978.35	9.05	0.0314
211.70	1978.40	8.61	0.0332
212.04	1978.43	8.23	0.0350
212.31	1978.45	7.88	0.0367
212.54	1978.47	7.58	0.0383
212.71	1978.48	7.31	0.0398

Figure 44 shows the comparison between the upstream steam temperatures acquired from Flownex and the upstream steam temperature calculated from the model. Figure 45 shows the comparison between the downstream steam temperatures acquired from Flownex and the downstream steam temperature calculated from the model.

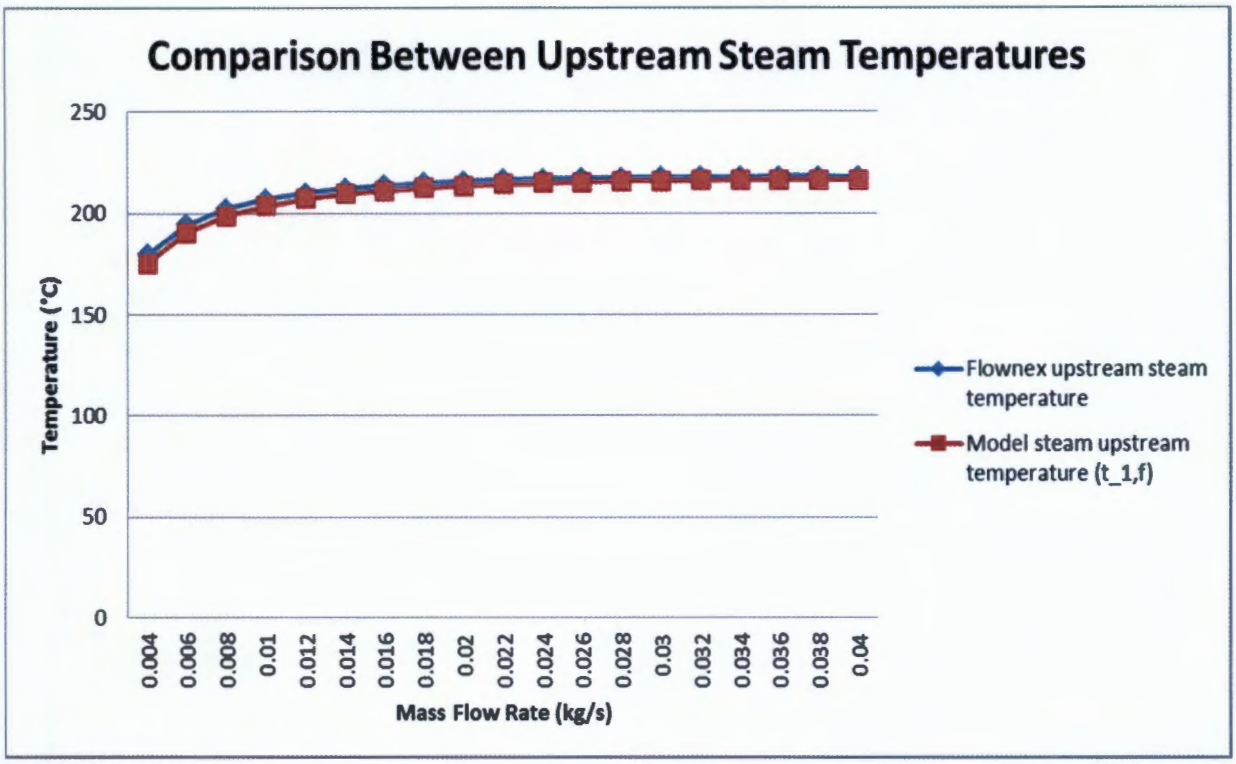

Figure 44: Comparison between upstream steam temperatures generated from Flownex and calculated from Excel model

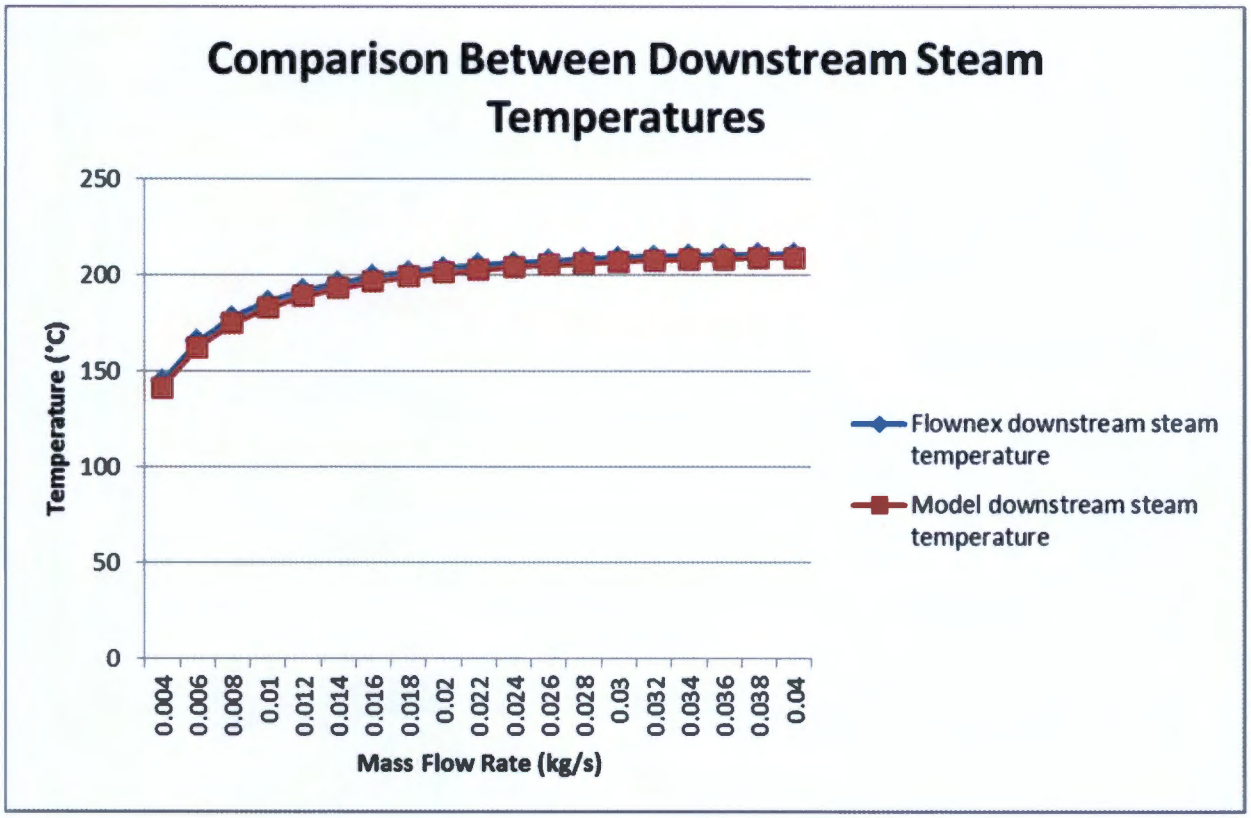

Figure 45: Comparison between downstream steam temperatures generated from Flownex and calculated from Excel model

Figure 44 shows that the upstream steam temperature calculated using the model trends the upstream temperature generated in Flownex fairly accurately. Figure 44 shows that the downstream steam temperature calculated using the model trends the downstream temperature generated in Flownex fairly accurately as well.

Figure 46 below shows the change in steam temperature calculated from the model compared to the change in steam temperature acquired from Flownex.

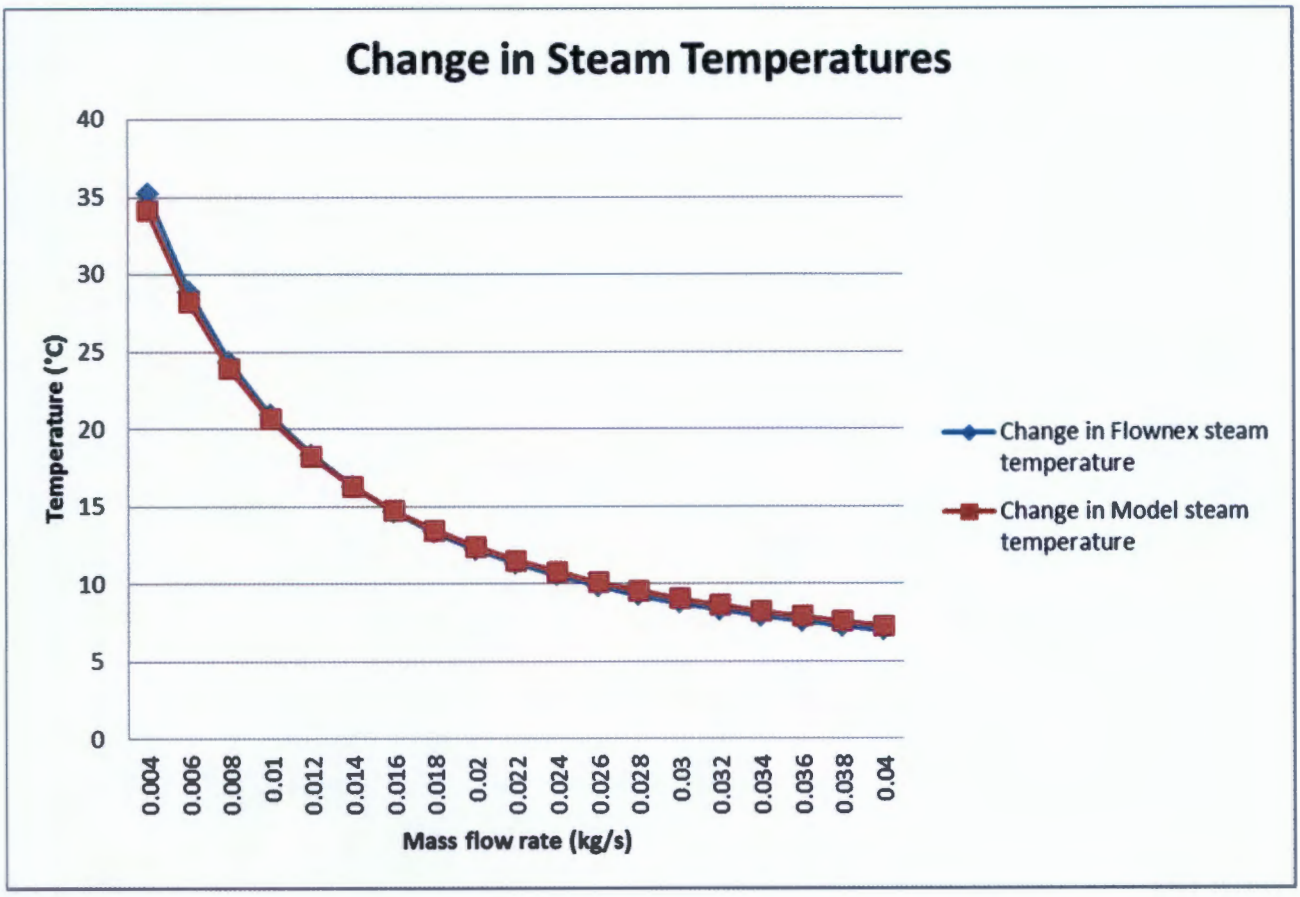

Figure 46: Change in steam temperature calculated from the proposed method compared to the change in steam temperature acquired from Flownex

It can be seen from the above graph that the change in steam temperature calculated using the model trends the change in steam temperature acquired from the Flownex simulation fairly accurately. This proves the validity of the method proposed to calculate the steam temperature at upstream and downstream points of the un-insulated pipe.

Figure 47 below shows a comparison between the mass flow rates calculated by the mathematical model using the change in pipe surface temperature, change in steam temperature and the Flownex mass flow rate. It can be seen from this graph that the mass flow rate calculated by the mathematical model using the change in pipe surface temperature has a significantly larger error than the mass flow rate calculated by the mathematical model using the change in steam temperature compared to the Flownex mass flow rate. This indicates that a better approximation of the true mass flow rate can be achieved when using the change in steam temperature compared to the change in pipe surface temperature.

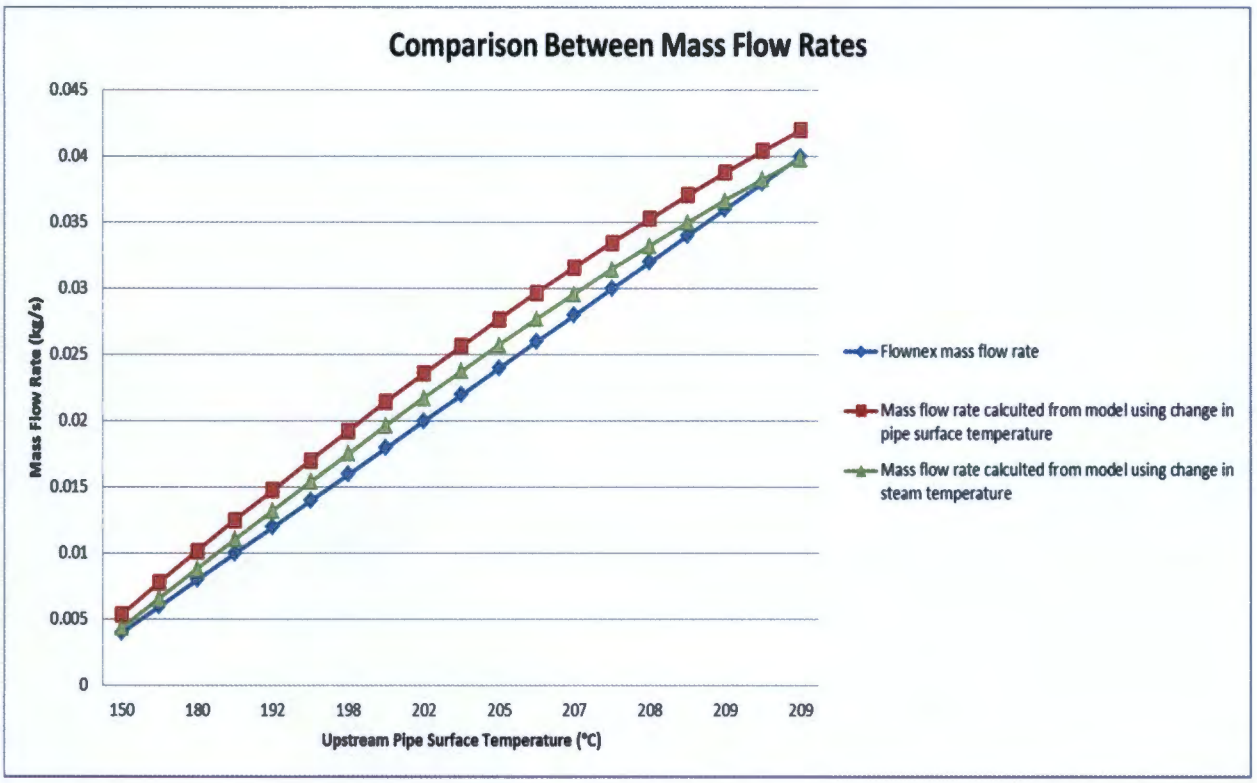

Figure 47: Comparison between mass flow rates

6.7 Applying method to experiment 1

In section 6.4, the mass flow rate for the tests performed on the experimental test rig was calculated using the mathematical model which assumed that the change in pipe surface temperature is equal to the change in steam temperature for the length of un-insulated pipe. In this section the mass flow rate, for experiment 1, was recalculated using the same mathematical model, which instead of equating the change in steam temperature to the change in pipe surface temperature, it calculates the change in steam temperature from the method derived in section 6.6. The Excel model that contain all input and calculation data is shown in appendix E. Figure 48 below shows the comparison between the mass flow rates calculated using the mathematical model which assumes the pipe surface temperature is equal to the steam temperature, the mass flow rate calculated using the mathematical model which calculates the steam temperature and the mass flow rate calculated from the orifice plate. Table 11 below shows the difference in the mass flow rates and the percentage deviation as well as the average deviation and difference for all results in experiment 1.

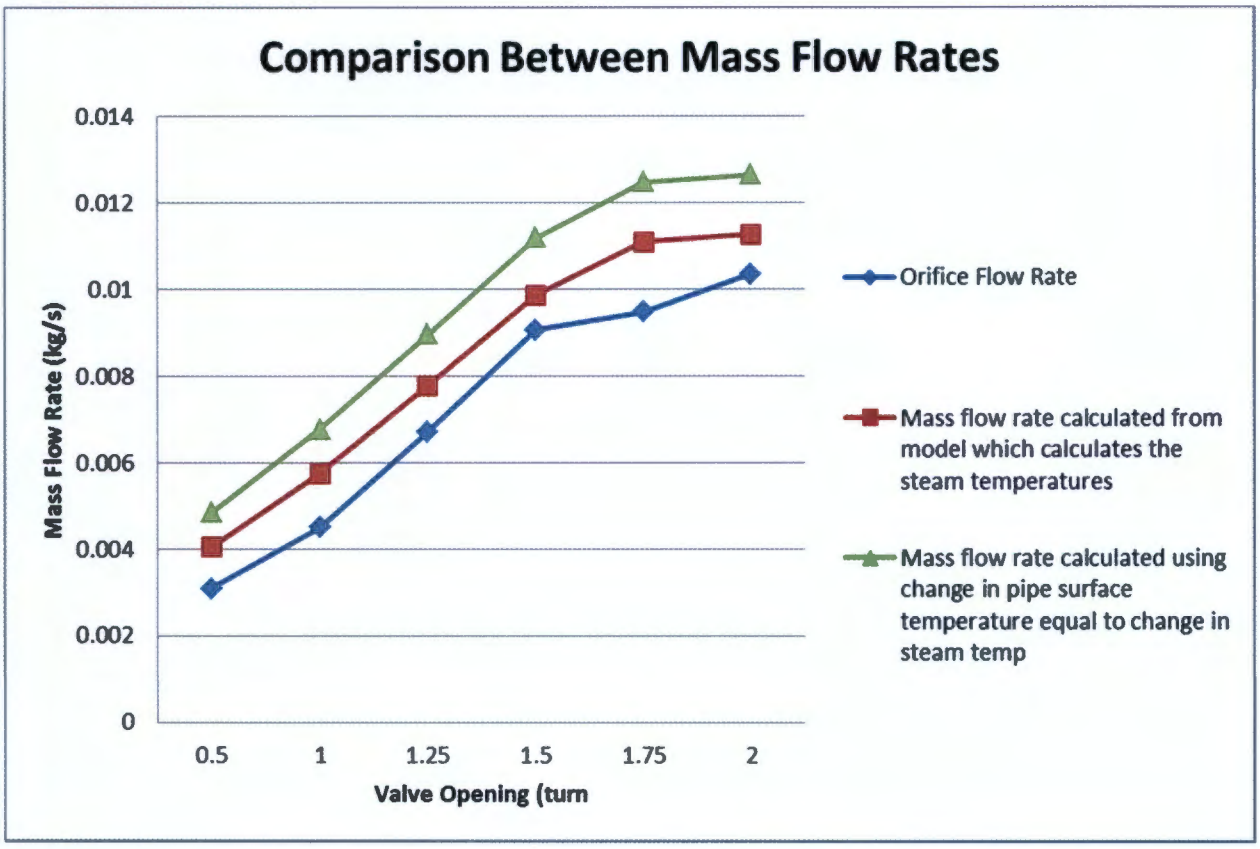

Figure 48: Comparison of mass flow rates for experiment 1

Table 11: Difference in Mass Flow Rates for Experiment 1

Mass Flow Rate calculated from model, assuming change in pipe surface temp is equal to change in steam temp	Verification mass flow rate from Orifice	Difference in Flow Rates	Percentage Deviation
[kg/s]	*[kg/s]*	*[kg/s]*	*[%]*
0.0048	0.0031	0.0018	57.0828
0.0068	0.0045	0.0023	50.2473
0.0090	0.0067	0.0022	33.4731
0.0112	0.0091	0.0021	23.4907
0.0125	0.0095	0.0030	31.7229
0.0127	0.0104	0.0023	22.2329
	Average	**0.0023**	**36.3750**

Mass Flow Rate calculated from model which calculates steam temp	Verification mass flow rate from Orifice	Difference in Flow Rates	Percentage Deviation
[kg/s]	*[kg/s]*	*[kg/s]*	*[%]*
0.0040	0.0031	0.0010	31.1744
0.0057	0.0045	0.0012	27.3207
0.0078	0.0067	0.0011	15.7114
0.0099	0.0091	0.0008	8.7963
0.0111	0.0095	0.0016	17.0512
0.0113	0.0104	0.0009	8.7087
	Average	**0.0011**	**18.1271**

It can be seen from the above graph that the error reduces significantly by utilising the change in steam temperature compared to the change in pipe surface temperature in the mathematical model.

6.8 Interpretation of model and results

The experimental results in section 6.4 indicated that the mass flow rate calculated using the proposed technique trended the actual mass flow rate, although an error existed which decreased with an increase in mass flow rate. This error was found to be as a result of the assumption which equated the change in pipe surface temperature to the change in steam temperature across the length of un-insulated pipe. Computational simulations performed in Flownex indicated that the change in pipe surface temperature deviated from the change in steam temperature at low mass flow rates whilst equalling it at higher mass flow rates.

A method was derived in section 6.6 which calculated the steam temperatures at upstream and downstream locations of the un-insulated pipe, using heat transfer equations, empirical correlations and conservation laws. The method was tested using Flownex, and found to be

accurate in calculating the upstream and downstream steam temperatures and the resulting change in steam temperature across the length of un-insulated pipe. This allowed for the rejection of the assumption that equated the change in pipe surface temperature to the change in steam temperature in the mathematical model. This improved the accuracy of the mass flow rate calculated from the mathematical model as can be seen in figure 48 and table 11.

The average difference in error, for all test points in experiment 1, shown in table 11, decreased from 0.0023 kg/s to 0.0011 kg/s. The average percentage error for the actual mass flow rate measured and the mass flow rate calculated from the mathematical model using the change in pipe surface temperature was 36.3 % whilst the average percentage error improved to 18.1 % for the mass flow rate calculated from the model using the change in steam temperature across the length of un-insulated pipe. It should be noted that the mathematical model uses heat transfer equations with empirical correlations and an error of 10 to 20 % can be expected. Coupled to this the expected error from an orifice plate and associated equipment is in the region of 3 to 5 %.

Since the average error is below 20 %, it can be concluded that the mathematical model proposed to calculate the mass flow rate of the leakage steam is suitable in approximating the actual mass flow rate of the leakage steam. This validates the proposed technique as a suitable method in determining internal leakages through steam valves.

7. Practical Application on Power Station

Majuba power station, where the author of this report is employed, was selected to conduct on site testing of the proposed technique. Majuba is Eskom's second largest power plant with an installed capacity of 4110 MW. It is a coal fired power station with no dedicated mine and currently purchases coal through short/medium term supply contracts. Coal is usually railed and trucked to site, making the cost of electricity higher than power plants that have a dedicated mine in close proximity. Therefore, improving efficiency of the current operating plant at Majuba will have a greater financial impact than at other power plants.

7.1 On site tests

Before entering the HP turbine, the steam contains the most amount of energy in the entire cycle. A leak at this point will have the most significant impact on plant efficiency. Steam is transported by four main steam pipe lines from the boiler to the turbine; each line contains a quarter of the HP turbines steam requirements. At the lowest point on each of these pipe lines, a drain line is installed to facilitate draining of the pipe lines in shut down and emergency conditions. Figure 49 below shows a schematic of the drain lines.

Tests, using the technique, were conducted on two of the four drain lines to identify which motorised isolation valve was internally leaking.

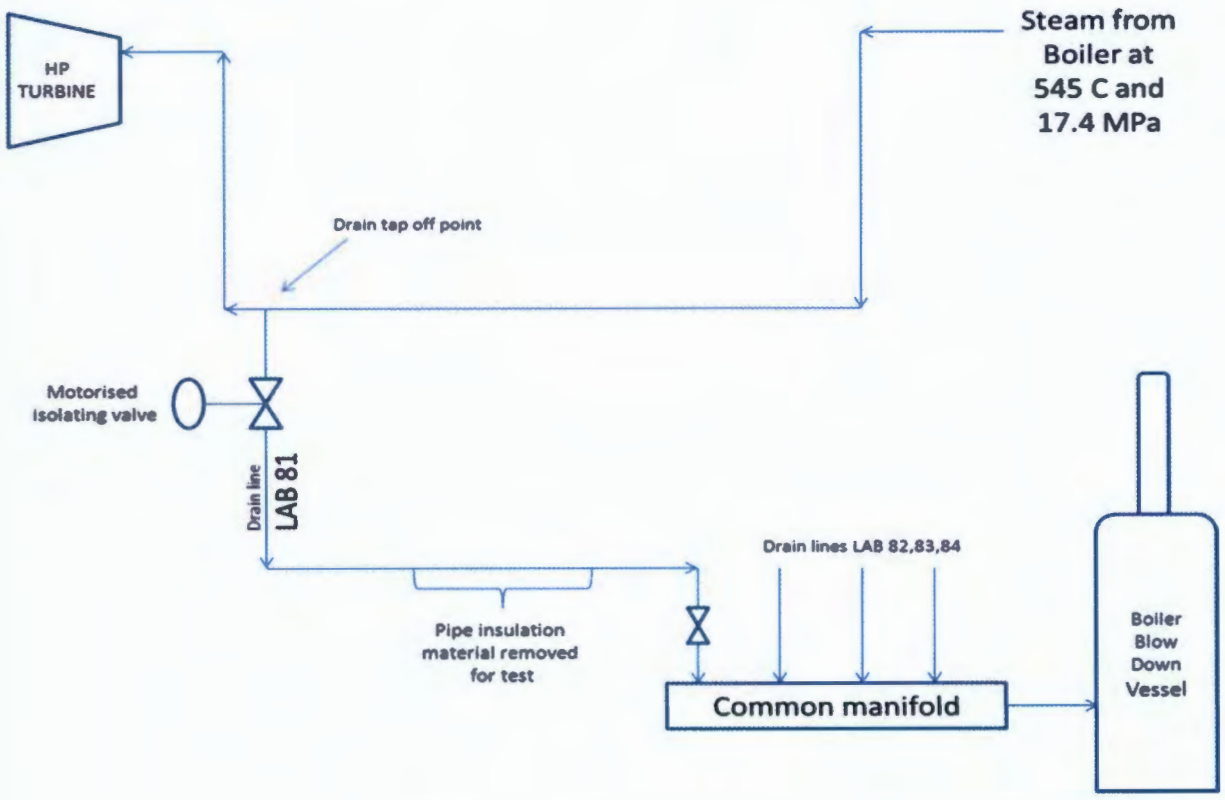

Figure 49: Schematic of steam drain lines

7.2 On site test set-up and procedure

The drain line tap off is located underneath the turbine hall, whilst the boiler blow down vessel is located in the boiler area. The distance between both is approximately 15 meters. Along a horizontal section of the drain pipe line a length of insulation material was removed to facilitate the test to be conducted. Figure 50 shows a schematic of the test length.

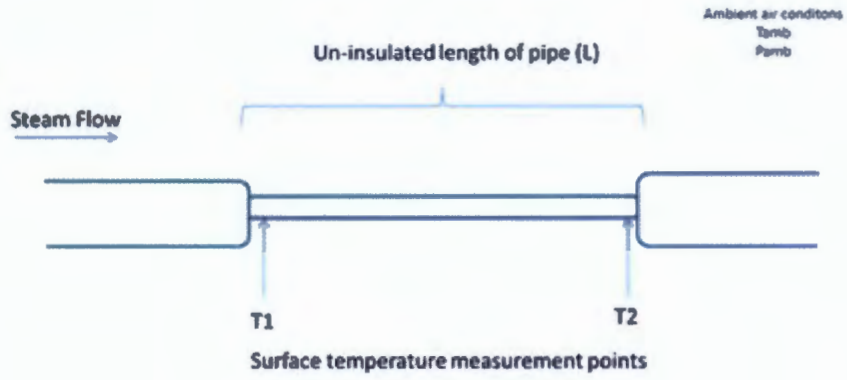

Figure 50: Schematic of test section

Surface temperature measurements were conducted on the upstream and downstream points of the un-insulated pipe, T_1 and T_2 respectively. Ambient conditions, the length of the un-insulated pipe and pipe dimensions were also recorded and are shown in table 12 below. The emissivity of the pipe surface was set at 0.95 whilst the convection coefficient was calculated using the Nusselt number approximation shown in equations 19 to 22. The proposed technique was then employed to detect and quantify if any drain valves were internally leaking.

7.3 Results from on-site tests

Table 12 below is the Excel model used to calculate the mass flow rate. All relevant data is contained in the table. The format of the below table is identical to table 10 shown in section 6.6.3 therefore table 9, which explains each column of the model, can be used here as well.

Table 12: On-site test results and mass flow rate calculation using model

	Experimental Data- Input Data								
	Pipe Properties						Temperatures		
	1	2	3	4	5	6	7	8	9
	Length of un-insulated pipe	Outer Diameter of Pipe	Inner Diameter of Pipe	Pipe Wall Thichness	Pipe emissivity	Thermal conductivity of pipe	Ambient Temperature	Upstream un-insulated Pipe Surface Temperature	Downstream un-insulated Pipe Surface temperature
	L	Do	Di	t	ε	k-pipe	Tamb	T1,s	T2,s
	[m]	[m]	[m]	[m]		[W/mK]	[°C]	[°C]	[°C]
1	2.7	0.0761	0.0441	0.016	0.95	50	24	24.30	24.30
2	2.7	0.0761	0.0441	0.016	0.95	50	24	148.00	135.00

First Estimate of Mass Flow Rate (1)											
Heat Loss from the entire length of un-insulated pipe				Thermophysical Properties of Air							
10	11	12	13	14	15	16	17	18	19	20	21
Average Pipe Surface Temperature	Surface Area of un-insulated pipe	Radiation Heat Transfer from un-insulated pipe surface	Convection Heat Transfer from un-insulated pipe surface	Film Temperature	Density of air	Specific heat of air	Dynamic viscosity	Thermal conductivity of air	Kinematic viscosity	Thermal diffusity	Thermal expansion coefficient
Ts,avg	A_ps	Qrad_ps	Qconv,ps	Tfilm	ρ_a	Cp_a	μ_a	k_a	v_a	α_a	β_a
[°C]	[m^2]	[W]	[W]	[k]	[kg/m^3]	[J/kgK]	[kg/sm]	[W/mk]	[m^2/s]	[m^2/s]	[1/K]
24.30	0.645503	1.09	0.31	297.15	1.19	1006.85	1.8337E-05	0.0260	1.5438E-05	2.1741E-05	0.0034
141.50	0.645503	755.83	551.84	355.75	0.99	1010.35	2.096E-05	0.0304	2.1127E-05	3.0358E-05	0.0028

First Estimate of Mass Flow Rate (2)							
Free convection coefficients for horizontal cylinder				Mass flow rate calculation			
22	23	24	25	26	27	28	29
Prandtl Number	Raleigh Number	Nusselt Number	Convection coefficient	Total Heat Loss	Speciic heat of steam	change in pipe surface temperature	Estimated mass flow rate
Pr	Ra	Nu	h	Q_tot	Cp_s	ΔTps	ṁ_est
			[W/m^2 k]	[W]	[J/kg o C]	[° C]	[kg/s]
0.71	13004.52	4.66	1.59	1.40	4182.24	0.00	#DIV/0!
0.70	2226448.67	18.19	7.28	1307.66	1986.97	13.00	0.0506

Calculating Estimate of upstream steam temperature (1)												
					Thermophysical Properties of Air							
30	31	32	33	34	35	36	37	38	39	40	41	42
Length of increment on upstream pipe surface	Surface Area of increment	Pipe Surface temperature at increment	Radiation heat transfer from increment	Convection heat transfer from increment	Film Temperature	Density of air	Specific heat of air	Dynamic viscosity	Thermal conductivity of air	Kinematic viscosity	Thermal diffusity	Thermal expansion coefficient
x_1	A_1x	T_1s	Q_rad, 1s	Q_conv,1s	Tf	ρ_a	Cp_a	μ_a	k_a	v_a	α_a	β_a
[m]	[m^2]	[° C]	[W]	[W]	[k]	[kg/m^3]	[J/kgK]	[kg/sm]	[W/mk]	[m^2/s]	[m^2/s]	[1/K]
0.005	0.001195	24.30	0.0020	0.0006	297.15	1.19	1006.85	1.834E-05	0.026	1.5438E-05	2.1741E-05	0.0034
0.005	0.001195	148.00	1.5217	1.0906	359.00	0.98	1010.63	2.11E-05	0.031	2.1463E-05	3.0867E-05	0.0028

Calculating Estimate of upstream steam temperature (2)												
Free convection coefficients for increment				Calculating internal pipe wall temperature		Upstream steam properties						
43	44	45	46	47	48	49	50	51	52	53	54	55
Prandtl Number	Raleigh Number	Nusselt Number	Convection coefficient	Total heat transfer from increment	Upstream Pipe wall internal temperature	Dynamic viscosity of steam flow	Reynolds Number	Prandtl Number	Nusselt Number	Thermal conductivity of steam	Convection coefficient	Upstream steam temperature Estimate
Pr	Ra	Nu	h	Q_1,s	T_1,i	μ_steam	Re_steam	Pr_steam	Nu_steam	k_steam	h_steam	T_1,f
			[W/m^2 k]	[W]	[° C]	[Pa.s]				[W/mK]	[W/m^2 k]	[° C]
0.71	13004.52	4.66	1.59	0.003	24.30	0.000904444	#DIV/0!	6.24	#DIV/0!	0.606	#DIV/0!	#DIV/0!
0.70	2254049.55	18.26	7.36	2.612	148.56	1.41265E-05	103466.07	0.98	234.83	0.029	152.69	173.26

Calculating Estimate of Downstream steam temperature (1)												
					Thermophysical Properties of Air							
56	57	58	59	60	61	62	63	64	65	66	67	68
Length of increment on Downstream pipe surface	Surface Area of increment	Downstream pipe surface temperature increment	Radiation heat transfer from increment	Convection heat transfer from increment	Film Temperature	Density of air	Specific heat of air	Dynamic viscosity	Thermal conductivity of air	Kinematic viscosity	Thermal diffusity	Thermal expansion coefficient
x_2	A_2s	T_2,s	Q_rad, 2,s	Q_conv, 2,s	Tf	ρ_a	Cp_a	μ_a	k_a	v_a	α_a	β_a
[m]	[m^2]	[° C]	[W]	[w]	[k]	[kg/m^3]	[J/kgK]	[kg/sm]	[W/mk]	[m^2/s]	[m^2/s]	[1/K]
0.005	0.001195	24.30	0.002	0.001	297.15	1.19	1006.85	1.8337E-05	0.03	1.5438E-05	2.174E-05	0.00
0.005	0.001195	135.00	1.283	0.954	352.50	1.00	1010.08	2.0819E-05	0.03	2.0793E-05	2.985E-05	0.00

Calculating Estimate of Downstream steam temperature (2)												
Free convection coefficients for increment				Calculating internal pipe wall temperature		Downstream steam properties						
69	70	71	72	73	74	75	76	77	78	79	80	81
Prandtl Number	Raleigh Number	Nusselt Number	Convection coefficient	Total heat transfer from increment	Downstream Pipe wall internal temperature	Dynamic viscosity of steam flow	Reynolds Number	Prandtl Number	Nusselt Number	Thermal conductivity of steam	Convection coefficient	Downstream steam temperature estimate
Pr	Ra	Nu	h	Q_2,s	T_2,i	μ_steam	Re_steam	Pr_steam	Nu_steam	k_steam	h_steam	T_2,f
			[W/m^2 k]	*[W]*	*[° C]*	*[Pa.s]*				*[W/mK]*	*[W/m^2 k]*	*[° C]*
0.71	13004.52	4.66	1.59	0.00	24.30	0.00090444	#DIV/0!	6.24	#DIV/0!	0.61	#DIV/0!	#DIV/0!
0.70	2193359.05	18.12	7.19	2.24	135.48	1.3617E-05	107334.77	0.99	242.14	0.03	151.31	156.82

Second Estimate of Mass Flow Rate			
82	83	84	85
Average steam temp	Specific Heat of Steam	Change in steam temperature	Mass flow rate estimate 2
	Cp_steam	ΔT	ṁ_2est
[° C]	*[J/kg o C]*	*[° C]*	*[kg/s]*
#DIV/0!	#VALUE!	#DIV/0!	#VALUE!
165.04	1978.61	16.44	0.0402

Iterative solver to calculate mass flow rate and steam temperatures (1)									
86	87	88	89	90	91	92	93	94	95
Estimate mass flow rate for iterative solver	Internal Diameter	Estimated upstream steam temp	Estimated downstream steam temp	upstream steam temp	downstream steam temp	Heat loss from increment 1	Heat loss from increment 2	Pipe upstream internal temp	Pipe downstream internal temp
ṁ_est	Di	T_1f_est	T_2f_est	T_1f_est	T_2f_est	Q_1s	Q_2s	T_1i	T_2i
[kg/s]	*[m]*	*[° C]*	*[° C]*	*[° C]*	*[° C]*	*[W]*	*[W]*	*[° C]*	*[° C]*
#VALUE!	0.0441	#DIV/0!	#DIV/0!	#VALUE!	#VALUE!	0.003	0.003	24.30	24.30
0.0387	0.0441	173.26	156.82	178.67	161.56	2.612	2.237	148.56	135.48

Iterative solver to calculate mass flow rate and steam temperatures (2)													
Upstream steam properties							Downstream steam properties						
96	97	98	99	100	101	102	103	104	105	106	107	108	109
Dynamic viscosity of steam flow	Reynolds Number	Prandtl Number	Nusselt Number	Thermal conductivity of steam	Convection coefficient	Upstream steam temperature	Dynamic viscosity of steam flow	Reynolds Number	Prandtl Number	Nusselt Number	Thermal conductivity of steam	Convection coefficient	Downstream steam temperature
μ_steam	Re_steam	Pr_steam	Nu_steam	k_steam	h_steam	T_1,f	μ_steam	Re_steam	Pr_steam	Nu_steam	k_steam	h_steam	T_2,f
[Pa.s]				*[W/mK]*	*[W/m^2 k]*	*[°C]*	*[Pa.s]*				*[W/mK]*	*[W/m^2 k]*	*[°C]*
#VALUE!	#VALUE!	#VALUE!	#VALUE!	#VALUE!	#VALUE!	#VALUE!	#VALUE!	#VALUE!	#VALUE!	#VALUE!	#VALUE!	#VALUE!	#VALUE!
1.5319E-05	72909.98	0.96	176.08	0.031	125.26	178.67	1.4638E-05	76299.83	0.97	183.14	0.030	123.84	161.56

Iterative solver to calculate mass flow rate and steam temperatures (3)			
110	111	112	113
Average steam temperature	Specific Heat of Steam	Change in steam temperature	Mass flow rate
	Cp_steam	ΔT	ṁ
[°C]	*[J/kg o C]*	*[°C]*	*[kg/s]*
#VALUE!	#VALUE!	#VALUE!	#VALUE!
170.11	1975.66	17.11	0.0387

It can be seen that the pipe surface temperatures on line LBA 83 remained at a constant 24.3 °C which indicates that the line is at ambient temperature and no steam flow is passing through this drain line. This indicates that the motorised isolation valve on line LBA 83 is in a good working condition and is not leaking steam internally.

On the other hand it can be seen that the upstream pipe surface temperature on line LBA 84 is 148 °C and the downstream temperature is 135 °C. This indicates that there is flow of steam through this line and the motorised drain isolating valve is leaking steam internally. Using the mathematical model the steam flow was calculated to be 0.039 kg/s.

Table 17 below shows the accumulative financial loss per annum for valve LBA 84 leaking internally steam at 0.039 kg/s using the equations derived in section 5.3. Table 13-16 shows the calculation of each loss mentioned in section 5.3.

Table 13: Calculation of loss of revenue per annum for leakage rate of 0.039 kg/s

Energy lost from leakage flow			
Upstream temperature before valve	T_o	[°C]	540
Upstream pressure before valve	P_o	[bar]	164
Enthalpy	h_o	[KJ/kg]	3407.64
Leakage mass flow rate	$\dot{m}$	[kg/s]	0.039
Energy lost through leakage flow	P_leak	[KW]	132.90
Loss in Revenue Calculation			
Energy lost through leakage flow	P_leak	[KW]	132.90
Turbine efficiency	η_t	[%]	92
Cost of electricity		[R/KWh]	0.89
Time on full load		[%]	31
Loss of revenue per hour			R 33.73
Loss of revenue per annum			**R 295 503.47**

In the above table, the enthalpy is a function of the temperature and pressure of the steam flow. The turbine efficiency was acquired from the turbine manuals found in the power station. Majuba is a load following station, generation is linked to demand, and it was calculated that the generating unit is required to be on full load 31 % of the time. The cost of electricity, acquired from the power station was fixed at R 0.89/KWh.

Table 14: Calculation of cost of excess coal per annum from leakage flow

Cost of excess coal required			
Energy required from excess coal	P_excess coal	[KW]	149.32
Boiler efficiency	η_b	[%]	89
Calorific value of coal	Cv,coal	[MJ/kg]	33.3
Cost of coal per ton		[R/ton]	351.03
Excess coal per hour		[kg/h]	16.14
Excess coal per annum		[tons]	141.41
Cost of excess coal per annum			**R 49 640.43**

In the above table, the boiler efficiency was acquired from boiler manuals located in the power station. The calorific value is the average calorific value for the coal received by Majuba for the 2012/13 financial year. Majuba Power Station currently pays R 351.03 per ton for coal.

Table 15: Calculation of the cost of excess demineralised water required

Cost of Demin Water			
Leakage mass flow rate	$\dot{m}$	[kg/s]	0.039
Steam density	p	[kg/m3]	49.06
Leakage volumetric flow rate	Q	[m3/s]	0.0008
Leakage volumetric flow rate	q	[l/s]	0.80
cost of demin water per mega liter		[R/Ml]	483.81
excess water per annum		[l]	25071564
Cost of excess demin water per annum			**R 12 129.87**

The average cost for 2013 to produce a mega litre of demineralised water at Majuba power station was calculated to be R 483.81.

Table 16: Calculation of the cost of excess power required by BFP's

Excess Power from BFP's			
BFP mass Flowrate	$\dot{m}$	[kg/s]	258
BFP Speed	N_1	[rpm]	5340
BFP Power consumed	P_1	[KW]	5562
Feed water Density	p_1	[kg/m3]	928.74
BFP volumetric flowrate	V_1	[l/s]	277.80
Leakage volumetric flow rate		[l/s]	0.40
NEW BFP volumetric flow rate	V_2	[l/s]	278.19
New BFP Speed	N_2	[rpm]	5347.64
New Power consumed	P_2	[KW]	5585.91
Excess Power consumed per pump	P_excess	[KW]	23.91
Excess Power consumed by both pumps		[KW]	47.82
Cost of excess power consumed by BFP'S		[R/h]	42.56
Cost per annum			**R 372 834.24**

Above data for BFP's were acquired from the pump manuals located on the power station.

Table 17: Total financial loss per year for valve LAB 84 internally leaking steam at 0.039 kg/s

Revenue loss at full load (30% of time)	R 295 503.47
Cost of excess coal required	R 49 640.43
Cost of demineriliised water	R 12 129.87
Cost of excess auxillary power required	R 372 834.24
Total Cost	R 730 108.02

It can be seen from the above that a relatively small leakage flow of 0.039 kg/s results in a total financial loss of R 730 108.02 per annum. The cumulative leakages from all boiler drain valves will result in substantial financial losses to the power plant and could possibly provide a significant saving if problematic valves are identified and refurbished timeously.

It should also be noted that table 15 indicates that for a leakage of 0.039 kg/s, there will be 25 million litres of excess water being used by the power station. This alone can justify one to give internally leaking valves due regard and consideration as the country is currently suffering severe water shortages.

8. Valve Monitoring Program

There are many drain valves installed on a power plant, making testing each valve a massive task. Figure 51 below illustrates a process that plant personnel can follow in the determination of internally leaking valves.

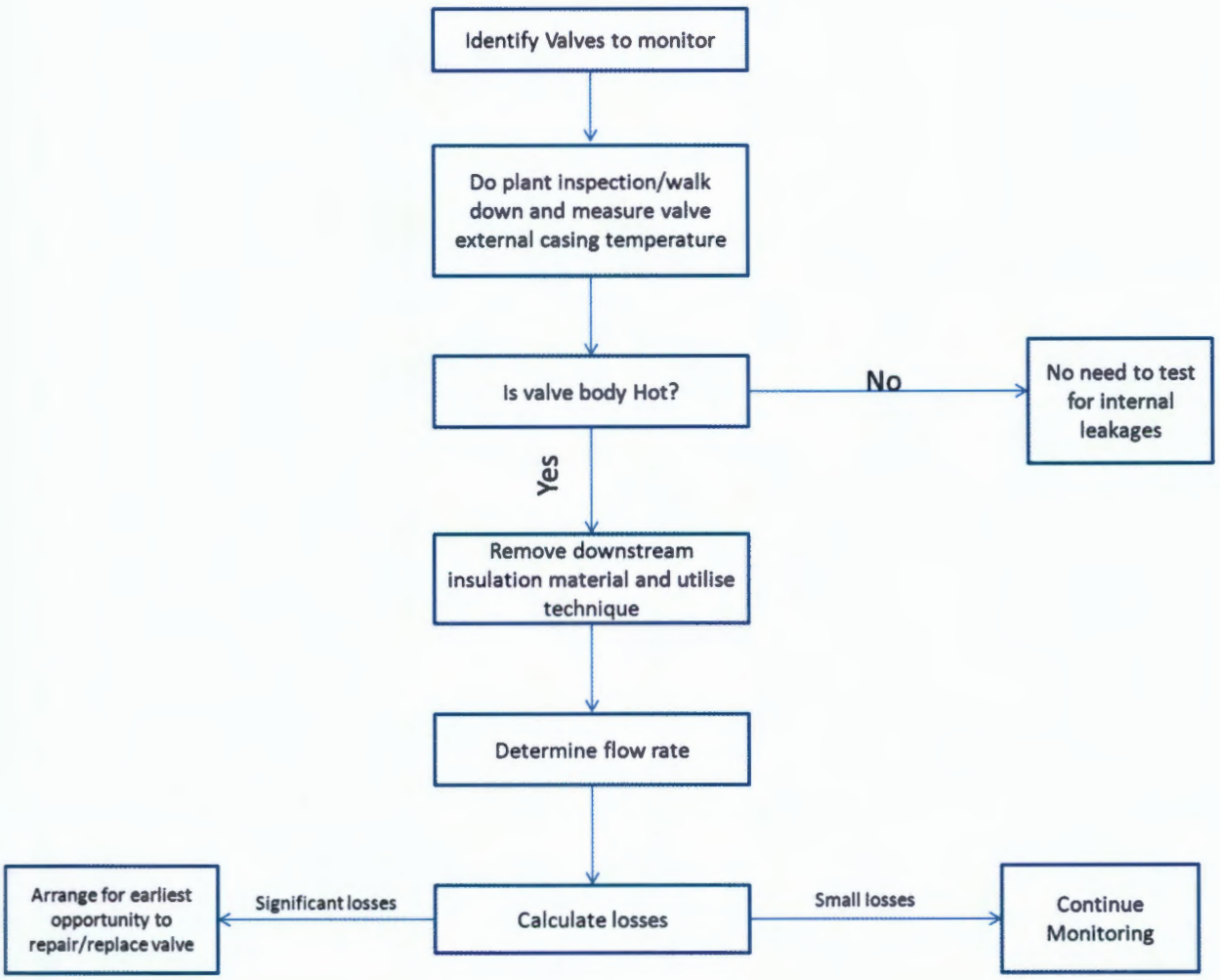

Figure 51: Process to implement valve monitoring using proposed technique

The first step in implementing a valve monitoring program will be to identify which valves should be considered. All valves will not have the same impact on the cycle and considering all drain valves will be a futile exercise. The identification of valves can be done by reviewing plant piping and instrumentation diagrams (P&ID's). The P&ID's contain information on all piping,

instrumentation, and fluid properties of the system. The valves to include are normally closed and isolate high energy steam from a lower energy sink, such as the boiler blow down vessel or the condenser.

In most drain lines on a power plant the drain valves are situated at a distance from the fluid it separates. This is shown in figure 52 below. If a drain valve is leaking fluid internally the energy level of the fluid upstream and downstream of the drain valve will be greater than if the valve is not leaking fluid internally. This elevated energy level will result in the temperature of the valve body and associated pipework upstream and downstream of the leaking valve to be greater than ambient temperature. A drain valve that is not internally leaking fluid will restrict the fluid from flowing to the downstream pipework resulting in the temperature of the valve body and associated pipework to be at ambient temperature. This is shown in figures 52 and 53 below.

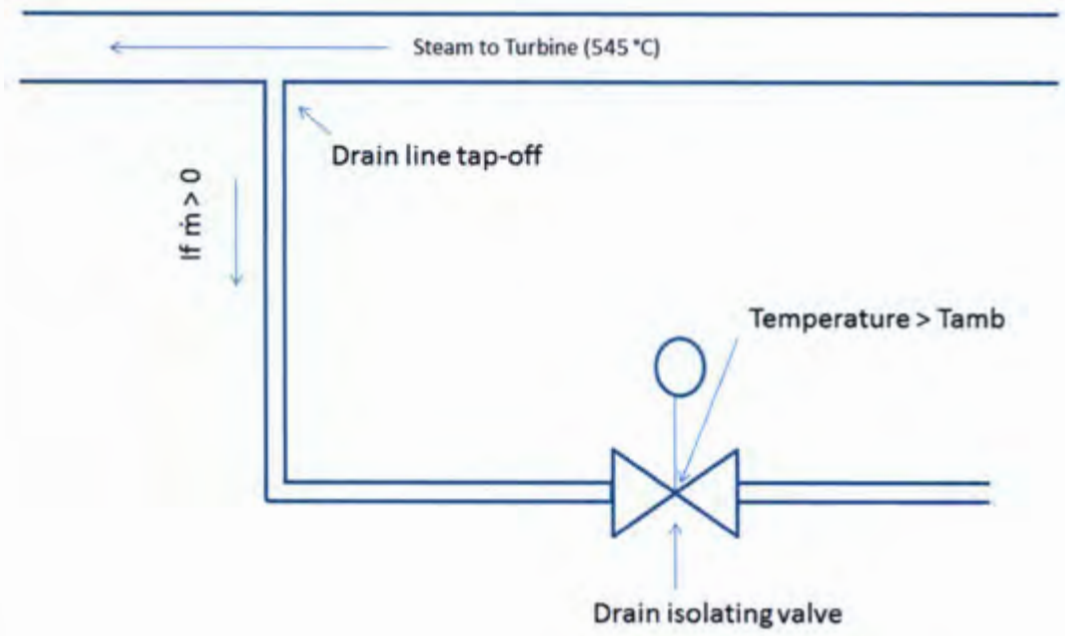

Figure 52: Drain valve that is internally leaking will cause an increase in temperature of the valve body as well as the associated pipework

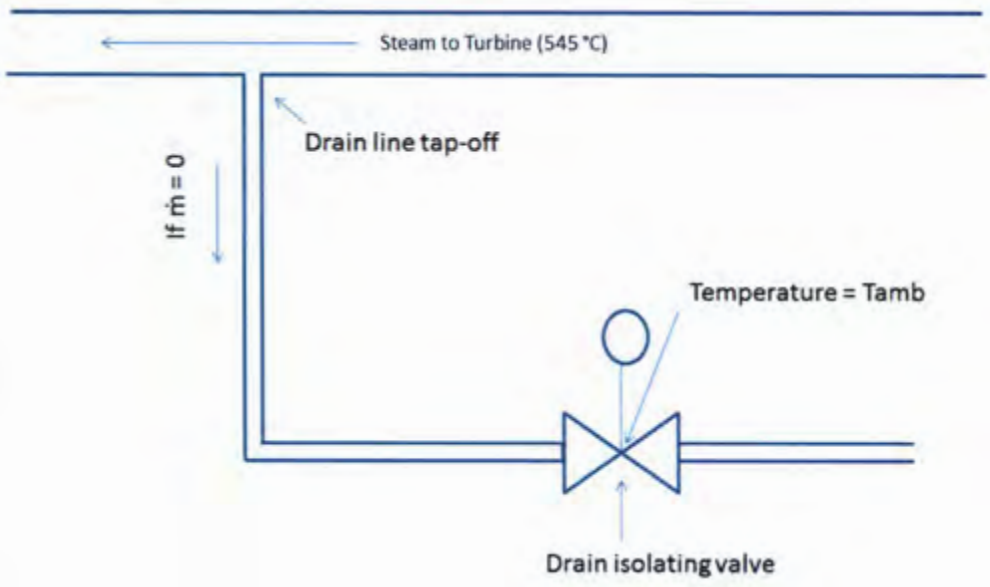

Figure 53: Drain valve that is not internally leaking steam will not increase the temperature of the valve body and associated pipe work

If one measures the temperature of the exposed valve casing one can predict if the valve is internally leaking steam or not. This will require plant personnel to point an infrared thermal camera on an exposed surface of the valve to measure the identified valves surface temperature. A relatively low temperature, close to ambient temperature, will indicate that the identified valve is not internally leaking. A high temperature will indicate that there is a possible leakage of fluid internally through the valve. Figure 54 below shows a valve body at 33.1 °C and another at 265 °C. It is clearly evident that the latter valve is leaking steam internally whilst the former is completely shut and not leaking steam. Thus, a plant operator, by measuring the temperature of the valve body can have an idea if the valve is leaking internally or not.

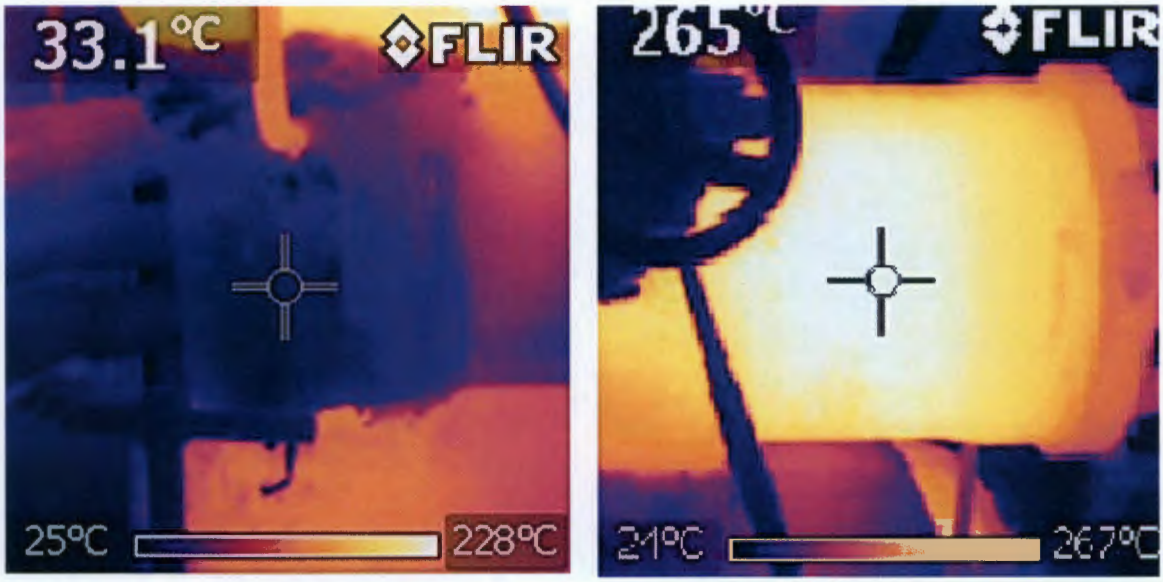

Figure 54: Thermal images of drain valve body

If the valve casing temperature is relatively low, close to ambient temperature, there is no need to utilise the technique to determine the flow rate. If the temperature is significantly greater than ambient temperature, it could either mean that the valve is leaking steam internally or the valve is located very close to the main steam line and it is getting heated up by the steam it is isolating. In this case, the technique can be employed to detect and quantify the leakage flow.

The following factors needs to be taken into consideration when choosing a suitable location to utilise the technique:

- A length of insulation material needs to be removed downstream of the identified internally leaking valve to facilitate usage of the technique.
- The location of the test length should be preferably horizontal to the floor.
- The location of the un-insulated pipe should be away from the sink so that choked flow effects and kinetic energy effects don't influence results.

Once the insulation material is removed, the operator should wait a period of time for the surface temperatures to reach equilibrium after which the technique can be employed to determine the leakage flow from the drain valve. During experimentation, the author experienced that after approximately 30 minutes the surface temperatures reached an equilibrium state. This will vary depending on the thickness of the pipe. As a precaution, one should take temperature measurements at different periods of time and only commence with test once three consecutive surface temperature readings are the same. This will ensure that the heat transfer will be at a steady state.

The leakage flow can then be used to calculate the losses experienced. Once all identified valves have been accounted for, an accumulated loss can be calculated for all valves that are leaking internally on a power generating unit. This information can assist management in

making a decision as to the most suitable time to address the losses by repairing or replacing identified internally leaking valves.

9. Conclusion

The objectives of this research were to develop an understanding of high energy valves and identify valves that are main contributors to energy losses in a power plant, to evaluate, by practical application, the suitability of different techniques to detect and quantify internal leakages through valves and to evaluate all losses associated with valves that are leaking internally.

An assessment of the water-steam cycle on a power plant indicated that the highest amount of energy added to the cycle is in the boiler which increases the energy contained in the working fluid from 1074 kJ/kg to 3400 kJ/kg. Any leakage of fluid around the boiler will result in the greatest loss to power plant efficiency. For this reason, this study identified boiler drain valves as the main contributors to energy losses in a power plant and focussed on finding a suitable technique to detect and quantify internal leakages through them.

A literature survey was conducted and it was found that techniques previously developed to detect and quantify the onset of internal valve leakages use mainly acoustic emission and infrared thermography technologies. This research mentions all techniques available, evaluates each one and chooses the most suitable one based on a set of criteria established for boiler drain valves. Amongst other requirements, the proposed technique needs to be relatively simple and straight forward and should not be reliant on pressure gauges, thermocouples, sensors etc. having to be installed into the piping network which would be not feasible and too cumbersome a solution.

The technique chosen was proposed by Sherikar [17] which uses infrared thermography to measure pipe surface temperatures of an un-insulated length of pipe located downstream of an identified valve. The underlying principal of the technique is that heat loss from the un-insulated pipe will cause a temperature drop of the flow through the un-insulated pipe which corresponds to a loss of enthalpy of the steam flow, and a means to calculate the flow rate of the leakage flow. Using fundamental principles and relevant heat transfer equations with empirical correlations, a mathematical model to calculate the mass flow rate was derived. This model was theoretically derived and needed to be experimentally validated, before it could be used in a power plant environment.

An experimental test rig was designed and connected to a mini power plant to validate the proposed mathematical model. The results obtained from the experiments indicated that although the mass flow rate calculated using the model trends the actual mass flow rate measured, there was a significant error between the two results. The error was found to be as

a result of an assumption used in the mathematical model which equated the change in steam temperature across the length of un-insulated pipe to the change in pipe surface temperature across the same pipe length.

A method was derived to calculate the upstream and downstream steam temperatures of the un-insulated pipe from the pipe surface temperatures. This method was applied to a computational simulation and found to be accurate in calculating the upstream and downstream steam temperatures of the un-insulated pipe. The mathematical model was then changed to use the change in steam temperature along the length of un-insulated pipe instead of assuming that the change in pipe surface temperature is equal to the change in steam temperature. The mathematical model, which used the change in steam temperature, was applied to a set of experimental data and the resulting mass flow rate calculation of the leakage flow was found to be more accurate than the previous mathematical model, which used the change in pipe surface temperature. The average percentage error for the actual mass flow rate measured and the mass flow rate calculated from the mathematical model using the change in pipe surface temperature was 36.3 % whilst the average percentage error improved to 18.1 % for the mass flow rate calculated from the model using the change in steam temperature across the length of un-insulated pipe. It should be noted that the mathematical model uses heat transfer equations with empirical correlations and an error of 10 to 20 % can be expected. Since the average error is below 20 %, it can be concluded that the mathematical model proposed to calculate the mass flow rate of the leakage steam is suitable in approximating the actual mass flow rate of the leakage steam.

The proposed technique was applied to two main steam drain lines on the unit 1 generator at Majuba power station. It was found that the surface temperatures on a length of un-insulated pipe downstream of the drain valve LAB 83 was at ambient temperature whilst downstream of valve LAB 84 the surface temperatures were 148 °C for the upstream of the un-insulated pipe and 135 °C for the downstream of the un-insulated pipe. From this it was evident that valve LAB 83 is not internally leaking whilst valve LAB 84 was internally leaking steam. Applying the proposed technique it was found that valve LAB 84 was internally leaking steam at 0.039 kg/s. This indicates that the technique can be utilised on a power plant environment.

The loss of high energy steam from internally leaking valves, results in a loss of power plant efficiency. More energy needs to be added to the system to maintain the generating capacity, resulting in a higher consumption of coal, higher auxiliary power consumption to feed the excess water required and higher demineralised water consumption. The loss of high energy steam can also impede the power plant from attaining maximum generation capacity due to limitations in plant components. It was found that for a relatively small leak of 0.039 kg/s from valve LAB 84 there is a total financial loss of R 730 108 per annum. It is thus fair to assume that the financial losses from a combination of all valves that are leaking internally in a power plant would be substantial.

Due to the vast amount of boiler drain valves installed on a power plant, it will be a massive task to test each valve for internal leakages. For this reason a process for plant personnel to follow in identifying internally leaking valves has been proposed in chapter 8. The process firstly requires plant personnel to identify drain valves that are required to isolate high energy steam from process and instrumentation diagrams. Thereafter the surface temperatures of the identified valves casings should be measured. An elevated temperature on the valve casing will indicate a possible leakage as explained in chapter 8. Once a possible leakage has been identified, the proposed technique can be used to calculate the flow rate of the leakage flow. The flow rate can then be used to calculate the accumulative financial losses which will be experienced from the leakage steam. This information can be used by management to make an executive decision either to shut down the generating unit to complete all maintenance activities or to continue operation beyond a planned maintenance interval as is currently the norm.

10.Recommendations

The proposed technique has been experimentally validated in this research for calculating a fairly accurate mass flow rate of a leakage steam flow through an internally leaking valve expanding to atmospheric pressure. The experiments conducted were done on a mini steam plant that only allowed for the generation of steam at a maximum temperature and pressure of 250 °C and 6 bar respectively, which was allowed to flow through relatively small pipe diameters of 15mm. Typically, in a power plant the temperatures, pressures and pipe diameters are greater. Rudimentary computational simulations performed in Flownex indicated that the proposed technique can be successfully utilised for all steam temperatures above the saturation temperature of the fluid and for all pipe diameters, hence the proposed technique can be utilised on a power plant environment. However, it will be useful for a live test rig to be installed on a power plant to validate the technique for use in a power plant environment. This will allow for greater confidence in the use of the proposed technique.

Chapter 8 proposes steps to follow in implementing a valve monitoring program on a power plant. It will be of value for a comprehensive maintenance procedure to be drawn up by relevant personnel in the power station to effectively assist maintenance personnel in implementing this valve monitoring program. The maintenance procedure should encompass all valves that could potentially have the greatest impact on power plant efficiency, methods and procedures of conducting the proposed technique and the relevant equations that make up the mathematical model to calculate a leakage flow rate from an identified internally leaking valve.

For the valve monitoring program to add value to the operation of the power plant an interpretation of the leakage flow rate and the financial impact is paramount. It is recommended that plant management understand the impact of internally leaking valves to the bottom line, and decide at what point it is no longer feasible to continue operating the plant with internally leaking valves. When the cumulative losses for all valves that are internally leaking exceed this point, the power plant should be shut-down to repair identified valves. This will ensure that the proposed technique is used effectively in eliminating losses caused by internally leaking valves and will allow for cost savings and excess power generating capacity.

11. References

[1] "Introduction to valves." Internet: www.varjepc.com/admin/upload/handbooks/Valve%20Handbook.pdf, [Dec. 5, 2013]

[2] T. C. Dickenson. *Valves, Piping and Pipeline Handbook.* Oxford: Elsevier Advanced Technology, 1999, pp 41-91.

[3] W.Kawewwaewnoi, A. Prateepasen, P. Kaewtrakulpong. "Measurement of valve leakage rate using acoustic emission." *ECTI-CON 2005*, pp. 597-600, May 2005.

[4] W.Kawewwaewnoi, A. Prateepasen, P. Kaewtrakulpong. "Investigation of the relationship between internal fluid leakage through a valve and the acoustic emission generated from the leakage." *Measurement*, vol.43, pp. 274-282, Feb. 2010.

[5] T.F. Drouillard. "A history of acoustic emission." *Journal of Acoustic Emission,* vol. 14, pp. 1-34, Oct. 1996.

[6] V. Delarue. "Leak detection and location for gas transmission pipelines." *Proceedings of the 1st International Conference on Pipelines,* vol. 2, pp 1109-1115, Nov. 1996.

[7] J.M Rajtar and R. Muthiah. "Pipeline leak detection system for oil and gas flow lines." *Journal of Manufacturing Science and Engineering,* vol. 119, pp 105-109, Oct. 1997.

[8] R.V Williams. *Acoustic Emission*. Bristol: Adam Hilger Ltd, 1980, pp. 52-70.

[9] M.A. Sharif, R.I. Grosvenor. "Internal valve leakage detection using an acoustic emission measurement system." *Transactions of the Institute of Measurement and Control,* vol. 20, pp. 233-242, Dec. 1998.

[10] A. Prateepasen, W. Kaewwaewnoi, P. Kaewtrakulpong. "Smart portable noninvasive instrument for detection of internal air leakage of a valve using acoustic emission signals." *Measurement*, vol. 44, pp. 378–384, Feb. 2011

[11] E. Meland, N.F. Thornhill, E. Lunde, M. Rasmussen. "Quantification of valve leakage rates." *AIChE Journal,* vol. 58 pp. 1181-1193, Apr. 2012

[12] E. Meland, V. Henrikson, E. Hennie, M. Rasmussen. "Spectral analysis of internally leaking shut-down valves." *Measurement,* vol. 44, pp 1059-1072, Mar. 2011.

[13] S. Dudic, I. Ignjatovic, D. Seslija, V. Blagojevic, M.Stojiljkovic. "Leakage quantification of compressed air using ultrasound and infrared thermography." *Measurement*, vol. 45, pp.1689-1694, Aug. 2012.

[14] C. Meola, G.M. Carlomagno. "Recent advances in the use of infrared thermography." *Measurement Science and Technology,* vol. 15, pp R27-R58, Jul. 2004.

[15] G.L. Orlove, R.P. Madding. " A primer on infrared thermography." Internet: http://files.aws.org/itrends/2009/04/it200904/it0409-16.pdf, [Dec. 5, 2013]

[16] S. Korellis. "Cost-benefit assessment of cycle alignment." *Electric Power Research Institute,* technical update 1024640, Nov. 2011.

[17] S. Sherikar. "Method of determining valve leakage based on upstream and downstream temperature measurements." U.S. Patent 7 031 851, Apr. 18, 2006.

[18] "Differential pressure: a difference you can see." Internet: http://www.wika.us/AN_0711_en_us.WIKA, [Nov. 29, 2013]

[19] G. Thompson, G. Zolkiewski. "An experimental investigation into the detection of internal leakage of gases through valves by vibration analyses." *Proceedings of the Institute of Mechanical Engineers,* vol. 211, pp 195-207, Aug. 1997.

[20] "Vibration." Internet: http://www.azimadli.com/vibman/whatisvibration.htm, [Dec. 5, 2013].

[21] A. Freidman. "How vibration works- the importance of trending." Internet: http://www.mobiusinstitute.com/articles.aspx?id=1680, [Dec.5, 2013].

[22] G. Thompson, L.S Wijesundera. "Leak rate measurement and leak detection through standard design process valves by vibration monitoring." *Second Cairo MDP Conference*, pp. 289-296, Nov. 1982.

[23] F. Incropera, D. Dewitt, T Bergman, A. Lavine. *Fundamentals of Heat and Mass Transfer.* New York: Wiley, 2007, pp.571-582.

[24] I.J. Karassik, J.P. Messina, P. Cooper, C.C. Heald. *Pump Handbook*. New York: McGraw Hill, 2008, chapter 2.

[25] D.G. Kroger. *Air-Cooled Heat Exchangers and Cooling Towers*. Oklahoma: PennWell Corparation, 2004, A.1-3.

[26] Measurement of fluid flow by means of pressure differential devices inserted in circular cross-section conduits, ISO Standard 5167, 2003

[27] M.A. Boles, Y.A. Cengel. Thermodynamics: An Engineering Approach. New York: McGraw Hill, 2006, pp.239-240.

[28] M.J. Moran, H.N. Shapiro. Fundamentals of Engineering Thermodynamics. Chichester: Wiley, 2006, pp.147-148.

[29] J.H. Leinhard IV, J.H. Leinhard V. A Heat Transfer Textbook. Massachusetts: Phlogiston Press, 2006, pp. 355-365.

[30] M.J. Moran, H.N. Shapiro, B.R. Munson, D.P. Dewitt. Introduction to Thermal Systems Engineering. New York: Wiley, 2003,pp. 424-437.

Appendices

Appendix A

Upstream and Downstream Fluid Properties of an Internally Leaking Valve

In order to select an appropriate monitoring technique to detect and quantify internal leakages of drain valves in a power plant environment, the fluid properties upstream and downstream of an internally leaking drain valve first needs to be understood. To accomplish this, a computational simulation was carried out in Flownex SE. Flownex SE is a computational simulation software that enables one to model systems and study how systems will behave in the real world, where fluid is the driving factor. The software is extensively used in the power generation sector throughout the world. It should be noted that most components in Flownex takes into consideration compressible flow effects.

The model created in Flownex SE was based on a typical main steam drain line configuration at Majuba Power Station. The main steam line transports steam to the turbine at pressures and temperatures of 16.4 MPa and 540 °C respectively. At the lowest point of the main steam line, a drain line is inserted which serves the function of draining the main steam line in start-up, shutdown and emergency conditions. The control of this is accomplished by a motorised drain valve, installed to the drain line, which when in the fully opened position drains the main steam line, and in the fully closed position isolates (shuts-off) fluid flow through the drain line. The drain lines discharge into the boiler blow down vessel which is maintained at atmospheric conditions.

Figure A.1 below illustrates the model created in Flownex.

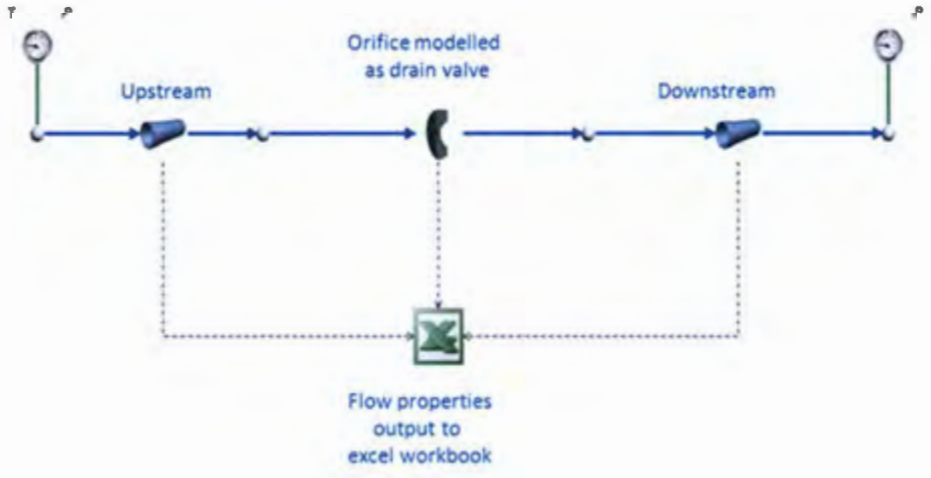

Figure A.1- Flownex model of typical drain valve

The model comprised a length of upstream and downstream piping connected to an orifice plate. It was decided to model an internally leaking valve as an orifice plate, since the orifice diameter can be varied in small percentages of pipe internal diameter. This enables one to better simulate flow through an internally leaking valve since the leak path of a valve that is internally leaking compared to the pipe diameter is extremely small.

In the simulations, the pipe lengths (10 meters), pipe diameters (44.1mm), upstream temperature (540 °C) and pressure (16.4 MPa), and the downstream pressures (1 bar) were kept constant, whilst the orifice diameter was varied between 0.1 – 10 % of pipe internal diameter. The upstream and downstream lengths of pipe were divided into 5 increments each. For each variation in orifice diameter, fluid properties were output to an excel workbook for each of the 10 increments. Table A.1 below shows the results from the simulation and section 3.5.1 contains the relevant graphs and explanations, relevant to this study.

Table A.1 Flownex simulation results for flow through an internally leaking drain valve.

Orifice Diameter	[m]	0.000441											
Mass Flow Rate	[kg/s]	0.002417178											
% of pipe internal diameter	[%]	1											
		UPSTREAM OF DRAIN VALVE						DOWNSTREAM OF DRAIN VALVE					
Node point along pipe	[m]	0	2	4	6	8	10	0	2	4	6	8	10
Pressure	[kPa]	16399.99998	16399.99993	16399.99989	16399.99984	16399.99982	16399.99982	101.0235746	101.0180102	101.0124513	101.0068938	101.0013626	100.9958068
Temperature	[°C]	539.9999998	538.5294613	538.5294611	538.5294609	538.5294608	538.5294608	461.0719769	461.0719439	461.0719113	461.0718789	461.071848	461.0718156
Enthalpy	[kJ/kg]	3406.153599	3406.153599	3406.153599	3406.153599	3406.153599	3406.153599	3406.139539	3406.139537	3406.139536	3406.139534	3406.139533	3406.139531
Velocity	[m/s]	0.031847485	0.031751417	0.031751418	0.031751418	0.031751418	0.031751418	5.303073633	5.30336603	5.303658181	5.303950296	5.304241115	5.304533209
Density	[kg/m3]	49.84005784	49.84005784	49.84005771	49.84005758	49.84005748	49.84005744	0.298402203	0.298385758	0.298369323	0.298352927	0.298336534	0.298336534
Speed of Sound	[m/s]	655.0969863	654.2027787	654.2027787	654.2027787	654.2027787	654.2027787	658.5257221	658.5257255	658.5257289	658.5257324	658.5257365	658.52574
Mach Number	[]	4.75681E-05	4.74675E-05	4.74675E-05	4.74675E-05	4.74675E-05	4.74675E-05	0.008052154	0.008052598	0.008053042	0.008053485	0.008053927	0.008054371

Orifice Diameter	[m]	0.000882											
Mass Flow Rate	[kg/s]	0.009668826											
% of pipe internal diameter	[%]	2											
		UPSTREAM OF DRAIN VALVE						DOWNSTREAM OF DRAIN VALVE					
Node point along pipe	[m]	0	2	4	6	8	10	0	2	4	6	8	10
Pressure	[kPa]	16399.99965	16399.99903	16399.99845	16399.9978	16399.99717	16399.99662	101.455977	101.3515666	101.247055	101.1424285	101.0376972	100.932858
Temperature	[°C]	539.9999971	538.5294562	538.5294538	538.5294512	538.5294485	538.5294463	460.9757637	460.9749522	460.9741396	460.9733251	460.9725093	460.971692
Enthalpy	[kJ/kg]	3406.153592	3406.153592	3406.153592	3406.153592	3406.153592	3406.153592	3405.93059	3405.930129	3405.929668	3405.929204	3405.928738	3405.92827
Velocity	[m/s]	0.127391416	0.127007145	0.127007149	0.127007154	0.127007159	0.127007162	21.11920795	21.14098069	21.16281965	21.18472782	21.20670346	21.2287475
Density	[kg/m3]	49.84005619	49.84005619	49.84005445	49.84005266	49.84005081	49.84004909	0.29957485	0.299266014	0.298956858	0.298647376	0.29833758	0.29833758
Speed of Sound	[m/s]	655.0969854	654.2027777	654.2027775	654.2027773	654.2027772	654.202777	658.4839364	658.4839174	658.4838982	658.4838786	658.4838588	658.4838387
Mach Number	[]	0.000190275	0.000189872	0.000189872	0.000189872	0.000189872	0.000189872	0.032069374	0.032102454	0.032135634	0.032168919	0.032202307	0.032235799

Orifice Diameter	[m]	0.001323											
Mass Flow Rate	[kg/s]	0.021755157											
% of pipe internal diameter	[%]	3											
		UPSTREAM OF DRAIN VALVE						DOWNSTREAM OF DRAIN VALVE					
Node point along pipe	[m]	0	2	4	6	8	10	0	2	4	6	8	10
Pressure	[kPa]	16399.9982	16399.99549	16399.99266	16399.98987	16399.98706	16399.98452	102.9606969	102.5045522	102.0463329	101.5860217	101.1235881	100.6590042
Temperature	[°C]	539.9999855	538.529436	538.5294243	538.5294127	538.5294011	538.5293907	460.5725831	460.565371	460.558063	460.5506574	460.5431517	460.5355433
Enthalpy	[kJ/kg]	3406.153559	3406.153559	3406.153559	3406.153559	3406.153559	3406.153559	3405.058622	3405.048859	3405.03892	3405.0288	3405.018494	3405.007996
Velocity	[m/s]	0.286634653	0.285770066	0.285770114	0.28577016	0.285770206	0.285770245	46.79696188	47.00511679	47.21609122	47.42994448	47.64674343	47.8665557
Density	[kg/m3]	49.84004954	49.84004954	49.84004149	49.84003332	49.84002519	49.84001744	0.303679061	0.302328216	0.300971215	0.299607987	0.298238445	0.298238445
Speed of Sound	[m/s]	655.0969815	654.2027732	654.2027724	654.2027716	654.2027708	654.2027701	658.3097344	658.3081114	658.3064546	658.3047634	658.3030366	658.3012733
Mach Number	[]	0.000428124	0.000427219	0.000427219	0.000427219	0.000427219	0.000427219	0.071080391	0.07139691	0.07171772	0.072042911	0.072372584	0.072706843

Orifice Diameter	[m]	0.001764											
Mass Flow Rate	[kg/s]	0.038676578											
% of pipe internal diameter	[%]	4											
		UPSTREAM OF DRAIN VALVE						DOWNSTREAM OF DRAIN VALVE					
Node point along pipe	[m]	0	2	4	6	8	10	0	2	4	6	8	10
Pressure	[kPa]	16399.99433	16399.98608	16399.9778	16399.96953	16399.96126	16399.95296	106.6782696	105.3611858	104.0268328	102.6745031	101.3034383	99.91282995
Temperature	[°C]	539.9999542	538.5293819	538.5293477	538.5293135	538.5292794	538.529245	459.5930372	459.5474193	459.4997229	459.4497843	459.397422	459.3424393
Enthalpy	[kJ/kg]	3406.15347	3406.153471	3406.153471	3406.153471	3406.153471	3406.153471	3402.938952	3402.858352	3402.773566	3402.684258	3402.590053	3402.490547
Velocity	[m/s]	0.509582597	0.508045692	0.508045937	0.508046182	0.508046427	0.508046673	80.18288681	81.18187524	82.2196374	83.29876855	84.42211633	85.59267516
Density	[kg/m3]	49.84003182	49.84003182	49.84000781	49.8399838	49.83995979	49.83993575	0.31384778	0.309936393	0.305973143	0.301955882	0.297882308	0.297882308
Speed of Sound	[m/s]	655.0969711	654.2027613	654.2027589	654.2027565	654.2027542	654.2027518	657.8859958	657.8708839	657.8549518	657.8381327	657.8203527	657.8015315
Mach Number	[]	0.000761123	0.000759515	0.000759515	0.000759516	0.000759516	0.000759516	0.121871997	0.123394226	0.124975664	0.126620282	0.12833244	0.130116723

Orifice Diameter [m] 0.002205
Mass Flow Rate [kg/s] 0.060433701
% of pipe internal diameter [%] 5

		UPSTREAM OF DRAIN VALVE						DOWNSTREAM OF DRAIN VALVE					
Node point along pipe	[m]	0	2	4	6	8	10	0	2	4	6	8	10
Pressure	[kPa]	16399.98615	16399.96693	16399.94765	16399.92836	16399.90905	16399.88982	114.0998806	111.1332385	108.0786712	104.9276538	101.6701689	98.29448486
Temperature	[°C]	539.9998882	538.5292708	538.5291912	538.5291114	538.5290317	538.5289522	457.930317	457.7402244	457.5295483	457.2944739	457.030157	456.7306459
Enthalpy	[kJ/kg]	3406.153283	3406.153285	3406.153285	3406.153285	3406.153285	3406.153285	3399.325836	3398.959592	3398.550903	3398.091814	3397.572218	3396.97967
Velocity	[m/s]	0.796243528	0.793842558	0.793843448	0.793844339	0.793845231	0.793846117	116.8568672	119.9500604	123.3101514	126.9786251	131.0067303	135.4542712
Density	[kg/m3]	49.83999548	49.83999548	49.83993953	49.83988356	49.83982755	49.83977163	0.334212883	0.325353534	0.316224848	0.306799962	0.297047243	0.297047243
Speed of Sound	[m/s]	655.0969491	654.2027363	654.2027308	654.2027252	654.2027197	654.2027142	657.162211	657.091349	657.0120868	656.9228416	656.8216003	656.7058869
Mach Number	[]	0.001189286	0.001186774	0.001186775	0.001186776	0.001186778	0.001186779	0.177815567	0.182546068	0.187686676	0.193301447	0.199469562	0.206283656

Orifice Diameter [m] 0.002646
Mass Flow Rate [kg/s] 0.087027444
% of pipe internal diameter [%] 6

		UPSTREAM OF DRAIN VALVE						DOWNSTREAM OF DRAIN VALVE					
Node point along pipe	[m]	0	2	4	6	8	10	0	2	4	6	8	10
Pressure	[kPa]	16399.97127	16399.93245	16399.89352	16399.85458	16399.81564	16399.77669	126.9442801	121.3551697	115.4566886	109.188522	102.4672986	95.17292777
Temperature	[°C]	539.9997682	538.5290703	538.5289093	538.5287484	538.5285875	538.5284265	455.8607562	455.327273	454.6838383	453.889528	452.8795846	451.5627844
Enthalpy	[kJ/kg]	3406.152943	3406.152947	3406.152947	3406.152947	3406.152947	3406.152947	3394.78393	3393.729112	3392.449305	3390.86125	3388.833411	3386.147031
Velocity	[m/s]	1.146629939	1.143173733	1.143176325	1.143178918	1.14318151	1.143184104	150.7956882	157.6355813	165.5553966	174.8848168	186.1192564	200.0328445
Density	[kg/m3]	49.8399299	49.8399299	49.83981689	49.83970388	49.83959087	49.83947784	0.369641308	0.352800315	0.334977693	0.315968922	0.295491392	0.295491392
Speed of Sound	[m/s]	655.0969091	654.202691	654.2026798	654.2026686	654.2026574	654.2026463	656.2479896	656.0402241	655.7869454	655.4710007	655.0651817	654.5310969
Mach Number	[]	0.001712631	0.001709015	0.001709019	0.001709023	0.001709027	0.001709031	0.229774975	0.240269242	0.252429192	0.266765965	0.28404993	0.305561678

Orifice Diameter [m] 0.003087
Mass Flow Rate [kg/s] 0.118459057
% of pipe internal diameter [%] 7

		UPSTREAM OF DRAIN VALVE						DOWNSTREAM OF DRAIN VALVE					
Node point along pipe	[m]	0	2	4	6	8	10	0	2	4	6	8	10
Pressure	[kPa]	16399.94678	16399.87618	16399.80535	16399.73453	16399.66371	16399.59288	146.870944	137.7447308	127.8269821	116.8531868	104.359456	89.37797469
Temperature	[°C]	539.9995705	538.528742	538.5284493	538.5281566	538.5278639	538.5275712	453.9524779	452.9010819	451.5091605	449.5599462	446.6205731	441.539346
Enthalpy	[kJ/kg]	3406.152382	3406.152389	3406.152389	3406.152389	3406.152389	3406.152389	3390.505379	3388.411475	3385.625683	3381.715482	3375.752893	3365.281704
Velocity	[m/s]	1.560759014	1.556057414	1.556063833	1.556070251	1.556076668	1.556083088	176.9080064	188.3726341	202.622394	221.0797039	246.5794282	285.9087143
Density	[kg/m3]	49.83982262	49.83982262	49.83961707	49.83941152	49.83920598	49.83900042	0.425060351	0.397251125	0.366806902	0.332735643	0.293068806	0.293068806
Speed of Sound	[m/s]	655.0968433	654.2026165	654.2025962	654.2025758	654.2025555	654.2025351	655.3770245	654.9607787	654.402581	653.610959	652.402531	650.2866566
Mach Number	[]	0.002331183	0.002326265	0.002326275	0.002326285	0.002326295	0.002326305	0.269875235	0.287532341	0.309511298	0.338035015	0.377683636	0.439477971

Orifice Diameter [m] 0.003528
Mass Flow Rate [kg/s] 0.154730111
% of pipe internal diameter [%] 8

		UPSTREAM OF DRAIN VALVE						DOWNSTREAM OF DRAIN VALVE					
Node point along pipe	[m]	0	2	4	6	8	10	0	2	4	6	8	10
Pressure	[kPa]	16399.90919	16399.79032	16399.67109	16399.55186	16399.4326	16399.31335	175.2258417	161.9700553	147.195542	130.1624488	109.183563	77.54613563
Temperature	[°C]	539.9992672	538.5282404	538.5277476	538.5272549	538.526762	538.5262691	452.6919615	451.1393667	448.9238809	445.4717506	439.0398938	419.4864307
Enthalpy	[kJ/kg]	3406.151522	3406.151534	3406.151534	3406.151534	3406.151534	3406.151534	3387.469881	3384.375702	3379.941793	3372.943792	3359.771673	3319.168973
Velocity	[m/s]	2.038652653	2.032517181	2.03253129	2.0325454	2.032559515	2.032573629	193.3065932	208.7002559	228.962036	257.7200347	304.5715925	417.0962168
Density	[kg/m3]	49.83965873	49.83965873	49.83931266	49.83896661	49.83862052	49.83827441	0.504749561	0.463968429	0.417878586	0.363171189	0.289819685	0.289819685
Speed of Sound	[m/s]	655.0967422	654.2025024	654.2024681	654.2024339	654.2023996	654.2023653	654.7513177	654.1347785	653.2410714	651.8271553	649.1495483	640.8235764
Mach Number	[]	0.003044976	0.003038561	0.003038583	0.003038605	0.003038626	0.003038648	0.295155348	0.318941362	0.350319458	0.395156493	0.468972599	0.651237821

Orifice Diameter [m] 0.003969
Mass Flow Rate [kg/s] 0.195842445
% of pipe internal diameter [%] 9

		UPSTREAM OF DRAIN VALVE						DOWNSTREAM OF DRAIN VALVE					
Node point along pipe	[m]	0	2	4	6	8	10	0	2	4	6	8	10
Pressure	[kPa]	16399.85452	16399.66589	16399.47664	16399.28738	16399.09813	16398.90887	213.2340832	195.6866425	175.8587179	152.4128112	121.6976434	55.38738104
Temperature	[°C]	539.998826	538.5275126	538.5267304	538.5259483	538.5251661	538.5243839	452.2302316	450.3884192	447.6589824	443.099928	433.0567873	369.4033676
Enthalpy	[kJ/kg]	3406.150271	3406.150291	3406.150291	3406.150291	3406.150291	3406.150291	3385.97999	3382.312118	3376.852024	3367.624505	3347.374113	3215.563106
Velocity	[m/s]	2.580336886	2.572581653	2.572610005	2.572638358	2.572666712	2.572695067	200.8661766	218.36429	242.0808787	277.5935701	342.8687408	617.3985654
Density	[kg/m3]	49.83942099	49.83942099	49.83887174	49.83832247	49.83777319	49.83722391	0.612782902	0.558510899	0.496012586	0.418718847	0.286991583	0.286991583
Speed of Sound	[m/s]	655.0965952	654.2023365	654.2022821	654.2022277	654.2021734	654.202119	654.4323441	653.7055667	652.6077949	650.7394304	646.5353534	618.6518991
Mach Number	[]	0.003854048	0.003845945	0.003845989	0.003846032	0.003846076	0.003846119	0.306852019	0.333958774	0.370793476	0.426370548	0.529725642	1

Orifice Diameter [m] 0.00441
Mass Flow Rate [kg/s] 0.241798258
% of pipe internal diameter [%] 10

		UPSTREAM OF DRAIN VALVE						DOWNSTREAM OF DRAIN VALVE					
Node point along pipe	[m]	0	2	4	6	8	10	0	2	4	6	8	10
Pressure	[kPa]	16399.77824	16399.49273	16399.20628	16398.91983	16398.63337	16398.3469	262.9924556	241.4439653	217.0985263	188.336637	150.7901264	55.34729836
Temperature	[°C]	539.9982104	538.526499	538.5253151	538.5241312	538.5229473	538.5217634	452.521883	450.6684154	447.9564722	443.3553305	433.287011	368.7926157
Enthalpy	[kJ/kg]	3406.148525	3406.148556	3406.148555	3406.148555	3406.148555	3406.148555	3385.941809	3382.286236	3376.841761	3367.680917	3347.790686	3215.422127
Velocity	[m/s]	3.185843318	3.176286187	3.176339172	3.17639216	3.176445151	3.176498145	201.0561659	218.4827869	242.1232686	277.3902758	341.6516165	617.6268662
Density	[kg/m3]	49.83908994	49.83908994	49.83825859	49.83742721	49.83659582	49.8357644	0.75603237	0.689334915	0.612488819	0.517905845	0.28792169	0.28792169
Speed of Sound	[m/s]	655.0963901	654.2021052	654.2020229	654.2019405	654.2018582	654.2017759	654.3955935	653.6755329	652.5982998	650.7270911	646.5308648	618.3743729
Mach Number	[]	0.004758447	0.004748471	0.004748552	0.004748633	0.004748715	0.004748796	0.307135836	0.334140879	0.370964287	0.425983899	0.527314522	1

Orifice Diameter [m] 0.004851
Mass Flow Rate [kg/s] 0.29259926
% of pipe internal diameter [%] 11

		UPSTREAM OF DRAIN VALVE						DOWNSTREAM OF DRAIN VALVE					
Node point along pipe	[m]	0	2	4	6	8	10	0	2	4	6	8	10
Pressure	[kPa]	16399.67526	16399.25947	16398.84229	16398.42511	16398.00791	16397.59071	323.947489	298.6226062	270.2433051	237.1990766	195.6015283	58.2779456
Temperature	[°C]	539.9973794	538.5251327	538.5234085	538.5216843	538.51996	538.5182357	453.2345992	451.4949252	449.0186787	445.0441013	436.7898939	367.9322863
Enthalpy	[kJ/kg]	3406.146169	3406.146213	3406.146213	3406.146212	3406.146212	3406.146212	3386.633248	3383.275164	3378.40018	3370.507253	3354.88902	3215.223631
Velocity	[m/s]	3.855198174	3.843662294	3.843755675	3.843849064	3.843942461	3.844035866	197.5872077	213.9085576	235.5988978	267.0069179	320.201749	617.9481671
Density	[kg/m3]	49.83864376	49.83864376	49.837433	49.8362222	49.83501136	49.83380047	0.932595281	0.854445793	0.765547959	0.658373085	0.309853019	0.309853019
Speed of Sound	[m/s]	655.0961132	654.201793	654.2016731	654.2015532	654.2014334	654.2013135	654.5027077	653.8419647	652.8767578	651.2856507	647.8823316	617.9680283
Mach Number	[]	0.005758212	0.005746186	0.005746329	0.005746472	0.005746615	0.005746759	0.301761519	0.32701637	0.360721175	0.409708689	0.492400916	1

Orifice Diameter	[m]	0.005292
Mass Flow Rate	[kg/s]	0.348242292
% of pipe internal diameter	[%]	12

		UPSTREAM OF DRAIN VALVE						DOWNSTREAM OF DRAIN VALVE					
Node point along pipe	[m]	0	2	4	6	8	10	0	2	4	6	8	10
Pressure	[kPa]	16399.54001	16398.95356	16398.36515	16397.77672	16397.18827	16396.5998	384.9779678	354.9109824	321.2002216	281.9420654	232.5482965	69.48823292
Temperature	[°C]	539.9962879	538.5233401	538.5209081	538.5184761	538.5160439	538.5136117	453.594585	451.8333074	449.3143844	445.3021106	436.996215	367.9657046
Enthalpy	[kJ/kg]	3406.143073	3406.143136	3406.143135	3406.143135	3406.143134	3406.143133	3386.583372	3383.224288	3378.332117	3370.418427	3354.797457	3215.231343
Velocity	[m/s]	4.588364766	4.574680606	4.574837372	4.574994156	4.575150959	4.57530778	197.8394717	214.1462677	235.8876149	267.339384	320.4875741	617.935687
Density	[kg/m3]	49.8380584	49.8380584	49.83635067	49.83464286	49.83293497	49.83122699	1.108627815	1.015737508	0.909921158	0.782735976	0.368778387	0.368778387
Speed of Sound	[m/s]	655.0957496	654.2013832	654.201214	654.2010449	654.2008758	654.2007068	654.4597436	653.8035778	652.8355367	651.246013	647.8418492	617.9264077
Mach Number	[]	0.00685329	0.006839048	0.006839288	0.006839528	0.006839769	0.006840009	0.302097285	0.32734679	0.361111219	0.410201978	0.49279109	1

Orifice Diameter	[m]	0.005733
Mass Flow Rate	[kg/s]	0.408728529
% of pipe internal diameter	[%]	13

		UPSTREAM OF DRAIN VALVE						DOWNSTREAM OF DRAIN VALVE					
Node point along pipe	[m]	0	2	4	6	8	10	0	2	4	6	8	10
Pressure	[kPa]	16399.36633	16398.56124	16397.75343	16396.94559	16396.13771	16395.32979	451.2725647	416.0429757	376.5487764	330.5546271	272.6459122	81.65941802
Temperature	[°C]	539.9948863	538.5210401	538.5177013	538.5143622	538.5110231	538.5076837	453.9869972	452.2001011	449.6553565	445.6044058	437.2266983	368.0195531
Enthalpy	[kJ/kg]	3406.139099	3406.139185	3406.139184	3406.139182	3406.139181	3406.139179	3386.534095	3383.172259	3378.27779	3370.353441	3354.694832	3215.24377
Velocity	[m/s]	5.385365095	5.369372523	5.369625139	5.369877796	5.370130493	5.370383231	198.0883907	214.3890923	236.117808	267.5823584	320.8076313	617.9155772
Density	[kg/m3]	49.83730746	49.83730746	49.83496298	49.83261834	49.83027355	49.82792859	1.299630408	1.190891925	1.067069313	0.917664323	0.432810198	0.432810198
Speed of Sound	[m/s]	655.0952826	654.200857	654.2006248	654.2003926	654.2001605	654.1999284	654.4141612	653.7620213	652.7995925	651.2126547	647.8009241	617.8892231
Mach Number	[]	0.008043714	0.008027105	0.008027492	0.008027879	0.008028266	0.008028653	0.302418694	0.327672497	0.361436727	0.410545959	0.493239621	1

Orifice Diameter	[m]	0.006174
Mass Flow Rate	[kg/s]	0.474056824
% of pipe internal diameter	[%]	14

		UPSTREAM OF DRAIN VALVE						DOWNSTREAM OF DRAIN VALVE					
Node point along pipe	[m]	0	2	4	6	8	10	0	2	4	6	8	10
Pressure	[kPa]	16399.14756	16398.06755	16396.98386	16395.90011	16394.81628	16393.73239	522.8783082	482.0475738	436.2987853	383.0313674	315.9566976	94.81654613
Temperature	[°C]	539.9931209	538.518145	538.5136657	538.509186	538.5047062	538.500226	454.4131004	452.595935	450.0240348	445.9473969	437.5005102	368.087851
Enthalpy	[kJ/kg]	3406.134093	3406.134208	3406.134205	3406.134203	3406.1342	3406.134198	3386.500814	3383.122081	3378.222841	3370.296978	3354.616837	3215.259531
Velocity	[m/s]	6.246192391	6.227743427	6.228136514	6.228529686	6.228922943	6.229316284	198.2563301	214.6230143	236.3504115	267.7932857	321.050658	617.8900695
Density	[kg/m3]	49.83636225	49.83636225	49.83321709	49.83007164	49.82692591	49.8237799	1.505702364	1.379814709	1.236526257	1.063696839	0.501931944	0.501931944
Speed of Sound	[m/s]	655.0946944	654.2001943	654.1998827	654.1995713	654.1992599	654.1989487	654.3664808	653.7175776	652.76148	651.1841659	647.7676879	617.8536356
Mach Number	[]	0.009329474	0.009310366	0.009310969	0.009311571	0.009312173	0.009312776	0.302607987	0.327975975	0.361758954	0.410868267	0.493564947	1

Orifice Diameter	[m]	0.006615
Mass Flow Rate	[kg/s]	0.54422511
% of pipe internal diameter	[%]	15

		UPSTREAM OF DRAIN VALVE						DOWNSTREAM OF DRAIN VALVE					
Node point along pipe	[m]	0	2	4	6	8	10	0	2	4	6	8	10
Pressure	[kPa]	16398.87651	16397.45634	16396.03131	16394.60616	16393.18089	16391.7555	599.7956018	553.0023018	500.4991405	439.4153896	362.5315086	108.968746
Temperature	[°C]	539.9909334	538.5145597	538.5086692	538.5027781	538.4968866	538.4909946	454.892895	453.036756	450.4183647	446.3185699	437.8213608	368.1739105
Enthalpy	[kJ/kg]	3406.12789	3406.12804	3406.128036	3406.128032	3406.128028	3406.128023	3386.490512	3383.109697	3378.173622	3370.244801	3354.581341	3215.279391
Velocity	[m/s]	7.170829929	7.149791909	7.150385385	7.150979029	7.151572842	7.152166825	198.3082847	214.6807077	236.5585698	267.9880552	321.161204	617.8579268
Density	[kg/m3]	49.83519184	49.83519184	49.83105598	49.82691963	49.82278279	49.81864546	1.728344113	1.583199083	1.418408287	1.220447383	0.576167651	0.576167651
Speed of Sound	[m/s]	655.0939655	654.1993733	654.1989636	654.198554	654.1981446	654.1977354	654.3254616	653.676982	652.7202553	651.155124	647.7436751	617.8211245
Mach Number	[]	0.010710548	0.010688833	0.010689742	0.010690651	0.010691561	0.010692471	0.302669705	0.328014548	0.362036282	0.411159812	0.493682297	1

Orifice Diameter	[m]	0.007056
Mass Flow Rate	[kg/s]	0.619229987
% of pipe internal diameter	[%]	16

		UPSTREAM OF DRAIN VALVE						DOWNSTREAM OF DRAIN VALVE					
Node point along pipe	[m]	0	2	4	6	8	10	0	2	4	6	8	10
Pressure	[kPa]	16398.54546	16396.7103	16394.8688	16393.02711	16391.18522	16389.34313	681.9838721	628.8255939	569.2035927	499.7091869	412.334683	124.1218803
Temperature	[°C]	539.9882617	538.5101825	538.50257	538.4949566	538.4873425	538.4797275	455.4034322	453.516233	450.864637	446.7107142	438.1686951	368.2820072
Enthalpy	[kJ/kg]	3406.120313	3406.120507	3406.1205	3406.120493	3406.120485	3406.120478	3386.473532	3383.099876	3378.178764	3370.19624	3354.544049	3215.304337
Velocity	[m/s]	8.159245904	8.13550515	8.136377873	8.137250917	8.138124282	8.138997968	198.3938906	214.7264515	236.5368285	268.1691987	321.2772977	617.8175507
Density	[kg/m3]	49.83376299	49.83376299	49.82841842	49.82307304	49.81772683	49.81237981	1.965895475	1.801281234	1.613508668	1.387892902	0.655507825	0.655507825
Speed of Sound	[m/s]	655.0930754	654.1983707	654.1978411	654.1973118	654.1967829	654.1962542	654.2815458	653.6379438	652.6872016	651.1225026	647.720209	617.7936326
Mach Number	[]	0.012186888	0.012162487	0.012163824	0.012165161	0.012166499	0.012167838	0.302784663	0.328058247	0.361955626	0.411425454	0.49381404	1

Orifice Diameter	[m]	0.007497
Mass Flow Rate	[kg/s]	0.699066563
% of pipe internal diameter	[%]	17

		UPSTREAM OF DRAIN VALVE						DOWNSTREAM OF DRAIN VALVE					
Node point along pipe	[m]	0	2	4	6	8	10	0	2	4	6	8	10
Pressure	[kPa]	16398.14616	16395.81093	16393.46755	16391.12384	16388.77982	16386.43548	769.3976888	709.4470283	642.2261633	563.9108261	465.2391641	140.2471085
Temperature	[°C]	539.9850391	538.5049045	538.4952165	538.4855272	538.4758366	538.4661446	455.9442383	454.0218625	451.3328953	447.1508231	438.5353811	368.4616147
Enthalpy	[kJ/kg]	3406.111175	3406.111419	3406.111408	3406.111396	3406.111385	3406.111373	3386.44914	3383.078814	3378.166181	3370.206083	3354.477351	3215.345786
Velocity	[m/s]	9.211391754	9.184857788	9.186111738	9.187366275	9.188621399	9.18987711	198.5167984	214.8245152	236.5900209	268.1324936	321.4848323	617.7504574
Density	[kg/m3]	49.83204023	49.83204023	49.82523903	49.81843651	49.81163267	49.8048275	2.218148832	2.032810949	1.821418116	1.566093599	0.739968313	0.739968313
Speed of Sound	[m/s]	655.0920016	654.1971614	654.1964873	654.1958138	654.1951407	654.1944682	654.2348337	653.5954485	652.6501541	651.0980914	647.6947155	617.793964
Mach Number	[]	0.013758424	0.013731295	0.013733216	0.013735138	0.01373706	0.013738984	0.302958919	0.32818395	0.361996951	0.411334159	0.494128546	1

Orifice Diameter	[m]	0.007938
Mass Flow Rate	[kg/s]	0.783728266
% of pipe internal diameter	[%]	18

		UPSTREAM OF DRAIN VALVE						DOWNSTREAM OF DRAIN VALVE					
Node point along pipe	[m]	0	2	4	6	8	10	0	2	4	6	8	10
Pressure	[kPa]	16397.66987	16394.73856	16391.79691	16388.85476	16385.91211	16382.96895	862.0624652	794.8938769	719.5967983	631.9008514	521.3870272	157.3569232
Temperature	[°C]	539.9811949	538.4986101	538.4864476	538.4742831	538.4621165	538.4499478	456.5169996	454.5560403	451.8251598	447.5986167	438.9408643	368.6477298
Enthalpy	[kJ/kg]	3406.100274	3406.100578	3406.100559	3406.100541	3406.100523	3406.100505	3386.420321	3383.050971	3378.142696	3370.195572	3354.447687	3215.388735
Velocity	[m/s]	10.32720001	10.29781034	10.29957537	10.30134144	10.30310854	10.30487669	198.6619205	214.9540823	236.6892664	268.1716918	321.5770909	617.6809293
Density	[kg/m3]	49.82998586	49.82998586	49.82144831	49.81290867	49.80436694	49.79582312	2.485110417	2.277812534	2.041364899	1.755990589	0.829519557	0.829519557
Speed of Sound	[m/s]	655.0907208	654.1957188	654.1948725	654.194027	654.1931823	654.1923383	654.1861443	653.5505862	652.6100015	651.0649679	647.6752464	617.7923824
Mach Number	[]	0.015425058	0.015395202	0.015397905	0.015400611	0.015403318	0.015406026	0.303169611	0.328359787	0.362110206	0.411333514	0.494256898	1

Orifice Diameter [m] 0.008379
Mass Flow Rate [kg/s] 0.873206538
% of pipe internal diameter [%] 19

		UPSTREAM OF DRAIN VALVE						DOWNSTREAM OF DRAIN VALVE					
Node point along pipe	[m]	0	2	4	6	8	10	0	2	4	6	8	10
Pressure	[kPa]	16397.10731	16393.4724	16389.8245	16386.17583	16382.52638	16378.87615	960.0542549	885.2493227	801.4089985	703.7900273	580.8666586	175.4586165
Temperature	[°C]	539.9766543	538.4911767	538.4760926	538.4610053	538.4459148	538.4308211	457.1208783	455.1221239	452.3462427	448.0699949	439.393895	368.8179054
Enthalpy	[kJ/kg]	3406.087399	3406.08777	3406.087742	3406.087714	3406.087686	3406.087658	3386.391305	3383.0222	3378.117118	3370.180019	3354.479619	3215.428005
Velocity	[m/s]	11.50658069	11.47430617	11.47674537	11.47918635	11.48162911	11.48407365	198.8079245	215.0878899	236.7973061	268.2296816	321.4777796	617.6173493
Density	[kg/m3]	49.82756	49.82756	49.81697267	49.80638213	49.79578838	49.78519141	2.766938305	2.536479614	2.273594028	1.956521458	0.924135884	0.924135884
Speed of Sound	[m/s]	655.0892079	654.1940149	654.1929651	654.1919166	654.1908693	654.1898232	654.1350539	653.504706	652.5686556	651.0297424	647.6654458	617.7785769
Mach Number	[]	0.017186657	0.017154127	0.017157863	0.017161602	0.017165344	0.017169089	0.303382487	0.328543973	0.362237775	0.411358681	0.494063487	1

Orifice Diameter [m] 0.00882
Mass Flow Rate [kg/s] 0.967490506
% of pipe internal diameter [%] 20

		UPSTREAM OF DRAIN VALVE						DOWNSTREAM OF DRAIN VALVE					
Node point along pipe	[m]	0	2	4	6	8	10	0	2	4	6	8	10
Pressure	[kPa]	16396.44874	16391.99052	16387.51614	16383.04059	16378.56388	16374.08599	1063.438036	980.4870164	887.6318214	779.5414319	643.5201192	194.5275867
Temperature	[°C]	539.9713385	538.4824752	538.4639714	538.4454627	538.4269491	538.4084307	457.7582117	455.7117792	452.8953563	448.5636707	439.8536591	368.9671178
Enthalpy	[kJ/kg]	3406.072326	3406.072774	3406.072732	3406.072689	3406.072647	3406.072605	3386.399332	3382.991817	3378.087833	3370.157103	3354.491925	3215.462437
Velocity	[m/s]	12.74941737	12.71426828	12.71758398	12.72090264	12.72422427	12.72754888	198.767543	215.2291033	236.9209465	268.3151013	321.4394967	617.5615971
Density	[kg/m3]	49.8247206	49.8247206	49.81173453	49.79874363	49.7857479	49.77274732	3.064604214	2.808663527	2.517949465	2.167521609	1.023800248	1.023800248
Speed of Sound	[m/s]	655.0874367	654.1920199	654.190732	654.1894459	654.1881615	654.186879	654.0825703	653.4544307	652.5260225	650.9920887	647.6481616	617.7503496
Mach Number	[]	0.019043051	0.019007961	0.01901304	0.019018124	0.019023212	0.019028304	0.303298847	0.328743682	0.362390705	0.411423192	0.493947311	1

Orifice Diameter [m] 0.009261
Mass Flow Rate [kg/s] 1.066566466
% of pipe internal diameter [%] 21

		UPSTREAM OF DRAIN VALVE						DOWNSTREAM OF DRAIN VALVE					
Node point along pipe	[m]	0	2	4	6	8	10	0	2	4	6	8	10
Pressure	[kPa]	16395.68392	16390.2699	16384.83594	16379.40025	16373.96284	16368.52371	1171.904131	1080.587301	978.0969835	858.9571189	709.0847164	214.4311069
Temperature	[°C]	539.9651648	538.4723701	538.4498946	538.427412	538.4049222	538.3824253	458.4261245	456.3450042	453.4580006	449.0719665	440.3000924	369.0780352
Enthalpy	[kJ/kg]	3406.054821	3406.055354	3406.055291	3406.055229	3406.055167	3406.055104	3386.414042	3383.009841	3378.047139	3370.112743	3354.454198	3215.488033
Velocity	[m/s]	14.0555609	14.01759359	14.02203401	14.02647926	14.03092934	14.03538426	198.693523	215.1453415	237.0926426	268.4803774	321.5568427	617.520149
Density	[kg/m3]	49.82142352	49.82142352	49.80565239	49.78987414	49.77408875	49.75829621	3.380270693	3.095340087	2.773916368	2.388288161	1.128474103	1.128474103
Speed of Sound	[m/s]	655.0853797	654.1897029	654.1881381	654.1865761	654.1850168	654.1834601	654.0286362	653.4087426	652.4764566	650.9494197	647.6155566	617.7003831
Mach Number	[]	0.02099402	0.020956556	0.020963358	0.020970168	0.020976984	0.020983808	0.303147569	0.328595341	0.362622401	0.411609329	0.494048814	1

Orifice Diameter [m] 0.009702
Mass Flow Rate [kg/s] 1.170418001
% of pipe internal diameter [%] 22

		UPSTREAM OF DRAIN VALVE						DOWNSTREAM OF DRAIN VALVE					
Node point along pipe	[m]	0	2	4	6	8	10	0	2	4	6	8	10
Pressure	[kPa]	16394.80214	16388.28645	16381.74632	16375.20369	16368.65856	16362.11093	1285.538948	1185.474575	1073.166547	942.2427646	777.8362514	235.3172513
Temperature	[°C]	539.9580465	538.4607192	538.4336639	538.4065984	538.3795224	538.352436	459.1204494	457.0054916	454.0748283	449.5985723	440.7657712	369.1876925
Enthalpy	[kJ/kg]	3406.034637	3406.035264	3406.035174	3406.035083	3406.034993	3406.034902	3386.417791	3383.027855	3378.072254	3370.068258	3354.412671	3215.513338
Velocity	[m/s]	15.42483129	15.38415556	15.39002222	15.39589656	15.40177859	15.40766832	198.6746559	215.0615969	236.9866898	268.6460201	321.6859629	617.479169
Density	[kg/m3]	49.81762255	49.81762255	49.7986409	49.77964891	49.76064658	49.7416339	3.710284552	3.398768223	3.042395754	2.61946076	1.23815404	1.23815404
Speed of Sound	[m/s]	655.0830079	654.187031	654.185147	654.1832669	654.1813907	654.1795184	653.9713501	653.360963	652.436733	650.9027591	647.5809871	617.6448954
Mach Number	[]	0.023039299	0.022999731	0.023008718	0.023017716	0.023026727	0.023035749	0.303079288	0.328436586	0.362425596	0.411795554	0.494160934	1

Orifice Diameter [m] 0.010143
Mass Flow Rate [kg/s] 1.27902535
% of pipe internal diameter [%] 23

		UPSTREAM OF DRAIN VALVE						DOWNSTREAM OF DRAIN VALVE					
Node point along pipe	[m]	0	2	4	6	8	10	0	2	4	6	8	10
Pressure	[kPa]	16393.79226	16386.01505	16378.20807	16370.39754	16362.58343	16354.76576	1404.287941	1295.044523	1172.495619	1029.505618	849.7706013	257.1839088
Temperature	[°C]	539.9498936	538.4473742	538.4150722	538.3827553	538.3504236	538.3180771	459.8412882	457.6865419	454.7196725	450.1641843	441.251417	369.2953407
Enthalpy	[kJ/kg]	3406.011521	3406.012248	3406.012119	3406.01199	3406.011861	3406.011732	3386.411394	3383.031576	3378.096896	3370.061617	3354.369297	3215.538179
Velocity	[m/s]	16.85700995	16.81379715	16.82145294	16.82912069	16.83680044	16.8444922	198.7068484	215.0442913	236.8826896	268.6707398	321.8207671	617.4389373
Density	[kg/m3]	49.81326954	49.81326954	49.79061099	49.76793772	49.7452497	49.72254691	4.05438713	3.715079842	3.327121055	2.860994353	1.352813501	1.352813501
Speed of Sound	[m/s]	655.0802914	654.1839703	654.1817203	654.1794759	654.177237	654.1750037	653.9111316	653.3086581	652.3967269	650.860969	647.5448778	617.5835469
Mach Number	[]	0.025178568	0.025137259	0.025148987	0.025160733	0.025172497	0.025184279	0.303087592	0.328371268	0.362235221	0.411769433	0.494273545	1

Orifice Diameter [m] 0.010584
Mass Flow Rate [kg/s] 1.392365153
% of pipe internal diameter [%] 24

		UPSTREAM OF DRAIN VALVE						DOWNSTREAM OF DRAIN VALVE					
Node point along pipe	[m]	0	2	4	6	8	10	0	2	4	6	8	10
Pressure	[kPa]	16392.64269	16383.42959	16374.18043	16364.92627	16355.6671	16346.40291	1528.236977	1409.394167	1276.133432	1120.760538	924.8814479	280.0279251
Temperature	[°C]	539.9406121	538.432181	538.3939035	538.3556051	538.3172859	538.2789459	460.5911374	458.3919199	455.3852093	450.7867708	441.7452561	369.4002327
Enthalpy	[kJ/kg]	3405.985205	3405.986039	3405.985858	3405.985677	3405.985495	3405.985313	3386.399218	3383.027235	3378.108886	3370.114282	3354.326549	3215.562385
Velocity	[m/s]	18.35183675	18.30632857	18.31620661	18.32610295	18.33601764	18.34595073	198.7681157	215.0644776	236.8320663	268.4746484	321.9535723	617.3997332
Density	[kg/m3]	49.80831441	49.80831441	49.78147003	49.75460498	49.72771921	49.70081268	4.412749706	4.04450171	3.62360696	3.114079687	1.472420835	1.472420835
Speed of Sound	[m/s]	655.0771988	654.1804854	654.1778183	654.1751591	654.1725076	654.169864	653.8490255	653.2533472	652.3532191	650.8321309	647.5021436	617.5160015
Mach Number	[]	0.027411441	0.027368866	0.027383999	0.027399159	0.027414346	0.027429562	0.303138431	0.328355763	0.362123214	0.411408573	0.494378407	1

Orifice Diameter [m] 0.011025
Mass Flow Rate [kg/s] 1.510409929
% of pipe internal diameter [%] 25

		UPSTREAM OF DRAIN VALVE						DOWNSTREAM OF DRAIN VALVE					
Node point along pipe	[m]	0	2	4	6	8	10	0	2	4	6	8	10
Pressure	[kPa]	16391.34147	16380.50303	16369.62112	16358.73228	16347.8365	16336.93376	1657.269537	1528.3929	1383.9347	1215.607128	1003.17029	303.8450185
Temperature	[°C]	539.9301052	538.4149796	538.3699339	538.3248593	538.2797558	538.2346233	461.3689708	459.1214083	456.0692172	451.4286722	442.2596773	369.5016273
Enthalpy	[kJ/kg]	3405.955416	3405.95636	3405.956109	3405.955858	3405.955606	3405.955353	3386.380452	3383.012662	3378.105261	3370.139419	3354.288353	3215.585783
Velocity	[m/s]	19.90900363	19.86152164	19.87413492	19.88677569	19.89944405	19.91214011	198.8625033	215.1322268	236.8473742	268.381001	322.0721886	617.361834
Density	[kg/m3]	49.80270531	49.80270531	49.77112196	49.73950997	49.70786929	49.67619984	4.784905263	4.386536858	3.931326563	3.380619619	1.596939057	1.596939057
Speed of Sound	[m/s]	655.0736978	654.1765394	654.1733997	654.1702708	654.1671526	654.1640452	653.7851781	653.1955415	652.3058498	650.8011756	647.4583323	617.4419287
Mach Number	[]	0.029737467	0.029694224	0.029713546	0.029732911	0.029752316	0.029771764	0.303237984	0.328411463	0.362108757	0.411231916	0.494452038	1

Orifice Diameter	[m]	0.011466
Mass Flow Rate	[kg/s]	1.633127864
% of pipe internal diameter	[%]	26

		UPSTREAM OF DRAIN VALVE						DOWNSTREAM OF DRAIN VALVE					
Node point along pipe	[m]	0	2	4	6	8	10	0	2	4	6	8	10
Pressure	[kPa]	16389.87622	16377.20745	16364.48647	16351.75601	16339.01605	16326.26656	1791.391588	1652.049493	1495.913825	1314.07021	1084.85354	328.5235243
Temperature	[°C]	539.9182726	538.3956047	538.3429315	538.2902188	538.2374664	538.1846743	462.1757041	459.8762503	456.7736219	452.0844231	442.8595671	369.6145337
Enthalpy	[kJ/kg]	3405.921869	3405.922924	3405.922581	3405.922237	3405.921892	3405.921546	3386.357028	3382.990423	3378.090068	3370.144854	3354.382291	3215.611838
Velocity	[m/s]	21.52815223	21.47910818	21.4950599	21.51105231	21.52708557	21.54315985	198.9802626	215.2355797	236.9115128	268.3607506	321.7803879	617.3196282
Density	[kg/m3]	49.79638868	49.79638868	49.75946748	49.72250711	49.68550748	49.6484685	5.170792142	4.741130659	4.250264344	3.656663004	1.726346036	1.726346036
Speed of Sound	[m/s]	655.0697551	654.1720946	654.1684218	654.1647637	654.1611202	654.1574915	653.7202172	653.1359623	652.255577	650.7657244	647.4416519	617.3688231
Mach Number	[]	0.032156114	0.032112942	0.032137379	0.032161878	0.032186438	0.03221106	0.303371119	0.328519757	0.362164965	0.41116524	0.493874149	1

Orifice Diameter	[m]	0.011466
Mass Flow Rate	[kg/s]	1.633127864
% of pipe internal diameter	[%]	27

		UPSTREAM OF DRAIN VALVE						DOWNSTREAM OF DRAIN VALVE					
Node point along pipe	[m]	0	2	4	6	8	10	0	2	4	6	8	10
Pressure	[kPa]	16389.87622	16377.20745	16364.48647	16351.75601	16339.01605	16326.26656	1791.391588	1652.049493	1495.913825	1314.07021	1084.85354	328.5235243
Temperature	[°C]	539.9182726	538.3956047	538.3429315	538.2902188	538.2374664	538.1846743	462.1757041	459.8762503	456.7736219	452.0844231	442.8595671	369.6145337
Enthalpy	[kJ/kg]	3405.921869	3405.922924	3405.922581	3405.922237	3405.921892	3405.921546	3386.357028	3382.990423	3378.090068	3370.144854	3354.382291	3215.611838
Velocity	[m/s]	21.52815223	21.47910818	21.4950599	21.51105231	21.52708557	21.54315985	198.9802626	215.2355797	236.9115128	268.3607506	321.7803879	617.3196282
Density	[kg/m3]	49.79638868	49.79638868	49.75946748	49.72250711	49.68550748	49.6484685	5.170792142	4.741130659	4.250264344	3.656663004	1.726346036	1.726346036
Speed of Sound	[m/s]	655.0697551	654.1720946	654.1684218	654.1647637	654.1611202	654.1574915	653.7202172	653.1359623	652.255577	650.7657244	647.4416519	617.3688231
Mach Number	[]	0.032156114	0.032112942	0.032137379	0.032161878	0.032186438	0.03221106	0.303371119	0.328519757	0.362164965	0.41116524	0.493874149	1

Orifice Diameter	[m]	0.012348
Mass Flow Rate	[kg/s]	1.892430962
% of pipe internal diameter	[%]	28

		UPSTREAM OF DRAIN VALVE						DOWNSTREAM OF DRAIN VALVE					
Node point along pipe	[m]	0	2	4	6	8	10	0	2	4	6	8	10
Pressure	[kPa]	16386.40263	16369.39354	16352.30994	16335.20922	16318.09131	16300.95615	2074.681232	1912.926437	1731.95363	1521.326621	1256.208499	380.2942327
Temperature	[°C]	539.8902163	538.3496483	538.2788644	538.2080089	538.1370813	538.0660816	463.8690709	461.4550299	458.2390811	453.4309626	444.059252	369.9437774
Enthalpy	[kJ/kg]	3405.842332	3405.843591	3405.842972	3405.84235	3405.841725	3405.841098	3386.323754	3382.921648	3378.02136	3370.088815	3354.404562	3215.687816
Velocity	[m/s]	24.95066855	24.90015206	24.92500817	24.94994955	24.97497669	25.00009005	199.1474126	215.554876	237.2013489	268.5694892	321.7111694	617.1965384
Density	[kg/m3]	49.78141108	49.78141108	49.7318273	49.68217279	49.63244731	49.58265064	5.982619194	5.48636504	4.920108448	4.235379314	1.999743951	1.999743951
Speed of Sound	[m/s]	655.0604063	654.1615505	654.1566102	654.1516963	654.1468087	654.1419477	653.5856091	653.0105	652.146399	650.6805905	647.3840401	617.2584044
Mach Number	[]	0.037268732	0.037228563	0.037266642	0.03730485	0.037343187	0.037381654	0.303527778	0.32890373	0.362510976	0.411406241	0.493579435	1

Orifice Diameter	[m]	0.012789
Mass Flow Rate	[kg/s]	2.028926116
% of pipe internal diameter	[%]	29

		UPSTREAM OF DRAIN VALVE						DOWNSTREAM OF DRAIN VALVE					
Node point along pipe	[m]	0	2	4	6	8	10	0	2	4	6	8	10
Pressure	[kPa]	16384.36805	16364.81564	16345.17463	16325.51095	16305.82451	16286.11521	2224.022327	2050.596034	1856.356052	1630.547066	1346.488205	407.6485746
Temperature	[°C]	539.8737794	538.3227128	538.2413011	538.1597943	538.078192	537.9964939	464.7713973	462.2890916	459.0069787	454.1370635	444.6869998	370.1298279
Enthalpy	[kJ/kg]	3405.795738	3405.79708	3405.79626	3405.795437	3405.794609	3405.793778	3386.341011	3382.912825	3377.984031	3370.055436	3354.400648	3215.730751
Velocity	[m/s]	26.75300994	26.70282135	26.73348306	26.76426582	26.79517041	26.82619764	199.0607413	215.5958002	237.3586702	268.6937456	321.723335	617.1269711
Density	[kg/m3]	49.7726359	49.7726359	49.71562903	49.65852859	49.60133424	49.5440456	6.417721416	5.877803101	5.271980842	4.539402305	2.143600116	2.143600116
Speed of Sound	[m/s]	655.0549292	654.1553699	654.1496847	654.1440343	654.1384186	654.1328379	653.5230402	652.9481755	652.0897943	650.6365832	647.353624	617.2058315
Mach Number	[]	0.039961186	0.03992432	0.039971294	0.040018451	0.040065791	0.040113316	0.303341102	0.328910272	0.362691069	0.411549717	0.493509199	1

Orifice Diameter	[m]	0.01323
Mass Flow Rate	[kg/s]	2.16991396
% of pipe internal diameter	[%]	30

		UPSTREAM OF DRAIN VALVE						DOWNSTREAM OF DRAIN VALVE					
Node point along pipe	[m]	0	2	4	6	8	10	0	2	4	6	8	10
Pressure	[kPa]	16382.11706	16359.74976	16337.27734	16314.7752	16292.24319	16269.68119	2378.215258	2192.979853	1984.970436	1743.457217	1439.807185	435.9834009
Temperature	[°C]	539.8555914	538.2928966	538.1997088	538.106396	538.0129578	537.9193935	465.6981113	463.1656881	459.7903465	454.8649615	445.3344297	370.3313472
Enthalpy	[kJ/kg]	3405.744183	3405.745583	3405.74451	3405.74343	3405.742344	3405.741252	3386.347976	3382.937827	3377.945655	3370.019067	3354.388655	3215.777255
Velocity	[m/s]	28.61527518	28.56630412	28.60385558	28.64157683	28.67946916	28.71753384	199.0257492	215.4798037	237.5202924	268.8290652	321.7606096	617.0516107
Density	[kg/m3]	49.76292508	49.76292508	49.69769973	49.63235178	49.5668807	49.50128595	6.866063827	6.287508078	5.634942157	4.853032516	2.292149978	2.292149978
Speed of Sound	[m/s]	655.0488684	654.148528	654.1420164	654.1355502	654.1291294	654.1227543	653.4591608	652.8925987	652.0286398	650.5919178	647.3228795	617.1556001
Mach Number	[]	0.042743225	0.042711143	0.042768673	0.042826459	0.042884503	0.042942807	0.303231688	0.328671865	0.362877605	0.411704676	0.493481462	1

Appendix B

Thermo physical properties of air

The proposed technique to determine internal leakages of high pressure and temperature drain valves requires one to calculate the heat loss from a length of un-insulated pipe. This heat loss is as a result of convection and radiation heat transfer. To calculate the heat loss as a result of convection, the thermo physical properties of air needs to be calculated. Kroger [25] gives the equations to calculate the thermo physical properties of dry air from 220K TO 380K at standard atmospheric pressure (101325 Pa). These equations are listed below. The results from these equations were checked against standard air property charts and found to be accurate.

Density: $$\rho_a = \frac{P_a}{287.08\,T}$$ Equation B.1

Specific heat: C_{p_a}

$$= 1.045356\,x\,10^{3} - 3.161783\,x\,10^{-1}\,T + 7.083814\,x\,10^{-4}\,T^{2} - 2.705209\,x\,10^{-7}\,T^{3}$$

Equation B.2

Dynamic Viscosity: μ_a

$$= 2.287973\,x\,10^{-6} + 6.259793\,x\,10^{-8}\,T - 3.131956\,x\,10^{-11} + 8.15038\,x\,10^{-15}\,T^{3}$$

Equation B.3

Thermal Conductivity: k_a

$$= -4.937787\,x\,10^{-4} + 1.018087x10^{-4}\,T - 4.627937x\,10^{-8}\,T^{2} + 1.250603\,x\,10^{-11}\,T^{3}$$

Equation B.4

Kinematic Viscosity: $v_a = \frac{\mu_a}{\rho_a}$ Equation B.5

Thermal diffusity: $\alpha_a = \frac{v_a}{\rho_a c_p}$ Equation B.6

Thermal expansion coefficient: $\beta_a = \frac{1}{T_f}$ Equation B.7

Film Temperature: $T_f = \frac{T_{amb} + T_{surface}}{2}$ Equation B.8

Appendix C

Measurement of fluid flow by means of a pressure differential device

Experiments were conducted to verify the accuracy of calculating a mass flow rate by the proposed technique. An orifice plate, pressure differential device, was installed in the experimental test rig to calculate the actual mass flow rate of the fluid flowing in the test rig. The mass flow rate calculated from the orifice plate was then compared to the mass flow rate calculated by the proposed monitoring technique for validation purpose.

In this section, the principals and equations used to compute mass flow rate from orifice plates are discussed. The design and calculations are based on ISO 5167-2003 [26], the international standard for Measurement of fluid flow by means of pressure differential devices inserted in circular cross-section conduits. Orifice plates are considered pressure differential devices since once installed in a pipe it causes a static pressure difference between the upstream and downstream sides of the plates. Computation of the mass flow rate is a purely arithmetic process and can be performed by replacing the right hand terms of the basic equation shown in equation C.1 below:

$$\dot{m} = \frac{C}{\sqrt{1-\beta^4}} \varepsilon \frac{\pi}{4} d^2 \sqrt{2\Delta p \rho_1} \qquad \text{Equation C.1}$$

Where:

$\dot{m}$ is the mass flow rate

C is the discharge coefficient

β is the ratio of orifice diameter to pipe internal diameter

ε is the expansibility factor

d is the orifice diameter

Δp is the differential pressure across the orifice

ρ_1 is the upstream density of the fluid

The discharge coefficient can be determined equation C.2 below. [26]

$$C = 0.5981 + 0.0261\,\beta^2 - 0.216\,\beta^8 + 0.000521\left(\frac{10^5\beta}{Re_D}\right)^{0.7} + (0.0188 + 0.0063A)\beta^{3.5}\left(\frac{10^6}{Re_D}\right)^{0.3} + (0.043 + 0.080e^{-10L_1} - 0.123e^{-7L_1})(1 - 0.11A)\frac{\beta^4}{1-\beta^4} - 0.031(M_2 - 0.8M_2^{1.1})\beta^{1.3} + 0.011(0.75 - \beta)\left(2.8 - \frac{D}{25.4}\right)$$

Equation C.2

For corner tapping's, as was the case in the installed orifice, ISO 5167-2003 [26] equates L_1, L_2 and M_2 to zero and equates $A = \left(\frac{19000\beta}{Re_D}\right)^{0.8}$. It can be seen in the above equation that the discharge coefficient is dependent on the Reynolds number which in turn is dependent on the mass flow rate, and thus has to be obtained by iteration.

The expansibility factor can be determined by equation C.3 which appears in ISO 5167-2003. [26]

$$\varepsilon = 1 - (0.351 + 0.256\,\beta^4 + 0.93\,\beta^8\left[1 - \left(\frac{P_2}{P_1}\right)^{\frac{1}{K}}\right]$$

Equation C.3

Appendix D

Comparison between change in pipe surface temperature and change in steam temperature along length of un-insulated pipe

The proposed technique assumes that the change in steam temperature is equal to the change in pipe surface temperature along the length of un-insulated pipe. To prove the validity of this assumption a Flownex SE model was created, which identically resembled the experimental test rig installed to the Cussons mini steam plant. Figure 38 in the report illustrates the model created in Flownex.

The model was simulated with steam flowing at 0.001 kg/s to 0.04 kg/s. The inlet temperature was kept constant at 230 °C and the downstream pressure was kept constant at atmospheric pressure. Relevant properties were output to an excel spread sheet and analysed. Table D.1 below shows results from the simulation whilst figure 39 in the text shows the graphical representation between the changes in pipe surface temperature compared to the change in steam temperature along the length of the un-insulated pipe.

Table D.1: Results from Flownex simulations

	Test Length Properties From FLOWNEX						
	Pipe Surface Temperatures			Steam Temperatures			
Mass Flow Rate	Upstream pipe surface Temp	Downstream pipe surface Temp	Change in Pipe Surface Temp	Upstream Temperature	Downstream Temperature	Change in steam Temperature	Difference between change in pipe surface temp and change in steam temp
$\dot{m}$	$T_{1,pipe\ surface}$	$T_{2,pipe\ surface}$	$\Delta_{pipe\ surface}$	$T_{1,steam}$	$T_{2,steam}$	Δ_{steam}	
[kg/s]	[°C]	[°C]	[°C]	[°C]	[°C]	[°C]	[°C]
0.004	150.28	122.71	27.56	179.67	144.47	35.20	7.64
0.006	169.04	145.17	23.86	194.34	165.43	28.91	5.05
0.008	179.89	159.14	20.75	202.10	177.80	24.30	3.55
0.01	186.97	168.71	18.26	206.81	185.92	20.90	2.63
0.012	191.93	175.62	16.32	209.93	191.61	18.32	2.00
0.014	195.59	180.85	14.74	212.11	195.82	16.29	1.56
0.016	198.36	184.92	13.44	213.69	199.01	14.67	1.23
0.018	200.54	188.18	12.35	214.85	201.50	13.35	1.00
0.02	202.28	190.83	11.45	215.73	203.47	12.27	0.81
0.022	203.70	193.01	10.69	216.41	205.05	11.35	0.66
0.024	204.86	194.83	10.03	216.92	206.35	10.57	0.54
0.026	205.78	196.33	9.46	217.26	207.37	9.89	0.43
0.028	206.54	197.59	8.95	217.51	208.21	9.30	0.35
0.03	207.17	198.66	8.51	217.68	208.89	8.79	0.28
0.032	207.70	199.58	8.12	217.80	209.45	8.35	0.23
0.034	208.14	200.37	7.77	217.87	209.92	7.95	0.18
0.036	208.51	201.04	7.46	217.90	210.30	7.60	0.14
0.038	208.81	201.63	7.18	217.90	210.61	7.29	0.10
0.04	209.07	202.13	6.94	217.87	210.86	7.01	0.07

Appendix E

Data to calculate mass flow rate for experiment 1.

In chapter 6.6, a method was given to calculate the steam temperatures of the un-insulated pipe as well as the resultant mass flow rate. In chapter 6.7, this method was applied to experiment 1 to compute the mass flow rate of a leakage flow and to compare mass flow rates calculated from model assuming change in pipe surface temperature is equal to change in steam temperature, mass flow rates calculated from model that calculates steam temperature and mass flow rates from orifice plate. The table below shows the Excel model used to calculate the mass flow rate using the model that calculates the steam temperature shown in chapter 6.6. Relevant graphs are shown in chapter 6.7.

Table E.1: Model to calculate mass flow rate for experiment 1

	Experimental Data- Input Data								
	Pipe Properties						Temperatures		
	1	2	3	4	5	6	7	8	9
	Length of un-insulated pipe	Outer Diameter of Pipe	Inner Diameter of Pipe	Pipe Wall Thichness	Pipe emissivity	Thermal conductivity of pipe	Ambient Temperature	Upstream un-insulated Pipe Surface Temperature	Downstream un-insulated Pipe Surface temperature
	L	Do	Di	t	ε	k-pipe	Tamb	T1,s	T2,s
	[m]	*[m]*	*[m]*	*[m]*		*[W/mK]*	*[°C]*	*[°C]*	*[°C]*
1	1.9	0.0213	0.01576	2.77	0.95	50	22.8	116.00	97.50
2	1.9	0.0213	0.01576	2.77	0.95	50	22.2	136.00	118.00
3	1.9	0.0213	0.01576	2.77	0.95	50	23	154.00	137.00
4	1.9	0.0213	0.01576	2.77	0.95	50	22.8	168.00	152.00
5	1.9	0.0213	0.01576	2.77	0.95	50	23.1	172.00	157.00
6	1.9	0.0213	0.01576	2.77	0.95	50	22.5	173.00	158.00

First Estimate of Mass Flow Rate (1)											
Heat Loss from the entire length of un-insulated pipe				Thermophysical Properties of Air							
10	11	12	13	14	15	16	17	18	19	20	21
Average Pipe Surface Temperature	Surface Area of un-insulated pipe	Radiation Heat Transfer from un-insulated pipe surface	Convection Heat Transfer from un-insulated pipe surface	Film Temperature	Density of air	Specific heat of air	Dynamic viscosity	Thermal conductivity of air	Kinematic viscosity	Thermal diffusity	Thermal expansion coefficient
Ts,avg	A_ps	Qrad_ps	Qconv,ps	Tfilm	ρ_a	Cp_a	μ_a	k_a	v_a	α_a	β_a
[°C]	*[m^2]*	*[W]*	*[W]*	*[k]*	*[kg/m^3]*	*[J/kgK]*	*[kg/sm]*	*[W/mk]*	*[m^2/s]*	*[m^2/s]*	*[1/K]*
106.75	0.12714	89.99	91.73	337.78	1.04	1008.95	2.0173E-05	0.0291	1.9305E-05	2.7598E-05	0.0030
127.00	0.12714	123.31	120.09	347.60	1.02	1009.68	2.0605E-05	0.0298	2.0293E-05	2.9095E-05	0.0029
145.50	0.12714	157.50	144.81	357.25	0.99	1010.48	2.1025E-05	0.0305	2.1282E-05	3.0593E-05	0.0028
160.00	0.12714	188.31	165.90	364.40	0.97	1011.11	2.1334E-05	0.0311	2.2026E-05	3.172E-05	0.0027
164.50	0.12714	198.26	171.94	366.80	0.96	1011.34	2.1437E-05	0.0312	2.2279E-05	3.2102E-05	0.0027
165.50	0.12714	200.98	174.36	367.00	0.96	1011.36	2.1446E-05	0.0313	2.23E-05	3.2134E-05	0.0027

First Estimate of Mass Flow Rate (2)							
Free convection coefficients for horizontal cylinder				Mass flow rate calculation			
22	23	24	25	26	27	28	29
Prandtl Number	Raleigh Number	Nusselt Number	Convection coefficient	Total Heat Loss	Speciic heat of steam	change in pipe surface temperature	Estimated mass flow rate
Pr	Ra	Nu	h	Q_tot	Cp_s	ΔTps	ṁ_est
			[W/m^2 k]	*[W]*	*[J/kg o C]*	*[° C]*	*[kg/s]*
0.70	44222.01	6.29	8.59	181.73	2026.22	18.50	0.0048
0.70	48410.13	6.44	9.01	243.40	1997.10	18.00	0.0068
0.70	49928.76	6.48	9.30	302.31	1983.33	17.00	0.0090
0.69	51086.38	6.52	9.51	354.21	1977.73	16.00	0.0112
0.69	51098.46	6.52	9.56	370.20	1976.75	15.00	0.0125
0.69	51548.48	6.54	9.59	375.34	1976.55	15.00	0.0127

Calculating Estimate of upstream steam temperature (1)												
					Thermophysical Properties of Air							
30	31	32	33	34	35	36	37	38	39	40	41	42
Length of increment on upstream pipe surface	Surface Area of increment	Pipe Surface temperature at increment	Radiation heat transfer from Increment	Convection heat transfer from increment	Film Temperature	Density of air	Specific heat of air	Dynamic viscosity	Thermal conductivity of air	Kinematic viscosity	Thermal diffusity	Thermal expansion coefficient
x_1	A_1x	T_1s	Q_rad, 1s	Q_conv,1s	Tf	ρ_a	Cp_a	μ_a	k_a	v_a	α_a	β_a
[m]	*[m^2]*	*[° C]*	*[W]*	*[W]*	*[k]*	*[kg/m^3]*	*[J/kgK]*	*[kg/sm]*	*[W/mk]*	*[m^2/s]*	*[m^2/s]*	*[1/K]*
0.005	0.000335	116.00	0.2747	0.2741	342.40	1.03	1009.29	2.038E-05	0.029	1.9768E-05	2.8299E-05	0.0029
0.005	0.000335	136.00	0.3675	0.3490	352.10	1.00	1010.04	2.08E-05	0.030	2.0752E-05	2.979E-05	0.0028
0.005	0.000335	154.00	0.4608	0.4130	361.50	0.98	1010.85	2.121E-05	0.031	2.1723E-05	3.1261E-05	0.0028
0.005	0.000335	168.00	0.5437	0.4671	368.40	0.96	1011.49	2.151E-05	0.031	2.2447E-05	3.2358E-05	0.0027
0.005	0.000335	172.00	0.5682	0.4813	370.55	0.95	1011.70	2.16E-05	0.032	2.2675E-05	3.2702E-05	0.0027
0.005	0.000335	173.00	0.5757	0.4877	370.75	0.95	1011.72	2.161E-05	0.032	2.2696E-05	3.2734E-05	0.0027

Calculating Estimate of upstream steam temperature (2)												
Free convection coefficients for increment				Calculating internal pipe wall temperature		Upstream steam properties						
43	44	45	46	47	48	49	50	51	52	53	54	55
Prandtl Number	Raleigh Number	Nusselt Number	Convection coefficient	Total heat transfer from increment	Upstream Pipe wall Internal temperature	Dynamic viscosity of steam flow	Reynolds Number	Prandtl Number	Nusselt Number	Thermal conductivity of steam	Convection coefficient	Upstream steam temperature Estimate
Pr	Ra	Nu	h	Q_1,s	T_1,i	μ_steam	Re_steam	Pr_steam	Nu_steam	k_steam	h_steam	T_1,f
			[W/m^2 k]	*[W]*	*[° C]*	*[Pa.s]*				*[W/mK]*	*[W/m^2 k]*	*[° C]*
0.70	46127.74	6.36	8.79	0.549	116.06	1.28735E-05	30424.07	1.00	88.88	0.026	146.52	131.19
0.70	49564.17	6.47	9.17	0.716	136.08	1.36408E-05	40101.40	0.99	110.28	0.028	193.19	151.07
0.69	50587.83	6.51	9.42	0.874	154.10	1.43441E-05	50500.32	0.98	132.17	0.029	244.55	168.54
0.69	51441.58	6.53	9.62	1.011	168.12	1.48981E-05	60700.77	0.97	152.82	0.030	294.86	181.97
0.69	51373.07	6.53	9.66	1.049	172.12	1.50574E-05	66987.89	0.97	165.27	0.031	322.70	185.26
0.69	51797.71	6.54	9.68	1.063	173.13	1.50973E-05	67745.91	0.97	166.74	0.031	326.54	186.28

Calculating Estimate of Downstream steam temperature (1)												
					Thermophysical Properties of Air							
56	57	58	59	60	61	62	63	64	65	66	67	68
Length of increment on Downstream pipe surface	Surface Area of increment	Downstream pipe surface temperature increment	Radiation heat transfer from increment	Convection heat transfer from increment	Film Temperature	Density of air	Specific heat of air	Dynamic viscosity	Thermal conductivity of air	Kinematic viscosity	Thermal diffusity	Thermal expansion coefficient
x_2	A_2s	T_2,s	Q_rad, 2,s	Q_conv, 2,s	Tf	ρ_a	Cp_a	μ_a	k_a	v_a	α_a	β_a
[m]	*[m^2]*	*[° C]*	*[W]*	*[w]*	*[k]*	*[kg/m^3]*	*[J/kgK]*	*[kg/sm]*	*[W/mk]*	*[m^2/s]*	*[m^2/s]*	*[1/K]*
0.005	0.000335	97.50	0.202	0.209	333.15	1.06	1008.64	1.9968E-05	0.03	1.8848E-05	2.69E-05	0.00
0.005	0.000335	118.00	0.284	0.284	343.10	1.03	1009.34	2.0408E-05	0.03	1.9838E-05	2.841E-05	0.00
0.005	0.000335	137.00	0.371	0.350	353.00	1.00	1010.12	2.0841E-05	0.03	2.0844E-05	2.993E-05	0.00
0.005	0.000335	152.00	0.450	0.406	360.40	0.98	1010.75	2.1162E-05	0.03	2.1608E-05	3.109E-05	0.00
0.005	0.000335	157.00	0.478	0.424	363.05	0.97	1010.99	2.1276E-05	0.03	2.1885E-05	3.151E-05	0.00
0.005	0.000335	158.00	0.484	0.430	363.25	0.97	1011.01	2.1285E-05	0.03	2.1906E-05	3.154E-05	0.00

Calculating Estimate of Downstream steam temperature (2)												
Free convection coefficients for increment				Calculating internal pipe wall temperature		Downstream steam properties						
69	70	71	72	73	74	75	76	77	78	79	80	81
Prandtl Number	Raleigh Number	Nusselt Number	Convection coefficient	Total heat transfer from increment	Downstream Pipe wall internal temperature	Dynamic viscosity of steam flow	Reynolds Number	Prandtl Number	Nusselt Number	Thermal conductivity of steam	Convection coefficient	Downstream steam temperature estimate
Pr	Ra	Nu	h	Q_2,s	T_2,i	μ_steam	Re_steam	Pr_steam	Nu_steam	k_steam	h_steam	T_2,f
			[W/m^2 k]	*[W]*	*[° C]*	*[Pa.s]*				*[W/mK]*	*[W/m^2 k]*	*[° C]*
0.70	41919.00	6.21	8.38	0.41	97.55	0.00028918	1354.40	1.80	9.32	0.68	400.07	101.70
0.70	46973.05	6.39	8.84	0.57	118.07	1.2949E-05	42242.24	1.00	115.52	0.03	191.58	130.04
0.70	49075.29	6.46	9.16	0.72	137.09	1.368E-05	52953.39	0.99	137.53	0.03	241.65	149.13
0.70	50591.25	6.51	9.40	0.86	152.10	1.4265E-05	63393.03	0.98	158.22	0.03	290.98	163.99
0.69	50708.51	6.51	9.46	0.90	157.11	1.4462E-05	69744.39	0.97	170.60	0.03	318.50	168.54
0.69	51185.73	6.52	9.49	0.91	158.11	1.4502E-05	70527.97	0.97	172.09	0.03	322.27	169.57

Second Estimate of Mass Flow Rate

82	83	84	85
Average steam temp	Specific Heat of Steam	Change in steam temperature	Mass flow rate estimate 2
	Cp_steam	ΔT	ṁ_2est
[° C]	*[J/kg o C]*	*[° C]*	*[kg/s]*
116.45	2025.33	29.49	0.0030
140.55	1992.76	21.03	0.0058
158.83	1980.97	19.41	0.0079
172.98	1976.55	17.98	0.0100
176.90	1975.89	16.72	0.0112
177.93	1975.75	16.71	0.0114

Iterative solver to calculate mass flow rate and steam temperatures (1)									
86	87	88	89	90	91	92	93	94	95
Estimate mass flow rate for iterative solver	Internal Diameter	Estimated upstream steam temp	Estimated downstream steam temp	upstream steam temp	downstream steam temp	Heat loss from increment 1	Heat loss from increment 2	Pipe upstream internal temp	Pipe downstream internal temp
ṁ_est	Di	T_1f_est	T_2f_est	T_1f_est	T_2f_est	Q_1s	Q_2s	T_1i	T_2i
[kg/s]	*[m]*	*[° C]*	*[° C]*	*[° C]*	*[° C]*	*[W]*	*[W]*	*[° C]*	*[° C]*
0.0040	0.01576	131.19	101.70	133.09	110.65	0.549	0.411	116.06	97.55
0.0057	0.01576	151.07	130.04	153.05	131.67	0.716	0.568	136.08	118.07
0.0078	0.01576	168.54	149.13	170.16	150.49	0.874	0.720	154.10	137.09
0.0099	0.01576	181.97	163.99	183.33	165.15	1.011	0.856	168.12	152.10
0.0111	0.01576	185.26	168.54	186.47	169.57	1.049	0.902	172.12	157.11
0.0113	0.01576	186.28	169.57	187.48	170.60	1.063	0.915	173.13	158.11

Iterative solver to calculate mass flow rate and steam temperatures (2)														
Upstream steam properties							Downstream steam properties							
96	97	98	99	100	101	102	103	104	105	106	107	108	109
Dynamic viscosity of steam flow	Reynolds Number	Prandtl Number	Nusselt Number	Thermal conductivity of steam	Convection coefficient	Upstream steam temperature	Dynamic viscosity of steam flow	Reynolds Number	Prandtl Number	Nusselt Number	Thermal conductivity of steam	Convection coefficient	Downstream steam temperature
μ_steam	Re_steam	Pr_steam	Nu_steam	k_steam	h_steam	T_1,f	μ_steam	Re_steam	Pr_steam	Nu_steam	k_steam	h_steam	T_2,f
[Pa.s]				*[W/mK]*	*[W/m^2 k]*	*[° C]*	*[Pa.s]*				*[W/mK]*	*[W/m^2 k]*	*[° C]*
1.3525E-05	24182.45	0.99	75.02	0.027	130.23	133.09	1.2669E-05	25816.85	1.01	78.16	0.026	126.78	110.65
1.4303E-05	32409.59	0.98	92.49	0.029	170.58	153.05	1.347E-05	34412.67	0.99	97.58	0.027	168.65	131.67
1.4979E-05	41923.92	0.97	113.25	0.031	219.85	170.16	1.4202E-05	44217.78	0.98	118.65	0.029	217.14	150.49
1.5505E-05	51383.09	0.96	133.00	0.032	268.38	183.33	1.478E-05	53904.30	0.97	138.60	0.030	265.08	165.15
1.5631E-05	57341.26	0.96	145.13	0.032	295.55	186.47	1.4956E-05	59930.69	0.97	150.75	0.031	292.13	169.57
1.5672E-05	58041.38	0.96	146.53	0.032	299.27	187.48	1.4997E-05	60654.49	0.97	152.18	0.031	295.79	170.60

Iterative solver to calculate mass flow rate and steam temperatures (3)			
110	111	112	113
Average steam temperature	Specific Heat of Steam	Change in steam temperature	Mass flow rate
	Cp_steam	ΔT	ṁ
[° C]	*[J/kg o C]*	*[° C]*	*[kg/s]*
121.87	2000.24	22.44	0.0040
142.36	1983.85	21.38	0.0057
160.32	1977.17	19.67	0.0078
174.24	1975.23	18.18	0.0099
178.02	1975.10	16.89	0.0111
179.04	1975.08	16.88	0.0113